Characterization of the Cell-Penetrating Properties of the Epstein-Barr Virus ZEBRA Trans-activator

Romy Rothe

UNIVERSITÉ DE GRENOBLE

THÈSE

Pour obtenir le grade de

DOCTEUR DE L'UNIVERSITÉ DE GRENOBLE

Spécialité : Sciences du Médicament

Arrêté ministériel : 7 août 2006

Présentée par

ROMY ROTHE

Thèse dirigée par Jean-Luc LENORMAND

préparée au sein du **Laboratoire TheREx-HumProTher TIMC-IMAG UMR CNRS**
dans **l'École Doctorale Chimie et Sciences du Vivant**

Caractérisation de la propriété de la protéine ZEBRA du virus Epstein-Barr à pénétrer dans les cellules

Thèse soutenue publiquement le **2 juin 2010**,
devant le jury composé de :

M. Emmanuel DROUET
Professeur, UJF Grenoble, Président
M. Alain JOLIOT
Professeur, Collège de France Paris, Rapporteur
Mme. Iréne JOAB
Docteur, Université Paris 11, Rapporteur
Mme. Sandrine BOURDOULOUS
Docteur, Université Paris Descartes, Examinateur
M. Jean-Luc LENORMAND
Professeur, UJF Grenoble, Examinateur

TABLE OF CONTENTS

1 ABBREVIATIONS

Amp	ampicillin
AA	amino acid
APS	Ammonium peroxide bisulfate
Bp	base pairs
BSA	bovine serum albumin
CHO	Chinese hamster ovary
CL	cationic lipids
dH2O	distilled Water
DMF	dimethylformamid
DMSO	dimethylsulfoxid
DNA	deoxyribonucleic acid
dNTPs	deoxyribonucleosid triphosphate
E. coli	*Escherichia coli*
EBV	Epstein-Barr virus
EDTA	ethylenediaminetetraacetic acid
EGFP	enhanced green fluorescent protein
FACS	fluorescence-activated cell sorter
FITC	fluorescein isothiocyanate
GAG	glycosaminoglycan
HIV	human immunodeficiency virus
HS	heparan sulfate
HSPGs	heparan sulfate proteoglycans
IPTG	isopropyl-β-D-thiogalactosid
Kan	kanamycine
kDa	kilo Dalton
LB	Luria Broth medium
MCS	multiple cloning side
Nt	nucleotide
O/N	over night
OD	optical density
ON	oligonucleotides
ORF	open reading frame
PBS	phosphate-buffered saline
PCR	polymerase chain reaction
PG s	proteoglycans
PTD	protein transduction domain
RNase	ribonuclease A
Rpm	repeats per minute
RT	room temperature
SDS	sodium dodecyl sulfate
TAT	transactivator of transcription of HIV
U	units
UV	ultraviolet
V/V	volume/ volume
W/V	weight/volume
X-Gal	5-brom-4-chlor-3-indolyl-β-D-galactosid

2 ACKNOWLEDGEMENTS

First, I would like to thank all the members of my jury for their willingness to evaluate my thesis project and for the participation at my defense. Especially, I would like to thank for their understanding and patience when adapting the date of thesis submission and defense to the unpredictable schedule of my little newborn Rosa.

I thank Pr Jean-Luc Lenormand for welcoming me in his lab and giving me the chance to work on this interesting project.

A lot of people supported me during my time in Grenoble at the HumProTher group. It is impossible to give to everybody the attention they deserve. But I will try…

I would like to thank Lavinia “Who is Who” Liguori and Madiha “DrMad” Derouazi. Without the two this work would have been almost impossible. I am very thankful for all the daily support, for helpful comments, scientific discussions, simply for making the everyday “Lablife” a lot easier. But most of all, I am very happy for your friendship, your encouragement and motivation, especially during the last months. You are not only the best colleagues ever; you are also great friends!

I am very grateful to Patricia “the best secretary in the world” Daubois for helping me with all the administrative forms and bureaucratic stuff. Without your support and engagement I would have been lost in France.

I thank Bruno “Mc Gyver” Marques for finding always a solution for every technical problem and resting patient among all the girls.

I appreciate the help of all the members of the TheREx team and the GREPI group.

A special thanks to Didier Grunwald for the precious help with the confocal microscopy in an enjoyable uncomplicated way.

Ich möchte an dieser Stelle meinen Eltern danken für ihre uneingeschränkte Unterstützung, ihr Vertrauen und ihre Liebe. Danke für die Wurzeln und Flügel!

Last but not least, the one and only: I thank my boyfriend Thomas Walther. You played an enormous part in the finishing of my thesis. It started by critical comments, helpful suggestions and proof reading of the manuscript and ended by providing chocolate whenever it was needed. Thank you for always being there for me!

3 SUMMARY

The basic-leucine zipper (bZIP) transcriptional activator ZEBRA of the Epstein - Barr virus was recently shown to cross the outer membrane of live cells and to accumulate in the nucleus of lymphocytes. During this PhD study, I investigated the potential application of ZEBRA as a transporter protein to facilitate transduction of cargo proteins. The analysis of different truncated forms of ZEBRA revealed that the minimal domain (MD) required for internalization was spanning residues 178-220. The MD efficiently transported reporter proteins, such as EGFP and β-galactosidase, into several normal and tumor cell lines. Functionality of internalized cargo proteins was confirmed by β-galactosidase activity in transduced cells, and no MD-associated cell toxicity was detected. Translocation of MD through the cell membrane required binding to cell surface associated heparan sulfate proteoglycans as shown by strong inhibition of protein uptake in presence of heparin. Furthermore, internalization was blocked at 4 °C, whereas no ATP was required as witnessed by an only 25 % decreased uptake efficiency in energy-depleted cells. Common endocytotic inhibitors had no significant impact on MD-EGFP uptake. Only methyl-β-cyclodextrin (MβCD) inhibited MD-EGFP uptake by 40 % indicating the implication of the lipid raft mediated endocytotic pathway. These data suggest that ZEBRA-MD-reporter protein transduction occurs mostly via direct translocation through the cell membrane and not by endocytosis.

Tissue distribution of ZEBRA-MD-EGFP or ZEBRA-MD-β-galactosidase was analyzed after administration into mice. ZEBRA coupled reporter proteins were found in single cells of various tissues contrary to application of EGFP and β-galactosidase alone.

In addition, the cell penetrating sequence of ZEBRA (MD) was fused to anti-tumor protein IL-24/MDA-7. Induced cell death after successful internalization of MD-IL-24/MDA-7 was proven by the cleavage of apoptosis specific caspases without showing difference between normal and tumor breast cells.

The mechanism of MD-mediated internalization is suitable for the efficient delivery of biologically active proteins.

4 RESUME

Il a été récemment démontré que l'activateur de transcription ZEBRA du virus Epstein-Barr contenant un motif «basic-leucine zipper (bZIP)» traverse la membrane externe des cellules vivantes et s'accumule dans le noyau des lymphocytes. Durant mon travail de thèse, j'ai étudié la possibilité d'utiliser ZEBRA comme protéine de transport afin de faciliter la transduction de protéines cargo. L'analyse de différentes formes tronquées de ZEBRA a permis de mettre en évidence que le domaine minimal (MD) nécessaire à l'internalisation inclut les résidus 178-220. Le MD a permis de transporter de manière efficace des protéines rapporteur comme la EGFP et la β-galactosidase dans plusieurs lignées cellulaires normales et tumorales. La fonction des protéines cargo internalisées a été confirmée par l'activité β-galactosidase dans les cellules transduites, et aucune toxicité cellulaire associée au MD n'a été détectée. La translocation du MD à travers la membrane cellulaire nécessite la liaison aux héparanes sulfates protéoglycans associés à la surface de la cellule comme cela a été démontré par la forte inhibition du transport de protéines en présence d'héparine. En outre, l'internalisation est également bloquée à basse température (4 °C). De plus, une réduction de seulement 25 % du transport de protéines cargo dans des cellules avec des stocks d'ATP épuisés démontre que l'internalisation est un processus indépendant de l'ATP. Les inhibiteurs classiques d'endocytose n'ont aucun effet significatif sur le transport de MD-EGFP. Seul le methyl-β-cyclodextrin inhibe de 40 % le transport de MD-EGFP, indiquant l'implication d'une voie d'endocytose médiée par les radeaux lipidiques. Ces résultats suggèrent que le transport de la protéine rapporteur ZEBRA-MD se produit principalement par translocation directe à travers la membrane cellulaire et non par endocytose.

La distribution tissulaire d'EGFP ou de la β-galactosidase couplés ou non avec ZEBRA-MD a été étudiée après injection dans la souris. Seules les protéines de fusion avec ZEBRA-MD ont pu être révélées dans les cellules de différents tissus.

De plus, la séquence de translocation de ZEBRA-MD a été fusionnée avec la protéine anti-tumorale IL-24/MDA-7. La mort cellulaire induite par l'internalisation de ZEBRA-MD-IL-24/MDA-7 a été mise en évidence par le clivage des caspases de la voie d'apoptose aussi dans des cellules normales que dans des cellules tumorales du sein.

En conclusion, le mécanisme d'internalisation de ZEBRA-MD est approprié pour un transport efficace de protéines biologiquement actives.

5 INTRODUCTION

Despite the great medical progress which is reflected by improved surgical intervention and more efficient medications there is still a high demand for innovative and specific therapies for the treatment of common diseases such as cancer, viral and bacterial infections, diabetes or stroke. Due to our increased understanding on the genetic and physiological causes for various diseases, it is now possible to assign the lack of growth-controlling mechanisms in cancerous cells, or fatal immunological reactions to the missing function of only one or few proteins.

Based on this knowledge, highly specific novel human therapy strategies were developed that allow for the specific repair of a molecular dysfunction: while *Gene Therapy* aims at compensating the lack of a protein by introducing a functional copy of the missing gene, *Protein Therapy* relies on the direct delivery of the missing protein itself. Particular efforts were invested in the development of new cancer therapies that ensure complete and efficient delivery of biomolecules in disease cells with no negative side-effects toward normal cells. Encouraging results using gene therapy have been recently obtained in the treatment of lung cancer by using an adenovirus-mediated gene transfer of a p53 wild type allele (Schuler *et al.*, 1998), or by using the replication-incompetent Mda-7/IL-24-expressing adenovirus in phase I-III clinical trials in treating solid tumor or breast cancers (Introgen Therapeutic Inc., company homepage). However, despite impressive progress in gene therapy, some major problems inherent to this technology are far from being solved, which is witnessed by cases of inflammation, toxicity of the virus vector itself, or random integration of virus vector DNA into the host chromosomes (Verma & Somia, 1997).

To circumvent problems associated with gene therapy, research focused on the delivery of pharmaceutically active (macro) molecules to live cells by non-viral strategies. The plasma membrane largely prevents direct uptake of therapeutic molecules into cells. To bypass this problem, new strategies to improve the internalization of those molecules were explored. Recent examples are the packaging of therapeutic molecules into liposomes which, upon contact with the hydrophobic cell membrane, release their cargo into the cytoplasm. Other strategies rely on the coupling of therapeutic molecules with cell-penetrating proteins or peptides, which are able to transduce cell membranes thereby transporting their cargo into the cells. Active research in the past decade has yielded a growing number of peptides capable of crossing plasma membranes. This was first shown for the trans-activating transcriptional factor (TAT) from HIV-1. It was soon followed by identification of the translocation capability of the homeodomain of the *Drosophila melanogaster* transcription

factor Antennapedia (Antp), and VP22 from the herpes simplex virus. Further modifications of the original proteins by site-directed mutagenesis and stepwise truncations lead to the discovery of minimal effective amino acid sequences denoted cell-penetrating peptides (CPPs) or peptide transduction domains (PTDs), respectively. Also new synthetic CPPs were created, namely model CPPs like polyarginine, which contain defined sequences derived from the original proteins, or which are synthesized from domains of different origins to achieve higher internalization efficiency (i.e. Transportan) (Pooga *et al.*, 1998).

This discovery of peptides with the ability to cross cell membranes in a seemingly receptor-independent manner offered a new tool for effective delivery for macromolecules, such as recombinant antibodies and proteins, siRNA, and peptides nucleic acids (PNAs). These approaches provide significant advantages over classical therapies. Possible applications include the restoration of mutated or deleted protein functions in diseased cells by delivering active molecules (Rousselle *et al.*, 2001), or the direct induction of apoptosis by introduction of tumor suppressor proteins or enzymes in cancerous cells (Snyder *et al.*, 2004). Furthermore, transduction systems can be exploited for efficient antigen loading of antigen presenting cells, such as dendritic cells (Kim *et al.*, 1997), or for vaccination purposes, including anti-tumor immune therapy (Justesen *et al.*, 2007). Depending on the biological cargoes, the transduction technology can be applied to address fundamental cellular questions relating to cell cycle regulation, to follow the pharmacokinetics of bioactive molecules in animal models, and also to increase the efficacy of existing therapeutic treatments (Ford *et al.*, 2001; Joliot & Prochiantz, 2004).

5.1 Aim of thesis

The aim of my PhD project was to characterize the delivery properties of a new potential transduction protein. The basic-leucine zipper (bZIP) transcriptional activator ZEBRA of the Epstein - Barr virus (EBV) was recently shown to cross the outer membrane of live cells and to accumulate in the nucleus of lymphocytes (Mahot *et al.*, 2005). The protein is composed of 245 residues containing an activation domain at the N-terminal part of the protein and DNA binding and dimerization domains at the C-terminus (see section 4.3.1) (Petosa *et al.*, 2006).

One of the key questions was the identification of the minimal domain (MD) required for internalization of ZEBRA. As it was demonstrated for other CPPs derived from natural proteins, e.g. Penetratin, TAT or VP22, stepwise truncation of the full-length ZEBRA protein were designed in order to identify the ***cell penetrating sequence***. In total 10 truncations encompassing sequences of the N-terminal and/or the C-terminal part of the full-length protein were analyzed to address this question.

Preceding to all cellular experiments, a major part of the PhD thesis was the optimization of the production and purification of all the ZEBRA fusion proteins. This work included testing diverse expression conditions, such as different bacterial strains or expression temperatures. The purification of the ZEBRA proteins using metal affinity chromatography was optimized by changing the purification buffer compositions.

A major objective of this work was to investigate the ability of the ZEBRA protein to deliver reporter proteins into different mammalian cell lines. Therefore, different truncated forms of ZEBRA were fused to the reporter proteins, i.e. the enhanced green fluorescence protein (EGFP) and β-galactosidase, and tested in several normal and tumor cell lines for internalization. These analyses revealed that the minimal domain (ZEBRA-MD) required for internalization spans over residues 178-220. For the potential use of ZEBRA-MD as a delivery tool for therapeutic proteins it was of great interest to understand the cell penetrating properties, including cytotoxicity, internalization mechanism and intracellular distribution of the internalized proteins. Consequently, the transport of EGFP into cells by ZEBRA-MD was evaluated in the presence of endocytotic inhibitors, at low temperature as well as applying different concentrations of the fusion protein to the cells. Furthermore, subcellular distribution of internalized protein was investigated using microscopical co-localization studies to confirm or exclude endocytic uptake. In addition to these *in vitro* data, additional information on tissue distribution, functionality, and stability of MD-EGFP were obtained by *in vivo* application in mice.

A second step of this project was to employ these findings on the development of a therapeutic application of ZEBRA-MD as a protein carrier. For this reason, various proteins with therapeutic relevance were genetically fused to the internalization domain of ZEBRA (ZEBRA-MD), including the melanoma differentiation associated gene-7 (*mda-7*). By the conjugation of MDA-7/IL-24 to ZEBRA-MD (see section 4.7) it was tested whether therapeutically relevant characteristics of both proteins, namely tumor specificity and intercellular delivery, respectively, could be combined to develop a novel cancer therapeutic. The specific apoptosis-inducing property of this fusion protein was evaluated in MCF10A (normal breast cell line) and MCF7 (tumor breast cell line). Induced programmed cell death was assessed by cell viability assays and Western blot analysis.

5.2 Introduction en française

Malgré des progrès importants dans les domaines de la recherche médicale dues entres-autres à des interventions chirurgicales mieux maitrisées et à des traitements plus efficaces, il existe toujours une forte demande pour des thérapies innovantes et spécifiques pour le traitement de maladies dites communes comme le cancer, les infections virales et bactériennes, les diabètes ou les maladies cardio-vasculaires. Grâce à une meilleure compréhension des causes génétiques et physiologiques des différentes maladies, il est maintenant possible d'assigner la perte des mécanismes moléculaires qui contrôlent la croissance des cellules tumorales ou des réactions immunologiques fatales, à la perte de fonctions de seulement une ou de quelques protéines.

Ainsi, sur la base de ces connaissances, des stratégies thérapeutiques spécifiques ont été développées permettant la réparation spécifique de disfonctionnements moléculaires : bien que la thérapie génique s'adresse à la compensation de la perte d'une protéine par l'introduction d'une copie fonctionnelle du gène manquant, la thérapie protéique se base elle, sur le transfert direct de la protéine manquante. Des efforts particuliers ont été ainsi réalisés dans le développement de nouvelles thérapies anti-cancéreuses qui permettent le transfert efficace de biomolécules dans les cellules malades sans effets secondaires dans les cellules saines. Des résultats encourageants utilisant la thérapie génique ont été récemment obtenus dans le traitement du cancer du poumon avec un adénovirus contenant le gène p53 sauvage (Schuler *et al.*, 1998) ou par l'utilisation d'un adénovirus déficient dans sa réplication et exprimant le gène Mda-7/IL-24 pour le traitement des tumeurs solides et des cancers du sein (essais cliniques de phase I/II; Introgen Therapeutic Inc.). Toutefois, malgré de nombreux progrès en thérapie génique, des problèmes sous-jacents à cette technologie sont loin d'être résolus comme par exemple, des cas d'inflammation, de toxicité du vecteur viral ou de l'intégration aléatoire de l'ADN viral dans les chromosomes de l'hôte (Verma & Somia, 1997).

Afin de palier aux problèmes associés à la thérapie génique, un très grand nombre d'études s'est focalisée sur la vectorisation des (macro-) molécules actives pharmaceutiques et de leurs transferts dans des cellules vivantes par des stratégies non-virales. Toutefois, la membrane plasmique prévient la capture directe des molécules thérapeutiques dans les cellules. De nouvelles stratégies d'internalisation de ces molécules ont donc été développées afin d'augmenter le transfert intracellulaire et le relargage de ces molécules dans les cellules. Ainsi, la vectorisation des molécules thérapeutiques dans des liposomes a permis le relargage de ces molécules dans le cytoplasme après contact avec la membrane cellulaire hydrophobe. D'autres approches utilisent le couplage de ces molécules thérapeutiques avec des peptides de transduction (Cell-Penentrating Peptides) qui sont

capables de transduire les cellules et de transporter leurs molécules cargos dans les cellules. Cette stratégie a permis, ces dix dernières années, à caractériser un nombre important de peptides capables de traverser la membrane plasmique. Le premier à avoir été isolé est le facteur de transcription TAT du virus VIH. Puis, rapidement après le facteur de transcription Antennapedia (Antp) de la drosophile *Drosophila melanogaster* et la protéine virale VP22 de l'herpès simplex virus ont été caractérisés. Des études par mutagénèse dirigée et par délétions ont permis la mise en évidence d'un domaine minimal effectif dénommé cell-penetrating peptides (CPPs) ou peptide transduction domains (PTDs). En dehors de ces peptides naturels, des peptides tels que la polyarginine ou des dérivés de peptides naturels (e.g. Transportan) ont été synthétisés permettant une meilleure internalisation (Pooga *et al.*, 1998).

La mise en évidence de peptides capables de traverser les membranes plasmiques, indépendamment des récepteurs de surface, offre de nouvelles perspectives pour le transfert efficace de macromolécules telles que les protéines et les anticorps recombinants, les siARN et les acides nucléiques peptidiques (ANP). Ces approches apportent des avantages significatifs par rapport aux thérapies classiques. Les applications possibles comprennent la restauration des fonctions des protéines mutées ou délétées dans les cellules malades en apportant des molécules actives (Rousselle *et al.*, 2001) ou par l'induction directe de l'apoptose en introduisant des protéines suppresseurs de tumeurs ou des enzymes dans les cellules cancéreuses (Snyder *et al.*, 2004). D'autre part, les systèmes de transduction peuvent être exploités pour la délivrance d'antigènes sur les cellules présentatrices d'antigènes telles que les cellules dendritiques (Kim *et al.*, 1997), ou à des fins de vaccination dont la thérapie anti-tumorale (Justesen *et al.*, 2007). Enfin, en fonction des cargos biologiques, la technologie de transduction peut être appliquée pour adresser des questions fondamentales sur la régulation du cycle cellulaire, pour suivre la pharmacocinétique des molécules bioactives dans des modèles animaux et aussi pour augmenter l'efficacité des traitements thérapeutiques existants (Ford *et al.*, 2001; Joliot & Prochiantz, 2004).

5.3 Buts de la these

Le but de mon projet de thèse était de caractériser les propriétés de transfert d'une nouvelle protéine de transduction. Le facteur d'activation transcriptionnelle ZEBRA du virus Epstein-Barr (EBV) a récemment été montré être capable de traverser la membrane externe des cellules vivantes et de s'accumuler dans le noyau des lymphocytes (Mahot *et al.*, 2005). La protéine est composée de 245 acides aminés et possède un domaine d'activation situé du côté N-terminal et des domaines de liaison à l'ADN et de dimérisation situés du côté C-terminal (voir section 4.3.1) (Petosa *et al.*, 2006). Une des questions posée fut l'identification

du domaine minimal (MD) nécessaire à l'internalisation de ZEBRA. Comme il a été déjà démontré pour les autres CPPs dérivés de protéines naturelles (e.g. Penetratin, TAT or VP22) des mutants de délétion de la protéine ZEBRA ont été dessiner afin d'identifier la séquence nécessaire à la pénétration cellulaire. Pour répondre à cette question, un total de 10 mutants de délétions comprenant les séquences N-terminales et/ou C-terminales de la protéine sauvage ont été analysées.

Avant les tests cellulaires, une majeure partie de ma thèse s'est focalisée sur l'optimisation de la production et de la purification de toutes les protéines de fusion ZEBRA. Ce travail comprend les tests de faisabilité d'expression sous diverses conditions telles que l'utilisation de différentes souches bactériennes ou les températures d'expression. La purification des protéines ZEBRA utilisant la chromatographie d'affinité a été optimisée en modifiant les compositions des tampons de purification.

Un des objectifs majeurs de ce travail a été d'investiguer la capacité de la protéine ZEBRA de transférer des protéines reportrices dans différentes lignées de cellules de mammifères. Ainsi, les différentes formes tronquées de ZEBRA ont été fusionnées à des protéines reportrices telles que la « enhanced green fluorescence protein (EGFP) » et la β-galactosidase, puis testées pour leur internalisation dans plusieurs lignées de cellules normales et tumorales. Ces analyses indiquent que le domaine minimal nécessaire pour l'internalisation est situé entre les résidus 178-220. Dans Le but d'utiliser le domaine minimal de ZEBRA (MD-ZEBRA) comme vecteur, il était important de comprendre les propriétés intrinsèques de pénétration dont la cytotoxicité, les mécanismes d'internalisation et la distribution intracellulaire des protéines internalisées. Ainsi, le transport de la protéine EGFP dans les cellules par MD-ZEBRA a été évalué en présence d'inhibiteurs de l'endocytose, à basse température et en présence de différentes concentrations de protéine de fusion dans les cellules. D'autre part, la distribution subcellulaire des protéines internalisées a été investiguée en utilisant la microscopie confocale afin de confirmer ou d'infirmer le processus d'endocytose. En addition à ces données in vitro, des études sur la distribution tissulaire, la fonctionnalité et la stabilité de la protéine MD-EGFP ont été obtenues in vivo sur un modèle animal.

Une deuxième étape de ce projet a été d'exploiter ces résultats pour les transposer à des études thérapeutiques en utilisant MD-ZEBRA comme carrier. Ainsi, plusieurs protéines d'intérêt thérapeutique ont été fusionnées au domaine d'internalisation de ZEBRA (MD-ZEBRA) comme par exemple, le melanoma differentiation associated gene-7 (*mda-7/IL24*). En conjuguant *mda-7*/IL24 à MD-ZEBRA (voir section 4.7), des analyses sur les caractéristiques biochimiques et thérapeutiques des 2 protéines ont été effectuées comme la

spécificité tumorale, et le transfert intracellulaire afin de développer une nouvelle molécule anti-cancéreuse. Les propriétés spécifiques d'induction de l'apoptose de cette molécule thérapeutique ont été évaluées sur des lignées de cellules normales (MCF10A) et des cellules de cancer du sein (MCF7). L'induction de la mort cellulaire a été analysée par des études de viabilité cellulaire et par Western blotting.

5.4 Epstein – Barr virus

The Epstein - Barr virus (EBV), also called Human Herpesvirus 4 (HHV4), belongs to the γ herpes virus family, and is one of the most common viruses in humans (Kuppers, 2003). EBV is an extremely successful virus, infecting more than 90 % of the human population worldwide and persisting in the vast majority of individuals as a lifelong, asymptomatic infection of the B-lymphocyte pool. In contrast to this almost always asymptomatic primary infection during childhood, a delayed infection during adolescence or young adulthood causes infectious mononucleosis (IM) in about half of the cases (Young & Rickinson, 2004).
Furthermore, EBV is tightly associated with a still growing spectrum of clinical disorders, ranging from acute and chronic inflammatory diseases to lymphoid and epithelial malignancies. In particular, the virus is thought to contribute in the pathogenesis of the endemic form of Burkitt's lymphoma, Hodgkin's disease, B and T cell lymphomas in immunocompromized individuals such as AIDS patients and organ transplant recipients, nasopharyngeal and gastric carcinoma (Middeldorp *et al.*, 2003; Rodriguez *et al.*, 1999; Young & Rickinson, 2004).
Like other herpesviruses, EBV has a toroid-shaped protein core wrapped around its DNA, a nucleocapsid, a protein tegument and an outer envelope. In virus particles, the genome presents itself as a linear, double-stranded DNA molecule of 172 kp. After infection of B cells, the virus DNA forms a circle and persists as an episome in the nuclei of infected cells (Middeldorp *et al.*, 2003).

5.4.1 Viral life cycle

The experiments of Georg and Eva Klein helped to define the two alternative life cycles of EBV, namely latent or lytic replication (Klein & Klein, 1984). At various stages of each life cycle, EBV employs distinct genetic programmes, which are characterized by a unique set of viral genes that are expressed (Miller *et al.*, 2007; Tsurumi *et al.*, 2005).
The incoming virus spreads throughout the lymphoid tissues as a latent (latency III) growth-transforming infection of B cells. It infects B lymphocytes through interaction of the viral gp350 protein with the CD21 receptor on the B cell surface. The viral envelope fuses with the host cell membrane and the nucleocapsid is then transported to the nucleus. After the release into the nucleus, the linear viral DNA is circulated at the terminal repeats to form the viral episome (Thorley-Lawson, 2001).
In vivo, EBV-infected B cells display two major programmes of gene usage depending on the location and differentiation state of the infected B cell. One of these programs is used to produce infectious virus, and refers to the above mentioned lytic viral replication. The other

one can be divided into three sub-programs that are associated to the latent infection in which no infectious virus is produced. The sub-programs are known as the growth program (Latency III), in which all nine latent proteins are expressed; the default program (Latency II), in which a restricted set of three latent proteins are expressed to provide necessary survival signals; and the latency program (Latency 0), in which few or no latent genes are expressed (Thorley-Lawson, 2001).

During so called latency III, a limited set of viral gene products, including six nuclear antigens (EBNA1, EBNA2, EBNA3A, EBNA3B, EBNA3C and EBNA-LP), three latent membrane proteins (LMP1, LMP2A and LMP2B) and two small RNAs (EBER1-2) are constitutively expressed, (Kuppers, 2003; Thorley-Lawson, 2001; Tsurumi *et al.*, 2005; Young & Rickinson, 2004). Expression of those proteins prompts infected B cells to start replication, to maintain continuous proliferation, and prevents cells from undergoing apoptosis (Tsurumi *et al.*, 2005). The latent nuclear proteins, i.e the EBNAs 1-3, influence both viral and cellular transcription to maintain continuous proliferation, they ensure integrity of the viral genome, and prevent cells from undergoing terminal differentiation or apoptosis. EBNA1, for example, is responsible for the replication of the virus episome and its distribution to the daughter cells. EBNA2 acts as a transactivator that regulates several key virus genes, such as *LMP1* and *LMP2A*, and many cellular genes. *LMP1* is a classical oncogene; its gene product inhibits apoptosis by upregulating anti-apoptotic protein expression (BCL2 or A20). Some of the proliferating infected B-cells escape from the latent-antigen-specific primary T-cell response by downregulating antigen expression and establishing a stable reservoir of resting viral-genome-positive memory cells, in which antigen expression is mostly suppressed (Latency 0) (Young & Rickinson, 2004). The virus uses the Latency 0 programme to persist *in vivo* in a transcriptionally quiescent state within resting memory B cells that circulate in the peripheral blood (Thorley-Lawson, 2001). Occasionally, these EBV-infected cells are recruited into germinal-centre reactions, entailing the activation of different latency programmes, after which they either re-enter the reservoir as memory cells, or activate the viral lytic cycle (Young & Rickinson, 2004).

The switch from latency to virus replication is determined by an intricate cascade of events initiating at the plasma membrane. Induction of the lytic cycle can be triggered by a variety of reagents, including anti-immunoglobulin, calcium ionophore, sodium butyrate, 5Aza2'deoxycytidine, trichostatin A or the phorbol ester 12-O-tetradecanoyl-phorbol-13-acetate (TPA) (Miller *et al.*, 2007; Speck *et al.*, 1997). Upon induction of the lytic program, the key EBV immediate-early (IE) lytic gene, *BZLF1,* is expressed. This gene encodes for the ZEBRA protein, a *trans*-activator of EBV early and late gene expression. For example, it directly activates the transcription of the second immediate-early gene product, Rta, a

transcriptional activator that functions in synergy with ZEBRA. Rta, like ZEBRA, is a sequence-specific DNA-binding protein. Both proteins activate viral and certain cellular promoters, leading to an ordered cascade of viral gene expression: activation of early gene expression followed by the lytic cascade of viral genome replication and late gene expression (Miller *et al.*, 2007; Tsurumi *et al.*, 2005). It was shown that the DNA recognition site of Rta is more complex than that of ZEBRA, suggesting that its function may be limited to activating expression of viral genes, while ZEBRA also acts as a lytic origin-binding protein (*oriLyt*). Seven essential core EBV replication genes were identified (*BZLF1*, *BALF5*, *BMRF1*, *BALF2*, *BBLF4*, *BSLF1*, *BBLF2* and *-3*) that are necessary and sufficient for *oriLyt*-specific DNA replication (Speck *et al.*, 1997). EBV productive DNA replication occurs at discrete sites in nuclei, called replication compartments (Speck *et al.*, 1997). Expression of ZEBRA results in the arrest of replication of cellular DNA concomitant with replication of viral DNA (Speck *et al.*, 1997).

Furthermore the lytic program greatly changes the cellular environment and arrests cell cycle progression by promoting an S-phase-like cellular condition, which favors viral lytic replication. Unlike many small DNA tumor viruses, such as SV40, adenovirus and human papilllomavirus, which require host cell proliferation for viral replication, EBV favors a nonproliferating host cell status for viral replication. Because herpes viruses, and so EBV, have much greater genomic complexity than many tumor viruses, and therefore encode proteins required for DNA synthesis (DNA polymerase, DNA metabolic enzymes, and other replication factors), they can replicate independently of host cell replication. It has been proven that ZEBRA is also involved in this process by inducing cell cycle arrest through interaction with a variety of cellular proteins, e. g. c-myb, p53, NF-κB or p27 (Cayrol & Flemington, 1996a; Cayrol & Flemington, 1996b; Rodriguez *et al.*, 1999; Speck *et al.*, 1997; Tsurumi *et al.*, 2005).
The structure, function and cellular interaction partners of ZEBRA will be explained in more detail in the next paragraph.

5.5 ZEBRA

The EBV immediate-early transcription factor ZEBRA (also known as EB1, Zta, BZLF1 or Z) is not only the central activator of the viral replicative cycle (Cayrol & Flemington, 1995; Sinclair, 2003; Speck *et al.*, 1997; Young & Rickinson, 2004). In addition, it interacts with DNA as both as a transcription and as a replication factor, alters intracellular signal transduction and interferes with cell cycle progression (Sinclair, 2003). This multifunctional protein is encoded by the *BZLF1* gene of EBV. Motivated by its key role in lytic infection, the

structure and function of ZEBRA has been extensively studied and will be subsequently reviewed here.

5.5.1 Structure of ZEBRA

ZEBRA is a 245 residue protein that belongs to the bZIP family of transcription factors (Farrell *et al.*, 1989; Sinclair, 2006); Petosa, *et al.,* 2006). The bZIP transcription factors, including Jun/Fos, C/EBPα and GCN4, are homo- or heterodimers that contain highly basic DNA binding regions adjacent to regions of α-helices that fold together as coiled coils, also called a leucine zipper. These proteins dimerize and bind DNA through their ~60 residues bZIP domain. ZEBRA's bZIP domain is unusual because it lacks the characteristic heptad repeat of leucine residues that normally mediates dimerization (Flemington & Speck, 1990; Kouzarides *et al.*, 1991; Petosa *et al.*, 2006). Furthermore, this region is insufficient to form a stable homodimer at physiological temperature or to bind DNA with high affinity (Hicks *et al.*, 2001; Petosa *et al.*, 2006). The general structure of the ZEBRA is illustrated in Figure 4.1. It contains an N-terminal transactivation domain, a basic region that mediates DNA contact, adjacent to a coiled-coil dimerization domain that together form the bZIP domain. Sometimes even a regulatory domain spanning residues 168–177 is described (Miller *et al.*, 2007).

The C-terminal part of ZEBRA (residues 175-237, Figure 4.1) in complex with a ZRE (ZEBRA responsive elements) from the promoter of the EBV early lytic gene *BSLF2/BMLF1* was successfully crystallized by Müller and colleagues, and revealed an additional structured motif, the C-terminal tail (CT). (Morand *et al.*, 2006; Petosa *et al.*, 2006). A continuous stretch of α-helix that encompasses both the basic region and the ZIP region (to residue Met221) was identified, as expected for a bZIP protein. Still, an unexpected twist was observed at the end of the α-helix, which comprises a one turn helix (Helix αC) followed by an extended stretch of residues running antiparallel to the coiled coil. A hairpin turn connects the bZIP and αC helices, which results in intra and intermolecular hydrophobic interactions between the CT and ZIP regions at the homodimer's DNA-distal end (Petosa *et al.*, 2006; Sinclair, 2006). The CT region stabilizes the coiled coil through numerous interactions and greatly enlarges the dimer interface. This explains the dimer's stability despite the missing leucine zipper motif and the loss of DNA binding caused by deletions affecting the tail's integrity (Hicks *et al.*, 2003; Petosa *et al.*, 2006).

ZEBRA interacts with a series of related DNA-binding sites termed ZEBRA-response elements (ZREs) and AP-1 sites (Sinclair, 2003). DNA binding assays undertaken in stringent conditions revealed that the C-terminal part of the dimerization region, CT, is absolutely required for DNA binding functions (Hicks *et al.*, 2003). Recently, the requirement

of interaction of the C-terminal tail and the core zipper for DNA replication was described assigning a functional role to this structural feature (McDonald *et al.*, 2009). In conclusion, ZEBRA presents a dimer interface of unique nature within the family of bZIP transcription factors.

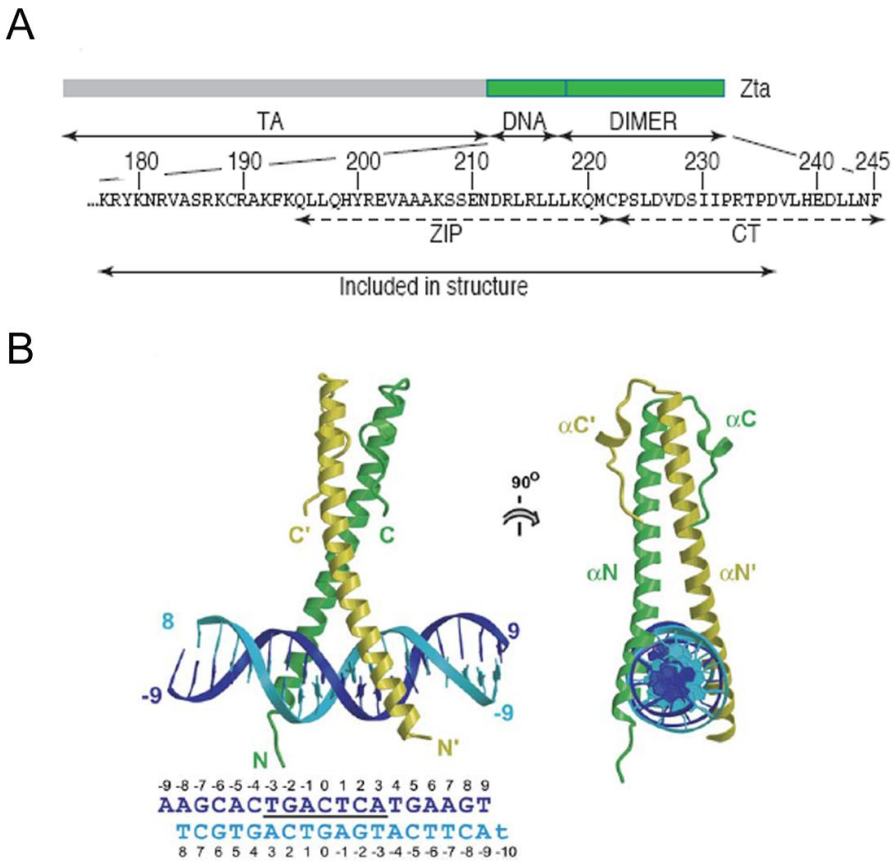

Figure 5.1 **Schematic representation of ZEBRA and the structure of the ZEBRA-DNA complex.** A - The entire ZEBRA protein can be divided in the N-terminal transactivation domain (TA), the DNA binding region (DNA) and the dimerization region (Dimer) extending through the C-terminus. Both the DNA-binding domain and the dimerization domain from a basic leucine zipper (bZIP) with and extension towards the C-terminus (CT). B - Orthogonal views of the Protein-DNA complex. The coiled coil bends towards one end of the DNA, with one bZIP helix curved (yellow) and the other essentially straight. The nucleotide sequence with the underlined AR-1 site is shown. Images were taken from (Petosa *et al.*, 2006; Sinclair, 2006).

5.5.2 Function of ZEBRA

ZEBRA has a variety of distinct functions that are involved in progression of the EBV lytic cycle. It acts in part as a transcription factor and in part as a replication factor (Figure 4.2). In particular, it triggers the switch from latency to lytic replication. It activates the promoters of EBV lytic genes by binding to its target sites, termed ZEBRA responsive elements (ZREs), and possibly by other mechanisms not involving direct contact with DNA. Overall, the

induction of over 50 viral genes is assigned to the function of ZEBRA (Miller *et al.*, 2007; Petosa *et al.*, 2006; Schepers *et al.*, 1996). Since ZEBRA fails to heterodimerize with other cellular bZIP proteins such as Fos, Jun, C/EBPα and CREB, it can exploit the cell's transcriptional activation pathways independently of these proteins (Wu *et al.*, 2004).

Generally, different functions during the lytic cycle activation of EBV by ZEBRA can be summarized (Figure 4.2). ZEBRA directly induces transcription of the *BRLF1* gene, which encodes for the second important EBV transcription factor, Rta. ZEBRA acts in synergy with Rta in the activation of downstream early lytic genes (Miller *et al.*, 2007). Besides its capacity to activate EBV early and late gene expression, ZEBRA also downregulates the latency-associated promoters, such as Cp and Wp (Kenney *et al.*, 1989; Speck *et al.*, 1997). At early stages in the viral lytic cycle, ZEBRA represses the Rta-mediated activation of late genes, e.g. *BLRF2*.

Additionally to its role as *trans*-activator, ZEBRA is an essential lytic replication factor, binding directly to the ZREs within the origin of replication of the EBV genome (oriLyt) (Fixman *et al.*, 1992; Schepers *et al.*, 1993; Schepers *et al.*, 1996; Speck *et al.*, 1997). Lytic replication is needed for late gene expression. Although Rta has the capacity to activate expression of some late genes early in the viral lytic cycle, such differing late gene expression might inhibit DNA replication by a feedback pathway (Miller *et al.*, 2007). Whether ZEBRA is acting as a repressor or as a replication factor, is mainly controlled by its phosphorylation state. ZEBRA can be phosphorylated by casein kinase 2 (CK2), Jun N-terminal kinase (JNK) and Protein kinase C (PKC). Phosphorylation of ZEBRA at its CK2 sites, especially S173, maximizes its DNA-binding activity. In this phosphorylated high-affinity DNA-binding state, ZEBRA represses the Rta-mediated activation of late lytic genes and acts as a lytic origin-binding protein, thus facilitating lytic viral DNA replication (El-Guindy & Miller, 2004; Miller *et al.*, 2007).

Interaction of ZEBRA with cellular pathways

In addition to its function as a *trans*-activator and replication factor, ZEBRA plays an active role in altering cellular expression pathways by interacting physically with several cellular proteins (Sinclair, 2003). ZEBRA is able to induce host cell cycle arrest (Cayrol & Flemington, 1996a; Cayrol & Flemington, 1996b), it alters cellular immune responses (Morrison *et al.*, 2001; Morrison & Kenney, 2004) and changes transcription factor activity (Adamson *et al.*, 2000). Some of these ZEBRA-interacting proteins are listed in Table 4.1. Since most of these interactions were analyzed by over-expression of at least one of the interaction partners, the biological relevance at physiological levels is not completely clarified (Sinclair, 2003).

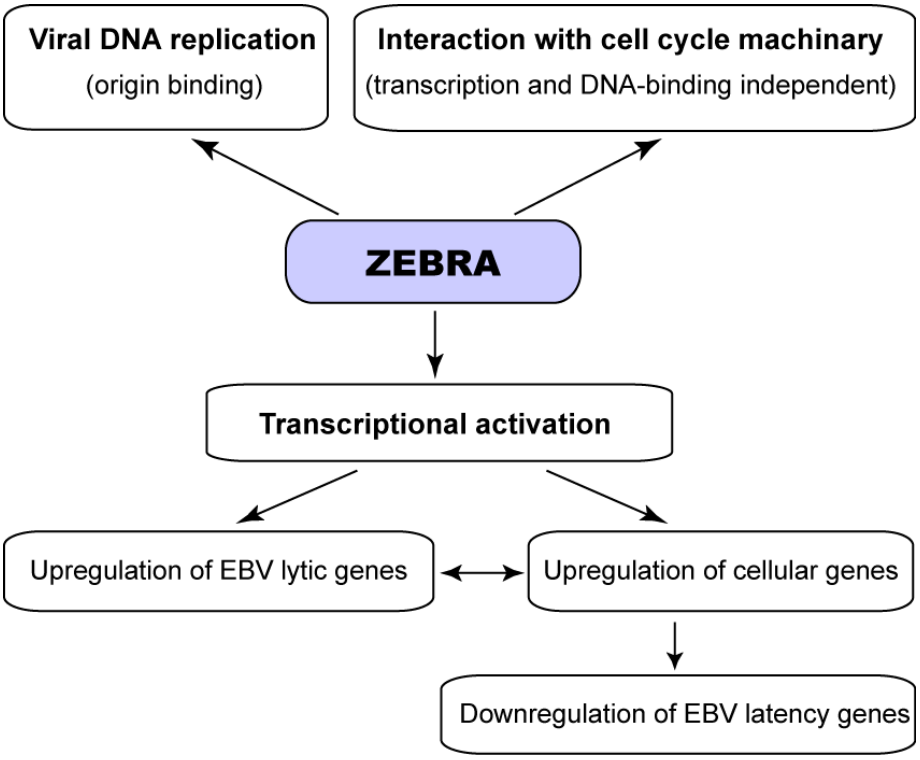

Figure 5.2 **Schematic illustration of the multiple functions of ZEBRA in the reactivation of Epstein-Barr virus (EBV).** ZEBRA acts as an immediate-early transcription factor and triggers the switch from latency to lytic virus replication. In this function it activates the promoters of EBV lytic genes, especially the second important EBV transcription factor Rta. This leads to an upregulation of downstream early lytic genes. Furthermore, ZEBRA plays an active role in altering cellular expression pathways by interacting physically with several cellular proteins. It is able to induce host cell cycle arrest; it alters cellular immune responses and changes transcription factor activity. Scheme was adapted and modified from (Speck *et al.*, 1997)

Examples of important cellular interaction partners

ZEBRA can not only interact with p53 *in vivo* and *in vitro.* It also interferes with the transactivation function of p53. Down-regulation of the p53-dependent transcription was observed upon binding of the ZEBRA bZIP domain to the C-terminal region of p53 (Sinclair, 2003). But ZEBRA can also affect the p53 function differently. An activation of p53-dependent expression in T-lymphoid cells by ZEBRA was shown by Dreyfuss et al. (Dreyfus *et al.*, 2000). Furthermore, Cayrol and Flemington described enhanced expression of p53 and induction of cell cycle arrest in several cell types (Cayrol & Flemington, 1996a; Cayrol & Flemington, 1996b).

The C-terminal half of ZEBRA directly interacts with C/EBPα and by this way activate the transcriptional function of C/EBPα, leading to enhanced expression of C/EBPα and a downstream target, $p21^{CIP1}$(Wu *et al.*, 2003).

The bZIP region and the transactivation domain of ZEBRA appear to be involved in the interaction with the retinoic acid receptors RARα and RXTα (Sista *et al.*, 1995). In addition, the bZIP region is also reported to bind the p65 subunit of NF-κB (Gutsch *et al.*, 1994; Zhang *et al.*, 1994).

Several other protein interactions with cellular proteins are described and, taken together, support the assumption that ZEBRA influences cellular regulatory pathways.

After a direct interaction with the cAMP response element-binding (CREB) an enhanced expression of ZEBRA as well as an inhibited transactivation activity of CREB was observed. Since CREB might play a role in the regulation of the ZEBRA promoter, it is thought that the repression of the CREB function by ZEBRA is an auto-regulatory feedback mechanism for the regulation of the *BZLF1* gene transcription (Sinclair, 2003).

Recently, a host DNA damage repair protein, 53BP1 that specifically interacts with ZEBRA was identified using a global proteomic approach. This interaction requires the C-terminal ends of both proteins. 53BP1 is implicated in the ATM signal transduction pathway which is activated during EBV replication. Furthermore, inhibited expression of 53BP1 reduced viral replication suggesting that the association between ZEBRA and 53BP1 is involved in the viral replication cycle (Bailey *et al.*, 2009).

Table 4.1 also lists a number of genes whose expression is perturbed by ZEBRA, involving a series of cell cycle regulatory genes such as $p21^{CIP1}$, p53, CDC25A and E2F1. The regulation at the RNA level implies that ZEBRA may act as transcription factor on the cellular promoters by direct binding or via its association with other transcription factors. Expression of these genes is regulated at both the RNA and proteins levels, as for example the expression of IFN-γ receptor by ZEBRA. The capacity of ZEBRA to disrupt the IFN-γ signal transduction pathway has implications for the ability of EBV to survive during primary infection and lytic cycle replication *in vivo* (Morrison *et al.*, 2001).

Regulation of cell cycle

ZEBRA stimulates multiple distinct growth arrest pathways and manipulates cell cycle control in a cell-lineage-dependent manner. Cell cycle arrest with some S-phase-specific gene expression is observed in a variety of cell lines in response to ZEBRA expression (Cayrol & Flemington, 1996a; Cayrol & Flemington, 1996b; Mauser *et al.*, 2002c; Sinclair, 2006; Wu *et al.*, 2003).

Interestingly, although ZEBRA can activate transcription through cellular AP-1 elements it was shown that ZEBRA can induce growth arrest independently of its ability to bind DNA (Rodriguez *et al.*, 2001). Furthermore, although DNA-binding is not required for ZEBRAs growth arrest functions, sequences within its DNA-binding domain are involved in eliciting

signals to cell cycle control pathways (Rodriguez *et al.*, 1999). Therefore, it is concluded that the DNA contact region has two independent roles: either to interact with specific DNA sequence elements or to interact with cellular proteins to promote cell cycle arrest (Rodriguez *et al.*, 1999). This explication is supported by interaction of ZEBRA with C/EBPα. It is claimed that one route by which ZEBRA halt the cell cycle is through the upregulation of C/EBPα expression (Wu *et al.*, 2002; Wu *et al.*, 2003). This assumption is evidenced by the failure of ZEBRA to halt the cell cycle in C/EBPα knock-out fibroblasts. ZEBRA protects C/EBPα from proteasome-dependent degradation and also directly interacts with C/EBPα to stimulate its ability to transactivate dependent promoters (Wu *et al.*, 2002; Wu *et al.*, 2003). The revelation that amino acids required for the interaction with C/EBPα are located deeply within the protein-DNA complex also suggests that the basic region of ZEBRA might have two exclusive binding partners: either DNA or C/EBPα. However, the situation is more complex as ZEBRA appears to use more than one route to halt the cell cycle. ZEBRA-induced cell cycle arrest is associated with the up-regulation of p53, and $p27^{KIP1}$, in addition to the upregulation of C/EBPα and $p21^{CIP1}$ (Cayrol & Flemington, 1996a; Cayrol & Flemington, 1996b; Mauser *et al.*, 2002a; Wu *et al.*, 2003). Genetic analysis has revealed that the basic region of Zta is required to mediate all of these events (Rodriguez *et al.*, 1999; Rodriguez *et al.*, 2001; Wu *et al.*, 2003). Furthermore, the contribution of the activation domain of ZEBRA to upregulate p53 and $p27^{KIP1}$, suggest more than one mechanism at work (Rodriguez *et al.*, 1999).

In contrast, this assumption is not true for all cells, as Mauser and colleagues revealed that ZEBRA does not cause cell cycle arrest in primary keratinocytes (Mauser *et al.*, 2002b). It was shown, that ZEBRA induced the expression of several genes that promote S-phase transition. Some differences in gene regulation were identified that may account for these different effects; in the cells that do not arrest or up-regulate p53, the S-phase transcription factor E2F1 is up-regulated (Mauser *et al.*, 2002b).

Table 5.1 List of cellular protein interaction and genes regulated by ZEBRA

Physical association of cellular proteins with ZEBRA		
Cellular protein	**Interaction site of ZEBRA**	**Reference**
p53	bZIP region	(Mauser *et al.*, 2002c; Zhang *et al.*, 1994)
CBP		(Zerby *et al.*, 1999)
C/EBPα	C-terminal half	(Wu *et al.*, 2003)
TFIIA-D		(Chi & Carey, 1993; Lieberman & Berk, 1991)

RXR, PAR	Transactivation domain and bZIP region	(Pfitzner *et al.*, 1995; Sista *et al.*, 1995)
NF-κB, p65 subunit	bZIP region	(Gutsch *et al.*, 1994)
Ubinuclein	Basic region	(Aho *et al.*, 2000)
RACK1	Transactivation domain	(Baumann *et al.*, 2000)
53BP1	C-terminal part	(Bailey *et al.*, 2009)
Cell genes regulated by ZEBRA		
Cell gene	**Regulation of Expression by**	**references**
TGFβinh3	RNA changes	(Cayrol & Flemington, 1995)
TGFβ	RNA changes	(Cayrol & Flemington, 1995)
α1 collagen	RNA changes	(Cayrol & Flemington, 1995)
TKT tyrosine kinase	RNA changes	(Lu *et al.*, 2000)
MMP1	RNA changes	(Lu *et al.*, 2000)
IFN-γ receptor	RNA changes	(Morrison *et al.*, 2001)
E2F1	RNA changes, Protein changes	(Mauser *et al.*, 2002b)
Stem-loop binding proteins	RNA changes, Protein changes	(Mauser *et al.*, 2002b)
CDC25, CD25	RNA changes, Protein changes	(Mauser *et al.*, 2002b)
CyclinE	RNA changes, Protein changes	(Mauser *et al.*, 2002b)
C/EBPα	RNA changes, Protein changes	(Wu *et al.*, 2003; Wu *et al.*, 2004)
p21	RNA changes, Protein changes	(Cayrol & Flemington, 1996a; Cayrol & Flemington, 1996b; Wu *et al.*, 2003)
p53	Protein changes	(Cayrol & Flemington, 1996a; Cayrol & Flemington, 1996b; Mauser *et al.*, 2002c)
p27	Protein changes	(Cayrol & Flemington, 1996a; Cayrol & Flemington, 1996b)
p65, NF-κB		(Morrison & Kenney, 2004)

The identification of cellular targets for ZEBRA is currently in the early stages. More detailed information about the mechanism by which ZEBRA reprograms the patterns of host gene expression during lytic cycle activation can be expected from future genome-wide transcription factor binding studies in a variety of cell lineages.

5.6 Gene delivery

For many - often fatal - genetic diseases, e. g. cystic fibrosis or muscular dystrophy, an ideal treatment would involve the replacement of the missing or mutated gene by the introduction of the relevant healthy transgene. A key factor for the success of gene therapy is the development of delivery systems that are capable of efficient gene transfer in a variety of tissues, without causing any associated pathogenic side effects. Vectors based upon many different viral systems, including retroviruses, lentiviruses, adenoviruses, and adeno-associated viruses, currently offer the best choice for efficient gene delivery (Verma & Somia, 1997). Current gene delivery technologies are also based on strategies using synthetic carriers, such as polymeric cationic peptides and cationic lipids (CLs) (Schatzlein, 2003).
Despite some initial success, vector development remains a concern for improved gene therapy technologies. The development of non-viral delivery systems is an important goal because viral gene transfer has many disadvantages, that is notably toxicity associated with the expression of structural viral proteins, insertional mutagenesis and potentially fatal immune responses (Crystal, 1995; Ferber, 2001).
Another major obstacle in gene therapy is the poor bioavailability of negatively charged or uncharged oligonucleotides (ON) analogues. Commonly used transfection systems include cationic lipids or viruses; however both have several limitations. Cationic lipids are restricted to *in vitro* applications, whereas viruses are sometimes immunogenic in *vivo* (Mae & Langel, 2006).

5.7 Endocytosis

The organization of the cell is highly complex. The cytoplasm is organized in multiple intracellular structures that have distinct properties and functions. Proteins, lipids and solutes are transported between these compartments by membrane trafficking pathways. Newly synthesized proteins traffic through the cell via biosynthetic pathways to their final cellular destination, such as lysosomes, the Golgi apparatus or, for secretory proteins, the extracellular space. The transport of molecules, such as receptor ligands and solutes, is controlled by the endocytotic pathway (Watson *et al.*, 2005).
In general, endocytosis is divided into phagocytosis (cell eating) and pinocytosis (cell drinking). Pinocytosis occurs by a number of pathways, including clathrin-mediated endocytosis, caveolin-mediated endocytosis, clathrin and caveolin independent endocytosis and macropinocytosis (Figure 4.3) (Conner & Schmid, 2003).

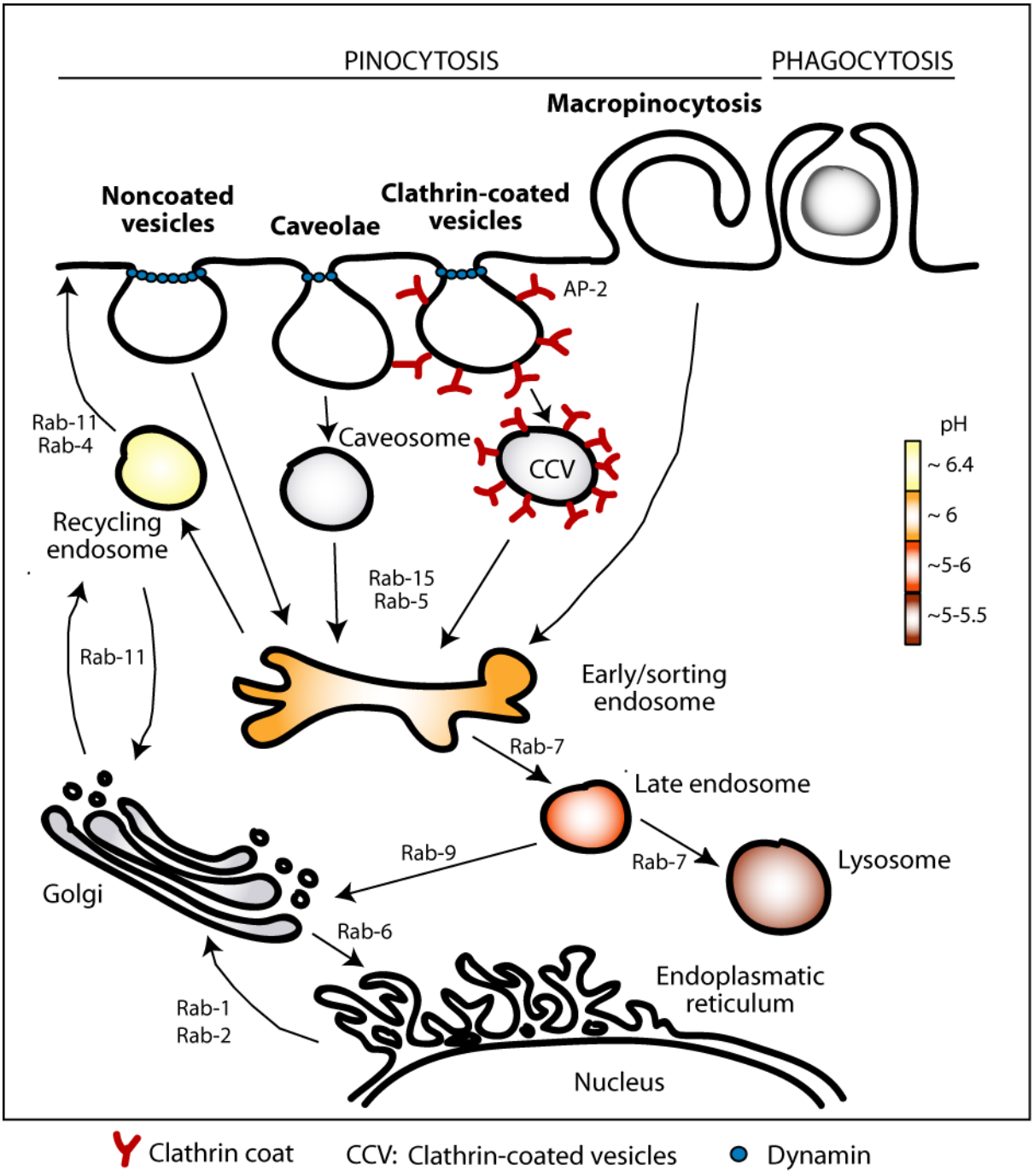

Figure 5.3 **Major pathways for endocytic trafficking.** Schematic diagram of the principle organelles and pathways involved in endocytosis and intracellular transport. Endocytosis can be subdivided in phagocytic and pinocytic uptake. It has been shown that four pinocytic pathways, i.e., clathrin-mediated endocytosis, caveolae-mediated endocytosis, macropinocytosis and clathrin-/caveolae-independent endocytosis are involved in the uptake of cationic CPPs. Acidification occurs during endosomal maturation. Rab and adaptor/accessory protein (AP) families of proteins are implicated in the control of transport. This scheme was adapted from (Langel, 2006; Watson *et al.*, 2005).

Clathrin-mediated endocytosis allows the cellular internalization of proteins and other molecules through the use of specific receptors expressed on the cell surface. Phagocytosis and macropinocytosis rely on the encapsulation of extracellular media through the extension and closure of large membrane ruffles. These two pathways are mainly performed by phagocytes and are essential for the internalization of large particles of around 300 nm in diameter. Additionally, macropinocytosis also facilitates uptake of fluid into the cell. Caveolae appear as 50 – 100 nm bulb-like invagination of the plasma membrane (Rothberg *et al.*, 1992). Caveolae share many characteristics with membrane lipid rafts suggesting that caveolae and rafts are part a common endocytotic pathway, which is defined by clathrin-independence, dynamin dependence, sensitivity to cholesterol depletion, and similar membrane lipid composition (Rothberg *et al.*, 1992). This unification of the caveolar endocytosis with noncaveolar raft endocytosis is referred to as caveolar/raft-dependent endocytosis (Langel, 2006).

Endocytosis and secretion are both linked through the endosomal network and controlled by the action of a family of small GTPases, the Rab proteins (Watson *et al.*, 2005). Endocytozed molecules experience a drop in pH from neutral to pH 5.9 – 6.0 in the lumen of early/recycling vesicles, with a further reduction to pH 6.0 – 5.0 during progression from late endosomes to lysosomes. The drop in pH within the sorting endosome dissociates many ligands from their receptor, allowing the recycling of the receptor back to the plasma membrane (Figure 4.3) (Watson *et al.*, 2005).

5.8 Protein Transduction

5.8.1 Discovery of cell penetrating peptides

The discovery of protein transduction domains (PTDs) or cell penetrating peptides (CPPs) takes its origin in the observation that some full-length transcription factors navigate between cells. It is now more than 20 years ago that Frankel and Pabo described the uptake of HIV-TAT by cells and its transport to the nucleus (Frankel & Pabo, 1988). In 1991, the group of Prochiantz and colleagues discovered that the Antennapedia homeodomain (DNA-binding domain) of *Drosophila melanogaster* was captured by neuronal cells (Joliot *et al.*, 1991).

This work was the origin of the discovery of the first PTD (or CPP) in 1994: a 16-mer peptide derived form the third helix of the homeodomain of Antennapedia termed Penetratin (RQIKIYFQNRRMKWKK) (Derossi *et al.*, 1994). This peptide corresponds exactly to the most conserved part of the homeodomain. It is capable of translocating across biological membranes, and to carry attached cargoes of various sizes and compositions into the cell interior (Derossi *et al.*, 1998).

In 1998, the group of Lebleu identified the minimal peptide sequence of TAT spanning residues 47 to 57 required for cellular uptake (YGRKKRRQRRR) (Vives *et al.*, 1997). The ability to define short peptide sequences, i.e. 11 amino acids in the case of TAT or 16 for Penetratin indeed opened the way to the fabrication of a large number of chemical CPP variants. This has permitted to develop new peptides, to identify key residues and to analyze the importance of physical conformations (Derossi *et al.*, 1996).

In 1997, the first non-covalent CPP (MPG) for delivery of nucleic acids was designed by the group of Heitz and Divita (Morris *et al.*, 1997). Whereas, the groups of Wender and of Futaki demonstrated that polyarginine sequences (R8) were sufficient to ferry molecules into cells, and proposed that their uptake mechanism involves a bidentate hydrogen-bonding interaction between the guanidinium group of the arginine residues and the phosphate group in the membrane (Futaki *et al.*, 2001; Wender *et al.*, 2000). There are quite a few other examples of CPPs, including Transportan, a 27 amino acid-long chimeric CPP derived form the N-terminal fragment of the neuropeptide galanin linked to mastoparan, a wasp venom peptide (Pooga *et al.*, 1998); VP22, a major structural component of Herpes simplex virus (HSV-1) (Elliott & O'Hare, 1997); an 18-mer amphipathic model peptide (MAP) with the sequence KLALKLALKALKAALKLA (Oehlke *et al.*, 1998); cationic peptides PTD-4 and PTD-5 synthesized using 12-mer peptide sequence from M13 phage library (Mi *et al.*, 2000) and a lot more other peptides.

A major breakthrough in the CPP field came from the first proofs-of-concept of their *in vivo* application. The groups of Dowdy and Langel demonstrated the delivery of small peptides and large proteins using the TAT peptide (Schwarze *et al.*, 1999), and delivery of PNAs using the chimeric peptide Transportan (Pooga *et al.*, 1998), respectively.

Up to now, the most intensively studied CPPs include the HIV-TAT peptide (TAT) or Penetratin from Antennapedia, together with synthetic oligomers of arginine (R4-R16). Twenty years after their discovery, CPPs are tested in first clinical trials (Heitz *et al.*, 2009).

5.8.2 Definition and classification

CPPs are generally short peptides of less than 40 amino acids, derived from natural or unnatural proteins or chimeric sequences. CPPs have the ability to enter the cell interior via different mechanisms, including endocytosis, with the capacity to mediate intracellular delivery of covalently or noncovalently conjugated bioactive cargoes. The first case requires chemical linkage with the cargo and the second involves formation of stable, non-covalent complexes.

Due to the lack of understanding of the true mechanisms of CPP cellular uptake, the classification of CPPs still remains to be clarified. A general classification based on the translocation mechanisms failed since many CPPs require more than one uptake mechanism that strongly depends on the cell type. Thus, the classification based on their origin presented in Table 4.2 is somewhat random and highly debatable, waiting to be taken forward by new information.

One possible classification:

1. Protein derived
    a. Protein transduction domains (PTDs), responsible for the parent protein translocation: penetratin, TAT, VP22
    b. Protein derived: pVEC, pIsl-1, LL-37, mPrP(1-28), hCT(9-32), NLS, mimicking peptides
2. Designed

    Amphiphilic: MAP

    Chimeric: Transportan, MPG

    Homing peptides: Lyp-1, F3, CGKRK, RGR

    Synthetic: Pep-1, MPG, KALA, KFFK, Pro-rich, polyarginines (R8-R11) (Langel, 2006)

Other categorizations are available based on different criteria. Frequently CPPs are subdivided according to their structure: they are as either polycationic, essentially containing clusters of polyarginine in their primary sequence, or amphipathic (Heitz *et al.*, 2009). One class would consist of amphipathic helical peptides, such as Transportan and model amphipathic peptide (MAP), where lysine is the main contributor to the positive charge. Another class includes arginine (Arg)-rich peptides, such as TAT and Antp or penetratin. But in view of the heterogeneity of their sequences and properties they would also need a further sub-classification into arginine-rich, amphipathic, non-basic and more specific criteria.
Based on their structural properties, another possible classification into three classes that behave differently, especially with respect their endocytotic uptake, was proposed by Langel (Langel, 2006).

1. Peptides with low amphipaticity where the charge contribution originates mostly from arginine residues (Penetratin, TAT)
2. Peptides with high degree of amphipaticity, where the charge contribution originates mainly from lysine residues (MAP, transportan)

3. Peptides where the charged and hydrophobic residues are separated lengthwise in the chain (pVEC and pep-1)

However, even this classification of CPPs lacks the power of generalization among all available cell penetrating peptides (Langel, 2006).

5.8.3 Intensively studied CPPs

When TAT protein is added to cell culture, it is internalized by cells in a concentration and time-dependent fashion (Gupta *et al.*, 2005). It localizes eventually to the nuclei where it trans-activates the viral promoter (Gupta *et al.*, 2005). Subsequently, it was found that the protein transduction sequence for TAT includes residues 47–57 (11-mer; YGRKKRRQRRR) (Vives *et al.*, 1997). Various other Arg-rich peptides, such as D-amino acid and Arg-substituted TAT (Futaki *et al.*, 2001) analogs; the RNA-binding peptides derived from virus proteins, such as HIV-1 Rev and flock house virus coat proteins; the DNA-binding segments of leucine zipper proteins, such as cancer-related proteins c-Fos and c-Jun; and the yeast transcription factor GCN4 also demonstrated the potential to translocate across membranes (Futaki *et al.*, 2001).

Penetratin also possess a high content in basic residues and by the presence of hydrophobic residues, most importantly tryptophanes (Joliot & Prochiantz, 2008). The role of specific hydrophobic residues in the uptake process is further supported by the limited internalization of Penetratin with Trp>Phe substitutions. Penetratin interacts with purely lipidic vesicles and these hydrophobic interactions involve Trp residues (Joliot & Prochiantz, 2008). Several biophysical studies involving artificial vesicles recently demonstrated that Penetratin can cross lipid bilayers and that it shows membrane destabilizing properties (Joliot & Prochiantz, 2008).

Table 5.2 Examples of cell penetrating peptides

Name	Sequence	Reference
Peptides deriving from protein transduction domains		
TAT_{49-57}	YG**RKKRR**Q**RRR***	(Vives *et al.*, 1997)
Penetratin (Antp)	**R**QI**K**IWFQN**RR**M**K**W**KK**	(Joliot & Prochiantz, 2004)
Transportan	GWTLNSAGYLLG**K**IN**K**ALAALA**KK**IL	(Pooga *et al.*, 1998)
VP-22	DAATAT**R**G**R**SAAS**R**PTE**R**P**R**APA**R**SAS**R**P**RR**	(Elliott & O'Hare, 1997)

	PVD	
Amphipathic peptides		
MAP (model amphipatic peptide)	**K**LAL**K**LAL**K**AL**K**AAL**K**LA	(Oehlke *et al.*, 1998)
MPG	GALFLGFLGAAGSTMGAWSQP**KKKRK**V	(Morris *et al.*, 1997)
SAP	V**R**LPPPV**R**LPPPV**R**LPPP	(Pujals *et al.*, 2006)
k-FGF	AAVALLPAVLLALLAP	(Lin *et al.*, 1995)
Prion peptide	MV**K**S**K**IGSWILVLFVAMWSDVGLC**KKR**P**K**P	(Magzoub *et al.*, 2006)
pVEC	LLIIL**RRR**I**RK**QAHAHS**K**	(Elmquist *et al.*, 2001)
Pep-1	KETWWETWWTEWSQP**KKKRK**V	(Gros *et al.*, 2006)
SynB1	**R**GG**R**LSYS**RRR**FSTSTG**R**	(Rousselle *et al.*, 2001)
Other cell-penetrating peptides		
Buforin II	T**R**SS**R**AGLQFPVG**R**VH**R**LLRK	(Kobayashi *et al.*, 2004)
Polyarginine	(**R**)n	(Futaki *et al.*, 2001; Wender *et al.*, 2000)
HN-1	TSPLNIHNGQ**K**L	(Hong & Clayman, 2000)

TAT, penetratin and Polyarginine are the most used CPPs. Several of the many other CPPs along with their sequence are listed. * Basic residues are presented in bold.

5.8.4 Mechanisms of internalization

The activity of therapeutic molecules depends on their availability and functionality after their delivery into cells, both of which are determined by the transduction mechanism of the particular CPP. Consequently, extensive research was directed to elucidate pathways underlying protein transduction. Earlier studies suggested a receptor, temperature and energy-independent internalization process, excluding the involvement of endocytosis, e. g. for TAT or Penetratin (Pooga *et al.*, 1998; Vives *et al.*, 1997). The energy-independent mechanism was shown to be an artifact due to strong fixation by acetone of the cell prior to the monitoring of protein uptake. According to Richard and colleagues, the cell-fixation procedure produces artificial redistribution of tightly membrane-bound positively charged peptides into the cell interior and nucleus. It was also impossible to distinguish between cell-associated peptides and truly internalized peptides using cytometric analysis without intensive washes (Richard *et al.*, 2003). In subsequent studies using live unfixed cells the uptake of TAT, R9-peptides and the Antp peptide was reexamined. Protein internalization

showed inhibition at low temperatures and depleted ATP pools, suggesting endocytosis as the major mechanism for internalization of the majority of the CPPs (Console *et al.*, 2003; Murriel & Dowdy, 2006; Nakase *et al.*, 2004; Richard *et al.*, 2003; Richard *et al.*, 2005; Wadia *et al.*, 2004).

Collectively, the recent data suggest the implication of more than one mechanism for CPP-mediated intracellular delivery of various molecules and particles. It is possible that some peptides use several entry routes and it is proven that the nature of the attached cargo can modify the mode of internalization, to the point that some cargoes will not be internalized at all (although possibly endocytozed) (Prochiantz, 2007). This complexity is further enhanced by other factors, in particular the membrane composition, the physiological state of the cells, and different uptake characteristics for one and the same peptide in different cell lines (Prochiantz, 2007).

At the moment it is widely agreed that CPP-mediated intracellular delivery of large molecules and nanoparticles proceeds via the energy-dependent endocytosis, with subsequent enhanced escape from endosome into the cell cytoplasm (Wadia *et al.*, 2004). In contrast, individual CPPs or CPP-conjugated small molecules penetrate cells via electrostatic interactions and hydrogen bonding and do not seem to depend on energy (Rothbard *et al.*, 2005). Also peptides from the Penetratin family do not need endocytosis to go across the plasma membrane. In addition, an alternative route of direct translocation of the small CPPs, such as SSHR-based peptide, was reported (Veach *et al.*, 2004).

There are certain structural requirements such as the importance of specific amino acids, for example a single amino acid substitution can almost completely inhibit CPP translocation (Joliot & Prochiantz, 2004). Also regions of secondary structure, such as amphipaticity and α-helical content seem to play a role (Joliot & Prochiantz, 2004). One fundamental difference between the cationic TAT and Penetratin is that the TAT peptide is composed of hydrophilic arginine residues, and mutating one of these strongly inhibits its energy-dependent translocation, but in contrast, translocation of Penetratin depends strictly on the presence of central hydrophobic core (Derossi *et al.*, 1994).

Although it remains difficult to establish a general scheme for CPP uptake mechanisms, there is a consensus that the first contacts between the CPPs and the cell surface take place through electrostatic interactions with proteoglycans, and that the cellular uptake pathway is controlled by several parameters including: (i) the nature and secondary structure of the CPP; (ii) its ability to interact with cell surface and membrane lipid components; (iii) the nature, type and active concentration of the cargo; and (iv) the cell type and membrane composition (Foged & Nielsen, 2008).

Therefore the uptake mechanism for cationic CPPs and amphipathic CPPs will be described separately at the following paragraph.

Cell surface binding

It is thought, that the direct contact between the CPPs and the negatively charged residues on cell surface is a prerequisite for successful translocation. A general assumption is the importance of highly positive charged residues in cationic CPPs for transduction (Mitchell 2000). It was shown that interactions with cell-surface heparan sulfate (HS) are required for the internalization of CPPs (Fuchs & Raines, 2004; Wadia *et al.*, 2004). Specifically, cellular treatment with exogenous heparan sulfate (heparin), an anti-HS antibody, or an HS-degrading enzyme (heparinase), all result in reduced polyarginine-peptide internalization, which shows that heparan sulfate proteoglycans (HSPGs) play a major role in peptide uptake (Belting, 2003; Poon & Gariepy, 2007).

In contrast, in a recent publication of Gump (Gump *et al.*, 2010) it is claimed that Tat-mediated transduction does not require cell surface associated neither HS, chondroitin sulfate (CS) nor sialic acids (SAs); and that it occurs efficiently in their absence. Furthermore, TAT-induced macropinocytotic fluid-phase uptake was revealed to be intact in glycan-deficient cells, indicating that TAT does not require these glycans to stimulate endocytosis. On the contrary, depletion of cell-surface proteins with proteases resulted in drastically reduced transduction efficiency, indicating that a cell-surface protein is necessary for TAT transduction (although not necessarily as a receptor). These data suggest that cationic peptides like TAT may induce transduction via binding to a protein on the cell surface rather than through interactions with glycans or direct interaction with the membrane (Gump *et al.*).

5.8.5 Uptake of cationic CPPs

Endocytosis

Numerous cationic peptides have been shown to permeate mammalian cells (Coeytaux *et al.*, 2003; Vives *et al.*, 1997). Cell entry of positive charged CPPs via endocytosis is the currently favored uptake mechanism (Vives *et al.*, 2003; Wadia *et al.*, 2004). Endocytosis is followed by passage from the vesicles to cytoplasm (Figure 4.4). Although, this implies vesicle disruption, the plasma membrane and cell viability is not affected. Macropinocytosis has been claimed as the major route of internalization of cationic CPPs, especially for TAT (Kaplan *et al.*, 2005; Wadia *et al.*, 2004), other endocytotic pathways including clathrin and caveolin-dependent endocytosis (Richard *et al.*, 2005; Ziegler *et al.*, 2005) and trans-Golgi network-mediated internalization (Fischer *et al.*, 2004) were shown to be implicated in the transport of other CPPs (Ferrari *et al.*, 2003; Fittipaldi *et al.*, 2003; Kaplan *et al.*, 2005; Nishi & Saigo, 2007; Richard *et al.*, 2005).

However, the basic character of a peptide alone is not sufficient for translocation. It has been demonstrated, that the length and composition of the cationic peptide is important for

internalization, as seven to nine cationic charges are optimal. Arginine residues are preferred over lysine, as in some studies peptides rich in lysine get transduced with much less efficiency than the arginine-rich peptides (Dietz & Bahr, 2004; Futaki *et al.*, 2001; Wender *et al.*, 2000). Increasing the local concentration of CPPs at the cell surface favors cellular uptake independently of endocytosis and leads to a more cytoplasmic distribution of CPPs. Once more, a single definition of the uptake pathway for cationic CPPs seems to be hindered by the observation that TAT cell entry differs depending on the size of the cargo. Large protein fusion conjugates were rather found to be entrapped in endocytotic vesicles, while small peptide conjugates seemed to enter the cell in a rapid manner that was dependent on the membrane potential (Tunnemann *et al.*, 2006).

To define the exact endocytotic pathway is challenging since some endocytotic mechanisms are distinguishably morphologically and can be associated with characteristic structural protein such as clathrin or caveolin, but biochemical probes of theses pathways can be unclear.

Many laboratories confirm an uptake by macropinocytosis for TAT and other cationic CPPs (Kaplan *et al.*, 2005). In the presence of inhibitors of macropinocytosis like cytochalasin D or amiloride, transduction of TAT peptides and cationic peptides is absent. Additionally, in the case of TAT, an uptake of neutral dextran, which is a marker of fluid phase endocytosis, was induced. This stimulation of macropinocytosis is significant because it indicates that cationic CPPs do not just passively enter cells but stimulate their own endocytotic pathway (Gump & Dowdy, 2007). Furthermore, the involvement of the small GTPase Rac for transduction was shown which is consistent with the role for Rac in the actin rearrangement during macropinocytosis (Nakase *et al.*, 2007). A similar mechanism for the internalization of VP22 was concluded, demonstrating an interaction with cell surface heparan sulfate proteoglycans and a subsequent lipid-raft-mediated endocytosis independent of clathrin, caveolin and Rho family GTPases but dependent on dynamin. Moreover, nearly all VP22-GFP signals were found in early endosomes (Nishi & Saigo, 2007).

Endosomal entrapment

Due to the endocytotic cell entry, one of the major challenges for the application of CPPs is to increase endosomal escape of CPP-cargoes to provide sufficient biologically active molecules at their intracellular destinations. Although, endocytozed CPP distribution can be observed in the cytosol and specific intracellular compartments, such as the nucleus, the vast majority of internalized polycations and their cargoes (>90 %) remains entrapped in endosomes, becomes degraded or is shuttled out of the cell (Poon & Gariepy, 2007). It has been assumed that endosomal acidification and cytosolic Hsp90 activity is required for the delivery of cationic CPPs to the cytoplasm (Fischer *et al.*, 2004), (Nishi & Saigo, 2007).

Clearly, endosomal escape remains a major limitation and the rate-limiting step of CPP-mediated drug delivery. Fusion of the CPP to pH-sensitive fusogenic peptides or co-administration of endosome-disruption agents, such as chloroquine, Ca^{2+}, sucrose or photosensitizers, result in an enhanced release of the CPP-cargoes from the endosomal compartments (Oliveira *et al.*, 2007; Oliveira *et al.*, 2008; Shiraishi & Nielsen, 2006; Wadia *et al.*, 2004). However, these strategies come along with considerable medical and technical disadvantages which consist in the cytotoxicity of disrupting agents, such as chloroquine, and the problematic application of photosensitizers for *in vivo* protein delivery.

Although it is now widely assumed that endocytosis is involved in the internalization of CPPs, it appears that different mechanisms may occur simultaneously. As it is the case for Penetratin or Transportan were both endocytosis and membrane translocation are reported as route of cell entry. A possible explanation can be found in the nature of the cargo linked to Penetratin. Recent comparative studies confirm the use of distinct uptake mechanisms by Penetratin and basic PTDs (Joliot & Prochiantz, 2008).

5.8.6 Uptake of Penetratin

Similar to the TAT peptide discovery, Penetratin derives from a natural protein. Penetratin is the translocation sequence in the third helix of the homeoprotein Antennapedia (Derossi *et al.*, 1994). Intensive studies on the third helix and several modified variants revealed the requirement of the helix. The syntheses of several peptides encompassing various sequences of the C-terminal part of the homeodomain lead to the identification of the minimal domain required for translocation. Penetratin varies from the large family of polycationic CPPs since besides the high content of basic residues it also possess hydrophobic residues. The region absolutely required tryptophan W48 in a cationic environment assuming that positively charged amino acids interact with negatively charged phospholipids. The change of one tryptophan into a phenylalanine reduces peptide internalization dramatically (Derossi *et al.*, 1994). This was proven after the deletion of phenylalanine and a tryptophan at positions 48 or 49, respectively, which abolished the peptide uptake. As tryptophanes are absent in most basic peptides, in particular in TAT and Poly-Arg, this observation additionally suggests that the mechanisms of internalization differ between peptides (Prochiantz, 2007).

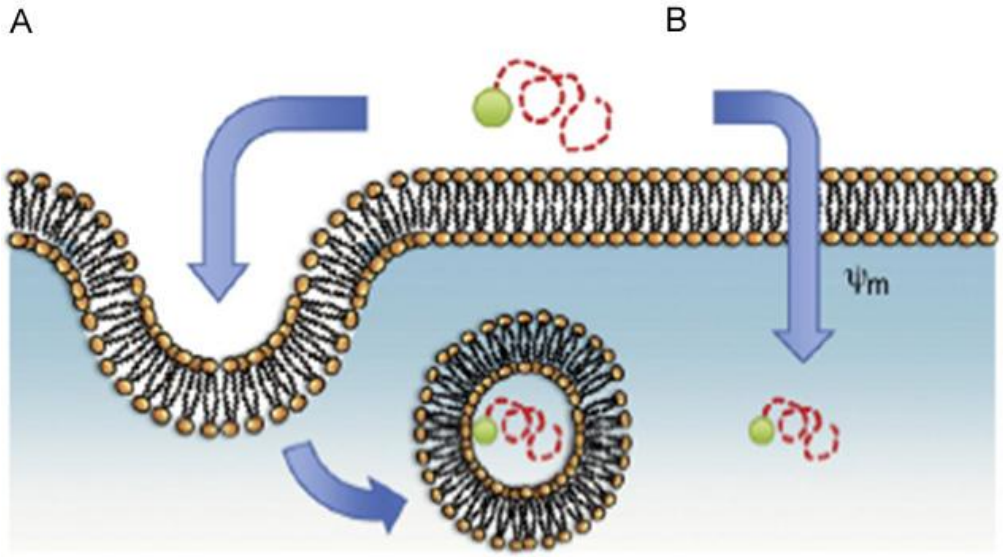

Figure 5.4 **Translocation mechanisms of CPP conjugates across the plasma membrane.** A – Internalization of CPPs via endocytotic mechanisms after interaction with negatively charged HSPGs at the membrane. B – Translocation of CPPs through direct diffusion in an energy independent manner that may be mediated by membrane potential. (Fonseca *et al.*, 2009)

Furthermore, an involvement of chiral receptors was excluded since both peptides independent of their D-amino acid composition or the retro-inverso peptides were internalized. Several biophysical studies indicate that Penetratin can cross lipid bilayers of artificial lipid vesicles, which confirms that receptors are not required for internalization (Joliot & Prochiantz, 2008; Prochiantz & Joliot, 2003). It is internalized independent of energy, at 4 °C and 37 °C, and can be found in the cytoplasm and the nucleus. Also the α-helical structure is not a prerequisite for the uptake. Current models of internalization involve peptide binding to the cell surface through charge interactions and membrane destabilization after W48 insertion in the bilayer. Destabilization might assist in the formation of inverted micelles, which would allow peptides to translocate across the membrane even at 4 °C (Figure 4.4). Micelles reopen inside the cell would than result in the release of the CPP-cargo construct into the cytoplasm (Joliot & Prochiantz, 2004; Prochiantz & Joliot, 2003). Based on this approach numerous cell penetrating peptides were developed commonly denoted as penetratin family. Up to now, a wide range of cargoes could be delivered into the cytoplasm and nucleus of various cultured cells and *in vivo* (Prochiantz, 2000).

5.8.7 Uptake of amphipathic peptides

Evidence for several routes of entry has been reported, some of which are independent of the endosomal pathway and involve the trans-membrane potential (Deshayes *et al.*, 2005; Rothbard *et al.*, 2004; Terrone *et al.*, 2003; Thoren *et al.*, 2003). To this group of CPPs belongs Transportan or the Model amphipathic peptide MAP. Amphipathic CPPs interact with

membrane lipids, mainly through their hydrophobic domains, and to form transient trans-membrane helical or β structures that temporarily affect membrane organization, thereby facilitating insertion into the membrane and initiation of the translocation process (Deshayes *et al.*, 2004a; Deshayes *et al.*, 2004b). The translocation of peptide that adopts an α-helical structure when in contact with membrane, as for instance MAP and, partly, Transportan, could be associated with pore formation (Zorko & Langel, 2005). The insertion of amphipathic peptides into the membrane forming a channel through oligomerization would not only allow efficient passage of hydrophilic cargoes, but would also be a threat to cell survival.

5.8.8 Delivered molecules

It exist two major strategies for the conjugation of cargoes to the carrier CPP. The first one is the covalent linkage of the molecule of interest to the CPP. This includes cloning and expression of a protein fused to the CPP and chemical crosslinking. The second way is described as the formation of a non-covalent complex. Up to now there are many examples for a successful delivery of covalently linked peptides or proteins into the cell. The risk with this strategy over lot of advantages is surely the possibility to alter the biological activity of the cargo (Morris *et al.*, 2008).

Several functional proteins and peptides were delivered using for example TAT, Penetratin or VP22. These include reporter proteins (GFP, β-galactosidase, Cre-recombinase) (Caron *et al.*, 2004; Schwarze *et al.*, 1999; Torchilin, 2007), cell cycle inhibitors or tumor suppressor proteins (p21, p53) (Snyder *et al.*, 2004), antigenic proteins (Ovalbumin) (Kim *et al.*, 1997; Shibagaki & Udey, 2002) and many more. CPPs can efficiently translocate a broad number of nanoparticles serving as diagnostic or therapeutic agents across the plasma membrane. Nanoparticles which were delivered inside the cells include dextran-coated MION (CLIO) particles (Lewin *et al.*, 2000), gold particles (Mandal *et al.*, 2009) and lipid-based nanoparticulates (liposomes or PEG-PE-based micelles), HPMA polymers, liposomes, adenovirus or paramagnetically labeled DOTA (Torchilin *et al.*, 2001; Tseng *et al.*, 2002).

Since CPPs are often cationic and are usually derived from DNA-binding domains of natural proteins, they have been also investigated as DNA delivery tools. Efficient delivery of oligonucleotides (ONs) such as small interfering RNAs (siRNAs), decoy-ONs and plasmids, and their analogues such as peptide nucleic acids (PNAs), locked nucleic acids (LNAs) and phosphorodiamidate morpholino oligomers (PMOs), is desired for controlling gene expression or silencing the activity of certain proteins (Mae & Langel, 2006). Nevertheless, one of the biggest problems of the antisense delivery strategies *in vivo* is the low stability of single-stranded DNA molecules. Due to the activity of DNA-directed nucleases (DNases)

these molecules are degraded within minutes in cellular plasma. Therefore, chemical modifications of the DNA backbone, such as 2' O-(2-methoxyethyl) (2' MOE), PNA, LNA or 2' fluoro, 2' methyl (2' OMe) are done to improve stability of the DNA (Mae & Langel, 2006).

5.8.9 Cell specificity

As mentioned above, CPPs have been successfully used to deliver a wide range of bioactive molecules such as proteins, peptides and nucleic acids in cultured cells. Furthermore, they were successfully applied for the delivery of therapeutic agents in many preclinical models of human diseases. The ability of CPPs to pass through the plasma membrane of very different cell types likely relies on a common mechanism of entry independent of a cell type specific receptor (see above). That could be an advantage for *in vitro* delivery systems where most of the time one cell type is present. However, it certainly presents a serious problem for *in vivo* drug delivery applications, because of the expected high loss of -most of the time- very expensive therapeutic drugs in untargeted tissues. Since the major drawback with CPPs is their inherent lack of cell type specific delivery the development of strategies to deliver macromolecules in a cell or tissue specific manner is gaining importance.

There are several attractive attempts to associate cell specificity to membrane permeable peptides. Several studies show an enhancement of cell directed delivery of therapeutic cargoes by fusing specific peptides (RGD, integrin receptor or NGRs), specific glycosides or antibodies to CPPs. The following section shall give some examples of the recent development of targeted CPPs.

One way to improved specificity is by incorporating novel targeting strategies, for example, homing peptides. The vasculature in tumors differs from that in normal tissue in morphology and in expression of molecular markers (Oh *et al.*, 2004; Ruoslahti, 2002). Laakonen describes the use of homing peptides, which utilize the molecular differences in the vasculature for specifically targeting a variety of organs as well as tumors. They screened phage-display libraries and discovered a number of homing peptides that selectively recognize those molecular markers on tumor blood vessels (Laakkonen *et al.*, 2002; Ruoslahti, 2000). This lead to the identification of tumor specific and cell internalizing properties. The F3 peptide is a 31 residue N-terminal peptide of the human mobility group protein 2 (HMGN2). It homes to blood vessels of all tumor types and is able to translocate to the nucleus of the target cell. The uptake mechanism was shown to be energy-independent and to rely on the cell surface receptor for F3, nucleolin. Another peptide, so called LYP-1, is limited to breast cancer. It does not only display cell type specificity and cell-penetrating properties, but also an anti-tumor activity by itself (Laakkonen *et al.*, 2002).

The group around Dowdy presented a multidomain approach to overcome the nonselective aspect of the TAT-mediated delivery system. In a wide variety of cancers, a number of cell-surface receptors, such as HER2 receptor in breast cancer, GnRH in ovarian carcinomas, and CXC chemokine receptor 4 (CXCR4) in multiple malignancies, are overexpressed. They linked a CXCR4 receptor ligand, DV3, to two transducible anticancer peptides, a p53-activating peptide (TATp53CV) and a cyclin-dependent kinase2 antagonist peptide (TAT-RxL). The treatment with targeted peptides resulted in an enhanced tumor killing compared to applied non-targeted peptides and may increase the therapeutic efficiency of CPPs (Snyder *et al.*, 2005).

Another possibility is to mask the membrane-interacting CPP sequence until the delivery system is in close proximity to the target cells. This very elegant new strategy for selectively delivering molecules to tumor cells was published by Jiang and colleagues (Jiang *et al.*, 2004). It was demonstrated that cellular association of polyarginine-based CPPs is effectively blocked when they are fused to an inhibitory domain made-up of negatively charged residues. These fusion peptides were called activatable CPPs (ACPPs) because cleavage of the linker between the polycationic and polyanionic domains, typically by a protease, releases the CPP portion and its attached cargo to bind to and enter cells. In normal tissues, the linker remains intact, whereas in tumor expressing appropriate proteases, the linker is cleaved allowing the CPP to accumulate in cells. In mice xenografts with human tumor cells secreting matrix metalloproteinases 2 and 9 (MMP-2, -9), ACPPs bearing a far-red-fluorescent cargo showed *in vivo* contrast ratios of 2–3 and a 3.1-fold increase in standard uptake value for tumors relative to normal tissue or control peptides with scrambled linkers. It was concluded that ACPPs offer a general strategy toward imaging and treating disease processes associated with linker-cleaving activities such as extracellular proteases (Jiang *et al.*, 2004).

Yet another very interesting approach was published by Yang (Yang *et al.*, 2008). In this study, the cell permeable capacity was used to load cells which possess tumor selectivity themselves. They used an enzyme-PTD complex of prodrug-activating enzymes, such as alkaline phosphatase (AP) and β-galactosidase, fused to PTD5 (RRQRRTSKLMKR) for loading interleukin-2-activated natural killer (A-NK) cells, tumor–seeking lymphocytes. These A-NK cells accumulate selectively at tumor sites and take their loaded cargo selectively to pulmonary metastases. They claimed a highly specific tumor targeting of the AP, since more than a fivefold higher concentration of AP was found in the tumor tissue compared to surrounding normal lung tissue at 24h after injection. Because the localizing capabilities of these tumor-seeking lymphocytes may also include infectious or inflammatory foci; they

hypothesized that PTD-transduced A-NK cells can also be used as carrier for the delivery of antimicrobial and anti-inflammatory compounds selectively to the site of infection.

Last to mention is the introduction of organelle-specific CPPs which can direct their cargo to specific sub-cellular organelles rather than to an explicit cell type. It was claimed that the benefit would be achieved if the cargo must be in particular location within the cell to function. The laboratory of Fonseca developed a CPP with additional mitochondria penetrating activity (MPPs) by introducing lipophilic residues (Fonseca *et al.*, 2009).

5.8.10 Medical and biological application

Taking into account the fast growing number of interesting publications concerning the medical or biological application of protein transduction the here mentioned applications can only represent a minor part of all possible treatments. Chosen examples are meant to give a small overview of recent therapies and potential application of CPPs, but they are certainly far from being complete.

CPPs in imaging and biosensing application

Nguyen et al published a method to visualize tumors during surgery using activatable cell penetrating peptides (ACPPs). The polycationic CPP is fluorescently labeled and coupled via a cleavable linker to a neutralizing peptide (see section 4.6.9). The authors provide evidence that fluorescent and gadolinium labeled ACPPs can be used for molecular navigation during complex surgical resection of large invasive tumors, thereby decreasing the amount of tumor left behind and increasing tumor-free survival as well as overall survival (Nguyen *et al.*, 2010).

Another strategy was described using Tat-conjugated quantum dots which were administered by a microcatheter intra-arterially and were found in the rats brain. The delivery of this quantum dots was so efficient that the visualization of the rat brain was possible with a low power UV lamp (Santra *et al.*, 2005).

Cancer therapy

CPPs have become useful tools for cancer therapies. These carriers have been employed in many innovative cancer applications to deliver both, pro-apoptotic proteins and chemotherapeutic drugs. In general, tumors are a result of an altered cell cycle leading to an increased cell proliferation. Consequently, peptides or proteins which have the ability to inhibit cell cycle progression or induce apoptosis are attractive conjugates of CPPs in cancer

therapies. Those cell cycle control proteins include for instance p21 or p27, as well as p53. (Snyder *et al.*, 2004). Tumor suppressor proteins, such as p53, arrest cell growth and induce apoptosis in response to cellular stress. Development of cancer often starts with mutations that inhibit tumor suppressor pathways. In line with this idea, the p53 protein is mutated or deleted in more than half of human tumors (Greenblatt *et al.*, 1994). For this reason, many cancer treatments are based on the restoration of the p53 function within abnormal growing cells. Wild-type p53 is effectively transported through the plasma membrane when fused to a CPP and inhibits the proliferation of human cancer cells once inside the cell. However, the transduced protein shows limited stability and is rapidly degraded in cells. Michiue et al presented a study using a degradation-resistant p53 protein fused to eleven arginines (R_{11}). They generated a mutant p53 in which several lysine residues in the C-terminal part of the protein were substituted by arginines. This mutant protein was resistant to ubiquitination and maintained its anti-tumor activity after transduction over a longer period of time (Michiue *et al.*, 2005).

A similar technique was presented by Snyder and colleagues. The C-terminal region of p53, namely the DNA-recognition site, binds specific DNA elements and triggers apoptosis. A structurally modified peptide (p53C') was synthesized, deriving from the region which induced programmed cell death by activating endogenous p53 and restoring function to proteins with DNA-binding mutations. Mice treated with the TATp53C' peptide showed significant tumor reduction and six times longer survival rates compared to the control mice (Snyder *et al.*, 2004).

A comparable approach was published by Senatus et al. using Antp as a carrier to deliver a C-terminal peptide of p53. Human and rat glioma cell lines containing endogenous mutant or wild-type p53 were induced into apoptosis after the exposure to p53p-Ant. But the peptide was nontoxic to proliferating non-malignant human and rat glial cell lines containing wild-type p53. It was concluded that p53p-Ant may serve as a new anticancer agents with unique selectivity for glioma cancer cells and that it can be successfully delivered *in vivo* into a brain tumor by a convection-enhanced delivery system which circumvents the blood-brain barrier (Senatus *et al.*, 2006).

Of course, many more proteins or peptides have been used to stop cell cycle progression in cancerous cells. Another strategy was demonstrated utilizing a novel TAT-based delivery system which can transport the therapeutic peptide, SAT3BP, in a target-specific manner. After internalization, SAT3BP inhibits STAT3 activation, thereby selectively inhibiting the growth of ErbB2-overexpressing breast cancer cells *in vitro* and *in vivo* (Tan *et al.*, 2006).

There are many more examples of excellent approaches in the field of cancer therapies using CPP delivery systems. They do not only concern delivery of full-length proteins, such

as tumor suppressor proteins or cell cycle regulators, much effort was directed to deliver oligonucleotides or oligopeptides. An additional therapeutic approach to the transport of functional proteins or peptides into the cell interior is the CPP-mediated delivery siRNAs. Short interfering RNAs (siRNAs) are used to inhibit translation of a specific target transcript without the need to extensively manipulate the cellular genome. Several siRNAs have been transported using Penetratin or TAT. Examples are caspase-3 siRNA or p38 MAPK (mitogen-activated protein kinase) (Davidson *et al.*, 2004; Moschos *et al.*, 2007).

Other therapies

In addition to cancer treatment, the protein transduction technology is also employed for protective therapies in neurodegenerative diseases, including brain ischemic injury or Parkinson's disease, using experimental animal models. The glial cell line-derived neurotrophic factor (GDNF) is a neuroprotectant. Kilic at al engineered a TAT-GDNF fusion which was intravenously injected in a mouse MCAO model and reduced the infarct volume and improved neuronal effects (Kilic *et al.*, 2003). Other anti-apoptotic proteins fused to TAT were injected in brain ischemia mice models for protective effects, such as the full-length BcL-x_L, the genetically engineered BcL-x_L, and the caspase inhibitor XIAP (Guegan *et al.*, 2006; Hotchkiss *et al.*, 2006; Kilic *et al.*, 2002). An additional application of CPPs has been demonstrated by its use in dendritic cell (DC) based cancer vaccines. TAT-mediated protein delivery showed potential as a therapeutic and prophylactic vaccine (Justesen *et al.*, 2007). Since exogenous proteins cannot enter the cytosol and access the MHC class I processing pathway, it is difficult to design a protein-based vaccine that induces class I – restricted cytotoxic T-lymphocyte (CTL) response. However, it has been shown that TAT-containing proteins cross cell membranes efficiently and accumulate in DCs at much lower extra-cellular protein concentrations compared to wild-type proteins which greatly reduces the cost for therapeutic protein production (Justesen *et al.*, 2007). After the fusion of a model antigenic protein, ovalbumin, to TAT, the conjugate was processed by antigen presenting cells, resulting in effective killing of the target cells by antigen-specific CTLs (Kim *et al.*, 1997; Shibagaki & Udey, 2002).

Another example for a successful vaccination was published by Justesen and colleagues. They had shown that recombinant TAT-p53 protein can be transduced into human monocytes-derived DCs and murine bone marrow-derived DCs. The ability of such p53-tranduced DCs to induce p53-specific immune response was determined by immunizing HLA-A*0201/Kb transgenic mice with these DCs. The authors demonstrated p53-specific CD4+ and CD8+ T-cell responses in the vaccinated mice (Justesen *et al.*, 2007).

It was also reported by Gavioli and colleagues that mice vaccinated with the HIV-1 Gag, Env, or V2-deleted Env antigens in combination with TAT show Th1-type and CTL responses

directed to a larger number of T cell epitopes, as compared to mice vaccinated with these proteins in absence of TAT (Gavioli *et al.*, 2008).

5.8.11 Clinical trials

Numerous preclinical and clinical trials of CPP-based delivery approaches are currently under evaluation. The first, CPP clinical trial was initiated a few years ago by Cell Gate Inc. for topical delivery of cyclosporine linked to polyarginine and entered phase II trials in 2003 (Rothbard *et al.*, 2004). Ever since, several companies are working on clinical development of CPPs for systemic administration of different therapeutic molecules. Avi Biopharma is working on the *in vivo* steric block splicing correction using 6-aminohexanoic acid spaced oligoarginine [(R-Ahx-R)4] (Lebleu *et al.*, 2008). Kai Pharmaceutical is currently evaluating a Tat-protein kinase C inhibitor peptide modulator of protein kinase C for acute myocardial infraction and cerebral ischaemia, which entered phase II in 2007 (Chen & Harrison, 2007). Other companies including Traversa Inc. and Panomics Inc. are currently evaluating CPPs in preclinical and clinical trials for TAT-based non-covalent siRNA delivery (TAT-RBD) or for secondary amphipathic peptide-based non-covalent delivery of siRNA, respectively (Heitz *et al.*, 2009).

5.8.12 Conclusions

The protein transduction technology has shown enormous potential to deliver a wide range of large molecules and small particles both *in vitro* and *in vivo*. A central task in the field of protein delivery remains the development of selective, efficient, safe, and easy-to-manufacture transduction vehicles. In this context, further biochemical and structural studies of the exact internalization pathways of each CPP together with its conjugates will be necessary. These studies are prerequisite to efficiently design carriers having structural specificity for target cells or tissues.

5.9 MDA-7/IL-24

The melanoma differentiation associated gene-7 (*mda-7*) was identified by subtraction hybridization from a human melanoma cell line (HO-1), induced to lose growth potential and terminally differentiate after treatment with IFN-β and mezerein (MEZ). Since the level of *mda-7* expression correlates with induction of irreversible growth arrest, cancer reversion, and terminal differentiation in human melanoma cells it was named melanoma differentiation associated gene-7 (*mda-7*). It is expressed at high levels in proliferating normal melanocytes and expression decreases progressively during the process of melanoma transformation and progression to metastatic disease. Therefore, it was suggested that this gene is associated with terminal differentiation of metastatic human melanoma cells (Jiang *et al.*, 1995).

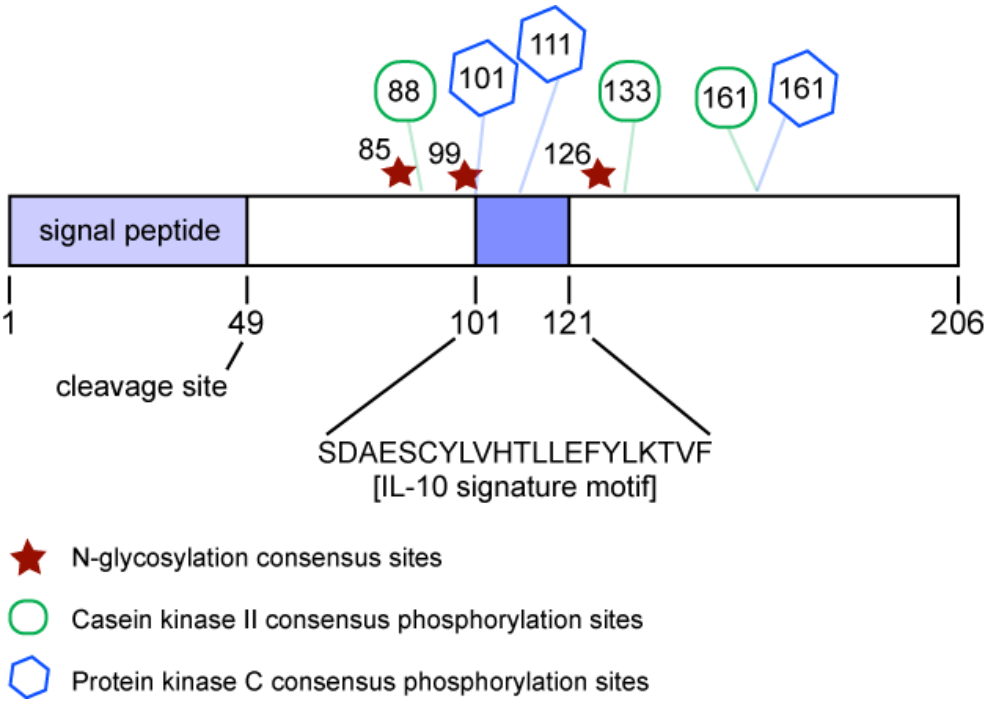

Figure 5.5 **Schematic presentation of the MDA-7/IL-24 protein showing various important protein motifs.** Drawing adapted from (Sauane *et al.*, 2003a).

5.9.1 Gene structure and expression

The *mda-7* cDNA encodes a novel and evolutionary conserved protein of 206 amino acids with a predicted molecular weight of 23.5 kDa. Analysis of the MDA-7 peptide sequence revealed few important features, comprising three N-glycosylation sites (amino acids 85, 99 and 126), six consensus phosphorylation sites (casein kinase II at 101,111 and 161; protein kinase C sites at 88,133 and 161) as well as an interleukin (IL)-10 signature motif at amino

acids 101-121 which is also shared by other members of the IL-10 family of cytokines (Figure 4.5) (Chaiken & Williams, 1996; Lebedeva *et al.*, 2007; Sauane *et al.*, 2003a). The N-terminal end consists of a consensus signal peptide with a proteolytic cleavage site at position 50. The cleaved and secreted product has a size of 18.3 kDa (Sauane *et al.*, 2003a).
IL-10 cytokines are secreted α-helical proteins and mediate their function through activation of the JAK/STAT signaling pathway. JAKs are represented by a family of four non-receptor tyrosine kinases, Jak1, Jak2, Jak3 and Tyr2 and the STATs by seven structurally and functionally-related proteins: Stat1α, Stat2, Stat3, Stat4, Stat5a and Stat5b. Selectivity of signaling is based at least partially on activation of specific JAK/STAT combinations by different cytokines (Pestka *et al.*, 2004).

Several features like its structure, sequence homology, translational regulation, murine and rat ortholog expression, and chromosomal location of *mda-7* suggest that it may be a member of the IL-10 family. It contains a predicted secretory motif of 49 residues, an IL-10 signature motif (Figure 4.5) and belongs to the four-helix bundle family of cytokine molecules. Furthermore, it was experimentally proven that the MDA-7/IL-24 protein is secreted and binds to two different heterodimeric receptor complexes from the class II cytokine receptor family: IL-20R1/IL-20R2 and IL-20R2/IL-22 resulting in the activation of STAT signaling pathways (Kreis *et al.*, 2007; Sauane *et al.*, 2003b). Therefore, *mda-7* has been classified as a member of the IL-10 family of cytokines that includes IL-10, IL-19, IL-20, IL-22 and IL-26, and has been renamed interleukin-24 or IL-24 (Chaiken & Williams, 1996; Sauane *et al.*, 2003a).

Physiological expression of the *mda-7/IL-24* gene occurs in a highly restricted manner in human cells with immunological function. These include normal unstimulated or LPS stimulated monocytes; anti-CD3 stimulated T-cells and normal human melanocytes (Caudell *et al.*, 2002; Huang *et al.*, 2001; Sauane *et al.*, 2003a). Analysis of a large collection of normal and cancer cell types demonstrate a lack of constitutive expression of *mda-7/IL-24,* with the exception of melanocytes. The analysis of *mda-7/IL-24* expression in normal tissues by Northern blots confirmed *mda-7/IL-24* expression restricted to tissues of the immune system, including spleen, thymus and peripheral blood mononuclear cells (PBMCs) derived from normal human tissues (Huang *et al.*, 2001; Lebedeva *et al.*, 2007). Secreted MDA-7/IL-24 stimulates monocytes and specific populations of T lymphocytes (Caudell *et al.*, 2002). It also promotes proinflammatory cytokine production (Sauane *et al.*, 2003a). Although normally restricted to specific cell types, *mda-7/IL-24* mRNA can be induced under appropriate conditions with IFN-β + MEZ in a spectrum of normal and tumor cells that are not of melanocytic or hematopoietic lineage (Sauane *et al.*, 2003a).

The constitutive or endogenous level of *mda-7/IL-24* is higher in normal melanocytes versus growth arrested and differentiation-induced human melanoma cells or metastatic human melanoma cells. The expression loss observed with melanoma progression raised the idea that *mda-7/IL-24* might display a tumor suppressive effect, particularly in a melanoma context (Jiang *et al.*, 1996; Lebedeva *et al.*, 2002; Lebedeva *et al.*, 2007; Sauane *et al.*, 2003a).

Indeed, when expressed at supraphysiological levels, for example through an adenovirus expression system or by transfection with cDNA, *mda-7/IL-24* induces growth suppression and programmed cell death (apoptosis) in a wide range of human cancers, including melanoma, glioblastoma multiforme, osteosarcoma and carcinomas of the breast, cervix, colon, lung, nasopharynx and prostate (Chada *et al.*, 2005; Gopalan *et al.*, 2005; Gupta *et al.*, 2006; Lebedeva *et al.*, 2003; Yacoub *et al.*, 2008b). In contrast, *mda-7/IL-24* has a negligible effect on growth and does not induce apoptosis in normal breast and prostate epithelial, melanocyte or skin and lung fibroblast cells (Gopalan *et al.*, 2005; Huang *et al.*, 2001; Jiang *et al.*, 1996; Saeki *et al.*, 2000; Sarkar *et al.*, 2002; Sauane *et al.*, 2003a). The inherent tumor-specific cytotoxicity of MDA-7/IL-24 could be confirmed by a wide range of *in vitro* and *in vivo* experiments in animal models containing human breast, lung and colorectal carcinomas, and glioma xenografts (Saeki *et al.*, 2002; Su *et al.*, 1998; Yacoub *et al.*, 2003).
Based on these unique properties, namely its antiangiogenic activity, its systemic immune activation, its ability to radiosensitize cancer cells and the “bystander antitumor effect” of MDA-7/IL-24*,* made the protein a promising new and widely applicable antitumor therapeutic molecule.

5.9.2 Mechanism of tumor cell-specific activity

The cancer selective properties and prospective application of MDA-7/IL-24 as novel therapeutic molecule inspired numerous scientific investigations. Although much research was spent on the underlying mechanisms of this tumor specific killing, it is still not fully understood why apoptosis is induced in cancer cells but not in normal cells. It is assumed that the cytokine exerts its antitumor activity in a spectrum of cancer cells via multiple cell type-dependent signaling pathways resulting in apoptosis. However, current experimental data revealed involvement of several proteins important for growth inhibition, including BCL-2 family members (Lebedeva *et al.*, 2003; Su *et al.*, 2006).
Apparently, MDA-7/IL-24 lethality is controlled by different pathways in different cell lines. Detailed studies in prostate cancer cells identified a reactive oxygen species (ROS) as an active component in MDA-7/IL-24-induced apoptosis and proofed that mitochondrial dysfunction and ROS production represent key components associated with prostate cancer killing (Lebedeva *et al.*, 2005; Sauane *et al.*, 2008). It was shown, that induction of apoptosis

after expression of MDA-7/IL-24 correlates with an up-regulation of the pro-apoptotic protein BAX in breast carcinoma and combination treated mutant K-*ras* pancreatic carcinoma cells. However, in human DU–145 human prostate cancer cells and in H1299 human lung carcinoma cells no changes in BAX levels were observed. These findings indicate that MDA-7/IL-24 can induce apoptosis in cancer cells in both, a BAX-dependent and a BAX-independent way (Saeki *et al.*, 2000; Sauane *et al.*, 2003a; Su *et al.*, 1998). Furthermore, transfection of *mda-7/IL-24* into a human prostate carcinoma cell line (DU-145) which contains a mutated *Rb* gene and human osteosarcoma cell (Saos2) that do not express *Rb* results in inhibition in colony formation. This indicates that growth inhibition by *mda-7/IL-24* is independent of a functional *Rb* gene (Jiang *et al.*, 1996). The laboratory of Paul Fisher has presented evidence that activation of the $p38^{MAPK}$ pathway followed by induction of the DNA damage-inducible (GADD) family of genes also plays a crucial role in Ad.*mda-7/IL-24*-mediated apoptosis in glioblastoma multiform, prostate cancer and melanoma cells (Sarkar *et al.*, 2002; Su *et al.*, 2003; Yacoub *et al.*, 2008b).

Moreover, an up-regulation of double-stranded RNA-dependent protein kinase (PKR) in Ad.*mda-7/IL-24* induced apoptosis was confirmed. After Ad.*mda-7/IL-24* infection activation of PKR leads to phosphorylation of downstream targets including eIF-2α, Tyk2, Stat1, and Stat3 even though the mechanism of activation of PKR by *mda-7/IL-24* is not clear (Pataer *et al.*, 2002). Other groups have reported that inhibition of phosphatidylinositol-3-kinase (PI3K) signaling promotes Ad.*mda-7/IL-24*-induced killing in breast and lung cancer cells (Chada *et al.*, 2005). Several studies documented that intracellular MDA-7/IL-24 localizes to the endoplasmic reticulum (ER) and induces ER stress response, also known as unfolded protein response (UPR), triggered by a temporal overexpression of recombinant *mda-7/IL-24* in the ER, which eventually promotes apoptosis of cancer cells (Sauane *et al.*, 2008).

In conclusion, multiple signal transduction pathways are induced by MDA-7/IL-24 including $p38^{MAPK}$, PKR and Stat3. But only $p38^{MAPK}$ and PKR appear to be necessary components for MDA-7/IL-24-mediated apoptosis since blocking the latter inhibits killing. The particular mechanism of cancer cell killing appears to follow one of several alternative proapoptotic pathways that are likely depending on the cell context. Proapoptotic molecules including *GADD* genes, TRAIL, caspase-3, -8 and -9 activation, Bid and PARP cleavage are all observed. Additionally, Ad.*mda-7/IL-24* -treated tumor cells show a more elevated G_2/M cell cycle arrest than control tumor cells or normal cells. Associated with the cell cycle arrest was the induction of apoptosis in Ad.*mda-7/IL-24* -infected tumor cells, as evidenced by the activation of caspase-3 and caspase-9 and cleavage of poly (ADP-ribose) polymerase (PARP) (Gopalan *et al.*, 2005; Lebedeva *et al.*, 2002; Saeki *et al.*, 2000).

5.9.3 Radiosensitization

It was documented that Ad.*mda-7/IL-24* enhances radiosensitivity independent of the p53, Fas, and BAX status in lung cancer cells (Sauane *et al.*, 2003a). Ad.*mda-7/IL-24* infection of glioma cells enhanced radiosensitivity in a cell cycle-independent manner via JNK signaling (Yacoub *et al.*, 2003). Additionally, treatment with a purified GST-MDA-7 fusion protein has also radiosensitive effects on malignant gliomas cells (Su *et al.*, 2003). Several studies in multiple tumor model systems, including malignant glioma and carcinoma of the lung, breast, prostate, and ovary confirmed the radiosensitizing ability of the *mda-7/IL-24* gene (Lebedeva *et al.*, 2007; Su *et al.*, 2006; Yacoub *et al.*, 2008c).

5.9.4 Angiogenesis

Angiogenesis facilitates metastasis of solid tumors and, when inhibited, has negative effects on tumor growth and spread. *In vivo,* tumors treated with Ad.*mda-7* demonstrated a reduced vascularization (Saeki *et al.*, 2002). This antiangiogenic activity was tested in several *in vitro* and *in vivo* studies. The antiangiogenic effect of Mda-7/IL-24 was also confirmed on human umbilical vein endothelial cells (HUVEC). Additional proof that MDA-7/IL-24 inhibits angiogenesis comes from experiments showing downregulation of vascular endothelial growth factor (VEGF) and transforming growth factor (TGF-β) (Saeki *et al.*, 2002). Therefore, it can be concluded that the anti-tumor activity of MDA-7/IL-24 is also partly mediated by inhibiting angiogenesis.

5.9.5 Involvement of receptors

The secreted MDA-7/IL-24 protein binds to IL-20 and IL-22 receptor complexes resulting in JAK/STAT activation. Since a treatment with tyrosine kinase inhibitor does not alter Ad.*mda-7/IL-24* -induced apoptosis, it is concluded that it is tyrosine kinase independent and can be distinguished from MDA-7/IL-24 cytokine function (Sauane *et al.*, 2003a; Su *et al.*, 2005). Ad.*mda-7* infection of different cell lines triggers several independent pathways which might not arise solely from its cytokine properties. However, since it was demonstrated that activation of the JAK/STAT pathway is negligible for Ad.*mda-7/IL-24*-induced apoptosis it is assumed that cell death occurs through a receptor-independent mechanism (Sauane *et al.*, 2003b).

5.9.6 Bystander effect

Adding another puzzling property of this cytokine it has been reported that infection, transfection or transduction of cells with full-length Mda-7/IL-24 leads to secretion of functional protein, which than elicits so-called “bystander” effect in surrounding cancer cells. Results indicate that MDA-7/IL-24 protein induces the bystander antitumor effect through an

ER stress mechanism mediated by strong activation of its own protein expression. Exogenous MDA-7/IL-24 protein induces growth inhibition and apoptosis only in cancer cells through a mechanism identical to Ad.*mda-7* infection (Sauane *et al.*, 2008).

5.9.7 Clinical trials

Ongoing research using an adenovirus expressing MDA-7/IL-24 (Ad.*mda-7/IL-24*) show an enhancement of the survival of animals implanted with GBM6 and GBM12 tumors (glioblastoma), and significant increase of survival benefit of irradiation in animals bearing GBM12 tumors (Yacoub *et al.*, 2008c). Furthermore, based on these exciting results, a phase I dose-escalation study using a replication-incompetent MDA-7/IL-24-expressing adenovirus (drug designation: INGN 241) in patients with advanced carcinoma was conducted by Introgen Therapeutics Inc. and the Baylor Sammons Cancer Center. This study demonstrated that intratumoral administration of Ad.*mda-7* (INGN 241) was safe with only mild toxicities observed (Mhashilkar *et al.*, 2001). Phase II-III clinical trials on melanomas or head and neck solid tumors and clinical trial I study in breast tumor indicate that the *in vitro* anti-tumor effects are recapitulated *in vivo,* when Ad.*mda*-7 is injected intratumorally (Introgen Therapeutics Inc., http://www.introgen.com).

In summary, Mda-7/IL-24 as an anti-cancer therapeutics has several obvious advantages over other candidate molecules. Beneficial properties include high tumor cell specificity, anti-angiogenic properties, ability to radiosensitize, as well as to cause growth-suppressive effects that are independent of p53, p16, Rb and BAX mutational status.

6 MATERIALS AND METHODS

6.1 Equipment and chemicals

Table 6.1 Frequently used equipment

product	company
Equipment	
Thermocycler	Eppendorf
Fluorescence Nikon Eclipse TE2000-E microscope	Nikon
Confocal microscope TCS-SP2	Leica Mannheim
FACScalibur	Becton Dickinson
MagneHis™ Protein Purification System	Promega
HisGraviTrap Purification Column	Amersham GE Healthcare
Enzymes	
Isis polymerase	Q-Biogene
Pfu polymerase	Promega
DNase I	Roche Diagnostics
Restriction endonucleases	Roche Diagnostics
Rapid DNA Ligation Kit	Roche Diagnostics
Kits	
QIAprep Spin Miniprep Kit	Qiagen
HiSpeed Plasmid Midi Kit	Qiagen
QIAquick Gel Extraction Kit	Qiagen
Cytotoxicity Detection Kit (LDH)	Roche Applied Science
β-galactosidase staining Kit	Sigma Aldrich
LightShift Chemiluminescent EMSA Kit	Pierce
Cell Compartmentation Kit	Pierce
Antibodies and dyes	
Anti-mouse Alexa-fluor 488	Molecular Probes
Anti-rabbit Alexa-fluor 456	Molecular Probes
DNA dye Hoechst 33342	Molecular Probes
Amino-Actinomycin D (7-AAD)	Sigma Aldrich
Peroxidase-labeled secondary Antibody anti-mouse	Amersham
Anti-GFP	Euromedex
Anti-His	Euromedex
Anti-EEA1	Calbiochem
Anti-Rab7	Cell Signaling Technology®
Anti-clathrin	Santa Cruz Biotechnology
Anti-cavoilin1	Santa Cruz Biotechnology

Peroxidase conjugated Anti-His	Sigma Aldrich
Apoptosis Sampler Kit	Cell signaling Technology®
Rabbit (cleaved) Caspase-3 Antibody	
Rabbit (cleaved) Caspase-7 Antibody	
Rabbit caspase-9 Antibody	
Anti-rabbit IgH, HRP-linked secondary Antibody (Goat)	

In general, all chemicals and drugs were purchased from Sigma Aldrich if not otherwise specifically stated.

6.2 Microorganisms

Table 6.2 List of bacterial strains

Name	Genotype
E. coli DH5α	*E. coli* B endA⁻I, hsdR17 (r_k, m^+k) , supE44,thi⁻I, recAl, gyrA96, relAl,Jθ80dlacZΔM15)
E. coli (DE3) BL21 (Novagen)	*E. coli* B F^- *ompT hsdS*$_B$ (r_B^- m_B^-) *gal dcm* (DE3)
E. coli BL21-CodonPlus (DE3)-RIPL (Stratagene)	*E. coli* B F^- *ompT hsdS* (rB^- mB^-) *dcm*$^+$ Tet^r *gal* λ(DE3) *endA* Hte [*argU proL* Cam^r] [*argU ileY leuW* Strep/Spec^r]
E. coli (DE3) Origami (Novagen)	*E. coli* B F-, *ompT, hsdSB* (rB-,mB-), *dcm*, (sr1-recA), 306::Tn10, gal

The *E. coli* strain DH5α was used for amplification of plasmid DNA. Because it is an endA⁻ strain it can be used for high quality plasmid DNA preparation.
BL21 strains are general protein expression strains that lack both the Lon and the ompT protease. The designation (DE3) indicates that the host is a lysogen of lDE3, and therefore carries a chromosomal copy of the T7 RNA polymerase gene under control of the *lacUV5* promoter and is therefore suitable for production of proteins from target genes cloned in pET vectors by induction with IPTG. The Origami™ strains are K-12 derivates that have mutations in both the thioredoxin reductase (*TrxB*) and glutathione reductase (*gor*) genes, which enhance disulfide bond formation in the cytoplasm.

6.3 Mammalian cells

Table 6.3 List of mammalian cells and the corresponding culture media

Cell line	Culture medium
C2C12	DMEM with 4,5 g/L glucose and 2 mM L-glutamine, 15 % FBS and 1 % Penicillin/Streptavidin
HCT116 p53+/+, p53-/-	Mc Coy's 5A Medium with 2 mM L-glutamine, 10 % FCS and 1 % Penicillin/Streptavidin
HeLa	DMEM with 4,5 g/L glucose and 2 mM L-glutamine, 10 % FBS and 1 % Penicillin/Streptavidin
MCF10A	F12 DMEM (containing bicarbonate, HEPES, 2 mM L-glutamine), 10 % FBS, 10 µg/ml insulin, 0.5 µg/ml hydrocortisone, 100 ng/ml cholera toxin, 20 ng/ml epidermal growth factor (EGF) and 1 % Penicillin/Streptavidin
MCF7	DMEM with 4,5 g/L glucose and 2 mM L-glutamine, 10 % FBS, 1 mM sodium pyruvate, 10 µg/ml insulin, 0.1 mM non-essential aa and 1 % Penicillin/Streptavidin
Saos2	Mc Coy's 5A Medium with 2 mM L-glutamine, 15 % FBS and 1 % Penicillin/Streptavidin
Raji	RPMI and 2 mM L-glutamine, 10 % FBS and 1 % Penicillin/ Streptavidine

All tissue culture media and supplementaries were purchase at Gibco.

6.4 Plasmids

Bacterial expression plasmids were obtained from Novagen EMDBiosciences. The pET15b vector carries an N-terminal His-Tag sequence, a *bla* coding sequence and a MCS with three cloning sites. The pET21b(+) carries an N-terminal T7-Tag sequence plus an optional C-terminal His-Tag as well as a *bla* coding sequence. The pET30b(+) vector provides an N-terminal His-Tag, a thrombin site, a S-Tag™ and enterokinase configuration plus an optional C-terminal His-Tag sequence together with a Kan coding sequence. All three plasmids supply a cloning and expression region of the coding strand which is transcribed by a T7 RNA polymerase. The included T7 promoter is inducible with IPTG.

Removal of the thrombin site from pET15b

In our lab we also utilize a modified version of the pET15b expression vector where the thrombin cleavage site is deleted (Figure 5.1). The two primers (Sense Primer Thrombin

deletion 5'-CATCATCATCATCATCACCATATGCTCGAGGATCCG-3', Antisense Primer Thrombin deletion 5'- CGGATCCTCGAGCATATGGTGATGATGATGATGATG -3') were used to remove the thrombin site by performing a mutagenesis reaction using the Quickchange Site-Directed Mutagenesis kit according to the manufacturer's instructions.

Figure 6.1 Removal of the thrombin site in the pET15b vector.

6.5 Primers

Table 6.4 List of primers

Name	Sequence 5' → 3'	Restriction site
	Construction of full-length ZEBRA	
ZebraXhoIfor	CCGCTCGAGATGATGGACCCAAACTCGAC	*Xho*I
ZebraBamHIrev	CGCGGATCCGAAATTTAAGAGATCCTCGTG	*Bam*HI
ZebraBamHIStoprev	CGCGGATCCTTAGAAATTTAAGAGATCCTCGTG	*Bam*HI
	Construction of truncated ZEBRA proteins	
ZebraAS1NdeIfor	GGAATTCCATATGGACCAAACTCGAC	*Nde*I
ZebraAS195BamHIrev	CGCGGATCCTTATTGCTTAAACTTGGCCCGGC	*Bam*HI
ZebraAS170BamHIrev	CGCGGATCCTTATTCCTCCAGCGATTCTGGC	*Bam*HI
ZebraAS140BamHIrev	CGCGGATCCTTACTGTTGTCCTTGGTTAGCCC	*Bam*HI
ZebraAS170NdeIfor	GGAATTCCATATGCAGCTAGCAGACATTGGTGTTCC	*Nde*I
ZebraAS195NdeIfor	GGAATTCCATATGCAACTGCTGCAGCACTACC	*Nde*I
ZebraBamHIStoprev	CGCGGATCCTTAGAAATTTAAGAGATCCTCGTG	*Bam*HI
ZebraAS50NdeIfor	GGAATTCCATATGCCGGTGCTGCCAGAGCC	*Nde*I
ZebraAS100NdeIfor	GGAATTCCATATGGACATAACCCAGAATCAACAG	*Nde*I
ZebraAS50XhoIrev	CCGCTCGAGCGGCCACAGCACACAAGG	*Xho*I
ZebraAS100XhoIrev	CCGCTCGAGTATGTCGGAGACTGGGAACAG	*Xho*I
ZebraAS140XhoIrev	CCGCTCGAGCTGTTGTCCTTGGTTAGCCC	*Xho*I

ZebraAS245XhoIrev	CCGCTCGAGGAAATTTAAGAGATCCTCGTG	*Xho*I
ZebraAS195XhoIrev	CCGCTCGAGTTGCTTAAACTTGGCCCGGC	*Xho*I
ZebraAS140XhoIrev	CCGCTCGAGCTGTTGTCCTTGGTTAGCCC	*Xho*I
ZebraAS140NdeIfor	GGAATTCCATATGCAGCTAGCAGACATTGGTGTTCC	*Nde*I
ZebraAS195NdeIfor	GGAATTCCATATGCAACTGCTGCAGCACTACC	*Nde*I
ZebraAS170NdeIfor	GGAATTCCATATGGAGGAATGCGATTCTGAACTAG	*Nde*I
ZebraAS220XhoIrev	CCGCTCGAGGCACATCTGCTTCAACAGG	*Xho*I
ZebraAS100XhoIrev	CCGCTCGAGTATGTCGGAGACTGGGAACAG	*Xho*I
ZebraAS175NdeIfor	GGAATTCCATATGAAGCGATACAAGAATCGGGTGGC	*Nde*I
	GFP fusion	
GFPNdeIfor	GGA ATTCCATATGGTGAGCAAGGGCGAGGA	*Nde*I
GFPXhoIrev	CCGCTCGAGCTTGTACAGCTCG	*Xho*I
GFPXhoIfor	CCGCTCGAGATGGTGAGCAAGGGCGAG	*Xho*I
GFPBamHIrev	CGCGGATCCCTTGTACAGCTCGTCCATGC	*Bam*HI
	LacZ fusion	
lacZXhoIfor	CCGCTCGAGATGATTACGGATTCACTGGCCGTC GTTTTACAACGTCG	*Xho*I
LacZBamHIrev	CGCGGATCCTTTTTGACACCAGACCAACTGG	*Bam*HI
	MDA7 /IL-24 fusion	
Mda7 N (D1)	TAACGCCTCGAGAATTTTCAACAGAGGCTGCAAAG	*Xho*I
Mda7 N (R1)	ATTCTTATGGATCCTTAGAGCTTGTAGATTTTTGCATCC	*Bam*HI
MDA7AS51XhoIfor	CCGCTCGAGGGCCAAGAATTCCACTTTGG	*Xho*I
	eIF3 fusion	
eIF3-N (D1)	TAACGCCTCGAGGCCACACCGGCGGTACCAGTAAGTGC TCCTCCG	*Xho*I
eIF3-N (R1)	ATTCTTATGGATCCTTACAGGTTTACAAGTTTTTCATTG	*Bam*HI
	Sequencing primer	
LacZ-1 for	GGCGTTTCATCTGTGGTGC	
lacZ-2 for	CTGTGGTACACGCTGTGCG	

lacZ rev	CTGTGGTACACGCTGTGCG
	Oligos for hybridization of AP1-probe
AP1-probe	AGCACTGACTCATGAAGT
AP1-probe	TACTTCATGAGTCAGTGCT

Indicated endonuclease restriction sites are underlined.

Detailed descriptions and protocols including cloning, expression and purification of ZEBRA fusion proteins were published at Current Protocols of Protein Science (Rothe & Lenormand, 2008).

6.6 Molecular biology

6.6.1 PCR

For the construction of truncated coding sequences of ZEBRA and all DNA sequences encoding for EGFP, β-galactosidase, MDA7, respectively, specific sense and antisense PCR primers that contains 15-25 nucleotides homologous to the ZEBRA gene and additional nucleotides including the appropriate restriction sites as described in Table 5.4 were designed. They were used for the amplification of DNA sequences using PCR (polymerase chain reaction).
For the PCR reaction the following components were mixed in a final volume of 50 µl:

Components	**Final Concentration**
10× PCR buffer	1×
dNTPs (10 mM)	0.2 mM
Sense primer (100 pM)	1 pM
Antisense primer (100 pM)	1 pM
Template DNA	20 – 100 ng
25 mM $MgCl_2$	1.5 – 3 mM
DNA polymerase	2 units
ddH_2O	sufficient for a final reaction volume of 50 µl

To amplify the DNA sequences by PCR a proofreading DNA polymerase (such as *PfuUltra*™ High-Fidelity DNA Polymerase or Isis Proofreading DNA Polymerase) and the reaction conditions as described below were used:

1 cycle	3 min	95 °C	(initial denaturation)
30 cycles	30 sec	95 °C	(denaturation)
	60 sec	x °C [(1)]	(annealing)
	x sec[(2)]	72 °C	(extension)
1 cycle	5 min	72 °C	(final extension)

[(1)] The optimal annealing temperatures depend on the primers used in the reaction and generally will be 5 °C below the melting temperature (T_m = (A+T) x 2 + (G+T) x 4) of the primers.

[(2)] The extension time will depend on the length of the PCR product (1 min for every 1000 nucleotides).

6.6.2 Electrophoresis

Agarose gel electrophoresis was employed to check the progression of a restriction enzyme digestion, to quickly determine the yield and purity of a DNA isolation or PCR reaction, and to size fractionate DNA molecules, which then could be eluted from the gel. Prior to gel casting, agarose was dissolved in 0.5 x TAE buffer by heating and the warm gel solution then was poured into a mold. The percentage of agarose varied from 0.7 % to 2 % depending on the expected size of the fragment. To estimate the size of DNA fragments a DNA ladder (MassRuler, 1 µl corresponds to 103 ng DNA, Fermentas). DNA fragments were separated in 0.5 x TAE buffer and at 100 V. The agarose gel was stained with 1 µg/ml ethidium bromide and visualized under UV light.

6.6.3 Purification of DNA fragments

The PCR- or restriction reaction was mixed with an appropriate volume of 5× loading buffer and loaded on 0.8 – 2 % agarose gel, electrophoresed and stained with 1 µg/ml ethidium bromide. The band of interest was excised and purified by gel extraction using the QIAquick Gel Extraction kit (Qiagen) according to the manufacturer's instructions.

6.6.4 Restriction of DNA fragments

1 µg DNA was digested with 2 U of each restriction enzyme. Restriction enzymes and DNA were diluted in the respective reaction buffer and incubated at 37 °C for 2 h.

6.6.5 Ligation

The concentration of insert and plasmid DNA was estimated by agarose gel electrophoresis. A DNA ladder was loaded on same gel to compare the amount of DNA, e.g. MassRuler^{TM} (Fermentas, 1 µl corresponds to 103 ng DNA). The linearized vector and insert DNA were mixed in molecular ratio of 1 : 3. The ligation reaction was performed for 5 min at room temperature using the Rapid Ligation Kit according to manufacturer's protocol (Roche Applied Science). The ligation reaction mixture was used directly for the transformation of competent *E. coli* cells or was stored at -20 °C.

6.6.6 Transformation of plasmid DNA into *E. coli*

20 µl aliquots of ultracompetent *E. coli* DH5α, (DE3) BL21, (DE3) Origami or BL21-CodonPlus (DE3)-RIPL, respectively, cells were thawn on ice for 5 min. The bacterial cell suspension was mixed either with 1/10 volume of ligation mix or 0.5 µl of plasmid DNA, equaling approximately 1-10 ng of circular plasmid DNA. After a heat shock of 45 sec at 42 °C, cells were placed on ice for 2 min. 100 µl of SOC medium (Novagen) was added and cells were incubated with shaking at 37 °C for 1 h. Finally, 60 µl of cell suspension was plated on LB-agar plates supplemented with appropriate antibiotics incubated at 37 °C overnight for plasmid selection.

Concentration of antibiotics:	LB - ampicillin:	100 µg/ml
	(1000x dilution of stock solution 100 mg/ml)	
	LB - kanamycin:	10 µg/ml
	(1000x dilution of stock solution 10 mg/ml)	

6.6.7 Plasmid DNA preparation

Single colonies were selected from LB-agar antibiotics plates and inoculated individually into 2 ml of LB-antibiotic medium and incubated overnight on a shaker at 37 °C. Plasmid DNA was isolated using QIAprep Spin Miniprep Kit (Qiagen) from *E. coli* DH5α culture according to manufacturer's instructions. For a large scale plasmid preparation, 200 ml of LB-antibiotic medium were inoculated with 1/1000 of a 2 ml *E. coli* DH5α preculture and incubated at 37 °C under constant shaking overnight. Plasmid DNA was isolated using HiSpeed Plasmid Midi Kit (Qiagen) according to manufacturer's instructions.

6.7 Protein Biochemistry

6.7.1 Protein expression

E. coli BL21 (DE3), Origami (DE3), or BL21- CodonPlus (DE3)-RIPL competent cells, depending of the codon content of the gene of interest, were transformed by a heat-shock method with a bacterial expression vector pET15b containing the ZEBRA fusion constructs. Bacteria were plated out on LB-agar plates supplemented with ampicillin and incubated overnight at 37 °C. The day after, 3 ml Luria broth (LB) medium containing 100 µg/ml ampicillin were inoculated with a single colony and shaken at 37 °C overnight to obtain a bacterial preculture. 3 ml of LB-ampicillin were inoculated with 1/10 volume of the overnight preculture. At an OD_{600} of 0.6, bacteria were induced by adding 0.2 mM - 1 mM IPTG and incubate for 2 h at 37 °C, 15 h at 25 °C or 15 h at 16 °C.

6.7.2 Solubility Assays

A 2 ml bacterial culture (*E. coli* BL21 (DE3), BL21- CodonPlus (DE3)-RIPL or Origami) was pellet by centrifuging for 5 min at 10,000 x g at 4 °C. The supernatant was removed, the pellet washed in 500 µl lysis/ binding buffer (without protease inhibitors) and centrifuged again. After removal of the supernatant and a resuspention of the pellet in 500 µl of 25 mM Tris-HCl, pH 7 to 8, 250 mM NaCl, 5 % glycerol supplemented with a complete protease inhibitor cocktail tablet. The cells were lysed by sonicating the suspension (3 × 15 sec) using a microtip probe Sonicator (Branson sonic power) on ice. The resulting solution was centrifuged 30 min at 13,000 x g at 4 °C. The resultant supernatant represents the soluble protein fraction. The pellet was resuspended in 500 µl of 20 mM Tris-HCl, pH 7 or 8, 50 mM NaCl, 6 M urea and placed on an end-over-end incubator and leaved to dissolve for 16 h at 4 °C and clarified by centrifugation of 30 min at 13,000 x g, 4 °C. This supernatant represents the insoluble protein fraction or soluble fraction in urea. Alternatively the insoluble pellet was directly resuspended in 500 µl of 1x SDS loading buffer. 5 µl of each fraction, as well as a sample of the uninduced fraction, were analyzed by SDS-PAGE. The uninduced fractions was obtained by centrifuging 5 min at 10,000 x g, 4 °C, the pellet was resuspended in 1x SDS loading buffer, and heated for 5 min at 95 °C. A syringe was used to resuspend the pellet by flushing up and down several times to break the chromosomal DNA. A second step of denaturation by heating 5 min at 95 °C followed. The SDS page was either stained by Coomassie blue to estimate the expression of the produced protein or transferred to a nitrocellulose membrane and probed with Anti-histidine antibody.

6.7.3 Protein purification using affinity chromatography

In general, soluble ZEBRA minimal transduction domain fusion proteins were purified by affinity chromatography using batch or gravity-flow purification methods. All the purification steps were performed at 4 °C in the presence of protease inhibitors, such as complete protease inhibitor cocktail tablets, pepstatin, E-64, aprotinin, and pefabloc (Roche Applied Science) to avoid protein degradation. To test the purification conditions, purification tests were performed using MagnaHis^{TM} purification beads in batch mode.

6.7.4 Small scale purification using the MagnaHis^{TM} purification system

The bacterial pellet from a 3 ml overnight expression culture was resuspended in 500 µl of ice-cold lysis/binding buffer. For cell lysis, bacterial cells were sonicated three times, each time for 15 sec on ice. The suspension was clarified by centrifuging 30 min at 13,000 × g, 4 °C. During the centrifugation step, 60 µl of MagnaHis^{TM} beads were washed three times with 200 µl of the ice-cold lysis/binding buffer by using the magnetic stand (Promega) to remove the buffer between each washing step. After removing the last wash the clarified supernatant of the lysed bacteria was added to the beads. An incubation of the supernatant beads mixture for at least 30 min or up to 4 h at 4 °C on an end-over-end rotator followed. The solution was separated from the beads by inserting the microcentrifuge tube into the magnetic stand and kept on ice since it represents the flow through. The beads were washed four times with the ice-cold washing buffer by increasing the imidazole concentration of the washing buffer stepwise from 10 mM to 60 mM. Each wash fraction was kept separately on ice for SDS page analysis. Elution of the recombinant protein from the beads was carried out by adding 100 µl of elution buffer each time with an increasing concentration of imidazole (100, 250, 500 and 1000 mM). All fractions were analyzed by SDS-PAGE by loading between 5 and 20 µl of each fraction including the total lysate, followed Coomassie blue staining and immunoblotting using an anti-histidine antibody (Sigma).

6.7.5 Large scale purification using HisGraviTrap columns

The pellet from a 1 l bacterial culture was resuspended the in 20 ml prechilled lysis/binding buffer and sonicated 5 × 25 sec on ice/ethanol to lyse the cells. The cell lysate was treated with 25 µg/ml DNase I at 4 °C for 15 min to remove nucleic acids. Soluble protein fraction was clarified by centrifuging for 30 min at 13,000 × g, 4 °C. Before adding the supernatant to the HisGraviTrap column (Amersham GE Healthcare), it was equilibrated with 5 ml of ice-cold lysis/binding buffer containing protease inhibitors. All fractions passing the column were recovered to check for the protein content. The column was washed with an increasing concentration of imidazole (from 10 to 60 mM) and NaCl (from 0.5 to 1.5 M), each time with 10 ml of ice-cold washing buffer. The elution of the fusion protein started by adding 1 ml of

prechilled elution buffer containing 100 mM imidazole and was continued by a stepwise increase of the imidazole content from 150 mM, 250 mM, 500 mM to 1 M imidazole in 500 µl aliquots of elution buffer. All the fractions containing the eluted protein samples were stored at −80 °C after analysis by SDS-PAGE with Coomassie blue staining and immunoblotting.

6.7.6 SDS page

5x SDS loading buffer containing DTT as reducing agent was added to protein samples (purified proteins, total cell lysate) and heated to 95 °C for 5 min. Samples were loaded onto SDS PAGE with varying contains of acrylamid (7 – 15 %) according to the protein size. A prestained molecular weight marker (PageRuler™ Prestained Protein Ladder, Euromedex) was loaded to determine molecular weights. Separation of proteins was done by 120 V for 90 min.

6.7.7 Coomassie Blue staining

SDS page was boiled three times in ddH_2O for 60 sec in a microwave and then incubated for 10 min with PageBlue™ Protein Staining Solution (Euromedex). The protein gel was washed with ddH_2O until it was completely destained.

6.7.8 Western Immunoblotting

After electrophoresis proteins were electrically transferred to a nitrocellulose membrane (0.22 µm or 0.45 µm, Biorad) using a semi-dry method for one hour at 0.8 mA/cm^2 gel (~50 mA/gel). For verification of an efficient electrotransfer, the membrane was stained with a Ponceau Red solution for three minutes at RT. Nitrocellulose membranes were washed with Tris-buffered saline (TBS) with 0,1 % Tween-20 and then blocked in 1x TTBS with 5 % w/v nonfat dry milk for 1 h at RT. After three washing steps for five minutes each with 1x TTBS, the membrane was incubated with the primary antibody at the appropriate dilution in blocking solution for one hour at RT or overnight at 4 °C with gentle agitation. After three times washing with 1x TTBS and incubation with HRP-conjugated secondary antibody in 1x TTBS for one hour at RT and gentle agitation, the membrane was washed again. Proteins were detected using the ECL Western Blotting detection reagent (Amersham, GE Healthcare) and exposed to Hyperfilm ECL (Amersham, GE Healthcare) for appropriated time and developed in a dark room with (Developing and Fixation solution from Sigma).

6.7.9 Labeling of ZEBRA minimal domain fusion proteins

To remove the imidazole and glycerol, the purified fusion protein was dialyzed against 1000 × volume of sterile phosphate-buffered saline (PBS) at 4 °C for 3 h using a Slide-A-Lyzer Dialysis Cassette (Pierce, MWCO of 2 to 20 kDa). Followed by a concentration of the

desalted protein solution to ~1 mg/ml using centrifugation concentration columns (Amicon). Protein concentration was estimated by loading the sample together with a BSA standard ranging a concentration of 30 to 1000 µg/ml on a SDS Page. 100 µg of pure recombinant protein at a concentration of 1 mg/ml was used for the labeling reaction. The dye/protein molar ratio relative to the molecular weight of the fusion protein was calculated and the labeling reaction was performed according to manufacturer's protocol (Molecular Probes, Invitrogen). The labeled protein was purified from the free/unreacted dye using the provided spin column. Estimation of the degree of protein labeling was done spectrophotometrically and verified by flow cytometry.

6.7.10 Electrophoretic mobility shift assay (EMSA)

DNA binding reactions were performed for all purified recombinant proteins. The AP-1 probe was made by annealing two oligonucleotides (5'-AGCACTGACTCATGAAGT-3' and 5'-TACTTCATGAGTCAGTGCT-3'). The AP-1 oligonucleotides were denatured at 95 °C for 5 min, then annealed by cooling the reaction in successive steps, 10 min at 55 °C, 30 min at 37 °C and 1 h at room temperature. The labeling of the annealed AP-1 probe with biotin was done by mixing the AP-1 probe with biotin dUTPs, Klenow buffer, H_2O and 5 units of Klenow polymerase. The following program was chosen in a thermocycler:

1 cycle	1 h	37 °C
1 cycle	10 min	85 °C
1 cycle	10 min	55 °C
1 cycle	1 h	RT

The biotin-labeled AP-1 probe was purified over a Microspin G-25 spin column (Active Motif). Up to 500 µg full-length ZEBRA and truncated proteins were preincubated with 4 x Binding buffer B-1, 2x Stabilizing buffer (Pierce) and 1 mM DTT for 15 min on ice. The Biotin-labeled probe was mixed with 4x Binding buffer C-1, 2x Stabilizing buffer (Pierce), supplemented with 50 ng/µl poly(dI-dC) (Pierce) and added to protein-containing solution. After an incubation of the reaction mix for 15 min at 4 °C, a non-denaturating sample buffer was added and samples were loaded on a 4-8 % nondenaturating polyacrylamid gel. The samples were electrophoresed in 0.5 x TBE at 160 V for ~90 min and transferred to a Hybond N+ membrane (Amersham GE Healthcare) using a semi-dry transfer unit for 15 min at 100 V. The membrane was placed on Saran wrap and the DNA was fixed under UV for 5 min in a Stratalinker UV Crosslinker (Stratagene). The membrane can be stored at -20 °C for 1 – 2 weeks. The LightShift Chemiluminescent EMSA Kit (Pierce) was used for the detection according to kit manufacturer's instruction.

6.8 Cell Biology

6.8.1 Cultivation Condition

Mammalian cells were maintained in indicated media at 37 °C and 5 % CO_2 in a humidified atmosphere. When reaching approximately 70 % confluency, cells were passaged with an seeding density of about 0.7 x 10^6 cells/T-25 flask, 2.1 x 10^6 cells/T-75 and 4.6 x 10^6 cells/ T-150 cell culture flask.

6.8.2 Transduction experiments

7.5 x 10^5 cells/well were seeded on a 12-well plate 24 h before all transduction experiments. For microscopic analysis, 2.5 x 10^5 cells were plated on 4-well chamber slides at least 24 h before treatment. Internalization experiments were performed at 60-80 % confluency. Cells were rinsed twice with PBS before addition of fresh serum-free culture medium containing indicated amounts of ZEBRA proteins. At a maximum of 4 h culture medium was supplemented with 10 % heat-inactivated fetal bovine serum (Gibco) for long term incubation.

6.8.3 Drug treatment

HeLa and Saos2 cells were incubated for 30 min prior to Z10-EGFP fusion protein addition in serum-free media containing the indicated concentration of individual drugs (20 µg/ml heparin, 100 nM wortmannin, 50 µg/ml nystatin, 30 µM chlorpromazine hydrochloride and 5-10 mM methyl-β-cyclodextrin [MβCD]). For depletion of the cellular ATP pool, cells were preincubated for 30 min in PBS containing 6 mM 2-deoxy-D-glucose and 10 mM sodium azide. Subsequently, cells were incubated for 3 h in the presence of inhibitors and proteins at 37 °C or 4 °C, and trypsinized (0.5 % trypsin-EDTA, Gibco) to remove surface bound protein before analyzing fluorescence by flow cytometry.

6.8.4 Immunocytochemistry

For immunolocalization studies, cells were washed twice for 5 min with Heparin (20 µg/ml) in PBS and fixed for 10 min in 4 % PFA in PBS at RT. Cells were permeabilized and blocked with 0.25 % Tween X-100, 5 % BSA in PBS at RT for 1 h. Followed by an incubation at RT in blocking solution (0,1 % Tween X-100, 5 % BSA in PBS) for 1 h with the indicated primary antibodies. To detect endogenous endosomal proteins, an Anti-EEA1 (4 µg/ml), an Anti-Rab7 (5 µg/ml), an Anti-clathrin and an Anti-caveloelin1 (5 µg/ml) were applied. The fusion proteins ZEBRA-EGFP were detected using Anti-GFP. After three washes in PBS for 10 minutes cells were incubated with the corresponding secondary antibodies Anti-mouse Alexa Fluor® 555 and Anti-rabbit Alexa Fluor® 647 in blocking solution. Cells were washed 4 times

for 10 minutes with PBS and nuclei were counterstained with Hoechst 33258 (0.5 µg/ml in PBS, Sigma). Slides were mounted with ProLong Gold antifade reagent (Molecular Probes), covered with a cover slip and stored at the dark until analysis. Confocal microscopy was done at the iRTSV-TS - U873 INSERM, CEA-Grenoble CEA Grenoble by Didier Grunwald. Images were taken on a confocal microscope TCS-SP2 (Leica Mannheim, Germany). Cellular fluorescence on non-fixed cells was visualized using the an inverted fluorescence Nikon Eclipse TE2000-E microscope (Nikon) with a GFP (465- to 495 nm excitation and 515- to 555 nm emission) filter.

6.8.5 β-galactosidase staining

After transduction experiments cells were washed with PBS and 20 µg/ml Heparin for cell surface bound protein removal. Fixation and staining was done according to the β-galactosidase staining kit protocol (Sigma). Briefly, cells were incubated with 1 x Fixation solution containing 2 % formaldehyde and 0.2 % glutaraldehyde at RT for 10 min. After three washing steps with PBS cells were stained with a solution containing magnesium chloride (20 mM), potassium ferricyanide (40 mM), potassium ferrocyanide (40 mM) and 2 mg/ml of X-gal for 3 h at 37°C. Images were taken with a Nikon Eclipse TE2000-E.

6.8.6 Flow cytometry analysis

Flow cytometric analyses were used to measure the internalization of EGFP fusion proteins. To do so, cells were treated with 0.5 x trypsin/EDTA (Gibco) for 5 min to remove surface bound peptides and washed twice with 1 ml PBS before analyzing green fluorescence. At least 10.000 cells were counted and gated on live cells by FSC/SSC and 7-AAD (1 mg/ml Sigma) exclusion.

For cell cycle analysis, cells were collected by trypsinization and washed twice in PBS. Cells were fixed with 70 % ice cold ethanol, for one hour at -20 °C, and treated for 30 min with RNase A (60 U/ml) in a 0.1 % Triton X-100 and propidium iodide (40 µg/ml) solution. Flow cytometric analysis was carried out with a fluorescence-activated cell sorting (FACScalibur, Becton Dickinson).

6.8.7 LDH (lactate dehydrogenase) leakage assay

Lactate dehydrogenase (LDH) is an enzyme that exits in the cytosol of eukaryotic cells; it can be detected in the cell culture medium after the disruption of cell membranes. Membrane integrity was measured using the Cytotoxicity Detection Kit (LDH) from Roche Applied Science. In brief, 1x 10^4 HeLa or Saos2 cells were seeded in 96-well plates 24 h one day before treatment with ZEBRA fusion proteins at indicated concentrations in serum-free medium. After 24 h, LDH assay was carried out according to manufactures protocol.

Absorbance was measured at 560/590 nm. Untreated cells were defined as no leakage and 100 % leakage was defined as total LDH release by lysing cells in 2 % Triton X-100 in serum-free medium.

6.9 Mice experimentation

6 weeks old female C57BL/6 mice were injected intraperitonal (i.p.) or intravenous (i.v.) (via the tail vein) with 50 - 200 µg of ZEBRA-Z10-EGFP, Z10-β-galactosidase or the reporter proteins, such as EGFP and β-galactosidase, alone. Prior to organ harvesting, each mouse was anesthetized with 100 µl of a ketamine-xylazine mix (3 ml of 100 mg/ml ketamine, 1 ml of 20 mg/ml xylazine and 6 ml PBS) and perfused through the right heart chamber with freshly prepared and filtered (0.22 µm filter) 5 U/ml Heparin in PBS. Tissues were harvest after 3h of treatment and a single cell suspension was made using a Cell Strainer (Falcon). Cells were washed with PBS and red blood cells were lysed by incubation in 1 ml of Red blood cell lysis buffer (155 mM NH_4Cl, 10 mM $KHCO_3$, 0.1 mM EGTA, pH 7.4) for 7 min on ice. Each live cell suspension was diluted 1 : 4 in PBS and washed twice with ice-cold PBS. In case of Z10-EGFP injection, cells were analyzed by FACS after an incubation with 7-AAD for dead cell exclusion. After injection of Z10-β-galactosidase single cell suspension was stained using the β-galactosidase staining kit protocol (Sigma) as above described. For *ex vivo* studies, indicated tissues were harvest from untreated mice as above described. Cell suspension was resuspended in RPMI culture medium supplemented with 10 % FCS. 5 µg of Z10-EGFP or Z10-β-galactosidase, respectively, were added to the culture and cells were incubated for 3 h at 37 °C and 5 % CO_2 in a humidified atmosphere. Internalization was evaluated either by FACS or by microscopy after β-galactosidase staining.

6.9.1 Non-invasive optical imaging in mice

The proteins Z10-EGFP and EGFP were labeled with the near infra-red Alexa Fluor® 647(CY5) fluorochrome according to manufactures protocol. Both proteins were used for non-invasive imaging in animals. Accurate labeling was checked by FACS analysis in HeLa cells prior to the mouse experiment. The whole body optical imaging was conducted at the Institute Albert Bonniot, La Tronche, France. Female Swiss nude mice, at 6–8 weeks of age were used and maintained under specific pathogen-free conditions. The mice received intravenous (i.v.) injection of 50 µg Cy5-labeled Z10-EGFP or EGFP for each mouse. Fluorescence reflectance imaging was performed using a Hamamatsu optical imaging system described at (Jin *et al.*, 2006). In brief, imaging was carried out in a dark box, and anesthetized animal was illuminated with a monochromatic 633 nm light (50 $\mu W.cm^{-2}$). The reemitted fluorescence was filtered using a colored glass filter RG 665 (optical density > 5 at

the excitation wavelength 633 nm) and collected with a cooled (-70 °C) digital charge-coupled device (CCD) camera (Hamamatsu digital camera C4742-98-26LWGS, Hamamatsu Photonics K.K., Japan). All fluorescence images were acquired using 200 ms and 500 ms of exposure time, with other related parameters kept constant throughout the experiment.

7 RESULTS

7.1 Truncations of ZEBRA

7.1.1 Construction and generation of truncations of ZEBRA

The full-length ZEBRA protein contains three major regions: a *trans*-activation domain (TAD, residues 1-140), a highly basic DNA binding domain (DB, residues 175-195) and a dimerization domain (DIM, residues 195-220) (Miller *et al.*, 2007; Petosa *et al.*, 2006; Sinclair, 2006). To identify the minimal domain required for the translocation of ZEBRA into mammalian cells, eight different truncations of the full-length ZEBRA (Z-FL) protein were constructed that covered the entire amino acids sequence of the native protein (Figure 6.1). Proteins extending from residues 1 to 195 covering the TAD and DB (Z1), as well as shorter fragments of the N-terminal part of ZEBRA, were produced (Z2, Z3). The fragments Z5 and Z7 contained both, DB and DIM, and varied with respect to the regions flanking those functional domains. Furthermore, three fragments bearing either the DB (Z6, Z8) or the DIM (Z9) were constructed (Figure 6.1).

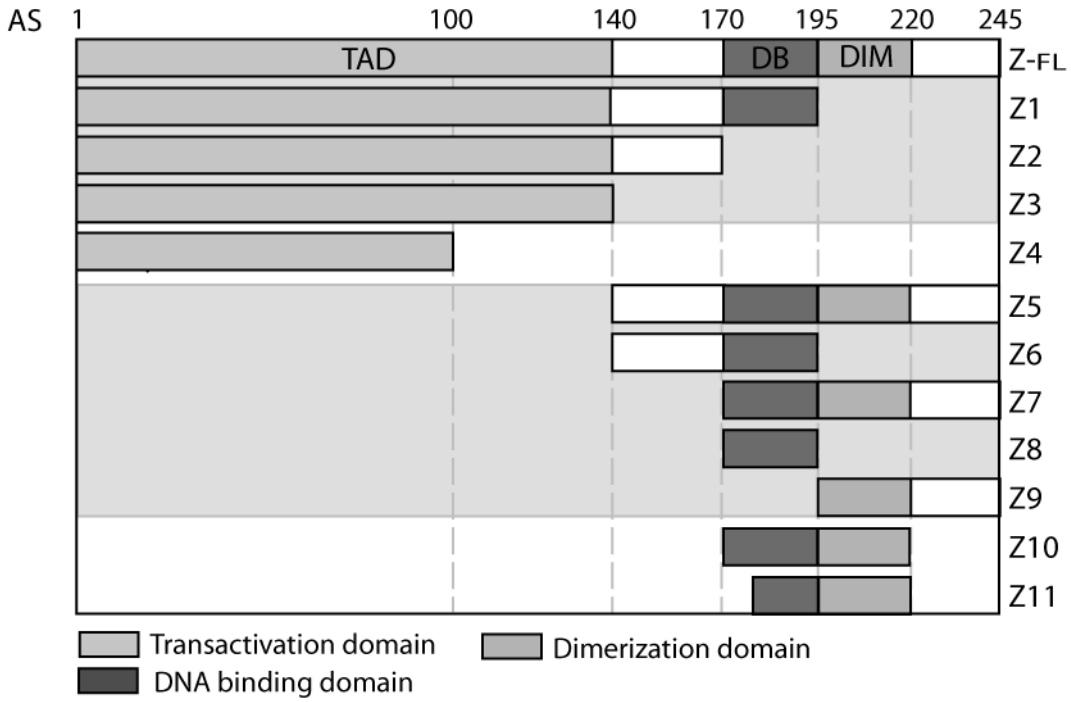

Figure 7.1 **Schematic presentation of the wild type ZEBRA protein and all corresponding protein truncations.** The full-length ZEBRA (ZEBRA-FL) protein contains activation, DB and DIM domain. Nine of the shown proteins were generated and expressed bearing only an N-terminal His-tag for purification purposes. These nine constructs are underlayed in grey.

7.1.2 Expression and purification conditions

Nine different gene fragments of ZEBRA (full-length and eight truncated forms) were produced by PCR. The amplified DNA fragments were cloned in a prokaryotic expression vector (pET15b) by standard cloning methods to generate a genetic in frame N-terminal hexa-His ZEBRA fusion protein to facilitate purification by nickel affinity chromatography.

Solubility

Due to their high hydrophobic content, most of the PTDs produced in *E. coli*, are insoluble. Several studies have described that the denaturated conformation of the PTDs does not interfere with the cellular uptake of the carriers and as well on the activity of the cargo (Schwarze *et al.*, 2000). However, none of these studies have clearly demonstrated the efficiency of the transduction of these denaturated carriers in comparison to a soluble native-like conformation of the PTDs. In order to avoid any conflicting results on the potency of ZEBRA to deliver cargos, only the soluble fractions of the fusion proteins were used throughout this study. Thus, it was analyzed whether the expressed proteins are found in the soluble or insoluble cell fraction. The bacterial lysates were separated into both fractions and analyzed by SDS-PAGE (Figure 6.2). Major portion of the expressed proteins was detected in the insoluble fraction. To optimize the solubility of each fusion protein, expression was induced with 0.1 mM, 0.5 mM or 1 mM IPTG at 37 °C or 16 °C (Figure 6.2). The data of solubility revealed that inducing the expression overnight at low IPTG concentrations (< 0.5 mM) and at low temperature (16 °C) lead to a slight increase of soluble proteins. Furthermore, depending on the composition of the protein domains expression levels and solubility varied strongly between these truncations.

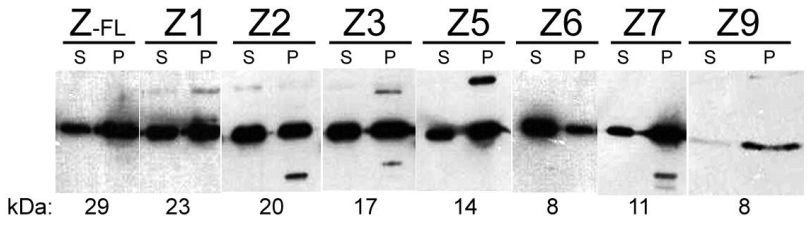

Figure 7.2 **Examination of the solubility of full-length ZEBRA and seven protein truncations.** The bacterial *E. coli* BL21 (DE3) lysates, expressing ZEBRA proteins, were separated in the soluble protein fraction (S) and the insoluble protein fraction (pellet=P) and analyzed by SDS-page and Western Blot analysis using an Anti-His Antibody.

The truncation Z6 presenting the DNA binding site of ZEBRA not only yields to the highest expression levels it also mainly soluble. Expression of all N-terminal truncation (Z1, Z2 and

Z3) is higher compared to the C-terminal truncated parts (Z5, Z7 and Z9) of ZEBRA. One half of the proteins Z1 to Z3 are found at the soluble protein fraction. The full-length, Z5 and Z7 yielding to a lesser extent to soluble proteins but still suffice for subsequent purification. The truncation Z9 covering the dimerization domain and the C-terminal part of ZEBRA is very little expressed and almost completely insoluble (Figure 6.2).

The soluble fraction was used afterwards to assess the purification procedure. Transduction experiments require large amount of purified recombinant proteins. Therefore, various buffer compositions were tested to determine the optimal conditions for purification of the fusion proteins. Small quantities of *E. coli* cultures (3 ml) expressing the ZEBRA proteins were used for purification with the MagnaHis^{TM} purification system (Promega). Figure 6.3 shows a summary of all purified truncated protein in small scale. Accordingly to the preceding expression analysis, deletions in the C-terminal part (Z1 to Z3) led to highest amounts of pure protein. The truncations Z5 and Z7, which are composed of both, the DB and the DIM, as well as Z6 were successfully purified and sufficient quantities of pure proteins were obtained. The Protein Z9 is expressed in a very low level at the soluble form, but also this purification yielded in acceptable amounts of pure protein in the small scale set-up. Afterwards, these conditions have been applied on scale-up experiments using > 500 ml of *E. coli* cultures and HisGraviTrap^{TM} columns (GE Healthcare).

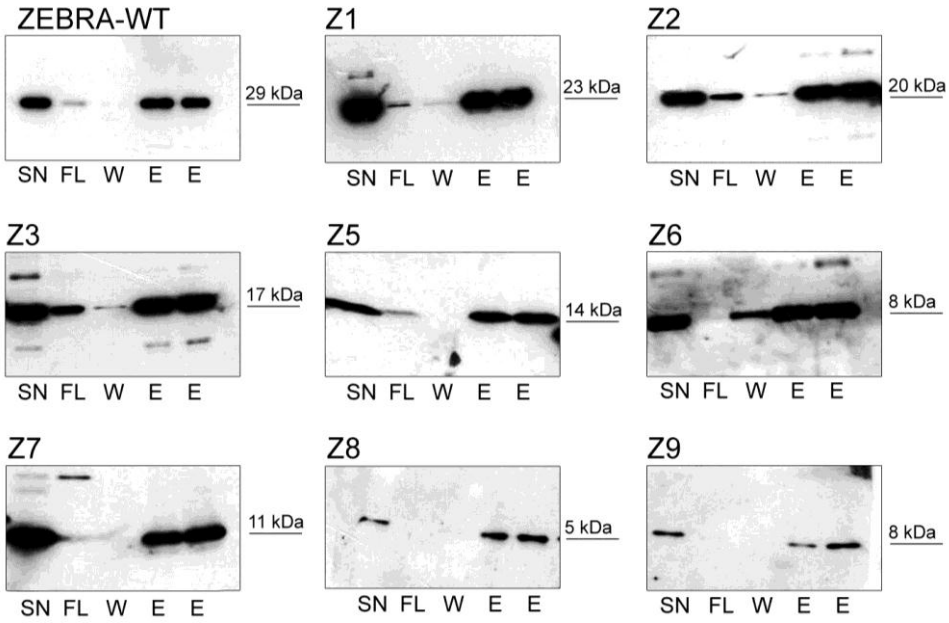

Figure 7.3 **Test purification using the MagnaHis^{TM} Protein Purification System.** Truncated ZEBRA proteins and the full-length protein were expressed in *E. coli* BL21 (DE3) and purified using various purification conditions. Proteins were separated on a SDS page and detected by Western blotting using an Anti-His antibody. SN – Supernatant (= soluble protein fraction), FL – Flow through, W – Wash, E – Elution.

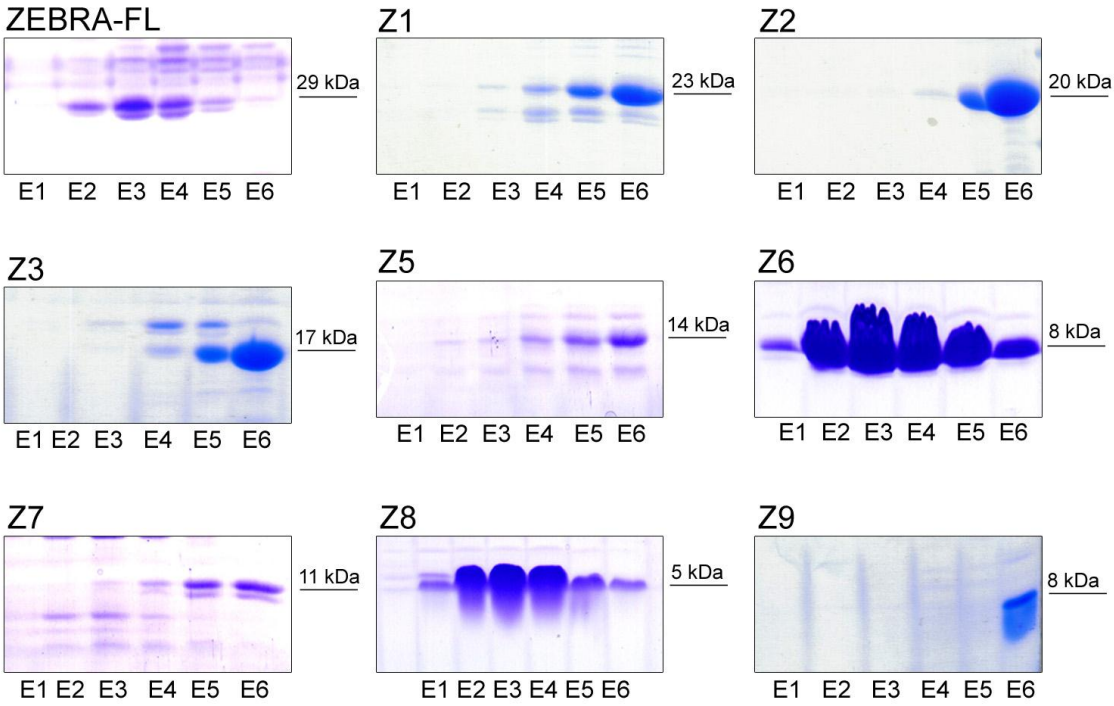

Figure 7.4 **Purification of full-length ZEBRA and eight truncated forms by nickel affinity chromatography.** After expression in *E. coli* BL21 (DE3), proteins were purified using the HisGraviTrap™ system. Equal amounts of each elution fraction were loaded on an acrylamide gel and separated by electrophoresis. The gel was stained by Coomassie blue staining. E – Elution.

In accordance with the small scale test purifications, high yields of pure protein were obtained of all N-terminal fragments (Z1, Z2, Z3) as well as Z6 and Z8. The protein fragments Z6 and Z8 content the DB site and yielded to 5 mg/liter of soluble pure recombinant protein. The truncation bearing the DIM domain are hydrophobic proteins which decrease their expression leading to smaller but sufficient quantities of pure proteins (Figure 6.4). Typical purification results in > 90 % purity in a single-step affinity purification.

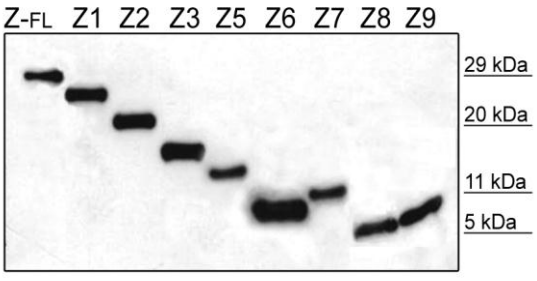

Figure 7.5 **Summary of all purified ZEBRA proteins.** Full-length ZEBRA and truncated ZEBRA proteins after expression in *E. coli* BL21 (DE3) and purification by nickel affinity chromatography were separated on a SDS page and detected by Western blotting using an Anti-His antibody.

In conclusion, ZEBRA protein fragments were expressed in *E. coli* BL21 (DE3) leading to proteins with a molecular weight of 29, 23, 20, 17, 15, 11, 9, 8 and 6 kDa (Figure 6.5). As shown in Figure 6.5, all truncated ZEBRA fragments could be successfully overexpressed and purified to near homogeneity.

7.1.3 Transduction

In recent publication artificial internalization due to strong fixation and permeabilization procedures were discussed (Richard *et al.*, 2005). To avoid these artifacts the translocation of ZEBRA and its truncations was preferentially studied on living cells. Therefore the truncated ZEBRA proteins were labeled with the fluorochrome Alexa Fluor®488 for direct visualization inside the cells by microscopic or cytometric analysis.

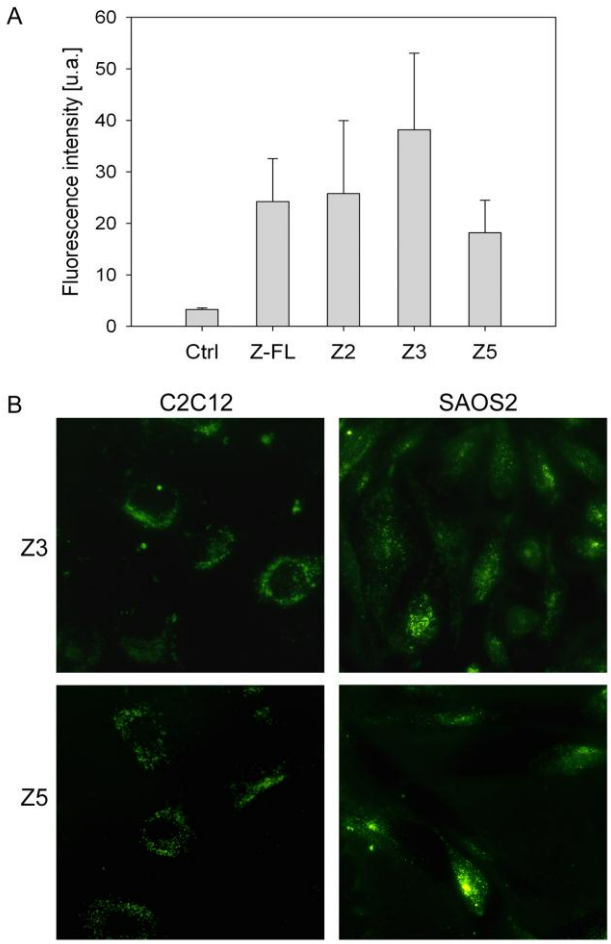

Figure 7.6 **Transduction of different Alexa Fluor®488 labeled ZEBRA truncations.** Analysis of intracellular fluorescence after 15 h of incubation with 0.2 µM of each ZEBRA truncation labeled with the fluorochrome Alexa®488. A - Flow cytometric analysis of live C3H10T1/2 cells after exposure to 0.2 µM Z-FL, Z2, Z3 and Z5 proteins. Cells were treated with Trypsin prior to flow FACS analysis. The mean cell fluorescence of three independent experiments and the ± S. D. is reported. B – Comparison of the uptake between Alexa Fluor®488 labeled Z3 and Z5 truncation of ZEBRA in live C2C12 and Saos2 cells by fluorescence microscopy.

Optimal labeling was only obtained for proteins >14 kDa. Labeling procedures for the smaller ZEBRA proteins led to insufficient staining. Examinations were carried out basically for the full-length ZEBRA (Z-FL), Z2, Z3, and Z5. The full-length protein as well as Z2, Z3 and Z5 showed translocation properties not only into lymphoid cells but also in several adherent growing cell lines (Figure 6.6).

In further studies, internalization was evaluated by flow cytometric analysis (Figure 6.6) using the described proteins. It was not possible to clearly identify a protein region of ZEBRA which is responsible for transduction. In general, uptake of each of these proteins was limited which was reflected by the low intensity of Alexa Fluor®488 fluorescence. Furthermore, all tested cells presented a similar vesicle-like distribution of the internalized proteins for every truncation which was added to the culture medium (Figure 6.6). Limitation in labeling reaction of small proteins and the resultant different grade of labeling made a clear comparison between each truncated form impossible. For this reason, transduction properties of the different truncated forms of ZEBRA when fused to the reporter protein EGFP were studied afterwards.

7.2 Full-length ZEBRA-EGFP fusion proteins

7.2.1 Construction and generation of full-length ZEBRA with EGFP

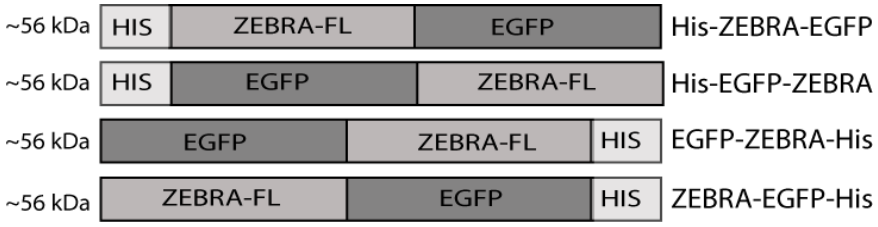

Figure 7.7 **Schematic presentation of the full-length ZEBRA protein fused to the reporter protein EGFP.** ZEBRA proteins were fused both at the N-terminus and C-terminus to EGFP. All four fusion proteins have an N-terminal or C-terminal His-tag for purification purposes.

Based on recent observations (Mahot *et al.*, 2005), the ability to deliver reporter proteins into different mammalian cell lines of the ZEBRA protein from the Epstein Barr virus was investigated. First, a series of fusion proteins containing a His-tag sequence and a reporter protein (EGFP) at the N- or C- terminus of the full-length ZEBRA (Figure 6.7) were designed and constructed. The goal of these experiments was to study whether the position of the reporter protein (EGFP) may interfere with the expression or the transduction ability of ZEBRA. All the constructs have been engineered by amplification of the coding sequences by PCR (see section 5.6.1). Depending of the position of the His-tag, the inserts have been subcloned into either a pET15b (N-terminal His-tag) or pET30b (C-terminal) expression vector.

7.2.2 Expression and purification of full-length ZEBRA with EGFP

For expression of these fusion proteins a suitable *E. coli* expression strain had to be determinate. Two different strains BL21 (DE3) and Origami were investigated (Data not shown). The expression of the N-terminal His tagged proteins showed no crucial difference between both *E. coli* strains. Only for the two other fusion proteins higher expression levels were observed with BL21 (DE3) compared to the origami strain. Due to these results the *E. coli* strain BL21 (DE3) is used for further expression experiments.

With the aim to increase the yield of each fusion proteins, the influence of culture temperature and time has been varied. At any evaluated expression condition, the fusion protein EGFP-ZEBRA-His was expressed at lower levels compared to the other constructs (Figure 6.8). No more than slight differences were obtained by expressing ZEBRA proteins at 37 °C for 2 h or at room temperature overnight after induction with 1 mM IPTG (Figure

6.8). Sufficient amounts of the three ZEBRA fusion proteins, including His-ZEBRA-EGFP, His-EGFP-ZEBRA and ZEBRA-EGFP-His have been obtained to carry out transduction experiments. The protein EGFP-ZEBRA-His could not be expressed and purified in sufficient amounts for subsequent studies.

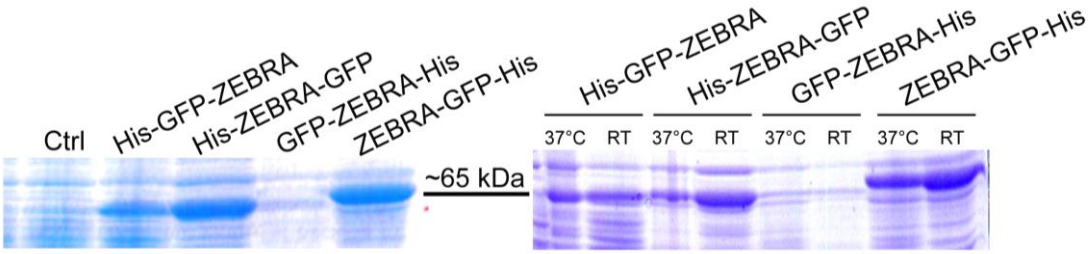

Figure 7.8 **Comparison of the expression of all four EGFP fusion proteins.** (A) Proteins were expressed at 25 °C overnight after induction with 1 mM IPTG in *E. coli* BL21. (Ctrl- *E. coli*-pET15b without induction). (B) Expression of the recombinant EGFP-ZEBRA fusion proteins at room temperature (RT) for 16h or at 37 °C for 2 h.

Furthermore, it was investigated whether the proteins are expressed in the soluble or insoluble cell fraction. The bacterial lysates were separated into both fractions by centrifugation and analyzed by SDS-page. Only a very small portion of the expressed proteins were soluble. To optimize the soluble protein production expression was induced with 0.1 mM, 0.5 mM and 1 mM IPTG carried out under different cultivation conditions. Generally can be concluded that inducing with low IPTG concentrations (< 0.5 mM) and expression at low temperatures over night leads to faintly increased amounts of soluble proteins (data not shown).

Various buffer compositions were tested in small scale purifications using the MagnaHis^{TM} purification system (Promega) to find optimal conditions for purifying these fusion proteins. For large scale purifications 500 ml of respective *E. coli* cultures were grown. To purify high amounts of protein the HisGraviTrap^{TM} (GE Healthcare) columns were used. After several purification of His-Zebra-GFP the washing and elution steps were optimized. The eluted protein was contaminated with co-eluted unspecific proteins and degradation products. Even applying high amounts of protease inhibitors the degradation by endogenous proteases of *E. coli* were not completely inhibited. Similar results were obtained for purification of His-EGFP-ZEBRA. For purification of ZEBRA-EGFP-His best conditions were found since eluted protein fractions show less contaminations with unspecific proteins. Nevertheless, sufficient amounts of three fusion proteins could be purified and were used in subsequent transduction experiments.

7.2.3 Transduction

The EBV positive lymphoid cell line (Raji cells) was used for transduction with three fusion proteins. After 15 h of incubation cells were carefully washed and analyzed by flow cytometry (Figure 6.9). Green fluorescence attribute to EGFP fusion was measured in about 50 % of all cells. The intensity of the detected green fluorescence was not very high for all three fusion protein. When transduced with 5 µg of His-ZEBRA-EGFP Raji cells show the highest fluorescence intensity compared to the other two tested fusion proteins. Consistent with these data, internalization of His-ZEBRA-GFP was detected by fluorescence microscopy in live C3H10 mouse fibroblasts (data not shown). Green fluorescence could be detected within these cells, showing that nearly 100 % of the cell population was transduced. The construct with an N-terminal His-tag and the C-terminal fusion to EGFP seemed to be internalized with the highest efficiency into live cells. Therefore, it was decided that the cargo protein is fused to the C-terminus of ZEBRA for all subsequent studies.

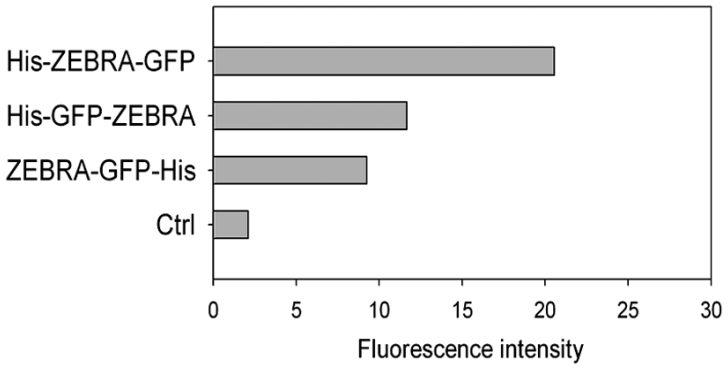

Figure 7.9 **Transduction of three full-length ZEBRA-EGFP fusion proteins into Raji cells.** 2×10^6 Raji (EBV positive lymphocytes) were incubated for 15 h in serum free RPMI medium with 5 µg of each fusion protein. Cells were washed and trypsinized prior to flow cytometric analysis.

7.3 ZEBRA truncation fused to reporter proteins

7.3.1 Construction ZEBRA protein truncations with EGFP

As it was described before, nine truncated forms of ZEBRA were generated by PCR and cloned into pET15b vector (Figure 6.10). All proteins are genetically fused in frame with the C-terminus of EGFP.

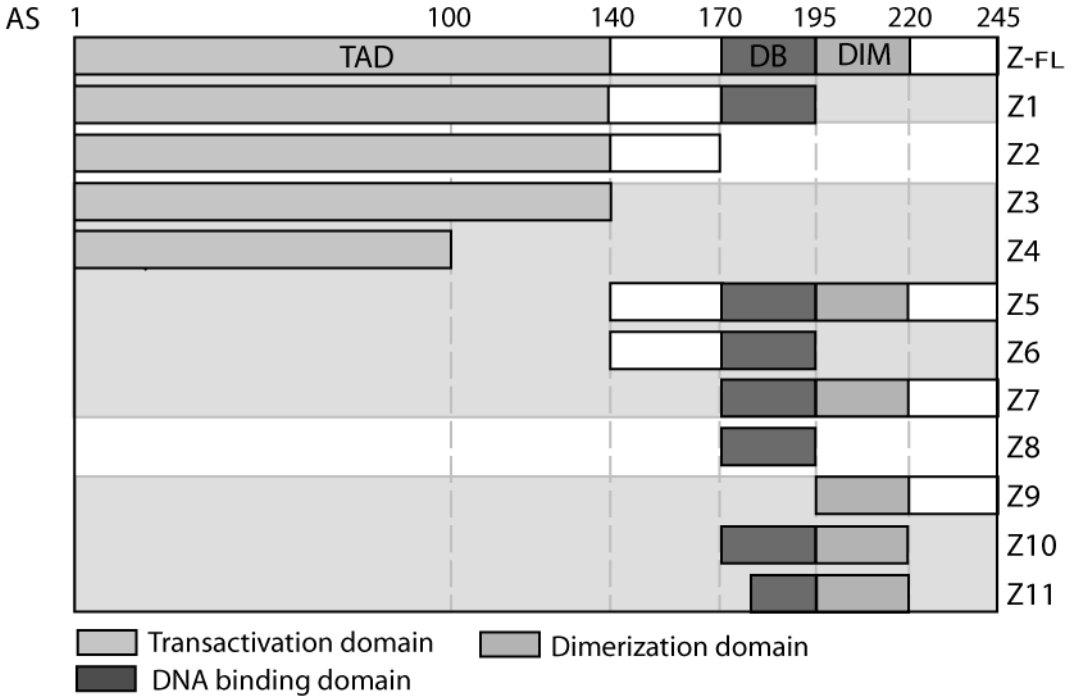

Figure 7.10 Schematic presentation of the full-length ZEBRA protein and all corresponding protein truncations. ZEBRA proteins underlined in grey were fused C-terminal to EGFP. Nine of the shown protein truncations were generated and expressed bearing only an N-terminal His-tag for purification purposes. (Underlined in grey)

7.3.2 Expression and purification of ZEBRA truncation fused to EGFP

The expression and purification by Ni^{2+} affinity chromatography was optimized for each protein regarding their biochemical properties. These fusion proteins were expressed in *E. coli* BL21 (DE3). The fusion to EGFP increased the expression of all truncations. Furthermore, fusion of ZEBRA truncations to EGFP resulted in higher yield of soluble purified protein when compared to β-galactosidase fusions. In accordance to the expression of ZEBRA fragment alone, all fusion truncations bearing the highly hydrophobic DIM domain exhibit decreased expression of soluble proteins in comparison with C-terminal deletions of ZEBRA. Figure 6.11 shows all ZEBRA-EGFP recombinants proteins after affinity chromatography purification and two examples of a purification outcome of Z10-EGFP and Z11-EGFP.

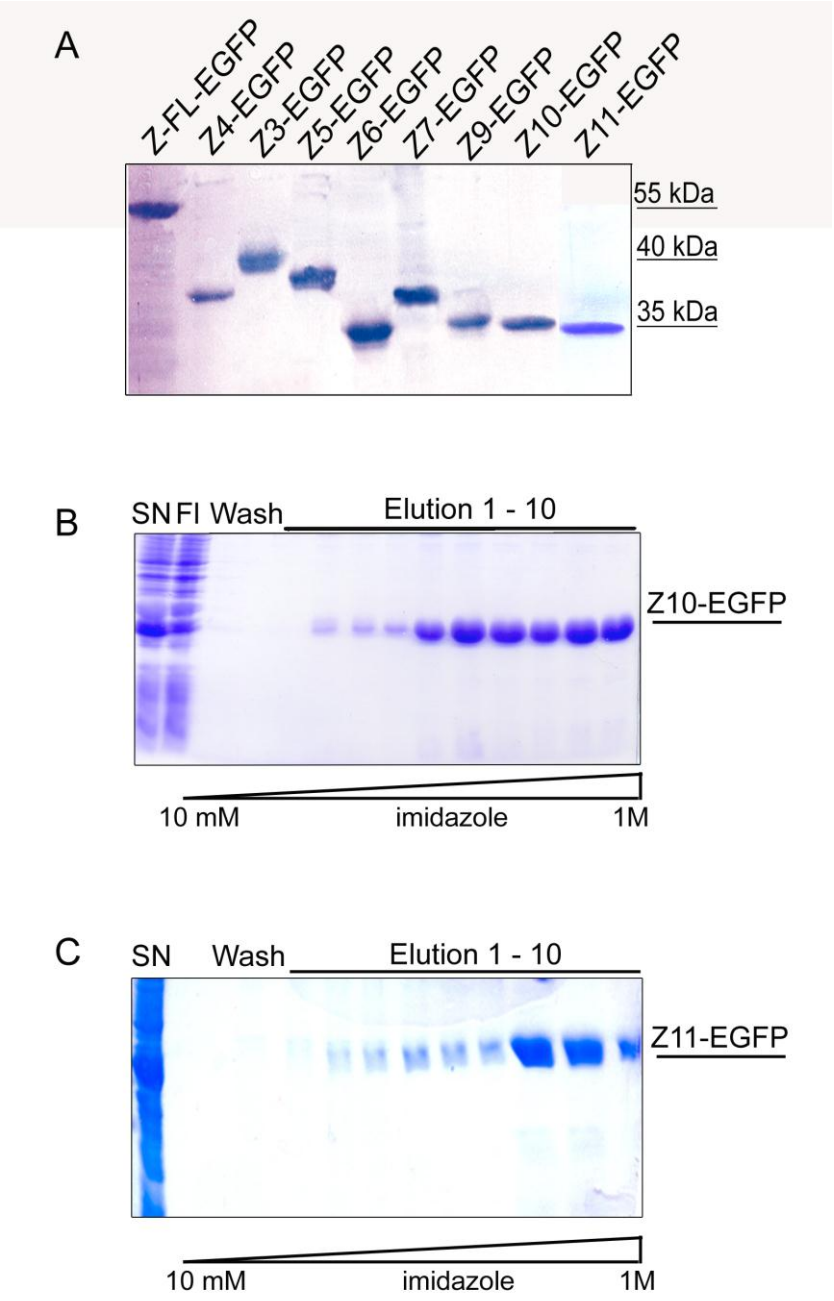

Figure 7.11 **Purification of ZEBRA truncation fused to the reporter protein EGFP.** A - Aliquots of ZEBRA-EGFP fusion proteins were loaded on a 13 % SDS page and separated by electrophoresis. B, C – Example of purification of Z10-EGFP and Z11-EGFP. SDS page was visualized by Coomassie Blue staining after electrophoresis.

7.3.3 Transduction

With the motivation to use ZEBRA as a protein carrier, the transduction properties of the full-length ZEBRA and several different truncations fused to EGFP, including Z2-EGFP, Z3-EGFP, Z4-EGFP, Z5-EGFP, Z6-EGFP, Z9-EGFP, Z10-EGFP and Z11-EGFP, were evaluated.

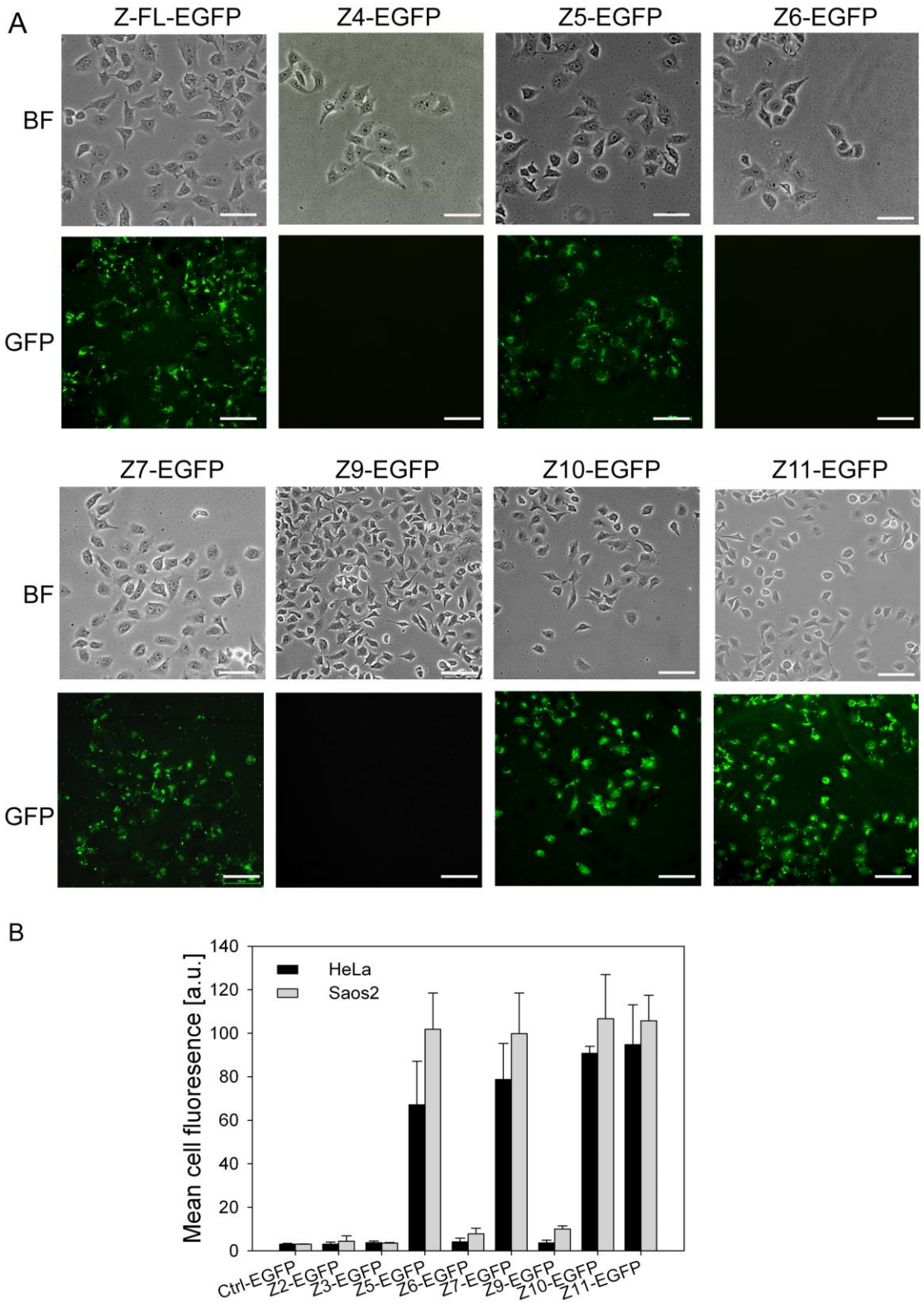

Figure 7.12 **Identification of the minimal protein domain required for protein translocation.** A - Analysis of intracellular fluorescence after 15 h of incubation with 0.2 µM of each ZEBRA-EGFP fusion protein in living HeLa cells by fluorescence microscopy. B - Flow cytometric analysis of live HeLa and Saos2 cells after exposure to 0.2 µM ZEBRA-EGFP fusion proteins. Cells were treated with Trypsin prior to flow FACS analysis. The mean cell fluorescence of three independent experiments and the ± S. D. is reported. White bar represent 100 µm.

The fusion proteins were added in the culture media of cervical cancer (HeLa) or osteosarcoma (Saos2) cells, incubated for 24 h and cell fluorescence was monitored either by flow cytometry or by fluorescence microscopy on live unfixed cells (Figure 6.12). It was found that only full-length Z-FL-EGFP, Z5-EGFP, Z7-EGFP, Z10-EGFP and Z11-EGFP proteins were efficiently transduced into HeLa cells (Figure 6.12). No fluorescence signal was observed in association with the EGFP-fused truncations containing only the N-terminal part (Z3-EGFP or Z4-EGFP) of the wild-type protein, an internal deletion in the zipper domain (Z6-EGFP), or a deletion of the basic domain (Z9-EGFP) (Figure 6.12). Transduction efficiency was further evaluated in HeLa and Saos2 cell lines by flow cytometry after 15 h incubation with 0.2 µM of each protein. The flow cytometric analyses confirmed the efficient uptake of Z5-EGFP, Z7-EGFP, Z10-EGFP and Z11-EGFP into the two cell lines (Figure 6.12).

From these results it was concluded that the presence of both the DB and the DIM domains are required and suffice for internalization. The smallest tested truncated protein containing both domains was Z10, which facilitated the delivery of EGFP with an almost 100 % efficiency (number of fluorescent cells over total cell number) into various mammalian cell lines. Therefore, all translocation experiments described below were performed using the Z10 peptide. The Z10 of ZEBRA is composed of 54 amino acid residues and combines two important domains of the ZEBRA protein, the DNA binding region and the dimerization domain, which together form the bZIP region (Figure 6.13). Additionally to 14 positively charged residues such as lysine and arginine, the Z10 provides 13 hydrophobic amino acids (leucine, alanine and valine), which are mainly located at the dimerization domain.
After studying the sequence of Z10, the length and amino acid composition of Z10 was optimized. By doing so, the first 8 amino acid (AA 170-177) were removed since a contribution of these aa for the uptake mechanisms of ZEBRA in terms of a high cationic charge was not expected. The new truncation of ZEBRA was named Z11 (AA 178-220) and fused to the reporter protein EGFP. Same expression and purification condition were used as previously described. The internalization of this fusion protein was assayed by live cell fluorescence microscopy and cytometry analysis. With both experiments it was proven that Z11 is able to deliver EGFP into Saos2 and HeLa cells (Figure 6.12). Since it was generated later during the presented work; most of the experiments for the characterization of the internalization were carried out using Z10-EGFP. But for all future application of ZEBRA as a protein carrier, the Z11 minimal domain will be used.

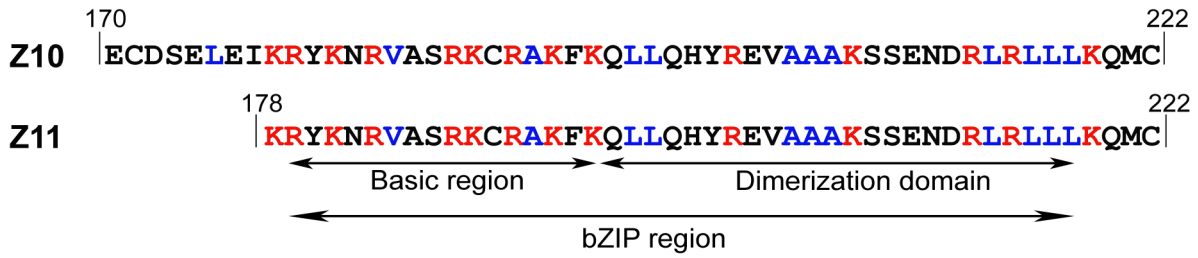

Figure 7.13 **Amino acid sequence of the cell penetrating sequences Z10 and Z11 of the ZEBRA protein.** Basic amino acids of both sequences (7 lysine and 7 arginine residues) are shown in red, whereas in hydrophobic amino acids (one valine, 5 alanine and 7 leucine residues [Z10] or 6 leucine [Z11]) are presented in blue. The presence of both, the DNA binding region and the dimerization domain, are absolutely required for the translocation property of the minimal transduction domain (MD) of ZEBRA.

Flow cytometric analysis of living cells from different cell lines HeLa, Saos2, HCT116p53-/- and C2C12 confirmed the ability of the C-terminal part of ZEBRA to translocate the cell membrane as shown in Figure 6.14. It should be emphasized that the majority of the lymphoid cells, Raji cells, is fluorescent which means not transduced. This result contradicts strongly with the previous published lymphoid specificity of the full-length ZEBRA.

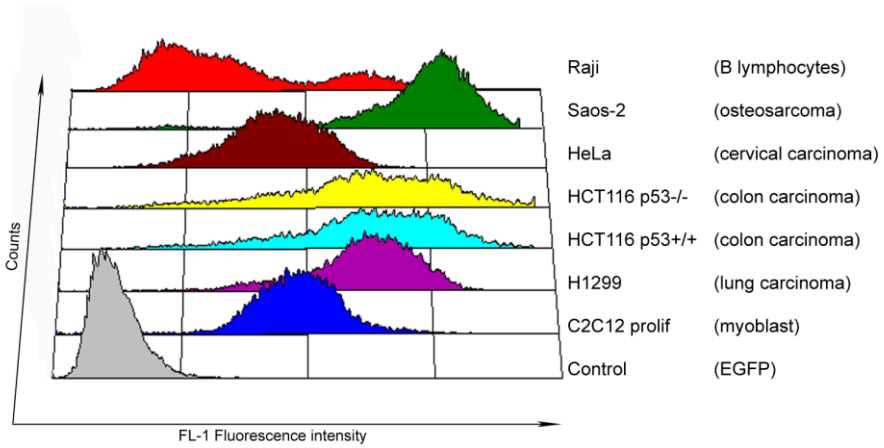

Figure 7.14 **Uptake of Z5-EGFP into various cell lines.** Cells were transduced with 0.3 µM of the fusion proteins and after 15 h cells were intensively washed and trypsinized. The fluorescence of GFP was analyzed using flow cytometry.

After the internalization of Z7-EGFP into the cell interior subsequent translocation into the nucleus could not be observed in microscopic images at any analyzed cell lines. In addition, whole cell lysate was recovered after 15 h incubation with 0.3 µM Z7-EGFP and separated into cytosolic and nucleic protein fraction using the Cell Compartmentation Kit from Pierce. Detection of EGFP by immunoblotting using an Anti-GFP antibody (Euromedex) confirmed the exclusive occurrence of this fusion protein in the cytosol (Figure 6.15). Interestingly, the same experiment was done using 0.3 µM of Z7-β-galactosidase. After 15 h, HeLa cells were

lysed and separated into two cell compartments, cytoplasm and nucleus. The Z7 fusion protein was detected in both cellular compartments using a mouse Anti-ZEBRA antibody (Figure 6.15). In line with this finding, β-galactosidase was found in both, the cytosol and the nucleus in transduced HeLa and Saos2 cells as shown in microscopic images (See section 6.3.7, Figure 6.25).

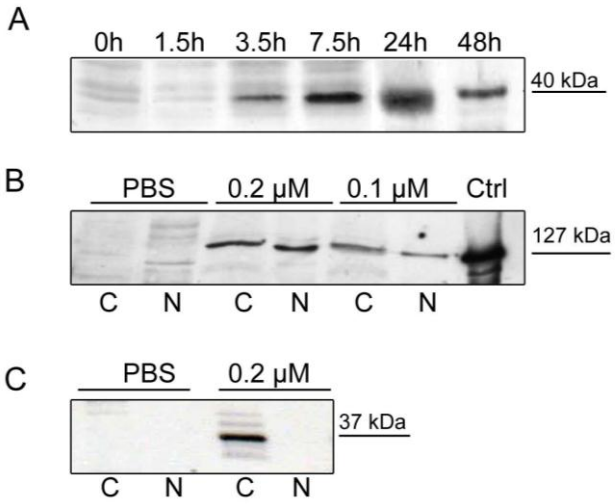

Figure 7.15 **Western blot analysis of internalized ZEBRA fusion proteins.** A - HCT116 (p53-/-) cells were incubated with 0.3 µM of Z5-EGFP. At indicated times total cell lysate was recovered and subjected to SDS gel electrophoresis. Z5-EGFP was detected using a mouse Anti-GFP antibody. B - After incubation for 15h with 0.3 µM of Z7-β-galactosidase HeLa cells were lysed and separated into two cell compartments, cytoplasm and nucleus. The Z7 fusion protein was detected in both cellular compartments using a mouse Anti-ZEBRA antibody. C - HeLa cells were incubated for 15 h with Z7-EGFP. The total cell lysate was separated into a cytosolic and a nucleic fraction using the Cell Compartmentation Kit from Pierce. The ZEBRA-EGFP fusion protein was detected exclusively at the cytoplasm of the transduced cells.

7.3.4 Kinetics of Z10-EGFP internalization and cytotoxicity

The translocation of Z10-EGFP was monitored by the measurement of fluorescence in live cells using flow cytometry analysis. The addition of low concentration of Z10-EGFP (0.2 µM) to the serum-free culture media of HeLa or Saos2 cells resulted in a rapid intracellular accumulation of the fusion protein (Figure 6.16). This cellular uptake was detected after removal of cell surface bound protein by extensive trypsin/heparin washes and remained stable for at least 24 h in the cells (Figure 6.16). The increased fluorescence intensity in Saos2 cells after transduction is most likely due to their larger size compared to smaller HeLa cells, and not caused by better translocation efficiency into the former.

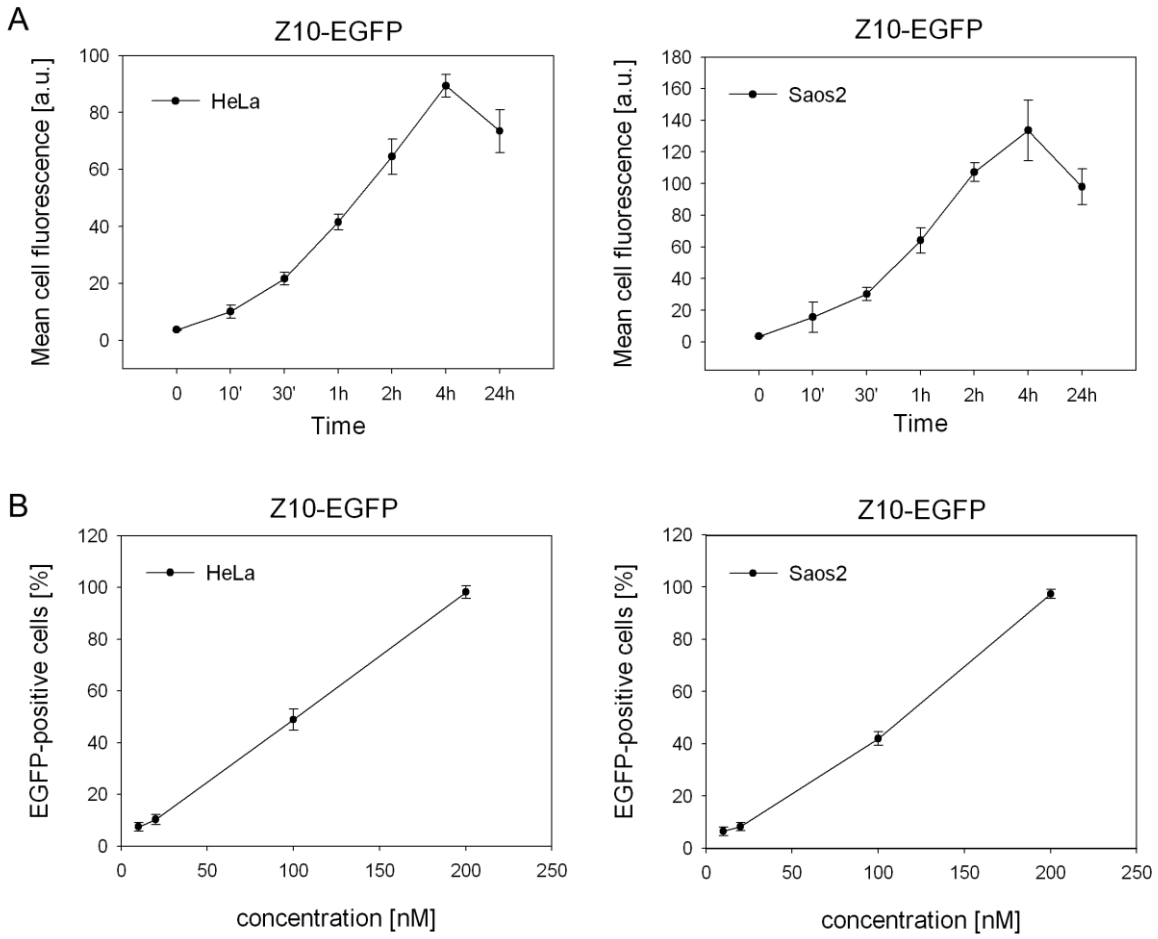

Figure 7.16 **Kinetics of Z10-EGFP internalization**. A - Time-dependent intracellular accumulation of MD-EGFP in HeLa and Saos2 cells. Both cell lines were incubated with 0.2 µM of MD-EGFP at 37 °C for the times indicated, and subsequently treated with trypsin for 10 min at 37 °C. The mean cell fluorescence was analyzed by flow cytometry. B - Dose-dependent uptake of MD-EGFP in live HeLa and Saos2 cells. Indicated concentrations of MD-EGFP were added to the serum-free cell culture medium. After 4 h cells were washed with PBS, trypsinized for 10 min at 37 °C and cell fluorescence was measured by flow cytometry. All transduction experiments were performed in triplicates in two independent analyses, and the ± S.D. are indicated.

The dose-dependent internalization of Z10-EGFP into these cell lines was also investigated. Cells were incubated during 4 h with different concentration of the fusion protein ranging from 10 to 200 nM. After extensive washing and trypzination, transduction efficiency was analyzed by flow cytometry. Transduced EGFP was already detected in HeLa and Saos2 cells after incubation with low amounts (10 and 20 nM) of Z10-EGFP (Figure 6.16). About 50 % of the cells were transduced in presence of 100 nM Z10-EGFP (Figure 6.16). Incubation of cells with higher concentrations (200 nM) of Z10-EGFP resulted in a 100 % transduced cell population. The fluorescence of internalized EGFP increased linearly with the concentration of Z10-EGFP in the culture medium and reached saturation at 200 nM (data not shown).

The toxicity of both Z10-EGFP and Z10-β-galactosidase (see section 5.8.7) fusion proteins was tested with a lactate dehydrogenase (LDH) based assay. The cytosolic enzyme LDH can be detected in the cell culture medium after the disruption of cell membranes. Saos2 and HeLa cells were incubated with different concentrations of the fusion protein ranging from 0.1 to 3 µM. 24 h after addition of the Z10 fusion proteins, no variation in the cell viability was observed as shown by the absence of extracellular LDH activity (Figure 6.17).

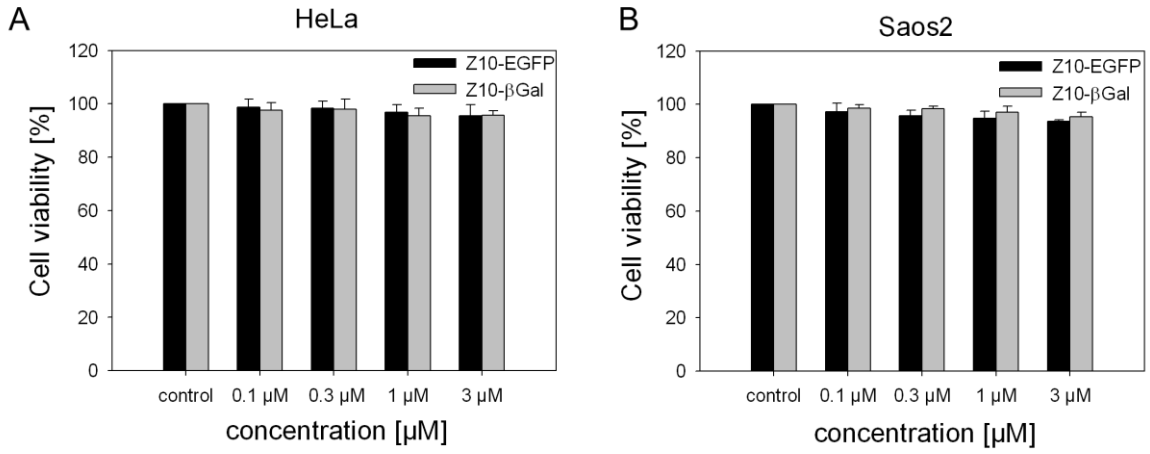

Figure 7.17 **Cytotoxicity of Z10-EGFP and Z10-β-galctosiadse**. Z10-mediated protein delivery caused no cytotoxicity. HeLa (A) and Saos2 (B) cells were exposed to indicate concentrations of Z10-EGFP and Z10-β-galactosidase and incubated in growth medium at 37 °C for 24 h. Cytotoxicity after the uptake of both fusion proteins was determined by the leakage of LDH into the culture medium. Each column represents the mean viability of two independent experiments performed in triplicates with indicated ± S.D.

7.3.5 Mechanisms of uptake

Several reports have described that cell surface heparan sulfate proteoglycans (HSPGs) play a key role for the cellular internalization of CPPs (Tyagi *et al.*, 2001; Ziegler & Seelig, 2004). Mutational analysis of cationic rich sequences demonstrated that the cellular uptake properties of TAT depends mostly on the presence of positively charged residues which facilitate binding to negatively charged HSPGs at the cellular surface (Ho *et al.*, 2001; Mukai *et al.*, 2006). To evaluate the role of HSPGs for the uptake of Z10-EGFP, HeLa and Saos2 cells were incubated for 30 min with 20 µg/ml heparin prior to addition of the fusion protein. Heparin is a structural homolog of HSPGs and may compete for binding of the latter to Z10-EGFP. The uptake of Z10-EGFP was significantly inhibited by presence of heparin in the culture medium when compared to the control condition without heparin (Figure 6.18). These data indicated that cellular internalization of Z10-EGFP required interactions between negatively charged HSPGs and the basic amino acids in the sequence of Z10 (Figure 6.18).

Recent studies on the uptake mechanisms of TAT or VP22 reported a significant contribution of endocytotic pathways to their cellular internalization (Fuchs & Raines, 2004; Kaplan *et al.*, 2005; Richard *et al.*, 2005; Wadia *et al.*, 2004). Therefore, we first investigated the effect of low temperature and ATP depletion on cellular uptake of Z10-EGFP. As shown in Figure 6.18, the intracellular EGFP signal for HeLa and Saos2 cells was strongly reduced after incubation at 4 °C. The cellular ATP pool was depleted by a treatment with sodium azide and 2-deoxy-D-glucose. We observed only a 20 – 30 % decrease in cell fluorescence in both cell lines (Figure 6.18), indicating that the uptake of Z10-EGFP is mostly ATP independent.

To clarify whether Z10-EGFP internalization involves endocytosis, the effect of several drugs that specifically inhibit caveolin, clathrin, or lipid raft-dependent endocytosis, respectively, was explored. Nystatin is a known inhibitor of caveolin-dependent endocytosis (Richard *et al.*, 2005). The internalization by a caveolae process is slow and occurs in general upon cell stimulation (Anderson, 1998). HeLa and Saos2 cells were treated with 50 µg/ml nystatin prior to addition of 0.2 µM Z10-EGFP and internalization was analyzed by flow cytometry. In both cell lines, the intracellular fluorescence signal for Z10-EGFP in presence of nystatin was identical to the control conditions (Figure 6.18). Thus, caveolin-dependent endocytosis is not involved in the uptake of Z10-EGFP. Macropinocytosis is a rapid and non-specific mechanism of internalization and has been described to be responsible for the cellular uptake of some CPPs (Kaplan *et al.*, 2005). Macropinocytosis depends on the activity of phosphatidylinositol-3-kinase (PI3K) and is inhibited by wortmannin (Araki *et al.*, 1996). The impact of wortmannin on the internalization of Z10-EGFP into HeLa and Saos2 cells was examined. The pretreatment of both cell lines with 100 nM wortmannin did not alter the cellular uptake of Z10-EGFP compared to untreated cells (Figure 6.18). Thus, Z10-mediated protein translocation does not occur via macropinocytosis. To test whether Z10-EGFP uptake involves clathrin-coated pit-mediated endocytosis, Z10-EGFP internalization was measured in presence of chlorpromazine. Saos2 and HeLa cells were incubated with 30 µM chlorpromazine. After 30 min incubation with chlorpromazine, the Z10-EGFP fusion protein was added. Interestingly, EGFP fluorescence was significantly reduced in Saos2 cells but not in HeLa cells (Figure 6.18). These results indicate that the internalization process of Z10-EGFP may differ depending on the cell type. Finally, the lipid raft-mediated endocytotic pathway, which has been also reported to be implicated in the uptake of CPPs (Kaplan *et al.*, 2005; Wadia *et al.*, 2004) was investigated. Cells were treated with methyl-β-cyclodextrin (MβCD) to deplete cell surface associated cholesterol resulting in a disruption of lipid rafts. As shown in Figure 6.18, an impaired uptake of Z10-EGFP into both cell lines was observed. These data suggest that lipid raft-mediated endocytosis contributes to the uptake of Z10-EGFP. However, 60 % of Z10-EGFP occurred through an alternative route of internalization.

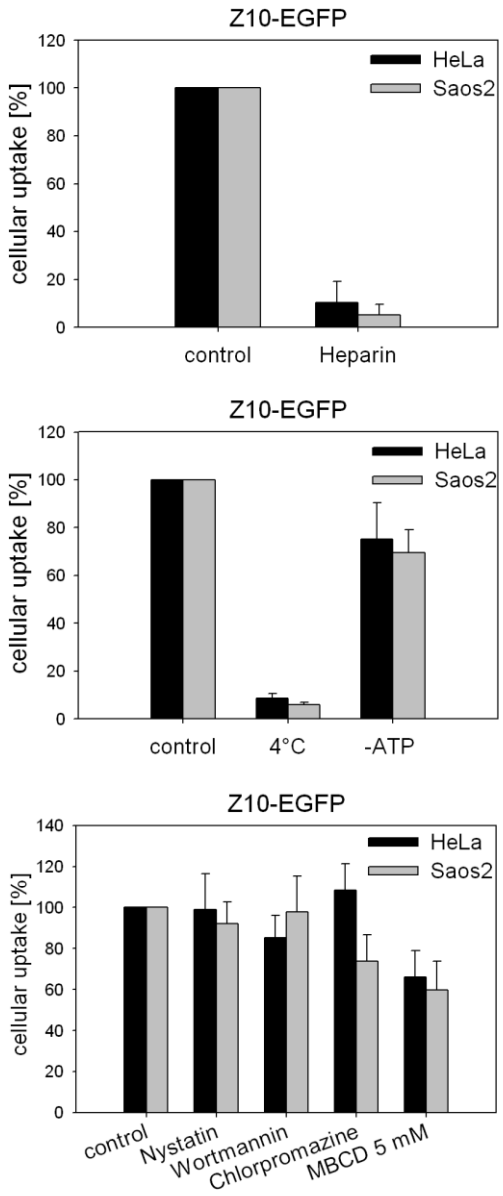

Figure 7.18 **Mechanisms of uptake.** A - HeLa and Saos2 cells were incubated with 20 µg/ml heparin for 30 min at 37 °C and afterwards exposed to 0.2 µM MD-EGFP for 3 h at 37 °C. Cells were trypsinized for 10 min at 37 °C and washed prior to flow cytometry analysis. B - The effect of low temperature and depletion cellular ATP on internalization of MD-EGFP. Both cell lines were incubated with 0.2 µM MD-EGFP for 1 h at 4 °C. To deplete the cellular ATP pool, HeLa and Saos2 cells were incubated for 1 h with 6 mM 2-deoxy-D-glucose and 10 mM sodium azide and then and exposed to 0.2 µM MD-EGFP for 1h. After trypzination, cells were analyzed by flow cytometry. C - Effect of endocytotic inhibitors on MD-EGFP transduction. Both cell lines were treated with 30 µM chlorpromazine, 100 nM wortmannin, 50 µg/ml nystatin, or 5-10 mM methyl-β-cyclodextrin (MBCD), respectively, 30 min prior to addition of 0.2 µM MD-EGFP. In general, cellular uptake of pre-treated cells was measured as mean fluorescence and normalized to mean cell fluorescence of untreated control. Each experiment was performed three times in triplicates and the means ± S.D. are indicated.

7.3.6 Intracellular localization of Z10-EGFP

In case of an endosomal-dependent pathway of Z10 uptake, colocalization with early and late endosomes would be expected. We performed immunofluorescence microscopy to study the subcellular co-localization of internalized Z10-EGFP with endosomal marker proteins, such as EEA1 (early endosomal marker), Rab7 (endosomal marker, Figure 6.19, 6.20, 6.21), caveolin-1 (caveosome marker), and clathrin (marker for clathrin coated pits, Figure 6.21) (Watson *et al.*, 2005). HeLa cells were incubated between 30 min to 15 h with Z10-EGFP at 37 °C and protein internalization was analyzed by confocal microscopy. The uptake of Z10-EGFP was confirmed by direct visualization of the intracellular fluorescence of EGFP or by antibody staining against EGFP.

The majority of the EGFP signals did not co-localize with EEA-1 or Rab-7 signals (Figure 6.19, 6.20, 6.21). However, a portion of the EGFP signals overlapped with endosomal markers. Variation of the incubation times did change this observation only slightly. At earlier time points (30 min) after the addition of Z10-EGFP to the cells we observed minor co-localization of the internalized protein with endosomal markers EEA-1 and at later time points (3 h) with Rab-7. Furthermore, Z10-EGFP did not co-localize with caveolin or clathrin signals at any analyzed time points (Figure 6.21)

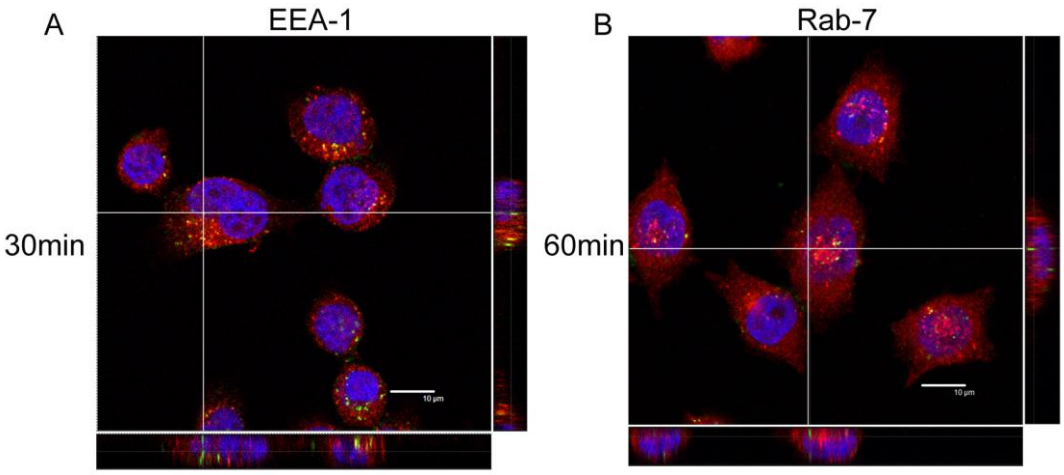

Figure 7.19 **Z10-EGFP internalization into HeLa cells.** HeLa cells were exposed to 0.2 µM MD-EGFP for 30 min to1 h at 37 °C. Surface bound proteins were removed by several heparin washes. Cells were then fixed, immuno-stained for endosomal marker proteins EEA-1 (A) or Rab-7 (B), detected with Alexa Fluor® 647 labeled second antibody, and nuclei were counterstained with Hoechst 33258. Cells were then visualized by confocal microscopy (TCS-SP2 – Leica Manheim, Germany). Images were acquired sequentially, as described in experimental procedures, with MD-GFP in green, EEA-1 or Rab7 in red, and DNA in blue. Square image (XY) corresponds to the central section of a Z-stack acquisition (22 optical sections, Δz = 500 nm), while bottom and right images correspond to sections of the stack (XZ and YZ respectively) defined by the cross lines in the XY representation.

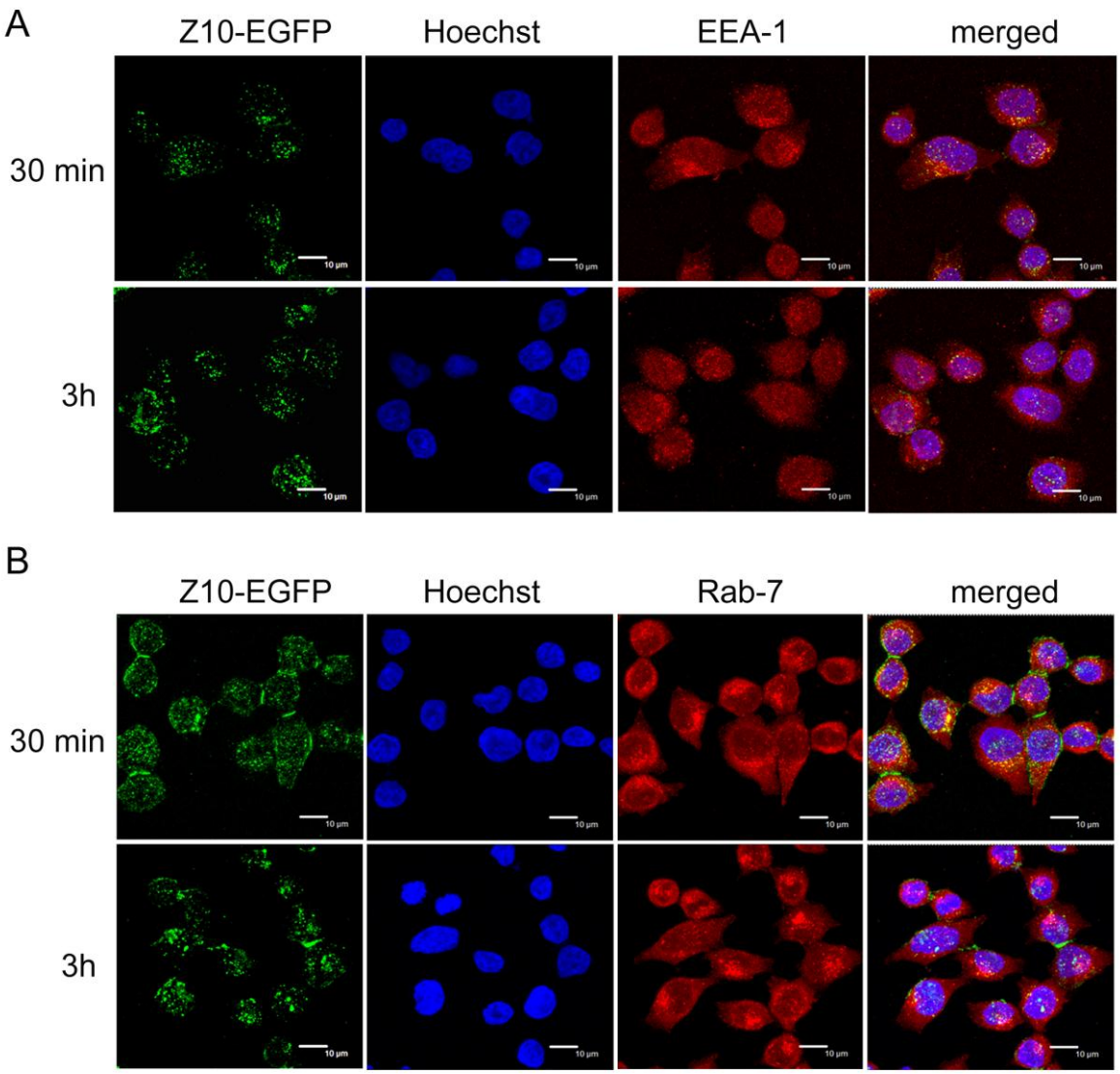

Figure 7.20 **Intracellular localization of Z10-EGFP in HeLa cells.** HeLa cells were exposed to 0.2 µM Z10-EGFP for 30 min to 3 h at 37 °C. Surface bound proteins were removed by several heparin washes. Cells were then fixed, immuno-stained for endosomal marker proteins EEA-1 (A) or Rab-7 (B) detected with Alexa Fluor® 647 labeled second antibody, and nuclei were counterstained with Hoechst 33258. Cells were then visualized by confocal microscopy (TCS-SP2 – Leica Mannheim, Germany). Images were acquired sequentially, as described in material and methods, with Z10-EGFP in green, EEA-1 or Rab7 in red and DNA in blue (A, B)

An additional proof of internalization of Z10-EGFP in HeLa cells was done by confocal microscopy studies. Intracellular Z10-EGFP proteins were detected inside the cell after immunofluorescence analysis by examining different Z-section of one cell. Four different endosomal markers (EEA-1, Rab-7, clathrin and caveolin) were stained as reference signals (red fluorescence). EGFP fluorescence was clearly found in the cell interior and was different from endosomal marker proteins (Figure 6.19).

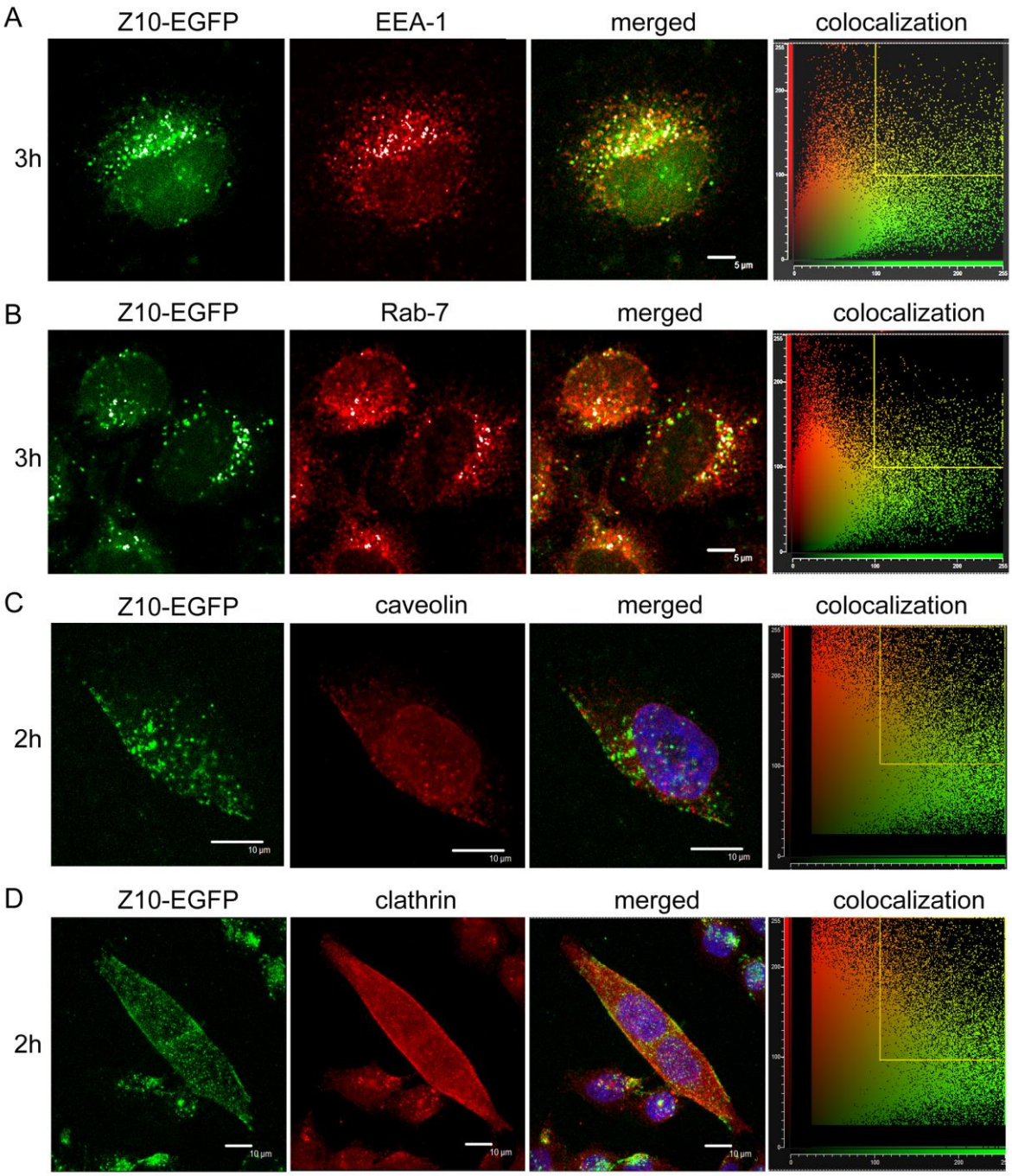

Figure 7.21 **Intracellular localization of Z10-EGFP compared to endosomal marker proteins in HeLa cells.** A, B HeLa cells were incubated for 2 h or 3 h with 0.2 µM Z10-EGFP at 37 °C. Cells were washed with 20 µg/ml heparin in PBS, fixed, and incubated with anti-EEA-1 (A), anti-Rab-7 (B), anti-caveolin-1 (C) or anti-clathrin (D) antibodies and the corresponding secondary anti-rabbit antibody (Alexa Fluor® 647). Fluorescence was analyzed sequentially by confocal microscopy (TCS-SP2 – Leica Mannheim), as previously described. Z10-EGFP signals are shown in green, nucleus in blue and EEA-1, Rab-7, clathrin or caveolin-1 marker in red. An estimation of colocalization was determined with the "CF2D" software from Leica. Diagrams (right) represent the relative intensity of the pixels in the green and red images. Dots gated in the yellow square, corresponding to colocalization, are represented in white in the images.

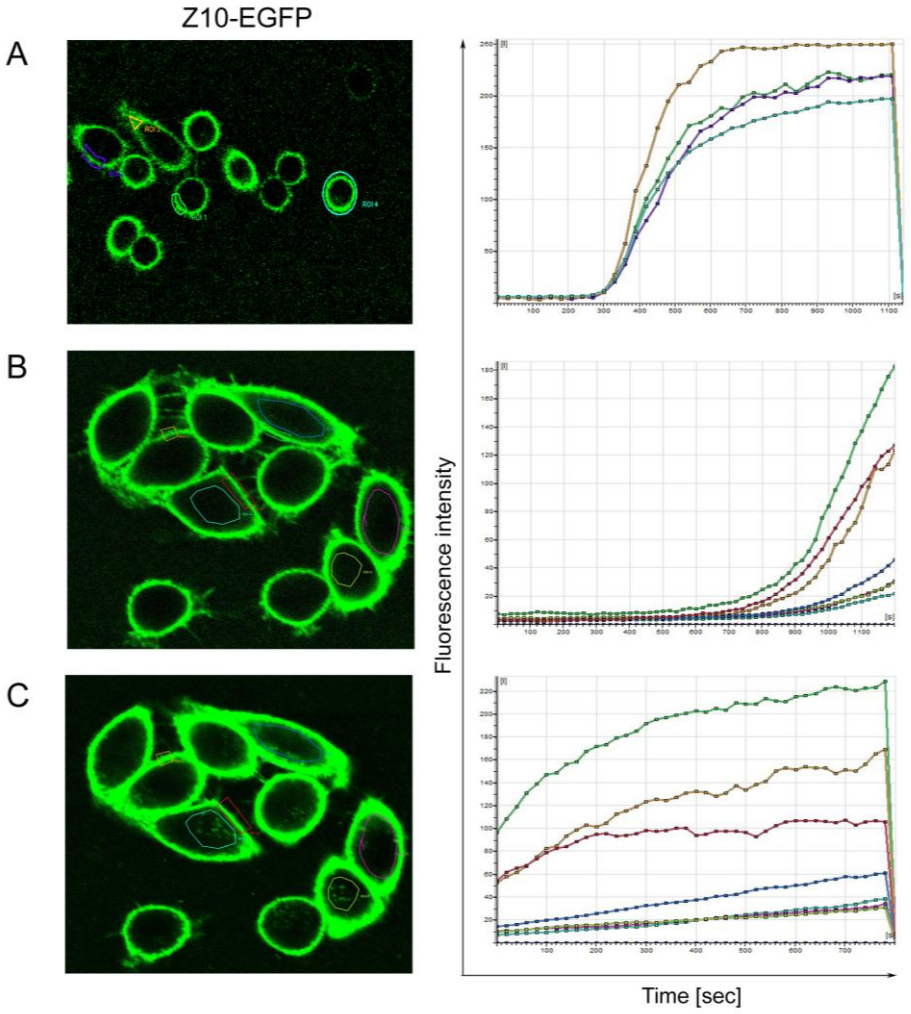

Figure 7.22 **Time lapse imaging of Z10-EGFP uptake in live HeLa cells.** Cells were exposed to 0.3 µM Z10-EGFP and fluorescence was directly measured by a time-lapse experiment using the Leica TCS-SP2 confocal microscope with 488 nm excitation for the Z10-EGFP (fluorescence collection between 500 and 540nm). Images correspond to fluorescent signals after different acquisition times. Increases in fluorescence intensity of defined cellular compartments over time are shown at the left panel. Associated films show 1 min of real time microscopy in 1 sec. A - Image represents 18 min of exposure with 0.3 µM MD-EGFP. B - Image corresponds to 20 min incubation with MD-EGFP. C - Second time lapse acquisition of the same cells for duration of 13 min, corresponding to 20 – 33 min after addition of MD-EGFP (PMT voltage was about half reduced, compared to B).

Cellular entry of Z10-EGFP was witnessed by live cell imaging in HeLa cells. 0.3 µM of the ZEBRA-EGFP fusion protein was added to the cells and directly visualized by fluorescence microscopy for 1 h (Figure 6.22). A fast accumulation at the cell membrane level was observed within the first 15 min, followed by a rapid trafficking of EGFP signals inside the cell.

7.3.7 Delivery of β-galactosidase into cells

With the prospect to use the cell penetrating domain of ZEBRA as a protein carrier, the intracellular functionality of Z10-delivered proteins using the 120 kDa enzyme β-galactosidase fused to Z10 as a model was tested. Therefore, the 120 kDa enzyme β-galactosidase was fused in frame to the C-terminal part of Z10 (Figure 6.23).

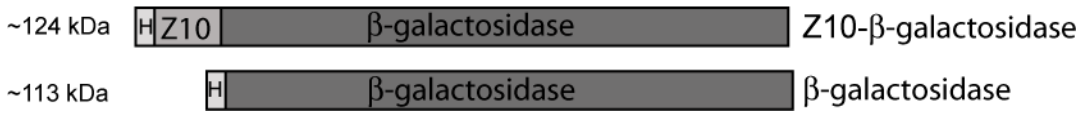

Figure 7.23 **Overview of ZEBRA-β-galactosidase constructs.** The Z10 of ZEBRA was fused N-terminal to the reporter enzyme β-galactosidase. The enzyme alone served as a control. The proteins contain a polyhistidine tag at the N-terminus for purification.

Both recombinant proteins, the enzyme β-galactosidase alone and in fusion to Z10, were expressed overnight at 16 °C in shaker flasks in *E. coli* BL21 (DE3) after induction with 0.5 mM IPTG. The soluble fraction containing the fusion protein was purified near homogeneity as previously described for the Z10-GFP fusion protein (Figure 6.24).

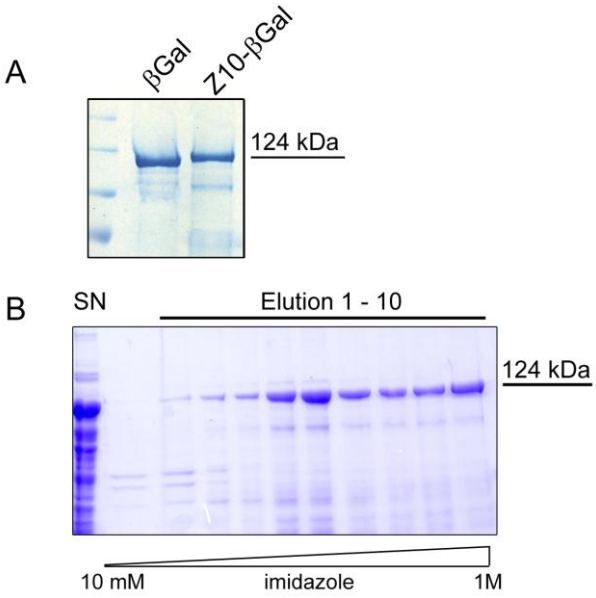

Figure 7.24 **Purification of β-galactosidase and Z10-β-galactosidase.** A – Aliquots of β-galactosidase and Z10-β-galactosidase proteins were loaded on a 10 % SDS page. B – Example of purification of Z10-β-galactosidase. SDS page was visualized by Coomassie Blue staining after electrophoresis.

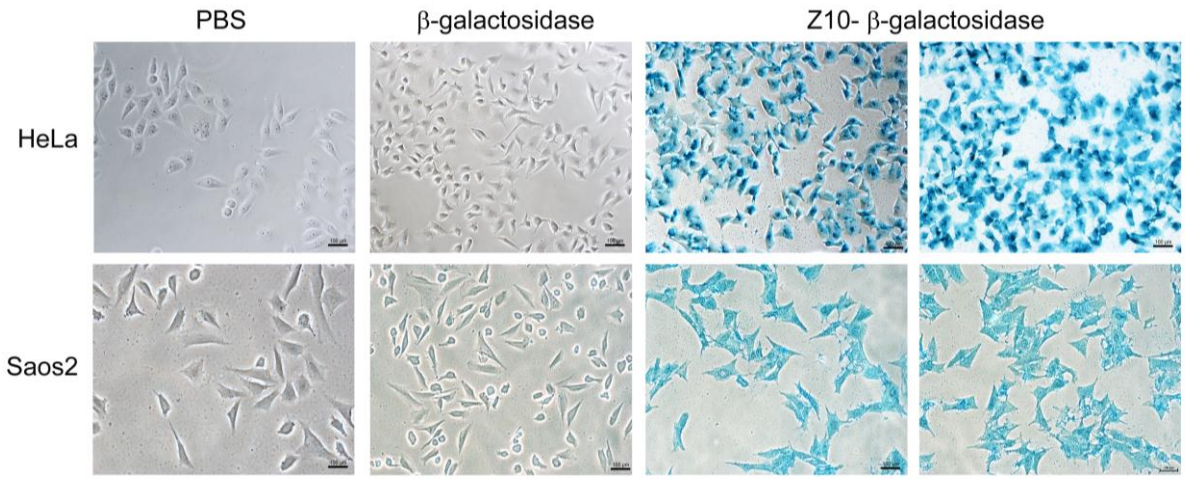

Figure 7.25 **Z10-mediated delivery of β-galactosidase into HeLa and Saos2 cells.** After 16 h incubation with 0.2 µM of Z10-β-galactosidase at 37 °C, cells were washed with 20 µg/ml heparin, fixed and stained according to the β-galactosidase Reporter Gene Staining Kit (Sigma). β-galactosidase staining was visualized by contrast phase microscopy.

The fusion protein was added to serum-free culture media of Saos2 and HeLa cells. 15 h after administration of each protein, cells were fixed and stained according to X-Gal staining Kit (Sigma). Figure 6.25 shows the successful delivery of functional β-galactosidase into HeLa and Saos2 cells as proven by the blue cellular staining. Analogous to the delivery of EGFP by ZEBRA-MD, we observed a 100 % transduced cell population using Z10-β-galactosidase. The reporter protein β-galactosidase alone was used as a negative control and no β-galactosidase activity was detected within these control cells (Figure 6.25). These results confirmed that β-galactosidase positive staining did not occur through a fixation artifact.

7.3.8 DNA binding activity

As ZEBRA is a transcription factor which binds DNA through its central basic region (DB, residues 175-195), we investigated whether the DNA binding activity is preserved in different ZEBRA truncations. It was previously shown that ZEBRA recognized the AP-1 consensus heptamer TGA $^{G}/_{C}$ TCA (Petosa *et al.*, 2006). This heptamer was used as a probe to evaluate the DNA binding activity with EMSAs (Figure 6.26). The truncations containing both, the DB and DIM domains, (Z4, Z6) bound the AP-1 probe with nearly the same efficiency as the full-length ZEBRA protein (Figure 6.26). In contrast, truncations carrying deletions in DB (Z8), DIM (Z5, Z7), or both domains (Z2, Z3), failed to bind the AP-1 probe (Figure 6.26). In agreement with (Petosa *et al.*, 2006), this data indicated that the presence of the DB and the DIM domain is required and sufficient for DNA binding. However, residual DNA-protein

complex formation was also detected for the Z1 truncation which only contained DB but no DIM domain.

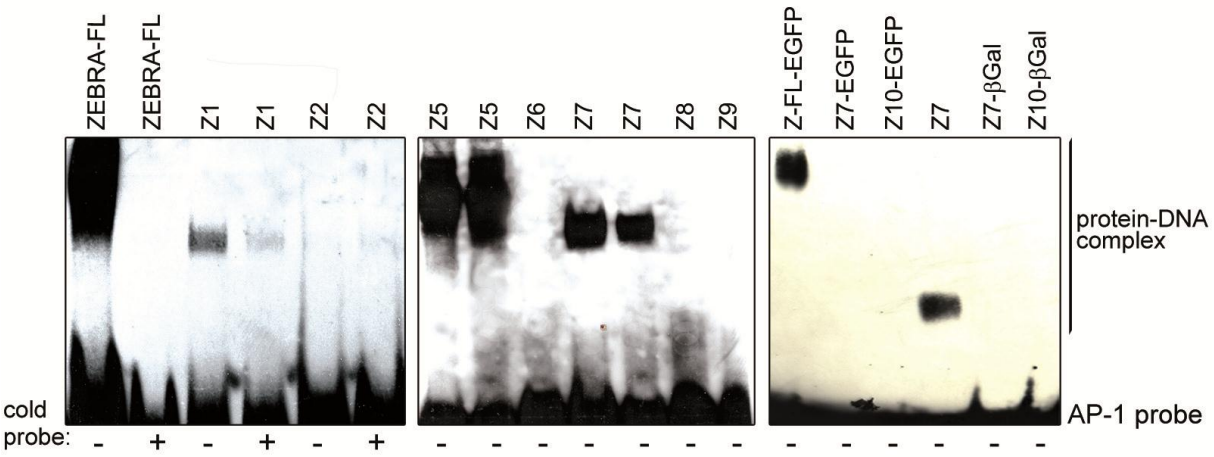

Figure 7.26 **DNA binding activity.** Electrophoretic mobility shift assay (EMSA) of recombinant ZEBRA variants. Truncated ZEBRA proteins and their respective fusion proteins were analyzed for their ability to bind AP-1 DNA probe. Signals were detected by a Chemiluminescent Assay (Pierce).

Because the truncated forms Z6 and Z10 were shown to transduce into cells, we further investigated the DNA binding activity of both peptides when fused N-terminally to EGFP or □-galactosidase reporter proteins. All fusion proteins failed to recognize the AP-1 probe as demonstrated by EMSA (Figure 6.26). In contrast, the fusion of EGFP to the full-length ZEBRA or Z4 (data not shown) had no effect on the DNA binding activity (Figure 6.26). These results suggested that conformational changes occurred after fusion of the reporter proteins with Z7 and Z10 compromising their ability to bind DNA.

7.4 Animal experimentation

7.4.1 *Ex vivo*

The spleen was recovered and a single cell suspension was made using the cell strainer (Falcon). Blood cells were lysed and cells washed twice with PBS. Spleen cells were subsequently resuspended in RPMI culture medium supplemented with 10 % serum and incubated for 3 h in presence of 5 µg/ml Z10-EGFP. Green cell fluorescence was analyzed by Flow cytometry. 7-AAD negative cells represent live cells. 67 % of the whole spleen cell population was positive for green cell fluorescence. 79 % of gated live lymphocytes and 93 % of live dendritic cells were transduced with Z10-EGFP.

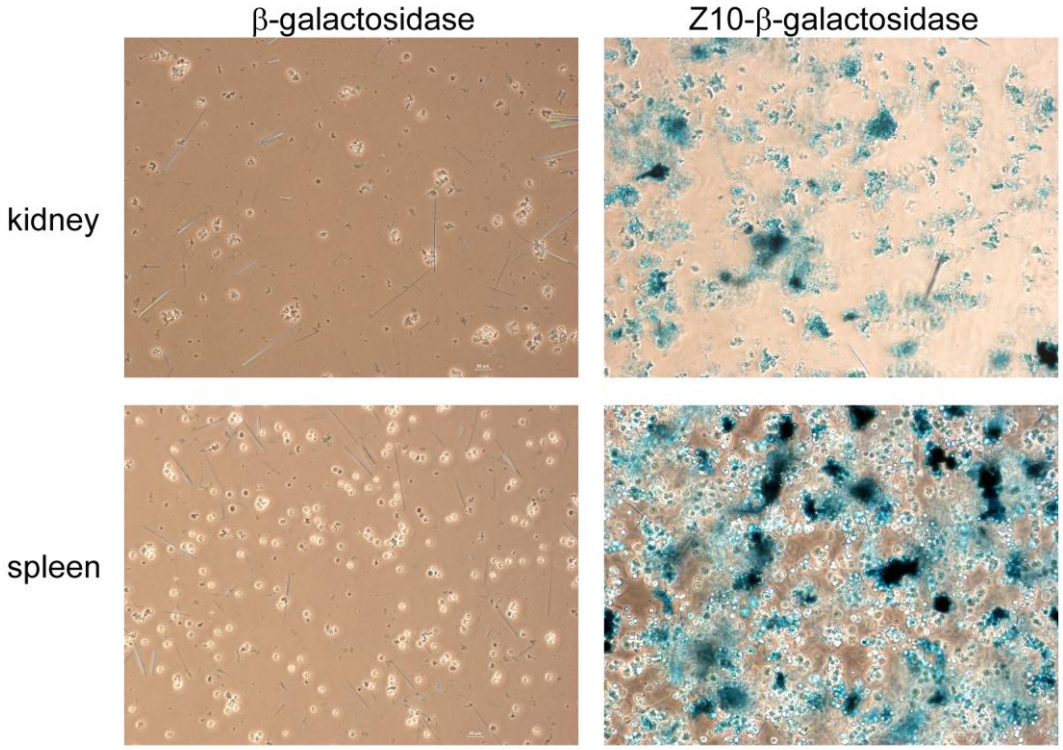

Figure 7.27 **β-galactosidase activity in kidney and spleen cells after transduction with Z10-β-gal.** For *ex vivo* studies, indicated tissues were harvest from untreated mice. A cell suspension was resuspended in RPMI culture medium supplemented with 10 % FCS. 5 µg of Z10-EGFP or Z10-β-galactosidase, respectively, were added to the culture and incubated for 3 h at 37 °C and 5 % CO_2 in a humidified atmosphere. Internalization was evaluated by microscopy after β-galactosidase staining.

These results were corroborated by the *ex vivo* transduction of spleen cells with Z10-β-galactosidase. Three organs were taken, that is, liver, spleen and kidney, and single cell suspensions were prepared as described and separately incubated with 5 µg/ml Z10-β-galactosidase. β-galactosidase positive cells were visualized by an X-Gal staining (Sigma)

and analyzed by microscopy. All three cell populations were transduced to 100 % shown by the blue cellular staining (Figure 6.27). In contrast to the cytometric analysis after the delivery of EGFP by Z10 dead cells could not be excluded. The protein β-galactosidase alone was used as a negative control and no β-galactosidase activity was detected within these control cells (Figure 6.27). These results confirmed that ZEBRA-Z10 is able to translocate not only in cell lines but also in live primary cells.

7.4.2 *In vivo*

Z10-EGFP and EGFP were labeled with a near infra-red Alexa Fluor® 647 fluorochrome (CY5) to conduct noninvasive optical imaging of mice. This experiment was carried out at the Institute Albert Bonniot, La Tronche, by assistance of Véronique Josserand. Nude mice received an intravenous injection of 50 µg Cy5-labeled Z10-EGFP or EGFP, and were imaged at different time points during 5 hours. Images were taken after 15 min, 1.5 h, 3 h and 5 h and revealed a clear difference of the distribution of both fluorescent signals in the mouse body. As shown in Figure 6.28, 15 min after injection a strong accumulation of fluorescence signals in the liver and bladder region was observed for the control mouse who received CY5-EGFP, while the CY-Z10-EGFP probe accumulated at the bladder but overall fluorescence is spread at different tissues. In the control mouse, the injected CY5-EGFP is quickly eliminated through the urinary system. Images taken from the back of the mice show concentrated signals for CY5-EGFP in both spleens of the control animal. In contrast, CY5-Z10-EGFP seemed to accumulated during the first 15 min at the spleen but is also present in other tissues. Furthermore, the fluorescence signal was washed-out quickly and could not be found in definitive spot as it was seen in the control mouse. The CY5-Z10-EGFP signal showed a somewhat stronger non-specific distribution at all-time points than the control CY5-EGFP which accumulated always in the bladder, liver, and both kidneys. CY5-Z10-EGFP fluorescence is presented as a uniform diffusion when looking at the side of the animal. One can assume the CY5-Z10-EGFP is distributed throughout various tissues and therefore failed to concentrate in specific organs. Consequently, specificity of CY5-Z10 for a single tissue or organ was not found. With this experimental setup it was possible to compare the behavior of CY5-Z10-EGFP and the control protein, CY5-EGFP alone, during 5 hours after injection to the tail vain. Even if one cannot specify the exact organs it is clear that CY5-Z10-EGFP is distributed differently than CY5-EGFP (Figure 6.28).

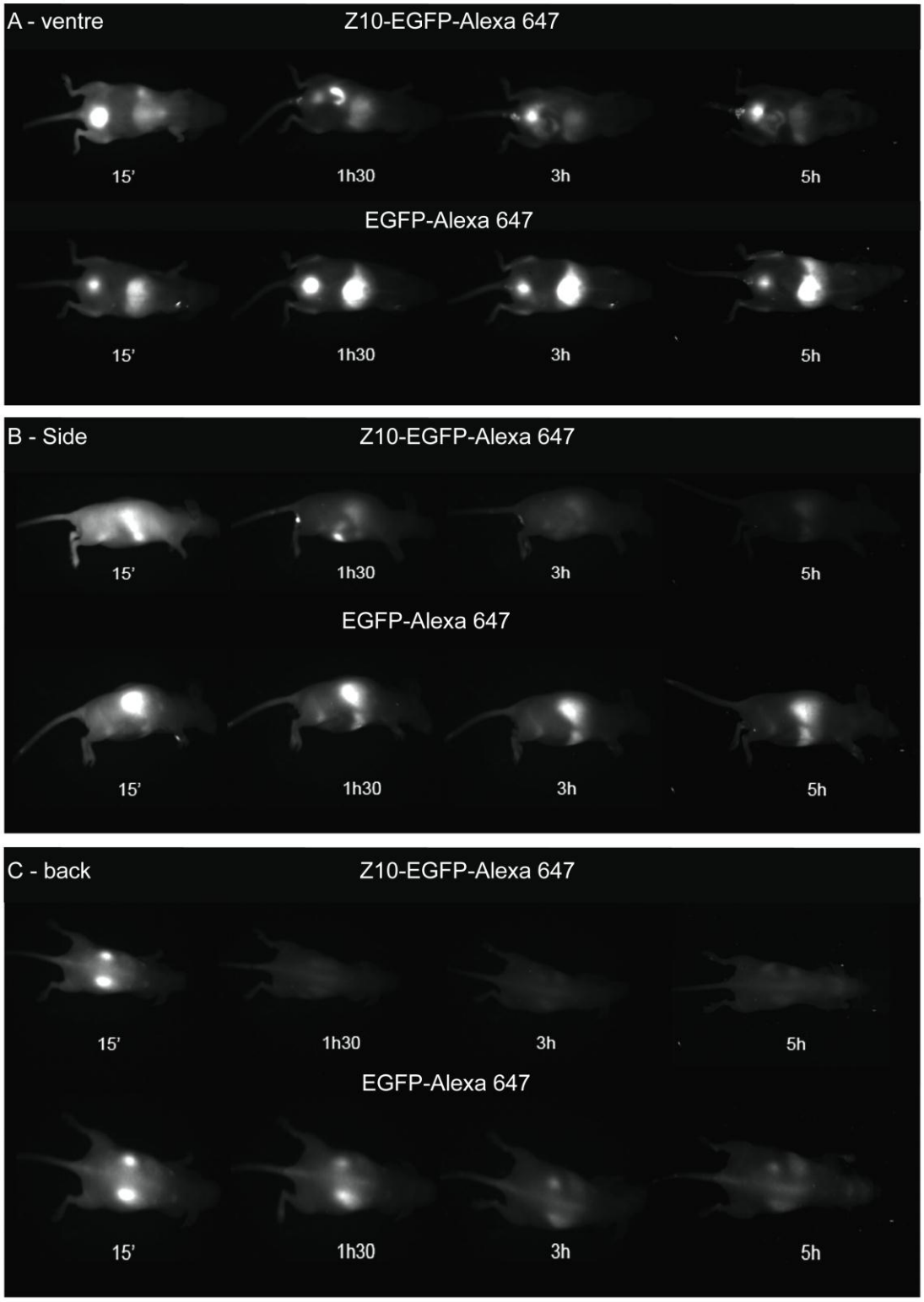

Figure 7.28 **Distribution of Z10-EGFP- Alexa Fluor® 647 and EGFP- Alexa Fluor® 647 in live mice.** 50 µg of each protein was injected intravenously. Images were taken at the indicated time points. Fluorescence reflectance imaging was performed using a Hamamatsu optical imaging system (Jin *et al.*, 2006). All fluorescence images were acquired using 200 ms and 500 ms of exposure time, with other related parameters kept constant throughout the experiment.

After 5 h both mice were sacrificed. Different organs and tissues were recovered and analyzed for fluorescence intensity (Figure 6.29). From the control mouse, the most intensive signals were found in the liver, bladder and kidney. The liver and kidney of the CY5-Z10-EGFP mouse display higher fluorescence intensity when compared to the other organs but in comparison to liver and kidney of the CY5-EGFP mouse, it is much weaker. The CY5-Z10 bladder is not fluorescent (Figure 6.29).

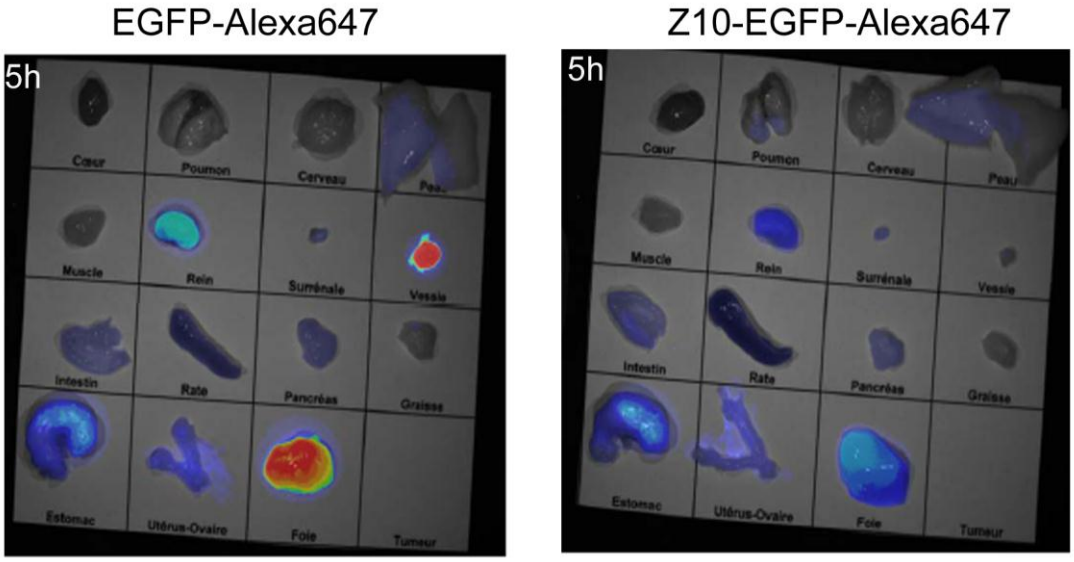

Figure 7.29 **Distribution of CY5-Z10-EGFP and CY5-EGFP.** 50 µg of each protein was injected intravenous into the tail vein. 5 hours after injection tissues were recovered and fluorescence reflectance imaging was performed using a Hamamatsu optical imaging system described at (Jin *et al.*, 2006). Fluorescence images were acquired using 1s of exposure time.

Based on these promising preliminary results a series of *in vivo* studies was carried out using either Z10-EGFP or Z10-β-galactosidase. 75 µg of the fusion proteins and control proteins without ZEBRA, respectively, were injected intraperitonally. 3 hours later, the mouse was sacrificed and liver, spleen and kidneys were recovered and used to produce a cell suspension. In case of Z10-EGFP, cells were examined for EGFP fluorescence by cytometric analysis. In one case, the entire lymphocyte population of the spleen was completely transduced as proven by EGFP positive cells. This finding was not reproducible. In 10 subsequent experiments, only a small percentage of live cells of liver (2,04 % ±1,24), spleen (9,41 % ±8,64) and kidney (3,35 % ±2,48) displayed green EGFP fluorescence after Z10-EGFP administration to the animal.

The same experiments were carried out using the Z10-β-galactosidase construct. 75 µg of protein was injected intraperitonally. Cell suspensions from liver, spleen and kidney were produced and stained with X-gal according to the protocol. In comparison to the high

throughput cytometric analysis only small quantities of the cell suspension could be examined. In all three organs, few cells displayed blue staining as an indication of functional β-galactosidase in these cells (Figure 6.30). This enzymatic activity was not found in cell suspensions from control mice (not shown), and can therefore, be considered as a proof of concept for Z10-mediated *in vivo* protein delivery. However, the fact that only few cells of the investigated organs exhibited staining showed that the overall efficiency of the transduction was low. In conclusion, ZEBRA-Z10 is capable to deliver the reporter proteins EGFP or β-galactosidase into various tissues when injected intravenously or intraperitonally into mice. It is distributed differently in the whole animal compared to the reporter proteins alone which was demonstrated by the noninvasive optical imaging in mice. Single positive cells after *in vivo* administration of Z10-EGFP or Z10-β-galactosidase in cells of liver, spleen or kidney confirmed the ability of ZEBRA-Z10 to translocate into live cells.

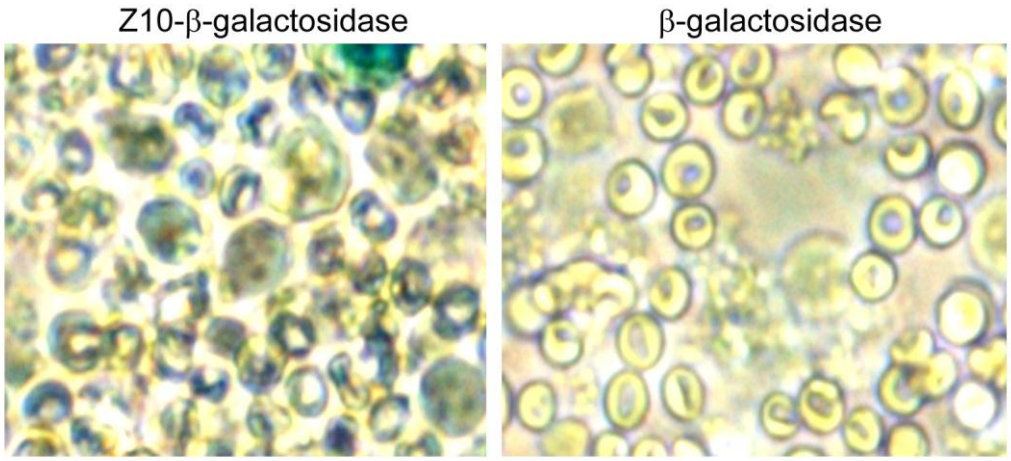

Figure 7.30 **Detection of β-galactosidase activity in single cell suspension of the liver tissues after administration of Z10-β-galactosidase and β-galactosidase.** 75µg Z10-β-galactosidase in 50 µl PBS and the same amount of β-galactosidase in PBS as a control were injected intraperitonally. Mice were sacrificed 3 h after injection. The liver was recovered and single cell suspensions were produced as described in section 5.8.5. Aliquots of these cells were stained according to the β-galactosidase staining Kit protocol (Sigma). Cells were analyzed by microscopy.

7.5 MDA-7/IL-24

7.5.1 Construction of ZEBRA-MDA-7/IL24 fusion proteins

After showing the ability of ZEBRA-MD to transport reporter proteins, such as EGFP or β-galactosidase, into the cell interior, the ZEBRA-MD transduction system was evaluated for the use in a therapeutical approach.

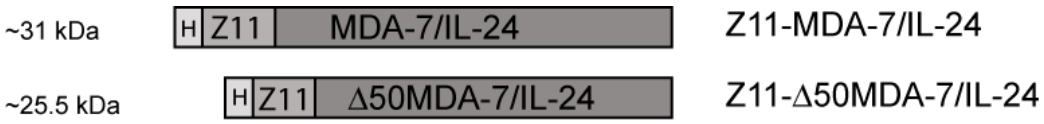

Figure 7.31 **Schematic presentation of the ZEBRA-Z11 fusion to MDA-7/IL24.** ZEBRA-MD (Z11) was fused N-terminal to full-length MDA-7/IL-24 and the truncated fragment of the protein in which the first 50 AA are deleted, respectively. Both proteins bearing an N-terminal hexa-histidine tag for purification purposes.

7.5.2 Expression and purification of Z11-MDA-7/IL24 fusion proteins

Briefly, two fusion proteins were generated as seen in Figure 6.31. In both constructs ZEBRA-Z11 served as the protein transduction domain. In-frame fusions of the C-terminus of ZEBRA-Z11 with the full-length MDA-7/IL-24 or a protein fragment of MDA-7/IL-24 carrying a deletion of its secretion sequence (AA 1-50, Δ50MDA-7/IL-24) were created using standard cloning procedures. Expression was performed in *E. coli* (DE3) BL21 after induction with 0.5 mM IPTG.

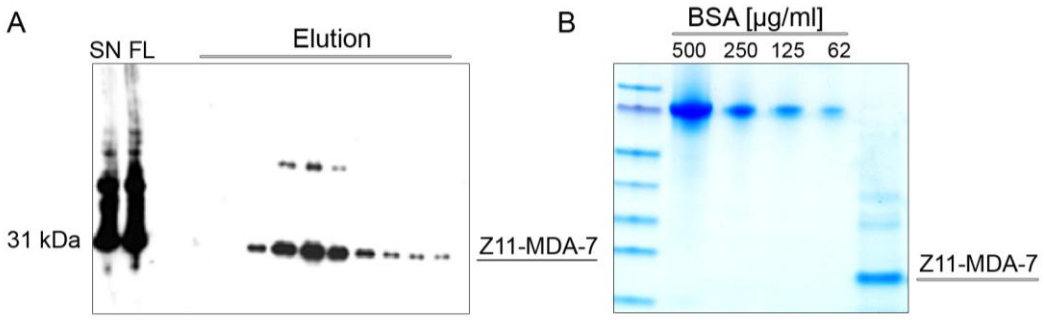

Figure 7.32 **Example of purification of Z11-MDA-7/IL-24.** A - Aliquots of each purification fraction of Z11-MDA-7/Il-24 were loaded on a 13 % SDS page, separated by electrophoresis and detected by immunoblotting using an Anti-Histidine antibody. B – Purified Z11-MDA-7/Il-24 after dialysis against PBS was loaded together with BSA concentration standards on a SDS page and visualized by Coomassie Blue staining after electrophoresis.

The soluble protein fraction was recovered from the bacterial lysate and bound to a nickel affinity column (HisGraviTrap™, Amersham) for purification. Eluted protein was separated by

SDS gel electrophoresis and visualized by Coomassie blue staining or western blotting (Figure 6.32). Positive fractions were dialyzed against 1000 volumes of PBS prior to cell culture experiments. In comparison to the Z10-EGFP or Z10-β-galactosidase recombinant proteins the MDA-7/IL-24 fusions were expressed in much lower quantities. A maximum protein yield of ~250 µg/ml of purified protein was achieved in relation to ~ 1 mg/ml of Z11-EGFP from the same bacterial expression volume. The 50 amino acids signal peptide of MDA-7/IL-24 is highly hydrophobic. A deletion of this sequence could improve the expression as well as the solubility of the recombinant protein. Unfortunately, this was not the case for Z11-Δ50MDA-7/IL-24. The deletion of the signal peptide did not lead to a higher yield of soluble protein when compared to Z11-MDA-7/IL-24 (data not shown).

7.5.3 Transduction of ZEBRA-MDA-7/IL-24

It was shown above that ZEBRA-Z11 is capable to deliver active macromolecules such as EGFP and β-galactosidase into mammalian cells. Thus, the tumor killing effect of MDA-7/IL-24 was evaluated after internalization using ZEBRA-11 as a carrier in a normal breast cell line (MCF10A) and a breast adenocarcinoma cell line (MCF7).

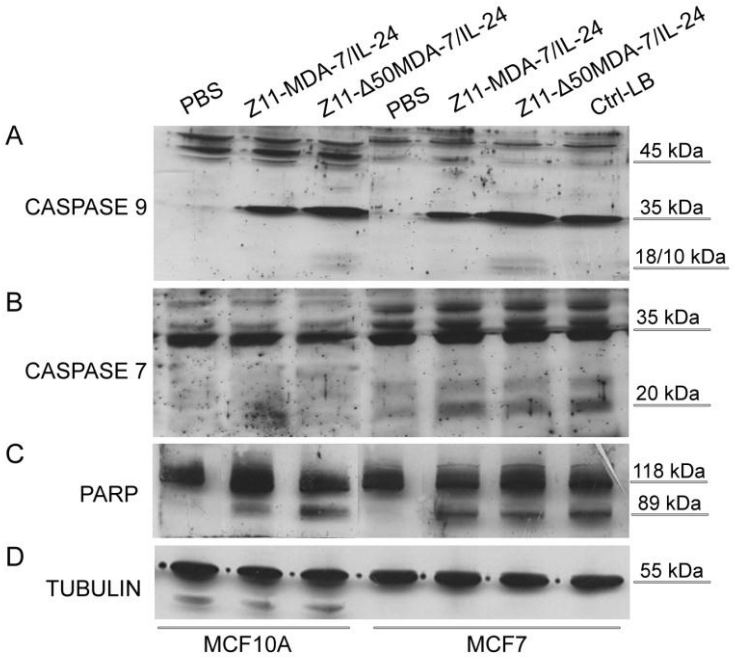

Figure 7.33 **Apoptotic protein activation by Z11-MDA-7/IL-24 fusion proteins.** Both cell lines were incubated with 0.2 µM of Z11-MDA-7/IL-24 and Z11-Δ50MDA-7/IL-24. After indicated time points, cells were lysed and the lysate was analyzed by immunoblotting. A - Caspase 9 activation was detected using an Anti-caspase 9 antibody after 15 h treatment. B - Caspase 7 and its cleaved forms were detected after 24 h treatment using an Anti-Caspase 7 antibody. C - PARP cleavage analysis after 24 h by immunological detection with an Anti-PARP antibody. As a positive control served MCF7 cells treated with pro-apoptotic Bak liposomes.

Caspase activation induced by Z11-MDA-7/IL-24

MCF7 and MCF10A cells were chosen as a model to verify the tumor specific cell-death induced by MDA-7/IL-24. In order to check the *in vitro* effect of both recombinant proteins, caspase activation was analyzed at different times. To confirm induction of apoptosis, immunoblotting was performed on cell lysate of MCF7 and MCF10A cells after Z11-MDA-7/IL-24 and Z11-Δ50MDA-7/IL-24 treatment. Antibodies against cleaved forms of different caspases were used to detect their activation. The pro-apoptotic protein Bak which is integrated in liposome was used as a positive control (Liguori *et al.*, 2008). As shown in Figure 6.33, treatment with Z11-MDA-7/IL-24 and Z11-Δ50MDA-7/IL-24 results in a total cleavage of caspase 9 in both cell lines. The antibody recognizes the full-length protein (46 kDa) and, when MDA-7/IL-24 proteins were added, the cleaved forms at 37/35, 18 and 10 kDa (Figure 6.33 A). The role of active caspase 9 is to generate the downstream executioner, caspase 7, by limited proteolysis, thereby transmitting the apoptotic signal to the execution phase. Likewise, a cleavage of PARP could be detected (Figure 6.33 C) in both, MCF7 and MCF10A, cells. PARP, a 118 kDa enzyme, is cleaved into 89- and 24-kDa fragments during drug-induce apoptosis. After 24 h treatment with both fusion proteins, faint cleaved forms of caspase 7 (20 kDa) were detected exclusively in MCF7 cells (Figure 6.33 B).

Cell viability

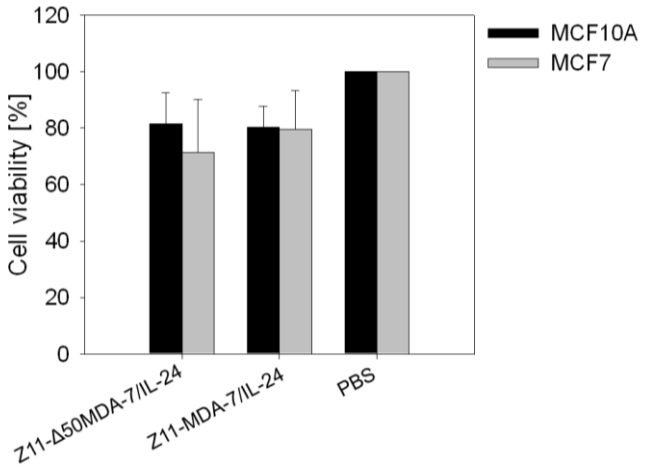

Figure 7.34 **Cytotoxicity of Z11-MDA-7/IL-24 and Z11-Δ50MDA-7/IL-24.** MCF10A and MCF7 cells were exposed to 0.2 µM of Z11-MDA-7/IL-24 and Z11-Δ50MDA-7/IL-24 and incubated in growth medium at 37 °C for 24 h. Cytotoxicity after the uptake of both fusion proteins was determined by the leakage of LDH into the culture medium. Each column represents the mean viability of two independent experiments performed in triplicates with indicated ± S.D

Another method applied for evaluating the induction of cell death was to estimate cell viability after incubation with Z11-MDA-7/IL-24 and Z11-Δ50MDA-7/IL-24. Lactate dehydrogenase (LDH) is an enzyme that is present in the cytosol of eukaryotic cells; its detection in the cell culture medium after the disruption of cell membranes can be used as an index of cell viability. MCF7 and MCF10A cells were tested accordingly and their response to 0.2 µM Z11-MDA-7/IL-24 and 0.2 µM Z11-Δ50MDA-7/IL-24 exposure was compared (Figure 6.34). After 24 h, MCF7 cells presented a loss in viability ranging between 29 % (Z11- Δ50MDA-7/IL-24) and 21 % in the presence of Z11-MDA-7/IL-24. Under the same experimental conditions, the MCF10A cell line presented cellular death of around 20 % after 24 h when treated with each of the ZEBRA fusion proteins. In conclusion, the incubation with either Z11-Δ50MDA-7/IL-24 or Z11-MDA-7/IL-24 lead to decreased cell viability in both cell lines. In agreement with the presence of apoptosis markers in healthy and cancerous cell lines, decrease of viability was the same in both cell lines.

8 DISCUSSION

With the prospect of developing ZEBRA as a protein delivery tool, it was of interest to identify the minimal transduction domain required for internalization. For this reason, numerous truncations of the full-length protein were engineered (see section 6.1). Representative protein fragments covering distinct protein domains of the full-length proteins were assessed regarding their ability to translocate into mammalian cells. In order to characterize their uptake capacities, truncations were labeled with the fluorochrome Alexa Fluor® 488 for the direct visualization of intracellular localization after internalization. All of these tested labeled proteins fragments were found in a clear vesicle-like distribution inside the cell. Furthermore, this observation was made in all of the assayed cell lines. Taken the variations in expression levels of each truncation and the consequential non-uniform fluorochrome labeling into account, a clear discrimination between truly internalized proteins and artificial uptake could not be made. Artifacts associated with fixation protocols as well as the use of fluorescent probes linked to CPPs can modify their penetrating behavior (Pichon *et al.*, 1999). Recent publications report that hydrophobic fluorescent dyes can have an impact on the uptake mechanism of CPPs and their interaction with the membrane (Morris *et al.*, 2008). In addition, it was demonstrated that not only the nature of the cargo but also the position of the probe in the peptide has an effect the interaction of the CPP with the cell membrane (El Andaloussi *et al.*, 2007). To circumvent these problems in the investigation of uptake characteristics of ZEBRA truncations, the peptides were covalently linked (by cloning and expression) to EGFP and β-galactosidase. Two different reporter proteins were used in order to estimate the impact of a specific cargo on uptake efficiency.

Characterization of transduction capacities of ZEBRA truncations was evaluated for constructs that were fused to the reporter protein EGFP. Thereby, four truncations of ZEBRA, namely Z5, Z7, Z10 and Z11 were identified, that had the ability to transfer EGFP into live cells. All truncations with protein translocation ability contained the basic positively charged DB domain, as well as the hydrophobic leucine-rich DIM domain of ZEBRA (Petosa *et al.*, 2006; Sinclair, 2006), whereas truncated proteins missing either of the two domains failed to translocate EGFP into cells. The 48 amino acid peptide Z11 was the smallest ZEBRA truncation with transduction abilities. It was therefore denoted minimal domain (MD).
The identification of the ZEBRA minimal domain and the characterization of protein uptake characteristics were carried out in partially overlapping periods of this thesis work. Therefore, the uptake mechanism, functionality of delivered proteins, as well as cell toxicity of ZEBRA-mediated protein uptake were investigated using the Z10 peptide which was already sufficiently small to expect loss of most of the functions of the natural ZEBRA protein.

The uptake of Z10-EGFP was temperature-dependent, presumably due to the fluidity loss of the lipid bilayer at low temperatures (Veach *et al.*, 2004). Since uptake of Z10-EGFP into ATP-depleted cells only decreased by 20 %, it was concluded that the Z10 fusion protein is internalized by a largely ATP-independent process. Furthermore, several endocytotic inhibitors, such as nystatin, wortmannin or chlorpromazine, did not interfere with Z10-EGFP uptake, indicating no participation of receptor-mediated endocytosis (Fuchs & Raines, 2004; Kaplan *et al.*, 2005; Richard *et al.*, 2005; Wadia *et al.*, 2004; Watson *et al.*, 2005). This finding was further supported by the lacking colocalization of Z10-EGFP with caveolin1 and clathrin. Furthermore, neither the early endosomal marker, EEA-1, nor the late endosomal marker Rab-7, are involved in transport of cargo from early to late endosomes, showed a complete co-localization in microscopic images. Only the incubation with methyl-β-cyclodextrin (MβCD), a drug that inhibits lipid raft mediated endocytosis (Wadia *et al.*, 2004), caused a 40 % decreased uptake of Z10-EGFP. Thus, the endocytotic pathway contributed significantly to the overall uptake of Z10-EGFP under the applied conditions, but did not account for the majority of the internalized fusion protein. In addition, uptake of Z10-EGFP required availability of cell surface HSPGs since its internalization was clearly impaired in the presence of heparin. Similar to other CPPs that are taken up in a HSPG-dependent manner, the cell surface binding of Z10 appears to be facilitated by the interaction of the highly positively charged DB region and the negatively charged HSPGs (Fuchs & Raines, 2006; Ziegler & Seelig, 2004; Zorko & Langel, 2005). However, as witness by the failure of the DB-containing Z5 truncation to enable protein uptake, the presence of a positively charged domain alone is not sufficient for protein internalization. Only when the DB was present together with the hydrophobic DIM domain, efficient protein uptake was observed. It was earlier established that DB and DIM domain together form a continuous stretch of an α-helix (Petosa *et al.*, 2006), which is similar to other amphipathic CPPs including MAP or Transportan (Lindgren *et al.*, 2000; Zorko & Langel, 2005). For those peptides, an increase in membrane permeability that correlates with the presence of amphiphilic α-helical structures has been observed (Dietz & Bahr, 2004). Accordingly, internalization of MD may require the α-helix formed by DB and DIM domain. Furthermore, the DB domain might mediate surface binding of MD while the DIM domain subsequently facilitates translocation through the lipid bilayer by hydrophobic interactions in a similar way as reported for Penetratin (Joliot & Prochiantz, 2008).

ZEBRA is internalized via a non-endocytotic, and receptor as well as transporter-independent pathway. Penetratin requires the hydrophobic tryptophan residues and crosses lipid bilayers without pore formation (Terrone *et al.*, 2003; Thoren *et al.*, 2000). In line with

these arguments, also the Z10-mediated protein translocation did not cause disruption or pore formation in the plasma membrane as shown by the absence of both, 7-AAD uptake and leakage of lactate dehydrogenase (LDH) in transduced cells. Taken together the energy-independent uptake of MD-EGFP, the decreased uptake of MD-EGFP into cells at low temperatures, as well as lacking exclusive colocalization with endosomal markers, and incomplete inhibition of MD-EGFP uptake by endocytotic inhibitors suggest that MD-EGFP is, at least in part, translocated directly across the lipid bilayer. This energy-independent internalization property of ZEBRA-MD-EGFP is highly advantages, since endosomal trapping can be circumvent, which seems to be the major bottleneck for most CPP, as for example TAT, which enters cell by macropinocytosis (Kaplan *et al.*, 2005) and fails to enter into liposomes (Kramer & Wunderli-Allenspach, 2003; Zorko & Langel, 2005).

Additionally, the ability of the truncated ZEBRA proteins to bind DNA was evaluated. As it was expected, constructs encompassing both the basic DB and the DIM domain recognized and bound the AP-1 site *in vitro*. Interestingly, this specific binding was lost when these proteins were fused C-terminal to either EGFP or β-galactosidase. As it was shown in the crystal structure of ZEBRA binding to the AP-1 promoter element, DNA binding of the protein requires complex conformation of its C-terminal part, and mutations in the latter were suggested to inactivate transcription factor activity of ZEBRA (Petosa *et al.*, 2006). Thus, the C-terminal fusion of proteins to truncated forms of ZEBRA may have compromised its ability to form protein-DNA complexes. The loss of its DNA-binding activity when fused to proteins is certainly to the best advantages for the development of a new potential protein delivery system. Even through a possible interaction between Zebras' MD and cellular proteins after its uptake into cells cannot be completely ruled out, since it was not examined in the presented study. As the full-length ZEBRA protein can induce growth arrest independently of its ability to bind DNA in host cells through direct interplay with cellular proteins and its basic region (Rodriguez *et al.*, 1999; Rodriguez *et al.*, 2001), possible effect on cellular proteins need to be analyzed.

In addition, a rapid internalization of Z10-EGFP into a wide range of different cells was observed. Z10-delivered proteins remained functional when transduced into cells, as demonstrated by the enzymatic activity of internalized Z10-β-galactosidase. In conclusion, Z10 is a new carrier suitable for the efficient transport of proteins into live mammalian cells. Since its uptake is largely independent from known endocytotic pathways, ZEBRA-MD can carry proteins into cells without being trapped in endosomal compartments. Additionally, it does not show any toxic side effects and transduce a wide range of mammalian cell with 100 % efficiency.

The reason why ZEBRA exhibit this translocation property is not clear. Some transcription factors can be transferred from cell to cell because of the presence of a specific protein domain. This is reported for homeoproteins, such as Antennapedia or Engrailed and TAT. The internalization of these transcription factors is part of a physiological process (Prochiantz, 2000; Prochiantz & Joliot, 2003). This could also be the case for the viral transcription factor ZEBRA. It can be assumed that, ZEBRA can exit EBV infected cells, either by secretion or cell lysis before it is re-internalized in neighbor cells to induce lytic cycle. Indeed, in the context of the EBV biological cycle, the protein is expressed during the productive cycle and thus could potentially be released by EBV infected cells. This paracrine function is also described for other transcription factors, namely TAT or Antennapedia (Prochiantz & Joliot, 2003).

Linkage of ZEBRA-MD to EGFP and β-galactosidase allowed the non-invasive import of these cargo molecules into cells *ex vivo* as well as in animals. *Ex vivo* cell suspensions were transduced with up to 100 % efficiency by both, Z10-EGFP and Z10-β-galactosidase. Moreover, after administrating Alexa Fluor® 647 (CY5) labeled Z10-EGFP to live mice a considerable difference to CY5-EGFP in terms of tissue distribution and clearance from the body was observed. The Alexa Fluor 647 labeled reporter protein EGFP was eliminated from the body via the urinary system, shown by a concentration in the kidney area and the bladder. Contrary to the control, the Z10-linked peptide appeared to show much wider tissue distribution and did not accumulate in distinct organs. This observation confirms the assumption that transduced proteins appear to be cleared from the body not by conventional mechanisms, but based on the half-life of the protein (Schwarze & Dowdy, 2000).

However, these data could not be confirmed in a complementary assay where tissue distribution of Z10-EGFP and EGFP alone was analyzed by cytometric analysis after intraperitonal administration to mice. This lack of agreement between both experimental approaches might have been caused by different sensitivities of the analytical methods, as well as the different route of administration of the fusion protein. Possibly the sensitivity to detect EGFP fluorescence in single cells by flow cytometry did not suffice even though Z10-EGFP was transduced into the cells. This could be a consequence of the relatively low amount (75 µg) of injected protein. Therefore, the fusion protein Z10-β-galactosidase was used for further *in vivo* studies. β-galactosidase is 120 kDa protein and has a high specific activity, therefore, requiring only a low level of internalized protein to be detected in tissues (Schwarze & Dowdy, 2000). Following *in vivo* administration of this construct, detection of blue-stained cells in several tissues revealed successful Z10-dependent delivery of galactosidase. In 1999, the Tat-β-galactosidase fusion protein was delivered into almost all

tissues including the brain, following intraperitonal injection into mice (Schwarze *et al.*, 1999). Intraperitonal injection of 200 µg of TAT–β-gal protein resulted in readably detectable TAT–β-gal enzymatic activity in all tissues assayed, with all regions of the brain demonstrating enzymatic activity.
Cell staining in the here presented experiments appears to be somewhat weaker than the one reported by Schwarze et al and Cai et al (Cai *et al.*, 2006; Schwarze *et al.*, 1999). However, the low dose of only 75 µg of Z10-galactosidase which was injected per animal may partially explain the low *in vivo* efficiency. Alternatively, Z10-mediated protein delivery might be less effective than the TAT-mediated process. Further studies are needed to clarify this question.

Contrary to earlier studies (Mahot *et al.*, 2005), cell type-specific internalization of Z10-EGFP was not observed in this work. The missing cell specificity *per se* was also observed for other cell penetrating peptides, such as TAT and Penetratin (Letoha *et al.*, 2003; Schwarze *et al.*, 1999), and represents a disadvantage compared to the so called homing peptides. These peptides are able to recognize specific cell type or tissues and can therefore function more efficiently because of a higher concentration at the site of action (Laakkonen *et al.*, 2002; Ruoslahti, 2000).

To circumvent the missing cell specificity of Zebras'-MD, Z11 was fused to the melanoma differentiation associated gene-7 (MDA-7/IL-24). A cancer-specific MDA-7/IL-24-mediated killing of cells was reported in many research publications (Lebedeva *et al.*, 2003; Sauane *et al.*, 2003a; Su *et al.*, 2006). By fusion of ZEBRA-MD to MDA-7/IL624 it was tried to combine the strong ability of crossing cell membranes, provided by ZEBRA-MD, and tumor specific function, provided by MDA7, to construct an efficient anti-tumor therapeutic. MDA-7/IL-24 induces apoptosis in wide range of cancer cells(Jiang *et al.*, 1996; Saeki *et al.*, 2000; Sarkar *et al.*, 2002; Su *et al.*, 1998) which can be monitored by the cleavage of apoptosis specific caspases. In this study, Z11-MDA-7/IL-24-induced cleavage of caspase 9 and 7 as well as PARP was detected in transduced cell lines. However, the cleaved form of caspase 9 and of PARP could be detected in both, the normal (MCF10A) and the tumor (MCF7) breast cell line. Only the activation of caspase 7 was observed solely in MCF7 cells. Moreover, cell viability of both cell lines was compared after exposure of Z11-MDA-7/IL-24 and Z11-Δ50MDA-7/IL-24. A decrease of viability by 20 % was observed for the normal as well as for the tumor cell line. This leads to the conclusion that by fusing MDA-7/IL-24 to the MD of ZEBRA the tumor specificity of MDA-7/IL-24-induced cell death is lost.

The cytokine MDA-7 exerts its antitumor activity in a spectrum of cancer cells via multiple cell type-dependent signaling pathways resulting in apoptosis (Lebedeva *et al.*, 2003; Lebedeva *et al.*, 2005; Sauane *et al.*, 2008; Su *et al.*, 2006). Several studies documented that intracellular MDA-7/IL-24 localizes to the endoplasmic reticulum (ER) and induces ER stress response after over-expression of recombinant MDA-7/IL-24 in supraphysiological levels, which eventually promotes apoptosis of cancer cells (Sauane *et al.*, 2008). It seems that only $p38^{MAPK}$ and PKR are necessary components for MDA-7/IL-24-mediated apoptosis since blocking these inhibits killing. The particular mechanism of cancer cell killing appears to follow one of several alternative pro-apoptotic pathways, likely depending on the cell context. Associated with the cell cycle arrest was the induction of apoptosis in Ad.mda-7-infected tumor cells, as evidenced by the activation of caspase-3 and caspase-9 and cleavage of poly(ADP-ribose) polymerase (PARP) (Gopalan *et al.*, 2005; Lebedeva *et al.*, 2002; Saeki *et al.*, 2000). Therefore the cleavage of the pro-apoptotic molecules such as caspase-9 and PARP was used to monitor induction of apoptosis by Z10-MDA-7/IL-24. Contrary to expectation, by fusing MDA-7/IL-24 to ZEBRA-MD the cancer cell specificity is lost. Due to time constraints, the control, the MDA-7/IL-24 protein alone, is missing. This result could give an explanation for the loss of tumor specificity when fused to ZEBRA. ZEBRA-MD facilitates the transfer of the cytokine into cell circumventing thereby an interaction of MDA-7/IL-24 with unidentified receptors or non-receptor mediators at the cell surface (Lebedeva *et al.*, 2007; Sauane *et al.*, 2003b). Thus, it is possible that the interaction at the membrane level is crucial for the cancer cell specific function of MDA-7/IL-24. Even if the delivery of MDA-7/IL-24 by ZEBRA-MD does not lead to the expected cancer cell specific killing, with additional experiments it can give an interesting insight into the mechanism of tumor cell specificity of MDA-7/IL-24.

Taken all these favorable characteristics together, ZEBRA-MD represents a novel and very promising delivery tool for biologically active proteins. In conclusion, with the identification of the minimal transduction domain of ZEBRA and the characterization of its cell penetration properties when fused to full-length cargo proteins, a big step forward to the development of a new, efficient and powerful protein delivery system was made.

8.1 Sommaire de discussion en française

Dans le but de développer ZEBRA comme système de transport de protéines, il était essentiel d'identifier le domaine de transduction minimal nécessaire pour l'internalisation. Pour cette raison, j'ai construit de nombreuses constructions tronquées et caractérisé leurs capacités de transduction après fusion avec la protéine rapporteuse EGFP. J'ai identifié quatre troncations de ZEBRA, Z5, Z7, Z10 et Z11, qui avaient la capacité de transférer EGFP dans les cellules vivantes. Tous les troncations avec la capacité de translocation de protéine contiennent aussi bien le domaine de fixation d'ADN que le domaine de dimérisation de ZEBRA (Petosa et al., 2006; Sinclair, 2006) alors que toutes les protéines tronquées ne contenant aucun de ces deux domaines ont échoué dans le transport d'EGFP vers les cellules. Les 48 acides aminés Z11 était la plus petite construction de ZEBRA avec des propriétés de transduction. Il a donc été appelé le domaine minimal (MD). Son mécanisme d'internalisation, la fonctionnalité des protéines livrées, aussi bien que toxicité cellulaire ont été caractérisée.

L'internalisation MD-EGFP était dépendante de la température, probablement en raison de la perte de fluidité de la double couche lipidique à des températures basses (Veach et al., 2004). Le transfert de MD-EGFP dans les cellules limitées en ATP ayant été réduite de 20 %, j'en ai conclu que la protéine de fusion MD est internalisée par un processus étant ATP-indépendant. En outre, plusieurs inhibiteurs endocytotiques, comme nystatin, wortmannin ou chlorpromazine, n'ont aucun effet significatif sur le transport de MD-EGFP, indiquant que l'endocytosis n'est pas impliqué dans le mécanisme de translocation (Fuchs & Raines, 2004; Kaplan *et al.*, 2005; Richard *et al.*, 2005; Wadia *et al.*, 2004; Watson *et al.*, 2005). Cette conclusion est soutenue par la faible colocalization de MD-EGFP avec caveolin1 et clathrin. En outre, ni le marqueur EEA-1, ni le marqueur Rab-7, que l'on retrouve respectivement dans les endosomes précoces et tardifs, ne co-localisaient avec MD-EGFP. Seule l'incubation avec le méthyle-β-cyclodextrin (MβCD), un médicament qui inhibe la voie d'endocytosis médiée par les radeaux lipidiques (Wadia et al., 2004), a diminué l'internalisation de MD-EGFP de 40 %.

Ainsi, la voie d'endocytosis contribue de façon significative à la translocation de MD-EGFP dans nos conditions expérimentales, mais ne représente à la voie majeure de translocation de MD. De plus, le transport de MD-EGFP nécessite la disponibilité de héparanes sulfates protéoglycans (HSPGs) associés à la surface de la cellule. En effet l'internalisation a été diminuée dramatiquement en présence d'héparine, un inhibiteur de HSPGs. Similaire à d'autres CPPs qui sont internalisés de manière HSPG-dépendante, la liaison de MD à la

surface de cellule est facilitée par l'interaction de la région de fixation d'ADN de charge hautement positive avec celle de HSPGs négativement chargée (Fuchs & Raines, 2006; Ziegler & Seelig, 2004; Zorko & Langel, 2005).

Pourtant, comme en témoigne l'échec de la troncation de Z6 à être internalisé, contenant le domaine DB, la présence d'un domaine positif chargé seul n'est pas suffisante pour la translocation de la protéine. Celle-ci a été observée seulement quand le DB et le domaine DIM étaient présents ensemble. Il a été établi plus tôt que le DB et le domaine DIM forment ensemble une étendue continue d'une α-hélice (Petosa et al., 2006), qui est similaire à d'autre CPPs amphipathic en incluant MAP ou Transportan (Lindgren *et al.*, 2000; Zorko & Langel, 2005). Pour ces peptides, une augmentation de la perméabilité de la membrane qui est en corrélation avec la présence de structures amphiphiliques et α-hélicoïdes a été observée (Dietz & Bahr, 2004). En conséquence, l'internalisation de MD peut exiger l'α-hélice formée par les domaines DB et DIM. En outre, le domaine de DB pourrait véhiculer la liaison de MD à la surface de la cellule, mais le domaine DIM facilite par la suite la translocation de membrane cellulaire par les interactions hydrophobes de façon semblable à celle décrite pour Penetratin (Joliot & Prochiantz, 2008). Ce CPP est intériorisé via une voie indépendante d'endocytose, aussi bien comme récepteur que comme transporteur. Penetratin besoin des résidus tryptophane et passe la membrane âpres la formation de pore (Terrone *et al.*, 2003; Thoren *et al.*, 2000). Conformément à ces arguments, aussi la translocation de MD n'a pas provoqué de perturbation ou la formation de pores dans la membrane comme le montre l'absence d'absorption de 7-AAD et la fuite de lactate dehydrogenase (LDH) dans les cellules après la transduction.

Finalement, j'ai aussi observé une translocation de MD-EGFP dans les liposomes synthétiques. Tous ces facteurs pris ensemble – l'internalisation indépendante de l'énergie de MD-EGFP, le transport inhibé de MD-EGFP dans les cellules à basses températures, ainsi que le manque de colocalisation exclusif avec les marqueurs endosomes et l'inhibition incomplète d'internalisation de MD-EGFP par les inhibiteurs endocytotiques - suggère que MD-EGFP traverse, au moins partiellement, la membrane cellulaire par translocation directe. Cette propriété d'internalisation indépendante de l'énergie de ZEBRA-MD-EGFP est hautement avantageuse puisque l'inclusion dans les endosomes peut être détourné, ce qui semble être un problème important pour la plupart des CPP, comme le montre l'exemple de TAT qui rentre dans la cellule par macropinocytose (Kaplan et al., 2005) et ne transloque pas dans les liposomes (Kramer & Wunderli-Allenspach, 2003; Zorko & Langel, 2005).

De plus, j'ai évalué la capacité des protéines de ZEBRA tronquées à fixer l'ADN. Comme attendu, les constructions couvrant le DB et le domaine DIM ont reconnu et attaché l AP1 *in vitro*. D'une façon intéressante, cette liaison spécifique a été perdue quand ces protéines étaient fusionnées en C-terminal à EGFP ou à β-galactosidase. Comme il a été montré dans

la structure en cristal de ZEBRA se liant à l'élément de promoteur AP 1 , la liaison de l'ADN avec la protéine nécessite une conformation complexe de sa partie de C-terminus et les mutations dans cette partie ont été suggérées pour inactiver l'activité du facteur de transcription de ZEBRA (Petosa et al., 2006). Ainsi, la fusion en C-terminus de protéines aux formes tronquées de ZEBRA peut avoir compromis sa capacité à former des complexes d'ADN-protéine. La perte de son activité de fixation à l'ADN lors de la fusion aux protéines est un avantage non négligeable pour le développement d'un nouveau système de transport de protéines. Comme la protéine entière de ZEBRA peut inciter l'arrêt de la croissance indépendamment de sa capacité à fixer l'ADN dans les cellules hôtes par interaction directe avec les protéines cellulaires et sa région DB (Rodriguez et al., 1999; Rodriguez et al., 2001), l'effet potentiel sur les protéines cellulaires doit être analysé.

Contrairement au transport de ZEBRA décrit précédemment dans les lymphocytes (Mahot et al., 2005) annoncé auparavant, j'ai observé une internalisation rapide de MD-EGFP dans une large gamme de différentes cellules. Les protéines transportées par MD sont restées fonctionnelles après internalisation dans les cellules, comme démontré par l'activité enzymatique de MD-β-galactosidase. En conclusion, MD est un nouveau transporteur prometteur pour la transduction efficace de protéines dans les cellules mammifères vivantes. Puisque son mécanisme d'internalisation est grandement indépendant d'une voie d'endocytose connu, le ZEBRA-MD peut transporter des protéines dans les cellules sans être retenu dans les compartiments endosomal. De plus, il ne montre pas d'effets indésirables toxiques et a une efficacité de translocation de 100% dans de nombreuses cellules mammifères. Toutes ces caractéristiques favorables prises ensembles montrent que le ZEBRA-MD représente un transporteur original et très prometteur pour les protéines thérapeutiques.

9 TABLE OF FIGURES

10 LIST OF TABLES

11 REFERENCES

Adamson, A. L., Darr, D., Holley-Guthrie, E., Johnson, R. A., Mauser, A., Swenson, J. & Kenney, S. (2000). Epstein-Barr virus immediate-early proteins BZLF1 and BRLF1 activate the ATF2 transcription factor by increasing the levels of phosphorylated p38 and c-Jun N-terminal kinases. *J Virol* **74**, 1224-1233.

Aho, S., Buisson, M., Pajunen, T., Ryoo, Y. W., Giot, J. F., Gruffat, H., Sergeant, A. & Uitto, J. (2000). Ubinuclein, a novel nuclear protein interacting with cellular and viral transcription factors. *J Cell Biol* **148**, 1165-1176.

Anderson, R. G. (1998). The caveolae membrane system. *Annu Rev Biochem* **67**, 199-225.

Araki, N., Johnson, M. T. & Swanson, J. A. (1996). A role for phosphoinositide 3-kinase in the completion of macropinocytosis and phagocytosis by macrophages. *J Cell Biol* **135**, 1249-1260.

Bailey, S. G., Verrall, E., Schelcher, C., Rhie, A., Doherty, A. J. & Sinclair, A. J. (2009). Functional interaction between Epstein-Barr virus replication protein Zta and host DNA damage response protein 53BP1. *J Virol* **83**, 11116-11122.

Baumann, M., Gires, O., Kolch, W., Mischak, H., Zeidler, R., Pich, D. & Hammerschmidt, W. (2000). The PKC targeting protein RACK1 interacts with the Epstein-Barr virus activator protein BZLF1. *Eur J Biochem* **267**, 3891-3901.

Belting, M. (2003). Heparan sulfate proteoglycan as a plasma membrane carrier. *Trends Biochem Sci* **28**, 145-151.

Cai, S. R., Xu, G., Becker-Hapak, M., Ma, M., Dowdy, S. F. & McLeod, H. L. (2006). The kinetics and tissue distribution of protein transduction in mice. *Eur J Pharm Sci* **27**, 311-319.

Caron, N. J., Quenneville, S. P. & Tremblay, J. P. (2004). Endosome disruption enhances the functional nuclear delivery of Tat-fusion proteins. *Biochem Biophys Res Commun* **319**, 12-20.

Caudell, E. G., Mumm, J. B., Poindexter, N. & other authors (2002). The protein product of the tumor suppressor gene, melanoma differentiation-associated gene 7, exhibits immunostimulatory activity and is designated IL-24. *J Immunol* **168**, 6041-6046.

Cayrol, C. & Flemington, E. K. (1995). Identification of cellular target genes of the Epstein-Barr virus transactivator Zta: activation of transforming growth factor beta igh3 (TGF-beta igh3) and TGF-beta 1. *J Virol* **69**, 4206-4212.

Cayrol, C. & Flemington, E. (1996a). G0/G1 growth arrest mediated by a region encompassing the basic leucine zipper (bZIP) domain of the Epstein-Barr virus transactivator Zta. *J Biol Chem* **271**, 31799-31802.

Cayrol, C. & Flemington, E. K. (1996b). The Epstein-Barr virus bZIP transcription factor Zta causes G0/G1 cell cycle arrest through induction of cyclin-dependent kinase inhibitors. *Embo J* **15**, 2748-2759.

Chada, S., Bocangel, D., Ramesh, R., Grimm, E. A., Mumm, J. B., Mhashilkar, A. M. & Zheng, M. (2005). mda-7/IL24 kills pancreatic cancer cells by inhibition of the Wnt/PI3K

signaling pathways: identification of IL-20 receptor-mediated bystander activity against pancreatic cancer. *Mol Ther* **11**, 724-733.

Chaiken, I. M. & Williams, W. V. (1996). Identifying structure-function relationships in four-helix bundle cytokines: towards de novo mimetics design. *Trends Biotechnol* **14**, 369-375.

Chen, L. & Harrison, S. D. (2007). Cell-penetrating peptides in drug development: enabling intracellular targets. *Biochem Soc Trans* **35**, 821-825.

Chi, T. & Carey, M. (1993). The ZEBRA activation domain: modular organization and mechanism of action. *Mol Cell Biol* **13**, 7045-7055.

Coeytaux, E., Coulaud, D., Le Cam, E., Danos, O. & Kichler, A. (2003). The cationic amphipathic alpha-helix of HIV-1 viral protein R (Vpr) binds to nucleic acids, permeabilizes membranes, and efficiently transfects cells. *J Biol Chem* **278**, 18110-18116.

Conner, S. D. & Schmid, S. L. (2003). Regulated portals of entry into the cell. *Nature* **422**, 37-44.

Console, S., Marty, C., Garcia-Echeverria, C., Schwendener, R. & Ballmer-Hofer, K. (2003). Antennapedia and HIV transactivator of transcription (TAT) "protein transduction domains" promote endocytosis of high molecular weight cargo upon binding to cell surface glycosaminoglycans. *J Biol Chem* **278**, 35109-35114.

Crystal, R. G. (1995). Transfer of genes to humans: early lessons and obstacles to success. *Science* **270**, 404-410.

Davidson, T. J., Harel, S., Arboleda, V. A., Prunell, G. F., Shelanski, M. L., Greene, L. A. & Troy, C. M. (2004). Highly efficient small interfering RNA delivery to primary mammalian neurons induces MicroRNA-like effects before mRNA degradation. *J Neurosci* **24**, 10040-10046.

Derossi, D., Joliot, A. H., Chassaing, G. & Prochiantz, A. (1994). The third helix of the Antennapedia homeodomain translocates through biological membranes. *J Biol Chem* **269**, 10444-10450.

Derossi, D., Calvet, S., Trembleau, A., Brunissen, A., Chassaing, G. & Prochiantz, A. (1996). Cell internalization of the third helix of the Antennapedia homeodomain is receptor-independent. *J Biol Chem* **271**, 18188-18193.

Derossi, D., Chassaing, G. & Prochiantz, A. (1998). Trojan peptides: the penetratin system for intracellular delivery. *Trends Cell Biol* **8**, 84-87.

Deshayes, S., Heitz, A., Morris, M. C., Charnet, P., Divita, G. & Heitz, F. (2004a). Insight into the mechanism of internalization of the cell-penetrating carrier peptide Pep-1 through conformational analysis. *Biochemistry* **43**, 1449-1457.

Deshayes, S., Plenat, T., Aldrian-Herrada, G., Divita, G., Le Grimellec, C. & Heitz, F. (2004b). Primary amphipathic cell-penetrating peptides: structural requirements and interactions with model membranes. *Biochemistry* **43**, 7698-7706.

Deshayes, S., Morris, M. C., Divita, G. & Heitz, F. (2005). Interactions of primary amphipathic cell penetrating peptides with model membranes: consequences on the mechanisms of intracellular delivery of therapeutics. *Curr Pharm Des* **11**, 3629-3638.

Dietz, G. P. & Bahr, M. (2004). Delivery of bioactive molecules into the cell: the Trojan horse approach. *Mol Cell Neurosci* **27**, 85-131.

Dreyfus, D. H., Nagasawa, M., Kelleher, C. A. & Gelfand, E. W. (2000). Stable expression of Epstein-Barr virus BZLF-1-encoded ZEBRA protein activates p53-dependent transcription in human Jurkat T-lymphoblastoid cells. *Blood* **96**, 625-634.

El-Guindy, A. S. & Miller, G. (2004). Phosphorylation of Epstein-Barr virus ZEBRA protein at its casein kinase 2 sites mediates its ability to repress activation of a viral lytic cycle late gene by Rta. *J Virol* **78**, 7634-7644.

El Andaloussi, S., Guterstam, P. & Langel, U. (2007). Assessing the delivery efficacy and internalization route of cell-penetrating peptides. *Nat Protoc* **2**, 2043-2047.

Elliott, G. & O'Hare, P. (1997). Intercellular trafficking and protein delivery by a herpesvirus structural protein. *Cell* **88**, 223-233.

Elmquist, A., Lindgren, M., Bartfai, T. & Langel, U. (2001). VE-cadherin-derived cell-penetrating peptide, pVEC, with carrier functions. *Exp Cell Res* **269**, 237-244.

Farrell, P. J., Rowe, D. T., Rooney, C. M. & Kouzarides, T. (1989). Epstein-Barr virus BZLF1 trans-activator specifically binds to a consensus AP-1 site and is related to c-fos. *Embo J* **8**, 127-132.

Ferber, D. (2001). Gene therapy. Safer and virus-free? *Science* **294**, 1638-1642.

Ferrari, A., Pellegrini, V., Arcangeli, C., Fittipaldi, A., Giacca, M. & Beltram, F. (2003). Caveolae-mediated internalization of extracellular HIV-1 tat fusion proteins visualized in real time. *Mol Ther* **8**, 284-294.

Fischer, R., Kohler, K., Fotin-Mleczek, M. & Brock, R. (2004). A stepwise dissection of the intracellular fate of cationic cell-penetrating peptides. *J Biol Chem* **279**, 12625-12635.

Fittipaldi, A., Ferrari, A., Zoppe, M., Arcangeli, C., Pellegrini, V., Beltram, F. & Giacca, M. (2003). Cell membrane lipid rafts mediate caveolar endocytosis of HIV-1 Tat fusion proteins. *J Biol Chem* **278**, 34141-34149.

Fixman, E. D., Hayward, G. S. & Hayward, S. D. (1992). trans-acting requirements for replication of Epstein-Barr virus ori-Lyt. *J Virol* **66**, 5030-5039.

Flemington, E. & Speck, S. H. (1990). Evidence for coiled-coil dimer formation by an Epstein-Barr virus transactivator that lacks a heptad repeat of leucine residues. *Proc Natl Acad Sci U S A* **87**, 9459-9463.

Foged, C. & Nielsen, H. M. (2008). Cell-penetrating peptides for drug delivery across membrane barriers. *Expert Opin Drug Deliv* **5**, 105-117.

Fonseca, S. B., Pereira, M. P. & Kelley, S. O. (2009). Recent advances in the use of cell-penetrating peptides for medical and biological applications. *Adv Drug Deliv Rev* **61**, 953-964.

Ford, K. G., Souberbielle, B. E., Darling, D. & Farzaneh, F. (2001). Protein transduction: an alternative to genetic intervention? *Gene Ther* **8**, 1-4.

Frankel, A. D. & Pabo, C. O. (1988). Cellular uptake of the tat protein from human immunodeficiency virus. *Cell* **55**, 1189-1193.

Fuchs, S. M. & Raines, R. T. (2004). Pathway for polyarginine entry into mammalian cells. *Biochemistry* **43**, 2438-2444.

Fuchs, S. M. & Raines, R. T. (2006). Internalization of cationic peptides: the road less (or more?) traveled. *Cell Mol Life Sci* **63**, 1819-1822.

Futaki, S., Suzuki, T., Ohashi, W., Yagami, T., Tanaka, S., Ueda, K. & Sugiura, Y. (2001). Arginine-rich peptides. An abundant source of membrane-permeable peptides having potential as carriers for intracellular protein delivery. *J Biol Chem* **276**, 5836-5840.

Gavioli, R., Cellini, S., Castaldello, A. & other authors (2008). The Tat protein broadens T cell responses directed to the HIV-1 antigens Gag and Env: implications for the design of new vaccination strategies against AIDS. *Vaccine* **26**, 727-737.

Gopalan, B., Litvak, A., Sharma, S., Mhashilkar, A. M., Chada, S. & Ramesh, R. (2005). Activation of the Fas-FasL signaling pathway by MDA-7/IL-24 kills human ovarian cancer cells. *Cancer Res* **65**, 3017-3024.

Greenblatt, M. S., Bennett, W. P., Hollstein, M. & Harris, C. C. (1994). Mutations in the p53 tumor suppressor gene: clues to cancer etiology and molecular pathogenesis. *Cancer Res* **54**, 4855-4878.

Gros, E., Deshayes, S., Morris, M. C., Aldrian-Herrada, G., Depollier, J., Heitz, F. & Divita, G. (2006). A non-covalent peptide-based strategy for protein and peptide nucleic acid transduction. *Biochim Biophys Acta* **1758**, 384-393.

Guegan, C., Braudeau, J., Couriaud, C., Dietz, G. P., Lacombe, P., Bahr, M., Nosten-Bertrand, M. & Onteniente, B. (2006). PTD-XIAP protects against cerebral ischemia by anti-apoptotic and transcriptional regulatory mechanisms. *Neurobiol Dis* **22**, 177-186.

Gump, J. M. & Dowdy, S. F. (2007). TAT transduction: the molecular mechanism and therapeutic prospects. *Trends Mol Med* **13**, 443-448.

Gump, J. M., June, R. K. & Dowdy, S. F. (2010). Revised role of glycosaminoglycans in TAT protein transduction domain-mediated cellular transduction. *J Biol Chem* **285**, 1500-1507.

Gupta, B., Levchenko, T. S. & Torchilin, V. P. (2005). Intracellular delivery of large molecules and small particles by cell-penetrating proteins and peptides. *Adv Drug Deliv Rev* **57**, 637-651.

Gupta, P., Su, Z. Z., Lebedeva, I. V. & other authors (2006). mda-7/IL-24: multifunctional cancer-specific apoptosis-inducing cytokine. *Pharmacol Ther* **111**, 596-628.

Gutsch, D. E., Holley-Guthrie, E. A., Zhang, Q., Stein, B., Blanar, M. A., Baldwin, A. S. & Kenney, S. C. (1994). The bZIP transactivator of Epstein-Barr virus, BZLF1, functionally and physically interacts with the p65 subunit of NF-kappa B. *Mol Cell Biol* **14**, 1939-1948.

Heitz, F., Morris, M. C. & Divita, G. (2009). Twenty years of cell-penetrating peptides: from molecular mechanisms to therapeutics. *Br J Pharmacol* **157**, 195-206.

Hicks, M. R., Balesaria, S., Medina-Palazon, C., Pandya, M. J., Woolfson, D. N. & Sinclair, A. J. (2001). Biophysical analysis of natural variants of the multimerization region of Epstein-Barr virus lytic-switch protein BZLF1. *J Virol* **75**, 5381-5384.

Hicks, M. R., Al-Mehairi, S. S. & Sinclair, A. J. (2003). The zipper region of Epstein-Barr virus bZIP transcription factor Zta is necessary but not sufficient to direct DNA binding. *J Virol* **77**, 8173-8177.

Ho, A., Schwarze, S. R., Mermelstein, S. J., Waksman, G. & Dowdy, S. F. (2001). Synthetic protein transduction domains: enhanced transduction potential in vitro and in vivo. *Cancer Res* **61**, 474-477.

Hong, F. D. & Clayman, G. L. (2000). Isolation of a peptide for targeted drug delivery into human head and neck solid tumors. *Cancer Res* **60**, 6551-6556.

Hotchkiss, R. S., McConnell, K. W., Bullok, K. & other authors (2006). TAT-BH4 and TAT-Bcl-xL peptides protect against sepsis-induced lymphocyte apoptosis in vivo. *J Immunol* **176**, 5471-5477.

Huang, E. Y., Madireddi, M. T., Gopalkrishnan, R. V. & other authors (2001). Genomic structure, chromosomal localization and expression profile of a novel melanoma differentiation associated (mda-7) gene with cancer specific growth suppressing and apoptosis inducing properties. *Oncogene* **20**, 7051-7063.

Jiang, H., Lin, J. J., Su, Z. Z., Goldstein, N. I. & Fisher, P. B. (1995). Subtraction hybridization identifies a novel melanoma differentiation associated gene, mda-7, modulated during human melanoma differentiation, growth and progression. *Oncogene* **11**, 2477-2486.

Jiang, H., Su, Z. Z., Lin, J. J., Goldstein, N. I., Young, C. S. & Fisher, P. B. (1996). The melanoma differentiation associated gene mda-7 suppresses cancer cell growth. *Proc Natl Acad Sci U S A* **93**, 9160-9165.

Jiang, T., Olson, E. S., Nguyen, Q. T., Roy, M., Jennings, P. A. & Tsien, R. Y. (2004). Tumor imaging by means of proteolytic activation of cell-penetrating peptides. *Proc Natl Acad Sci U S A* **101**, 17867-17872.

Jin, Z. H., Josserand, V., Razkin, J., Garanger, E., Boturyn, D., Favrot, M. C., Dumy, P. & Coll, J. L. (2006). Noninvasive optical imaging of ovarian metastases using Cy5-labeled RAFT-c(-RGDfK-)4. *Mol Imaging* **5**, 188-197.

Joliot, A., Pernelle, C., Deagostini-Bazin, H. & Prochiantz, A. (1991). Antennapedia homeobox peptide regulates neural morphogenesis. *Proc Natl Acad Sci U S A* **88**, 1864-1868.

Joliot, A. & Prochiantz, A. (2004). Transduction peptides: from technology to physiology. *Nat Cell Biol* **6**, 189-196.

Joliot, A. & Prochiantz, A. (2008). Homeoproteins as natural Penetratin cargoes with signaling properties. *Adv Drug Deliv Rev* **60**, 608-613.

Justesen, S., Buus, S., Claesson, M. H. & Pedersen, A. E. (2007). Addition of TAT protein transduction domain and GrpE to human p53 provides soluble fusion proteins that can be transduced into dendritic cells and elicit p53-specific T-cell responses in HLA-A*0201 transgenic mice. *Immunology* **122**, 326-334.

Kaplan, I. M., Wadia, J. S. & Dowdy, S. F. (2005). Cationic TAT peptide transduction domain enters cells by macropinocytosis. *J Control Release* **102**, 247-253.

Kenney, S., Kamine, J., Holley-Guthrie, E., Lin, J. C., Mar, E. C. & Pagano, J. (1989). The Epstein-Barr virus (EBV) BZLF1 immediate-early gene product differentially affects latent versus productive EBV promoters. *J Virol* **63**, 1729-1736.

Kilic, E., Dietz, G. P., Hermann, D. M. & Bahr, M. (2002). Intravenous TAT-Bcl-Xl is protective after middle cerebral artery occlusion in mice. *Ann Neurol* **52**, 617-622.

Kilic, U., Kilic, E., Dietz, G. P. & Bahr, M. (2003). Intravenous TAT-GDNF is protective after focal cerebral ischemia in mice. *Stroke* **34**, 1304-1310.

Kim, D. T., Mitchell, D. J., Brockstedt, D. G., Fong, L., Nolan, G. P., Fathman, C. G., Engleman, E. G. & Rothbard, J. B. (1997). Introduction of soluble proteins into the MHC class I pathway by conjugation to an HIV tat peptide. *J Immunol* **159**, 1666-1668.

Klein, G. & Klein, E. (1984). The changing faces of EBV research. *Prog Med Virol* **30**, 87-106.

Kobayashi, S., Chikushi, A., Tougu, S., Imura, Y., Nishida, M., Yano, Y. & Matsuzaki, K. (2004). Membrane translocation mechanism of the antimicrobial peptide buforin 2. *Biochemistry* **43**, 15610-15616.

Kouzarides, T., Packham, G., Cook, A. & Farrell, P. J. (1991). The BZLF1 protein of EBV has a coiled coil dimerisation domain without a heptad leucine repeat but with homology to the C/EBP leucine zipper. *Oncogene* **6**, 195-204.

Kramer, S. D. & Wunderli-Allenspach, H. (2003). No entry for TAT(44-57) into liposomes and intact MDCK cells: novel approach to study membrane permeation of cell-penetrating peptides. *Biochim Biophys Acta* **1609**, 161-169.

Kreis, S., Philippidou, D., Margue, C., Rolvering, C., Haan, C., Dumoutier, L., Renauld, J. C. & Behrmann, I. (2007). Recombinant interleukin-24 lacks apoptosis-inducing properties in melanoma cells. *PLoS ONE* **2**, e1300.

Kuppers, R. (2003). B cells under influence: transformation of B cells by Epstein-Barr virus. *Nat Rev Immunol* **3**, 801-812.

Laakkonen, P., Porkka, K., Hoffman, J. A. & Ruoslahti, E. (2002). A tumor-homing peptide with a targeting specificity related to lymphatic vessels. *Nat Med* **8**, 751-755.

Langel, Ü. (2006). *Handbook of Cell-Penetrating Peptides*, 2 edn.

Lebedeva, I. V., Su, Z. Z., Chang, Y., Kitada, S., Reed, J. C. & Fisher, P. B. (2002). The cancer growth suppressing gene mda-7 induces apoptosis selectively in human melanoma cells. *Oncogene* **21**, 708-718.

Lebedeva, I. V., Sarkar, D., Su, Z. Z., Kitada, S., Dent, P., Stein, C. A., Reed, J. C. & Fisher, P. B. (2003). Bcl-2 and Bcl-x(L) differentially protect human prostate cancer cells from induction of apoptosis by melanoma differentiation associated gene-7, mda-7/IL-24. *Oncogene* **22**, 8758-8773.

Lebedeva, I. V., Su, Z. Z., Sarkar, D., Gopalkrishnan, R. V., Waxman, S., Yacoub, A., Dent, P. & Fisher, P. B. (2005). Induction of reactive oxygen species renders mutant and wild-type K-ras pancreatic carcinoma cells susceptible to Ad.mda-7-induced apoptosis. *Oncogene* **24**, 585-596.

Lebedeva, I. V., Su, Z. Z., Emdad, L., Kolomeyer, A., Sarkar, D., Kitada, S., Waxman, S., Reed, J. C. & Fisher, P. B. (2007). Targeting inhibition of K-ras enhances Ad.mda-7-induced growth suppression and apoptosis in mutant K-ras colorectal cancer cells. *Oncogene* **26**, 733-744.

Lebleu, B., Moulton, H. M., Abes, R., Ivanova, G. D., Abes, S., Stein, D. A., Iversen, P. L., Arzumanov, A. A. & Gait, M. J. (2008). Cell penetrating peptide conjugates of steric block oligonucleotides. *Adv Drug Deliv Rev* **60**, 517-529.

Letoha, T., Gaal, S., Somlai, C., Czajlik, A., Perczel, A. & Penke, B. (2003). Membrane translocation of penetratin and its derivatives in different cell lines. *J Mol Recognit* **16**, 272-279.

Lewin, M., Carlesso, N., Tung, C. H., Tang, X. W., Cory, D., Scadden, D. T. & Weissleder, R. (2000). Tat peptide-derivatized magnetic nanoparticles allow in vivo tracking and recovery of progenitor cells. *Nat Biotechnol* **18**, 410-414.

Lieberman, P. M. & Berk, A. J. (1991). The Zta trans-activator protein stabilizes TFIID association with promoter DNA by direct protein-protein interaction. *Genes Dev* **5**, 2441-2454.

Liguori, L., Marques, B., Villegas-Mendez, A., Rothe, R. & Lenormand, J. L. (2008). Liposomes-mediated delivery of pro-apoptotic therapeutic membrane proteins. *J Control Release* **126**, 217-227.

Lin, Y. Z., Yao, S. Y., Veach, R. A., Torgerson, T. R. & Hawiger, J. (1995). Inhibition of nuclear translocation of transcription factor NF-kappa B by a synthetic peptide containing a cell membrane-permeable motif and nuclear localization sequence. *J Biol Chem* **270**, 14255-14258.

Lindgren, M., Gallet, X., Soomets, U., Hallbrink, M., Brakenhielm, E., Pooga, M., Brasseur, R. & Langel, U. (2000). Translocation properties of novel cell penetrating transportan and penetratin analogues. *Bioconjug Chem* **11**, 619-626.

Lu, J., Chen, S. Y., Chua, H. H., Liu, Y. S., Huang, Y. T., Chang, Y., Chen, J. Y., Sheen, T. S. & Tsai, C. H. (2000). Upregulation of tyrosine kinase TKT by the Epstein-Barr virus transactivator Zta. *J Virol* **74**, 7391-7399.

Mae, M. & Langel, U. (2006). Cell-penetrating peptides as vectors for peptide, protein and oligonucleotide delivery. *Curr Opin Pharmacol* **6**, 509-514.

Magzoub, M., Sandgren, S., Lundberg, P. & other authors (2006). N-terminal peptides from unprocessed prion proteins enter cells by macropinocytosis. *Biochem Biophys Res Commun* **348**, 379-385.

Mahot, S., Fender, P., Vives, R. R., Caron, C., Perrissin, M., Gruffat, H., Sergeant, A. & Drouet, E. (2005). Cellular uptake of the EBV transcription factor EB1/Zta. *Virus Res* **110**, 187-193.

Mandal, D., Maran, A., Yaszemski, M. J., Bolander, M. E. & Sarkar, G. (2009). Cellular uptake of gold nanoparticles directly cross-linked with carrier peptides by osteosarcoma cells. *J Mater Sci Mater Med* **20**, 347-350.

Mauser, A., Holley-Guthrie, E., Simpson, D., Kaufmann, W. & Kenney, S. (2002a). The Epstein-Barr virus immediate-early protein BZLF1 induces both a G(2) and a mitotic block. *J Virol* **76**, 10030-10037.

Mauser, A., Holley-Guthrie, E., Zanation, A., Yarborough, W., Kaufmann, W., Klingelhutz, A., Seaman, W. T. & Kenney, S. (2002b). The Epstein-Barr virus immediate-early protein BZLF1 induces expression of E2F-1 and other proteins involved in cell cycle progression in primary keratinocytes and gastric carcinoma cells. *J Virol* **76**, 12543-12552.

Mauser, A., Saito, S., Appella, E., Anderson, C. W., Seaman, W. T. & Kenney, S. (2002c). The Epstein-Barr virus immediate-early protein BZLF1 regulates p53 function through multiple mechanisms. *J Virol* **76**, 12503-12512.

McDonald, C. M., Petosa, C. & Farrell, P. J. (2009). Interaction of Epstein-Barr virus BZLF1 C-terminal tail structure and core zipper is required for DNA replication but not for promoter transactivation. *J Virol* **83**, 3397-3401.

Mhashilkar, A., Chada, S., Roth, J. A. & Ramesh, R. (2001). Gene therapy. Therapeutic approaches and implications. *Biotechnol Adv* **19**, 279-297.

Mi, Z., Mai, J., Lu, X. & Robbins, P. D. (2000). Characterization of a class of cationic peptides able to facilitate efficient protein transduction in vitro and in vivo. *Mol Ther* **2**, 339-347.

Michiue, H., Tomizawa, K., Matsushita, M., Tamiya, T., Lu, Y. F., Ichikawa, T., Date, I. & Matsui, H. (2005). Ubiquitination-resistant p53 protein transduction therapy facilitates anti-cancer effect on the growth of human malignant glioma cells. *FEBS Lett* **579**, 3965-3969.

Middeldorp, J. M., Brink, A. A., van den Brule, A. J. & Meijer, C. J. (2003). Pathogenic roles for Epstein-Barr virus (EBV) gene products in EBV-associated proliferative disorders. *Crit Rev Oncol Hematol* **45**, 1-36.

Miller, G., El-Guindy, A., Countryman, J., Ye, J. & Gradoville, L. (2007). Lytic cycle switches of oncogenic human gammaherpesviruses(1). *Adv Cancer Res* **97**, 81-109.

Morand, P., Budayova-Spano, M., Perrissin, M., Muller, C. W. & Petosa, C. (2006). Expression, purification, crystallization and preliminary X-ray analysis of a C-terminal fragment of the Epstein-Barr virus ZEBRA protein. *Acta Crystallogr Sect F Struct Biol Cryst Commun* **62**, 210-214.

Morris, M. C., Vidal, P., Chaloin, L., Heitz, F. & Divita, G. (1997). A new peptide vector for efficient delivery of oligonucleotides into mammalian cells. *Nucleic Acids Res* **25**, 2730-2736.

Morris, M. C., Deshayes, S., Heitz, F. & Divita, G. (2008). Cell-penetrating peptides: from molecular mechanisms to therapeutics. *Biol Cell* **100**, 201-217.

Morrison, T. E., Mauser, A., Wong, A., Ting, J. P. & Kenney, S. C. (2001). Inhibition of IFN-gamma signaling by an Epstein-Barr virus immediate-early protein. *Immunity* **15**, 787-799.

Morrison, T. E. & Kenney, S. C. (2004). BZLF1, an Epstein-Barr virus immediate-early protein, induces p65 nuclear translocation while inhibiting p65 transcriptional function. *Virology* **328**, 219-232.

Moschos, S. A., Williams, A. E. & Lindsay, M. A. (2007). Cell-penetrating-peptide-mediated siRNA lung delivery. *Biochem Soc Trans* **35**, 807-810.

Mukai, Y., Sugita, T., Yamato, T. & other authors (2006). Creation of novel Protein Transduction Domain (PTD) mutants by a phage display-based high-throughput screening system. *Biol Pharm Bull* **29**, 1570-1574.

Murriel, C. L. & Dowdy, S. F. (2006). Influence of protein transduction domains on intracellular delivery of macromolecules. *Expert Opin Drug Deliv* **3**, 739-746.

Nakase, I., Niwa, M., Takeuchi, T. & other authors (2004). Cellular uptake of arginine-rich peptides: roles for macropinocytosis and actin rearrangement. *Mol Ther* **10**, 1011-1022.

Nakase, I., Tadokoro, A., Kawabata, N. & other authors (2007). Interaction of arginine-rich peptides with membrane-associated proteoglycans is crucial for induction of actin organization and macropinocytosis. *Biochemistry* **46**, 492-501.

Nguyen, Q. T., Olson, E. S., Aguilera, T. A., Jiang, T., Scadeng, M., Ellies, L. G. & Tsien, R. Y. (2010). Surgery with molecular fluorescence imaging using activatable cell-penetrating peptides decreases residual cancer and improves survival. *Proc Natl Acad Sci U S A* **107**, 4317-4322.

Nishi, K. & Saigo, K. (2007). Cellular internalization of green fluorescent protein fused with herpes simplex virus protein VP22 via a lipid raft-mediated endocytic pathway independent of caveolae and Rho family GTPases but dependent on dynamin and Arf6. *J Biol Chem* **282**, 27503-27517.

Oehlke, J., Scheller, A., Wiesner, B., Krause, E., Beyermann, M., Klauschenz, E., Melzig, M. & Bienert, M. (1998). Cellular uptake of an alpha-helical amphipathic model peptide with the potential to deliver polar compounds into the cell interior non-endocytically. *Biochim Biophys Acta* **1414**, 127-139.

Oh, P., Li, Y., Yu, J., Durr, E., Krasinska, K. M., Carver, L. A., Testa, J. E. & Schnitzer, J. E. (2004). Subtractive proteomic mapping of the endothelial surface in lung and solid tumours for tissue-specific therapy. *Nature* **429**, 629-635.

Oliveira, S., van Rooy, I., Kranenburg, O., Storm, G. & Schiffelers, R. M. (2007). Fusogenic peptides enhance endosomal escape improving siRNA-induced silencing of oncogenes. *Int J Pharm* **331**, 211-214.

Oliveira, S., Hogset, A., Storm, G. & Schiffelers, R. M. (2008). Delivery of siRNA to the target cell cytoplasm: photochemical internalization facilitates endosomal escape and improves silencing efficiency, in vitro and in vivo. *Curr Pharm Des* **14**, 3686-3697.

Pataer, A., Vorburger, S. A., Barber, G. N. & other authors (2002). Adenoviral transfer of the melanoma differentiation-associated gene 7 (mda7) induces apoptosis of lung cancer cells via up-regulation of the double-stranded RNA-dependent protein kinase (PKR). *Cancer Res* **62**, 2239-2243.

Pestka, S., Krause, C. D. & Walter, M. R. (2004). Interferons, interferon-like cytokines, and their receptors. *Immunol Rev* **202**, 8-32.

Petosa, C., Morand, P., Baudin, F., Moulin, M., Artero, J. B. & Muller, C. W. (2006). Structural basis of lytic cycle activation by the Epstein-Barr virus ZEBRA protein. *Mol Cell* **21**, 565-572.

Pfitzner, E., Becker, P., Rolke, A. & Schule, R. (1995). Functional antagonism between the retinoic acid receptor and the viral transactivator BZLF1 is mediated by protein-protein interactions. *Proc Natl Acad Sci U S A* **92**, 12265-12269.

Pichon, C., Monsigny, M. & Roche, A. C. (1999). Intracellular localization of oligonucleotides: influence of fixative protocols. *Antisense Nucleic Acid Drug Dev* **9**, 89-93.

Pooga, M., Hallbrink, M., Zorko, M. & Langel, U. (1998). Cell penetration by transportan. *Faseb J* **12**, 67-77.

Poon, G. M. & Gariepy, J. (2007). Cell-surface proteoglycans as molecular portals for cationic peptide and polymer entry into cells. *Biochem Soc Trans* **35**, 788-793.

Prochiantz, A. (2000). Messenger proteins: homeoproteins, TAT and others. *Curr Opin Cell Biol* **12**, 400-406.

Prochiantz, A. & Joliot, A. (2003). Can transcription factors function as cell-cell signalling molecules? *Nat Rev Mol Cell Biol* **4**, 814-819.

Prochiantz, A. (2007). For protein transduction, chemistry can win over biology. *Nat Methods* **4**, 119-120.

Pujals, S., Fernandez-Carneado, J., Kogan, M. J., Martinez, J., Cavelier, F. & Giralt, E. (2006). Replacement of a proline with silaproline causes a 20-fold increase in the cellular uptake of a Pro-rich peptide. *J Am Chem Soc* **128**, 8479-8483.

Richard, J. P., Melikov, K., Vives, E., Ramos, C., Verbeure, B., Gait, M. J., Chernomordik, L. V. & Lebleu, B. (2003). Cell-penetrating peptides. A reevaluation of the mechanism of cellular uptake. *J Biol Chem* **278**, 585-590.

Richard, J. P., Melikov, K., Brooks, H., Prevot, P., Lebleu, B. & Chernomordik, L. V. (2005). Cellular uptake of unconjugated TAT peptide involves clathrin-dependent endocytosis and heparan sulfate receptors. *J Biol Chem* **280**, 15300-15306.

Rodriguez, A., Armstrong, M., Dwyer, D. & Flemington, E. (1999). Genetic dissection of cell growth arrest functions mediated by the Epstein-Barr virus lytic gene product, Zta. *J Virol* **73**, 9029-9038.

Rodriguez, A., Jung, E. J., Yin, Q., Cayrol, C. & Flemington, E. K. (2001). Role of c-myc regulation in Zta-mediated induction of the cyclin-dependent kinase inhibitors p21 and p27 and cell growth arrest. *Virology* **284**, 159-169.

Rothbard, J. B., Jessop, T. C., Lewis, R. S., Murray, B. A. & Wender, P. A. (2004). Role of membrane potential and hydrogen bonding in the mechanism of translocation of guanidinium-rich peptides into cells. *J Am Chem Soc* **126**, 9506-9507.

Rothbard, J. B., Jessop, T. C. & Wender, P. A. (2005). Adaptive translocation: the role of hydrogen bonding and membrane potential in the uptake of guanidinium-rich transporters into cells. *Adv Drug Deliv Rev* **57**, 495-504.

Rothberg, K. G., Heuser, J. E., Donzell, W. C., Ying, Y. S., Glenney, J. R. & Anderson, R. G. (1992). Caveolin, a protein component of caveolae membrane coats. *Cell* **68**, 673-682.

Rothe, R. & Lenormand, J. L. (2008). Expression and purification of ZEBRA fusion proteins and applications for the delivery of macromolecules into mammalian cells. *Curr Protoc Protein Sci* **Chapter 18**, Unit 18 11.

Rousselle, C., Smirnova, M., Clair, P., Lefauconnier, J. M., Chavanieu, A., Calas, B., Scherrmann, J. M. & Temsamani, J. (2001). Enhanced delivery of doxorubicin into the brain via a peptide-vector-mediated strategy: saturation kinetics and specificity. *J Pharmacol Exp Ther* **296**, 124-131.

Ruoslahti, E. (2000). Targeting tumor vasculature with homing peptides from phage display. *Semin Cancer Biol* **10**, 435-442.

Ruoslahti, E. (2002). Specialization of tumour vasculature. *Nat Rev Cancer* **2**, 83-90.

Saeki, T., Mhashilkar, A., Chada, S., Branch, C., Roth, J. A. & Ramesh, R. (2000). Tumor-suppressive effects by adenovirus-mediated mda-7 gene transfer in non-small cell lung cancer cell in vitro. *Gene Ther* **7**, 2051-2057.

Saeki, T., Mhashilkar, A., Swanson, X. & other authors (2002). Inhibition of human lung cancer growth following adenovirus-mediated mda-7 gene expression in vivo. *Oncogene* **21**, 4558-4566.

Santra, S., Yang, H., Stanley, J. T., Holloway, P. H., Moudgil, B. M., Walter, G. & Mericle, R. A. (2005). Rapid and effective labeling of brain tissue using TAT-conjugated CdS:Mn/ZnS quantum dots. *Chem Commun (Camb)*, 3144-3146.

Sarkar, D., Su, Z. Z., Lebedeva, I. V., Sauane, M., Gopalkrishnan, R. V., Dent, P. & Fisher, P. B. (2002). mda-7 (IL-24): signaling and functional roles. *Biotechniques* **Suppl**, 30-39.

Sauane, M., Gopalkrishnan, R. V., Sarkar, D., Su, Z. Z., Lebedeva, I. V., Dent, P., Pestka, S. & Fisher, P. B. (2003a). MDA-7/IL-24: novel cancer growth suppressing and apoptosis inducing cytokine. *Cytokine Growth Factor Rev* **14**, 35-51.

Sauane, M., Gopalkrishnan, R. V., Lebedeva, I. & other authors (2003b). Mda-7/IL-24 induces apoptosis of diverse cancer cell lines through JAK/STAT-independent pathways. *J Cell Physiol* **196**, 334-345.

Sauane, M., Su, Z. Z., Gupta, P., Lebedeva, I. V., Dent, P., Sarkar, D. & Fisher, P. B. (2008). Autocrine regulation of mda-7/IL-24 mediates cancer-specific apoptosis. *Proc Natl Acad Sci U S A* **105**, 9763-9768.

Schatzlein, A. G. (2003). Targeting of Synthetic Gene Delivery Systems. *J Biomed Biotechnol* **2003**, 149-158.

Schepers, A., Pich, D. & Hammerschmidt, W. (1993). A transcription factor with homology to the AP-1 family links RNA transcription and DNA replication in the lytic cycle of Epstein-Barr virus. *Embo J* **12**, 3921-3929.

Schepers, A., Pich, D. & Hammerschmidt, W. (1996). Activation of oriLyt, the lytic origin of DNA replication of Epstein-Barr virus, by BZLF1. *Virology* **220**, 367-376.

Schuler, M., Rochlitz, C., Horowitz, J. A. & other authors (1998). A phase I study of adenovirus-mediated wild-type p53 gene transfer in patients with advanced non-small cell lung cancer. *Hum Gene Ther* **9**, 2075-2082.

Schwarze, S. R., Ho, A., Vocero-Akbani, A. & Dowdy, S. F. (1999). In vivo protein transduction: delivery of a biologically active protein into the mouse. *Science* **285**, 1569-1572.

Schwarze, S. R. & Dowdy, S. F. (2000). In vivo protein transduction: intracellular delivery of biologically active proteins, compounds and DNA. *Trends Pharmacol Sci* **21**, 45-48.

Schwarze, S. R., Hruska, K. A. & Dowdy, S. F. (2000). Protein transduction: unrestricted delivery into all cells? *Trends Cell Biol* **10**, 290-295.

Senatus, P. B., Li, Y., Mandigo, C. & other authors (2006). Restoration of p53 function for selective Fas-mediated apoptosis in human and rat glioma cells in vitro and in vivo by a p53 COOH-terminal peptide. *Mol Cancer Ther* **5**, 20-28.

Shibagaki, N. & Udey, M. C. (2002). Dendritic cells transduced with protein antigens induce cytotoxic lymphocytes and elicit antitumor immunity. *J Immunol* **168**, 2393-2401.

Shiraishi, T. & Nielsen, P. E. (2006). Enhanced delivery of cell-penetrating peptide-peptide nucleic acid conjugates by endosomal disruption. *Nat Protoc* **1**, 633-636.

Sinclair, A. J. (2003). bZIP proteins of human gammaherpesviruses. *J Gen Virol* **84**, 1941-1949.

Sinclair, A. J. (2006). Unexpected structure of Epstein-Barr virus lytic cycle activator Zta. *Trends Microbiol* **14**, 289-291.

Sista, N. D., Barry, C., Sampson, K. & Pagano, J. (1995). Physical and functional interaction of the Epstein-Barr virus BZLF1 transactivator with the retinoic acid receptors RAR alpha and RXR alpha. *Nucleic Acids Res* **23**, 1729-1736.

Snyder, E. L., Meade, B. R., Saenz, C. C. & Dowdy, S. F. (2004). Treatment of terminal peritoneal carcinomatosis by a transducible p53-activating peptide. *PLoS Biol* **2**, E36.

Snyder, E. L., Saenz, C. C., Denicourt, C., Meade, B. R., Cui, X. S., Kaplan, I. M. & Dowdy, S. F. (2005). Enhanced targeting and killing of tumor cells expressing the CXC chemokine receptor 4 by transducible anticancer peptides. *Cancer Res* **65**, 10646-10650.

Speck, S. H., Chatila, T. & Flemington, E. (1997). Reactivation of Epstein-Barr virus: regulation and function of the BZLF1 gene. *Trends Microbiol* **5**, 399-405.

Su, Z., Emdad, L., Sauane, M. & other authors (2005). Unique aspects of mda-7/IL-24 antitumor bystander activity: establishing a role for secretion of MDA-7/IL-24 protein by normal cells. *Oncogene* **24**, 7552-7566.

Su, Z. Z., Madireddi, M. T., Lin, J. J., Young, C. S., Kitada, S., Reed, J. C., Goldstein, N. I. & Fisher, P. B. (1998). The cancer growth suppressor gene mda-7 selectively induces apoptosis in human breast cancer cells and inhibits tumor growth in nude mice. *Proc Natl Acad Sci U S A* **95**, 14400-14405.

Su, Z. Z., Lebedeva, I. V., Sarkar, D. & other authors (2003). Melanoma differentiation associated gene-7, mda-7/IL-24, selectively induces growth suppression, apoptosis and

radiosensitization in malignant gliomas in a p53-independent manner. *Oncogene* **22**, 1164-1180.

Su, Z. Z., Lebedeva, I. V., Sarkar, D., Emdad, L., Gupta, P., Kitada, S., Dent, P., Reed, J. C. & Fisher, P. B. (2006). Ionizing radiation enhances therapeutic activity of mda-7/IL-24: overcoming radiation- and mda-7/IL-24-resistance in prostate cancer cells overexpressing the antiapoptotic proteins bcl-xL or bcl-2. *Oncogene* **25**, 2339-2348.

Tan, M., Lan, K. H., Yao, J., Lu, C. H., Sun, M., Neal, C. L., Lu, J. & Yu, D. (2006). Selective inhibition of ErbB2-overexpressing breast cancer in vivo by a novel TAT-based ErbB2-targeting signal transducers and activators of transcription 3-blocking peptide. *Cancer Res* **66**, 3764-3772.

Terrone, D., Sang, S. L., Roudaia, L. & Silvius, J. R. (2003). Penetratin and related cell-penetrating cationic peptides can translocate across lipid bilayers in the presence of a transbilayer potential. *Biochemistry* **42**, 13787-13799.

Thoren, P. E., Persson, D., Karlsson, M. & Norden, B. (2000). The antennapedia peptide penetratin translocates across lipid bilayers - the first direct observation. *FEBS Lett* **482**, 265-268.

Thoren, P. E., Persson, D., Isakson, P., Goksor, M., Onfelt, A. & Norden, B. (2003). Uptake of analogs of penetratin, Tat(48-60) and oligoarginine in live cells. *Biochem Biophys Res Commun* **307**, 100-107.

Thorley-Lawson, D. A. (2001). Epstein-Barr virus: exploiting the immune system. *Nat Rev Immunol* **1**, 75-82.

Torchilin, V. P., Rammohan, R., Weissig, V. & Levchenko, T. S. (2001). TAT peptide on the surface of liposomes affords their efficient intracellular delivery even at low temperature and in the presence of metabolic inhibitors. *Proc Natl Acad Sci U S A* **98**, 8786-8791.

Torchilin, V. P. (2007). Tatp-mediated intracellular delivery of pharmaceutical nanocarriers. *Biochem Soc Trans* **35**, 816-820.

Tseng, Y. L., Liu, J. J. & Hong, R. L. (2002). Translocation of liposomes into cancer cells by cell-penetrating peptides penetratin and tat: a kinetic and efficacy study. *Mol Pharmacol* **62**, 864-872.

Tsurumi, T., Fujita, M. & Kudoh, A. (2005). Latent and lytic Epstein-Barr virus replication strategies. *Rev Med Virol* **15**, 3-15.

Tunnemann, G., Martin, R. M., Haupt, S., Patsch, C., Edenhofer, F. & Cardoso, M. C. (2006). Cargo-dependent mode of uptake and bioavailability of TAT-containing proteins and peptides in living cells. *Faseb J* **20**, 1775-1784.

Tyagi, M., Rusnati, M., Presta, M. & Giacca, M. (2001). Internalization of HIV-1 tat requires cell surface heparan sulfate proteoglycans. *J Biol Chem* **276**, 3254-3261.

Veach, R. A., Liu, D., Yao, S., Chen, Y., Liu, X. Y., Downs, S. & Hawiger, J. (2004). Receptor/transporter-independent targeting of functional peptides across the plasma membrane. *J Biol Chem* **279**, 11425-11431.

Verma, I. M. & Somia, N. (1997). Gene therapy -- promises, problems and prospects. *Nature* **389**, 239-242.

Vives, E., Brodin, P. & Lebleu, B. (1997). A truncated HIV-1 Tat protein basic domain rapidly translocates through the plasma membrane and accumulates in the cell nucleus. *J Biol Chem* **272**, 16010-16017.

Vives, E., Richard, J. P., Rispal, C. & Lebleu, B. (2003). TAT peptide internalization: seeking the mechanism of entry. *Curr Protein Pept Sci* **4**, 125-132.

Wadia, J. S., Stan, R. V. & Dowdy, S. F. (2004). Transducible TAT-HA fusogenic peptide enhances escape of TAT-fusion proteins after lipid raft macropinocytosis. *Nat Med* **10**, 310-315.

Watson, P., Jones, A. T. & Stephens, D. J. (2005). Intracellular trafficking pathways and drug delivery: fluorescence imaging of living and fixed cells. *Adv Drug Deliv Rev* **57**, 43-61.

Wender, P. A., Mitchell, D. J., Pattabiraman, K., Pelkey, E. T., Steinman, L. & Rothbard, J. B. (2000). The design, synthesis, and evaluation of molecules that enable or enhance cellular uptake: peptoid molecular transporters. *Proc Natl Acad Sci U S A* **97**, 13003-13008.

Wu, F. Y., Tang, Q. Q., Chen, H., ApRhys, C., Farrell, C., Chen, J., Fujimuro, M., Lane, M. D. & Hayward, G. S. (2002). Lytic replication-associated protein (RAP) encoded by Kaposi sarcoma-associated herpesvirus causes p21CIP-1-mediated G1 cell cycle arrest through CCAAT/enhancer-binding protein-alpha. *Proc Natl Acad Sci U S A* **99**, 10683-10688.

Wu, F. Y., Chen, H., Wang, S. E. & other authors (2003). CCAAT/enhancer binding protein alpha interacts with ZTA and mediates ZTA-induced p21(CIP-1) accumulation and G(1) cell cycle arrest during the Epstein-Barr virus lytic cycle. *J Virol* **77**, 1481-1500.

Wu, F. Y., Wang, S. E., Chen, H., Wang, L., Hayward, S. D. & Hayward, G. S. (2004). CCAAT/enhancer binding protein alpha binds to the Epstein-Barr virus (EBV) ZTA protein through oligomeric interactions and contributes to cooperative transcriptional activation of the ZTA promoter through direct binding to the ZII and ZIIIB motifs during induction of the EBV lytic cycle. *J Virol* **78**, 4847-4865.

Yacoub, A., Mitchell, C., Lister, A. & other authors (2003). Melanoma differentiation-associated 7 (interleukin 24) inhibits growth and enhances radiosensitivity of glioma cells in vitro and in vivo. *Clin Cancer Res* **9**, 3272-3281.

Yacoub, A., Gupta, P., Park, M. A. & other authors (2008b). Regulation of GST-MDA-7 toxicity in human glioblastoma cells by ERBB1, ERK1/2, PI3K, and JNK1-3 pathway signaling. *Mol Cancer Ther* **7**, 314-329.

Yacoub, A., Hamed, H., Emdad, L. & other authors (2008c). MDA-7/IL-24 plus radiation enhance survival in animals with intracranial primary human GBM tumors. *Cancer Biol Ther* **7**, 917-933.

Yang, Q., Larsen, S. K., Mi, Z., Robbins, P. D. & Basse, P. H. (2008). PTD-mediated loading of tumor-seeking lymphocytes with prodrug-activating enzymes. *Aaps J* **10**, 614-621.

Young, L. S. & Rickinson, A. B. (2004). Epstein-Barr virus: 40 years on. *Nat Rev Cancer* **4**, 757-768.

Zerby, D., Chen, C. J., Poon, E., Lee, D., Shiekhattar, R. & Lieberman, P. M. (1999). The amino-terminal C/H1 domain of CREB binding protein mediates zta transcriptional activation of latent Epstein-Barr virus. *Mol Cell Biol* **19**, 1617-1626.

Zhang, Q., Gutsch, D. & Kenney, S. (1994). Functional and physical interaction between p53 and BZLF1: implications for Epstein-Barr virus latency. *Mol Cell Biol* **14**, 1929-1938.

Ziegler, A. & Seelig, J. (2004). Interaction of the protein transduction domain of HIV-1 TAT with heparan sulfate: binding mechanism and thermodynamic parameters. *Biophys J* **86**, 254-263.

Ziegler, A., Nervi, P., Durrenberger, M. & Seelig, J. (2005). The cationic cell-penetrating peptide CPP(TAT) derived from the HIV-1 protein TAT is rapidly transported into living fibroblasts: optical, biophysical, and metabolic evidence. *Biochemistry* **44**, 138-148.

Zorko, M. & Langel, U. (2005). Cell-penetrating peptides: mechanism and kinetics of cargo delivery. *Adv Drug Deliv Rev* **57**, 529-545.

12 APPENDIX

REAGENTS AND SOLUTIONS

Use Milli-Q-purified water in all the protocols.

10× TBE (Tris-borate)	108 g Tris, 55 g boric acid, adjust volume to 1 l with H_2O Stored at RT
50× TAE (Tris-acetate)	242 g Tris-HCl pH 8.5, 18.6 g EDTA, 57.1 ml glacial acetic acid, adjust volume to 1 liter with H_2O, Stored at RT
SDS PAGE running buffer with H_2O	10 g SDS, 30.3 g Tris, 144.1 g glycerin, adjust volume to 1 l Stored at RT
Transfer buffer	2.9 g glycine, 5.8 g Tris, 0.37 g SDS, 200 ml methanol; adjust volume to 1 l with H_2O Stored at RT
1× TBS (Tris buffered saline)	50 mM Tris, 150 mM NaCl, pH 7.5, adjust volume to 1l with H_2O Stored at RT
1× TBST (Tris buffered saline Tween)	1 ml Tween 20 in 1 liter 1× TBS Stored at RT
10× PBS (phosphate buffered saline)	80 g NaCl, 2 g KCl, 26,8 g Na_2HPO_4-$7H_2O$, 2.4 g KH_2PO_4, adjust volume to 1 liter with H_2O, adjust pH 7.4 with 1 M HCl), sterilized by autoclaving, Stored at RT
Red blood cell lysis buffer	155 mM NH_4Cl, 10 mM $KHCO_3$, 0.1 mM EGTA, pH 7.4 Sterilized by filtration Stored at 4 °C

PURIFICATION BUFFERS

lysis/ binding buffer:	20 mM Tris-HCl, pH 6.8-8, 250 mM NaCl, 5 % glycerol 10 mM imidazole Sterilized by filtration Stored at RT
Washing buffer:	Wash 1: 20 mM Tris-HCl, pH 6.8-8, 5 % glycerol, 500 mM NaCl, 20 mM imidazole Wash 2: 20 mM Tris-HCl, pH 6.8-8, 5 % glycerol, 1M NaCl, 40 mM imidazole Wash 3: 20 mM Tris-HCl, pH 6.8-8, 5 % glycerol, 1.5M NaCl, 60 mM imidazole Stored at RT
Elution buffer:	20 mM Tris-HCl, pH 6.8-8, 500 mM NaCl, 75 mM KCl, 20 % glycerol, 100-250-500-1000 mM imidazole gradient Sterilized by filtration Stored at RT

SEQUENCES

1. Nucleotide sequence of ZEBRA

```
1    ATGATGGACC CAAACTCGAC TTCTGAAGAT GTAAAATTTA CACCTGACCC ATACCAGGTG
61   CCTTTTGTAC AAGCTTTTGA CCAAGCTACC AGAGTCTATC AGGACCTGGG AGGGCCATCG
121  CAAGCTCCTT TGCCTTGTGT GCTGTGGCCG GTGCTGCCAG AGCCTCTGCC ACAAGGCCAG
181  CTAACTGCCT ATCATGTTTC AACCGCTCCG ACTGGGTCGT GGTTTTCTGC CCCTCAGCCT
241  GCTCCTGAGA ATGCTTATCA AGCTTATGCA GCACCTCAGC TGTTCCCAGT CTCCGACATA
301  ACCCAGAATC AACAGACTAA CCAAGCCGGG GGAGAAGCAC CTCAACCTGG AGACAATTCT
361  ACTGTTCAAA CAGCAGCAGC AGTGGTGTTT GCTTGCCCCG GGGCTAACCA AGGACAACAG
421  CTAGCAGACA TTGGTGTTCC ACAGCCTGCA CCAGTGGCTG CCCCGGCACG ACGCACACGG
481  AAACCACAAC AGCCAGAATC GCTGGAGGAA TGCGATTCTG AACTAGAAAT AAAGCGATAC
541  AAGAATCGGG TGGCTTCCAG AAAATGCCGG GCCAAGTTTA AGCAACTGCT GCAGCACTAC
601  CGTGAGGTCG CTGCTGCCAA ATCATCTGAA AATGACAGGC TGCGCCTCCT GTTGAAGCAG
661  ATGTGCCCAA GCCTGGATGT TGACTCCATT ATCCCCCGGA CACCAGATGT TTTACACGAG
721  GATCTCTTAA ATTTCTAA
```

2. Amino acid sequence of ZEBRA

```
1      MMDPNSTSEDVKFTPDPYQVPFVQAFDQATRVYQDLGGPSQAPLPCVLWPVLPEPLPQGQ
61     LTAYHVSTAPTGSWFSAPQPAPENAYQAYAAPQLFPVSDITQNQQTNQAGGEAPQPGDNS
121    TVQTAAAVVFACPGANQGQQLADIGVPQPAPVAAPARRTRKPQQPESLEECDSELEIKRY
181    KNRVASRKCRAKFKQLLQHYREVAAAKSSENDRLRLLLKQMCPSLDVDSIIPRTPDVLHE
241    DLLNF-
```

3. Amino acid sequence of EGFP

```
1      MVSKGEELFTGVVPILVELDGDVNGHKFSVSGEGEGDATYGKLTLKFICTTGKLPVPWPT
61     LVTTLTYGVQCFSRYPDHMKQHDFFKSAMPEGYVQERTIFFKDDGNYKTRAEVKFEGDTL
121    VNRIELKGIDFKEDGNILGHKLEYNYNSHNVYIMADKQKNGIKVNFKIRHNIEDGSVQLA
181    DHYQQNTPIGDGPVLLPDNHYLSTQSALSKDPNEKRDHMVLLEFVTAAGITLGMDELYKL
241    E
```

4. Amino acid sequence of β-galactosidase

```
1     MITDSLAVVLQRRDWENPGVTQLNRLAAHPPFASWRNSEEARTDRPSQQLRSLNGEWRFA
61    WFPAPEAVPESWLECDLPEADTVVVPSNWQMHGYDAPIYTNVTYPITVNPPFVPTENPTG
```

121 CYSLTFNVDESWLQEGQTRIIFDGVNSAFHLWCNGRWVGYGQDSRLPSEFDLSAFLRAGE
181 NRLAVMVLRWSDGSYLEDQDMWRMSGIFRDVSLLHKPTTQISDFHVATRFNDDFSRAVLE
241 AEVQMCGELRDYLRVTVSLWQGETQVASGTAPFGGEIIDERGGYADRVTLRLNVENPKLW
301 SAEIPNLYRAVVELHTADGTLIEAEACDVGFREVRIENGLLLLNGKPLLIRGVNRHEHHP
361 LHGQVMDEQTMVQDILLMKQNNFNAVRCSHYPNHPLWYTLCDRYGLYVVDEANIETHGMV
421 PMNRLTDDPRWLPAMSERVTRMVQRDRNHPSVIIWSLGNESGHGANHDALYRWIKSVDPS
481 RPVQYEGGGADTTATDIICPMYARVDEDQPFPAVPKWSIKKWLSLPGETRPLILCEYAHA
541 MGNSLGGFAKYWQAFRQYPRLQGGFVWDWVDQSLIKYDENGNPWSAYGGDFGDTPNDRQF
601 CMNGLVFADRTPHPALTEAKHQQQFFQFRLSGQTIEVTSEYLFRHSDNELLHWMVALDGK
661 PLASGEVPLDVAPQGKQLIELPELPQPESAGQLWLTVRVVQPNATAWSEAGHISAWQQWR
721 LAENLSVTLPAASHAIPHLTTSEMDFCIELGNKRWQFNRQSGFLSQMWIGDKKQLLTPLR
781 DQFTRAPLDNDIGVSEATRIDPNAWVERWKAAGHYQAEAALLQCTADTLADAVLITTAHA
841 WQHQGKTLFISRKTYRIDGSGQMAITVDVEVASDTPHPARIGLNCQLAQVAERVNWLGLG
901 PQENYPDRLTAACFDRWDLPLSDMYTPYVFPSENGLRCGTRELNYGPHQWRGDFQFNISR
961 YSQQQLMETSHRHLLHAEEGTWLNIDGFHMGIGGDDSWSPSVSAEFQLSAGRYHYQLVWC
1021 QK

5. Amino acid sequence of MDA7/IL24

1 MNFQQRLQSLWTLARPFCPPLLATASQMQMVVLPCLGFTLLLWSQVSGAQGQEFHFGPCQ
61 VKGVVPQKLWEAFWAVKDTMQAQDNITSARLLQQEVLQNVSDAESCYLVHTLLEFYLKTV
121 FKNYHNRTVEVRTLKSFSTLANNFVLIVSQLQPSQENEMFSIRDSAHRRFLLFRRAFKQL
181 DVEAALTKALGEVDILLTWMQKFYKL

RELATED PUPLICATIONS

Rothe, R., Liguori, L., Villegas-Méndez, A.Marques, B., Drouet, E. and Lenormand, J.L. (2010) Characterization of the cell-penetrating properties of the Epstein-Barr virus ZEBRA protein. JBC, *in press*

Rothe, R. and Lenormand, J.L. (2008) "Expression and Purification of Truncated ZEBRA Proteins to Study Their Transduction Properties." Current Protocols in Protein Science, Chapter 18,

Liguori, L., Marques, B., Villegas-Méndez, A., Rothe, R. and Lenormand, J.L. (2008) Liposomes-mediated delivery of pro-apoptotic therapeutic membrane proteins. J Control Release. Mar 20;126(3):217-27.

Marques, B., Liguori, L., Paclet, M.H., Villegas-Méndez, A., Rothe, R., Morel, F. and Lenormand, J.L. (2007) Liposome-mediated cellular delivery of active gp91. PLoS ONE. Sep 12;2(9):e856.

Liguori, L., Marques, B., Villegas-Méndez, A., Rothe, R. and Lenormand, J.L. (2007) Production of membrane proteins using cell-free expression systems. Expert Rev Proteomics. Feb;4(1):79-90. Review.

RELATED POSTER

R. Rothe, L. Liguori, A. Villegas-Mendez, B. Marques and J.L. Lenormand: "ZEBRA as a new delivery system for therapeutic proteins" CDTM, Cardiff UK, June 2008

R. Rothe, A. Villegas-Mendez, L. Liguori, B. Marques and J.L. Lenormand: "ZEBRA as new promising delivery systems for a wide range of proteins" IDTM Grenoble, France, September 2007

R. Rothe, A. Villegas-Mendez, L. Liguori, B. Marques and J.L. Lenormand: "ZEBRA as a new delivery system for therapeutic proteins." Telford, UK, September 2006

Available online at www.sciencedirect.com
ScienceDirect
Journal of Controlled Release 126 (2008) 217–227
journal of controlled release
www.elsevier.com/locate/jconrel

Liposomes-mediated delivery of pro-apoptotic therapeutic membrane proteins

Lavinia Liguori, Bruno Marques, Ana Villegas-Mendez, Romy Rothe, Jean-Luc Lenormand *

HumProTher laboratory, GREPI, TIMC IMAG, UMR5525, UJF/CNRS, University of Joseph Fourier, CHU-Grenoble, BP217, 38043 Grenoble Cedex 9, France

Received 22 August 2007; accepted 3 December 2007
Available online 14 December 2007

Abstract

The delivery of functional therapeutic proteins by lipid vesicles into targeted living cells is one of the most promising strategies for treatment of different diseases and cancer. The use of this system in the delivery of membrane proteins directly into cells remains to be tested because the methods for producing membrane proteins are difficult to perform. Here we describe the effect of proteoliposomes containing the voltage-dependent anion channel (VDAC) and pro-apoptotic Bak, both produced with an optimized cell-free expression system. For the first time, recombinant VDAC and Bak proteins are synthesized and directly integrated into the lipidic bilayer of natural liposomes in a one-step reaction. VDAC has been shown to play an essential role in apoptosis in mammalian cells by regulating cytochrome *c* release from mitochondria and Bak modulates mitochondrial membrane permeability upon activation. Internalization of recombinant proteoliposomes into mammalian cells induces apoptosis by release of cytochrome *c* and caspases activation. These results highlight that membrane proteins integrated in natural liposomes can represent an excellent candidate for cancer protein therapy.

Keywords: Membrane proteins production; Membrane proteins delivery; Proteoliposomes; Protein therapy; Apoptosis

1. Introduction

In the search for effective cancer treatments, new strategies tend to focus on a combination of traditional chemotherapy with selective delivery of pro-apoptotic agents or by inhibiting blood vessel growth. In this context, the development of bio- and nanotechnologies enhances the process by engineering new drugs delivery systems such as nanoparticles, immunomicelles and liposomes. These systems are capable of carrying therapeutic agents which present low solubility in water [1].

Liposomes are microscopic vesicles composed of lipid membranes surrounding discrete aqueous compartments [2]. The integration of pro-apoptotic membrane proteins (MPs) into liposomes represents a new approach in the delivery of an immediate death stimulus in cancer cells. However, because of their hydrophobicity, over-expression of MPs *in vivo* frequently leads to protein aggregation, cell toxicity, mis-folding, and low yield [3]. Because of these tremendous difficulties during their production and purification, MPs are highly underrepresented in structural data banks [3]. Interest in obtaining high yields of MPs is evident in the case of structural studies, but is also crucial for functional studies.

The development of cell-free protein synthesis systems provides a method of performing biological processes without cellular proliferation. There is an increased interest in these technologies and recent progress has improved the volumetric productivity [4]. Cell-free protein synthesis technologies can be used to express cytotoxic, poorly expressed and unstable proteins [5–8]. An increasing number of MPs from diverse families such as prokaryotic small multidrug transporters or eukaryotic G-protein-coupled receptors have been produced in high amounts and in active forms with these systems [9,10].

The combination of a cell-free synthesis system and the use of lipid-based biotechnologies, which focus on liposomes, represent an original approach in facilitating the delivery of hydrophobic therapeutic agents into living cells. Previously, we reported that lipids from spinach thylacoids were suitable for

* Corresponding author. Tel.: +33 4 76 63 74 39; fax: +33 4 76 63 75 59.
E-mail address: JLLenormand@chu-grenoble.fr (J.-L. Lenormand).

0168-3659/$ - see front matter © 2007 Elsevier B.V. All rights reserved.
doi:10.1016/j.jconrel.2007.12.004

OPEN ACCESS Freely available online

PLoS one

Liposome-Mediated Cellular Delivery of Active gp91^{phox}

Bruno Marques[1], Lavinia Liguori[1], Marie-Hélène Paclet[2], Ana Villegas-Mendéz[1], Romy Rothe[1], Françoise Morel[2], Jean-Luc Lenormand[1]*

1 HumProTher, UMR-CNRS 5525, Université Joseph Fourier, Centre Hospitalier Universitaire, Laboratoire d'Enzymologie/DBPC/BP 217, Centre Hospitalier Universitaire de Grenoble, Grenoble, France, **2** GREPI, TIMC-Imag, UMR-CNRS 5525, Université Joseph Fourier, Centre Hospitalier Universitaire, Laboratoire d'Enzymologie/DBPC/BP 217, Centre Hospitalier Universitaire de Grenoble, Grenoble, France

Background. **Gp91^{phox} is a transmembrane protein and the catalytic core of the NADPH oxidase complex of neutrophils. Lack of this protein causes chronic granulomatous disease (CGD), a rare genetic disorder characterized by severe and recurrent infections due to the incapacity of phagocytes to kill microorganisms.** ***Methodology.*** **Here we optimize a prokaryotic cell-free expression system to produce integral mammalian membrane proteins.** ***Conclusions.*** **Using this system, we over-express truncated forms of the gp91^{phox} protein under soluble form in the presence of detergents or lipids resulting in active proteins with a "native-like" conformation. All the proteins exhibit diaphorase activity in the presence of cytosolic factors (p67^{phox}, p47^{phox}, p40^{phox} and Rac) and arachidonic acid. We also produce proteoliposomes containing gp91^{phox} protein and demonstrate that these proteins exhibit activities similar to their cellular counterpart. The proteoliposomes induce rapid cellular delivery and relocation of recombinant gp91^{phox} proteins to the plasma membrane. Our data support the concept of cell-free expression technology for producing recombinant proteoliposomes and their use for functional and structural studies or protein therapy by complementing deficient cells in gp91^{phox} protein.**

Citation: Marques B, Liguori L, Paclet M-H, Villegas-Mendéz A, Rothe R, et al (2007) Liposome-Mediated Cellular Delivery of Active gp91^{phox}. PLoS ONE 2(9): e856. doi:10.1371/journal.pone.0000856

INTRODUCTION

Gp91^{phox} protein is the catalytic subunit of the NADPH oxidase complex in human neutrophils and is involved in the electron transfer from NADPH to molecular oxygen O_2 [1]. Gp91^{phox} is a transmembrane glycoprotein which physiologically associates with the p22^{phox} subunit to form flavocytochrome b_{558} [2]. MALDI and nanospray LC-MS/MS methods have delineated the transmembrane domains of gp91^{phox} [3]. This protein contains six putative α-helices and three extracellular loops in which the glycosylation sites (Asn132, Asn149 and Asn240) are comprised in loops 2 and 3 [4]. In its active state, NADPH oxidase is a multi-component enzyme complex composed of cytochrome b_{558} (gp91^{phox} and p22^{phox}) and cytosolic factors (p67^{phox}, p47^{phox}, p40^{phox}, Rac and Rap1A) that translocate at the membrane surface from cytosol upon stimulation. From this transfer and through the assembly of the constituents, NADPH oxidase is activated [5]. Upon infection or stimulation with inflammatory mediators, NADPH oxidase from neutrophils generate O_2^- and then oxygen derivatives, or ROS, which are necessary for the defense of the organism.

Recent studies on the C-terminal part (amino acids 221 to 570) of gp91^{phox} protein show that the cytoplasmic domain retains a high NADPH diaphorase activity [6] that can be stimulated in the presence of cytosolic proteins Rac and p67^{phox}. This supports the hypothesis that p67^{phox} and Rac bind directly to gp91^{phox} and activates NADPH oxidase by inducing conformational changes in its flavoprotein domain [7]. Using a similar approach, different domains of p22^{phox} protein have been delineated and shown to be involved in the maturation of the gp91^{phox} protein before the assembly of the gp91^{phox}/p22^{phox} heterodimer [8].

Among these approaches, an internal domain in the N-terminal part of p22^{phox} is involved in the flavocytochrome assembly, whereas the proline-rich region (PRR motif) in the C-terminal portion is responsible for NADPH oxidase activity via the binding to the p47^{phox} SH3 domain [1].

Chronic granulomatous disease (CGD) is a rare immuno-deficiency disease caused by mutations in genes encoding one of the main constituents of NADPH oxidase [9]. Mutations in the *CYBB* gene encoding gp91^{phox} represent almost 60% of CGD cases. These defects largely result in a lack of protein expression (X° CGD) or, in less than 10% of CGD cases, in a decrease or a loss of oxidase activity while protein is present (X^- or X^+ CGD). Recently, gene therapy has been tested in animal models and in clinical trials to attempt to reconstitute NADPH oxidase activity in X-linked CGD mice or in X-linked CGD patients [10]. Although promising results have been reported, this method still employs a retrovirus that may deliver the corrective gene into the patient's genome in locations which affect essential genes such as those involved in cancer.

Beside gene therapy, recent progress has been made with methods for the delivery of functional proteins which are based on the direct delivery of active therapeutic proteins into targeted living cells or, in the case of monoclonal antibodies, for the stimulation of specific immune responses [11]. Different strategies are used for the delivery of functional proteins such as micro-injection, electroporation, liposomes or by fusion to a protein transduction domain (PTD). Among these delivery systems, liposomes represent a promising technology for the delivery of

Academic Editor: Mikhail Blagosklonny, Ordway Research Institute, United States of America

Received May 23, 2007; **Accepted** August 16, 2007; **Published** September 12, 2007

Funding: This work was supported by grants from the 'Ministère de l'Enseignement supérieur de la Recherche et Technologie', Paris, France; the 'UFR de Médecine, Université Joseph Fourier', Grenoble, France; the 'Région Rh?'ne Alpes, programme Emergence 2003', France; the CGD Research Trust, UK; the 'Groupement des Entreprises Françaises dans la lutte contre le Cancer', délégation de Grenoble, the 'Délégation Régionale de la Recherche Clinique', CHU Grenoble, France and the Marie Curie Excellence Grant (EXT014320).

Competing Interests: The authors have declared that no competing interests exist.

* **To whom correspondence should be addressed.** E-mail: JLLenormand@chu-grenoble.fr

Review

For reprint orders, please contact reprints@future-drugs.com

Production of membrane proteins using cell-free expression systems

Lavinia Liguori, Bruno Marques, Ana Villegas-Méndez, Romy Rothe and Jean-Luc Lenormand[†]

Different overexpression systems are widely used in the laboratory to produce proteins in a reasonable amount for functional and structural studies. However, to optimize these systems without modifying the cellular functions of the living organism remains a challenging task. Cell-free expression systems have become a convenient method for the high-throughput expression of recombinant proteins, and great effort has been focused on generating high yields of proteins. Furthermore, these systems represent an attractive alternative for producing difficult-to-express proteins, such as membrane proteins. In this review, we highlight the recent improvements of these cell-free expression systems and their direct applications in the fields of membrane proteins production, protein therapy and modern proteomics.

Expert Rev. Proteomics 4(1), 79–90 (2007)

CONTENTS

[†]*Author for correspondence*
University Joseph Fourier, HumPro Ther Laboratory, GREPI, CHU-Grenoble, 38043 Grenoble, France
Tel.: +33 476 765 483
Fax: +33 476 765 608
jllenormand@chu-grenoble.fr

KEYWORDS:
cell-free expression system, detergent, high-throughput protein expression, membrane protein, proteoliposome

Challenges for producing membrane proteins

Membrane proteins represent approximately 30% of the total proteins from an organism and are involved in essential biochemical processes. For instance, membrane proteins perform critical roles in the cell cycle by regulating signaling, metabolism, transport and recognition. Dysregulation of their biological activity is one of the primary responses of the cell from bacterial or viral infections, as well as in cancer or genetic diseases. One of the major difficulties in the study of membrane protein is to recover a suitable concentration of recombinant protein using the classical overexpression techniques or from natural sources. Any attempt to develop a new method for expressing membrane proteins must consider some challenging problems. Among these, membrane proteins must be integrated into a lipid bilayer in a correctly folded structure, the membrane insertion must neither result in cell toxicity nor in poor growth of the host system, and membrane proteins must be synthesized in sufficient concentration without any proteolytic degradation. Membrane proteins are highly under-represented in structural data banks due to tremendous difficulties that occur upon approaching their structural analysis. Our understanding of the function of this broad range of proteins is highly circumscribed by a lack of structural information, due to difficulties in obtaining crystals suitable for x-ray diffraction. Currently, there are more than 25,000 soluble proteins, but only 115 membrane proteins are characterized in their 3D structure. A large part of membrane protein research focuses on developing and implementing new technologies to solve the bottlenecks that preclude the determination, at high throughput, of high-resolution structures of membrane proteins and membrane protein complexes.

Considering that these proteins play a central role in drug discovery as potential pharmaceutical targets, it is now imperative to go deeper into their structure to understand their molecular and physiological functions. In fact, recombinant proteins as a new tool for treating diseases were recently highlighted by a report from Data Monitor (a market analyst company). This company predicted that, by 2010, the therapeutic proteins market will generate annual sales over US$59 billion [1]. The development of technologies for producing recombinant proteins (e.g., therapeutic proteins) in different systems has profoundly shaped biological research. These protein expression systems (*in vivo* prokaryotic and

10.1586/14789450.4.1.79

ISSN 1478-9450

Expression and Purification of ZEBRA Fusion Proteins and Applications for the Delivery of Macromolecules into Mammalian Cells

UNIT 18.11

Romy Rothe[1] and Jean-Luc Lenormand[1]

[1]HumProTher laboratory, TheREx-GREPI, University of Joseph Fourier, UFR de Médecine, France

ABSTRACT

The recent development of peptide carriers for efficient and specific delivery of biologically active molecules into mammalian cells represents a major advance in the study of both normal and uncontrolled cell growth. In the past few years, this technology has been successfully applied to the delivery of therapeutic molecules in animal models and now, some of these carriers are available in the clinic for the treatment of some human diseases. This unit describes the production in a bacterial expression system of reporter proteins (EGFP and β-galactosidase) fused to a transduction domain of the Epstein-Barr virus ZEBRA protein, as well as purification of the fusion proteins. The purified fusion proteins can be added to any of a large spectrum of mammalian cells and the internalization process measured by flow cytometry, fluorescence microscopy on live or fixed cells to study their intracellular distribution. *Curr. Protoc. Protein Sci.* 54:18.11.1-18.11.29.

Keywords: protein expression • fusion protein • protein delivery • endocytosis • intracellular distribution • therapeutic proteins

INTRODUCTION

The delivery of protein therapeutics is an effective and innovative strategy for treating cancer and infectious diseases. Internalization of exogenous biologically active molecules by live cells also represents an interesting approach for studying cellular functions. The prerequisite for the delivery of macromolecules, including proteins, enzymes, antibodies, peptide nucleic acids (PNAs), oligonucleotides, antisense nucleotides, DNA, and small interference RNAs (siRNAs) is to cross the cell membrane to exert their biological actions in the cytoplasm, the nucleus, or in specific organelles (e.g., mitochondria or endoplasmic reticulum; Gupta et al., 2005). However, the lipophilic composition of the membranes hinders the cellular uptake of these biomolecules. The development of carriers which can enhance and ensure the complete and specific delivery of therapeutic molecules, for example in disease cells, is therefore necessary.

Protein transduction technology with cell-penetrating peptides (CPPs) or protein transduction domains (PTDs) has recently emerged as an effective way of delivering macromolecules into normal and transformed cells. In 1988, two groups (Green and Loewenstein, 1988; Frankel and Pabo, 1988) independently reported that the TAT transcription factor, a viral protein from human immunodeficiency virus (HIV), was able to cross cell membranes and be internalized when added to the cell culture. A short domain of 11 amino acids (residues 47 to 57 of the TAT protein) responsible for this property has been identified and this minimal, highly basic domain (GRKKRRQRRRP) enables transduction of a variety of macromolecules, including full-length proteins and oligopeptides, into cells (Harada et al., 2006). Subsequent studies have identified a growing number of

Current Protocols in Protein Science 18.11.1-18.11.29, November 2008
Published online November 2008 in Wiley Interscience (www.interscience.wiley.com).
DOI: 10.1002/0471140864.ps1811s54

Characterization of the Cell-Penetrating Properties of the Epstein-Barr Virus ZEBRA *Trans*-Activator

Romy Rothe[1], Lavinia Liguori[2], Ana Villegas-Mendez[1], Bruno Marques[1], Didier Grunwald[3], Emmanuel Drouet[4] and Jean-Luc Lenormand[1]*

From the TheREx-HumProTher, TIMC-IMAG Laboratory, CNRS UMR5525, University Joseph Fourier, UFR de Médecine, 38700 La Tronche, France[1];

Fondation RTRA "Nanosciences", University Joseph Fourier, TIMC-GMCAO, 38706 La Tronche, France; [2]

iRTSV-TS - U873 INSERM - CEA-Grenoble - 17, rue des Martyrs, 38054 Grenoble cedex 9, France [3];

Unit of Virus Host Cell Interactions (UVHCI) UMR 5233 UJF-EMBL-CNRS B.P. 181. 6, rue Jules Horowitz. F-38042 Grenoble Cedex 9, France[4].

Running head: Transduction Properties of ZEBRA

*To whom correspondence should be addressed: TheREx-HumProTher, TIMC-IMAG Laboratory, CNRS UMR5525, University Joseph Fourier, UFR de Médecine, 38700 La Tronche, France. E-mail: JLLenormand@chu-grenoble.fr

Phone: 33(0)4 76 63 74 39; Fax: 33(0)4 76 63 75 59

The basic-leucine zipper (bZIP) transcriptional activator ZEBRA of the Epstein - Barr virus (EBV) was recently shown to cross the outer membrane of live cells and to accumulate in the nucleus of lymphocytes. We investigated the potential application of the EBV *trans*-activator ZEBRA as a transporter protein to facilitate transduction of cargo proteins. The analysis of different truncated forms of ZEBRA revealed that the minimal domain (MD) required for internalization was spanning residues 170-220. The MD efficiently transported reporter proteins, such as EGFP and β-galactosidase, into several normal and tumor cell lines. Functionality of internalized cargo proteins was confirmed by β-galactosidase activity in transduced cells, and no MD-associated cell toxicity was detected. Translocation of MD through the cell membrane required binding to cell surface associated heparan sulfate proteoglycans as shown by strong inhibition of protein uptake in presence of heparin. We found that internalization was blocked at 4°C, whereas no ATP was required as witnessed by an only 25% decreased uptake efficiency in energy-depleted cells. Common endocytotic inhibitors, such as nystatin, chlorpromazine, or wortmannin had no significant impact on MD-EGFP uptake. Only methyl-β-cyclodextrin (MβCD) inhibited MD-EGFP uptake by 40% indicating the implication of the lipid raft mediated endocytotic pathway. These data suggest that MD-reporter protein transduction occurs mostly via direct translocation through the lipid bilayer and not by endocytosis. This mechanism of MD-mediated internalization is suitable for the efficient delivery of biologically active proteins and renders ZEBRA-MD a promising candidate for therapeutic protein delivery applications.

Recently, cell penetrating peptides (CPP) were discovered that have the ability to cross lipid bilayers of mammalian cells which naturally constitutes a tight biological barrier allowing only the uptake of non-polar molecules smaller than 500 Dalton into the cell (1). Coupling of CPPs to molecules such as siRNA, peptide nucleic acids, and bioactive proteins facilitates delivery of therapeutic agents into live cells (2-5). The most intensively studied CPPs include the Tat peptide, which is derived from the human immunodeficiency virus protein (HIV-1) (6,7), the third helix of *Antennapedia* homeodomain (also referred to as Penetratin) from *Drosophila* (8), and the VP22 peptide of the herpes simplex virus (9,10).

The activity of therapeutic molecules depends on their availability and functionality after their delivery into cells, both of which are determined by the transduction mechanism of the particular CPP (11). Consequently, extensive research was directed to elucidate pathways underlying protein transduction. Because of its apparent temperature and ATP dependency, it is widely assumed that cell entry occurs via endocytosis after binding of

the CPP to negatively charged heparan sulphate proteoglycans (HSPGs) located on the cell surface (12-14). Tat-fusion proteins were shown to be internalized *via* macropinocytosis whereas different endocytotic pathways, such as clathrin-dependent or caveolin-dependent endocytosis, were shown to be implicated in the transport of other CPPs (10,12,15-17). In addition, an alternative route of direct translocation of the small CPPs, such as SSHR-based peptide, was reported (18). Currently, one of the major challenges for the application of CPPs is to increase endosomal escape of CPP-cargoes to provide sufficient biologically active molecules at their intracellular destinations. Fusion of the CPP to pH-sensitive fusogenic peptides or co-administration of endosome-disruption agents, such as chloroquine, Ca2+, sucrose or photosensitizers, result in an enhanced release of the CPP-cargoes from the endosomal compartments (19-22). However, these strategies come along with considerable medical and technical disadvantages which consist in the cytotoxicity of disrupting agents, such as chloroquine, and the problematic application of photosensitizers for *in vivo* protein delivery. Therefore, there is a strong need for the identification of alternative CPPs that ideally bypass the endocytotic uptake route, thereby facilitating efficient delivery of therapeutic molecules to their intracellular destinations.

The present study focuses on the characterization of the cell penetrating properties of the major Epstein-Barr Virus *trans*-activator, the ZEBRA protein (also referred to as Zta, Z, EB1 or BZLF1) (23,24). Recently, it was shown that this protein not only binds DNA, and exerts cell cycle control functions, but also has the ability to penetrate lymphoid cells (25). The ZEBRA protein belongs to the basic-leucine zipper (bZIP) family of transcription factors and is responsible for the initiation of the EBV lytic cycle (24,26). Furthermore, this multifunctional protein controls its own expression, virus replication, cell cycle arrest and DNA-damage response in the host cells (24,27-30). The structure of the 245 amino acids ZEBRA protein has recently been resolved in its DNA-bound form: the protein is divided into an N-terminal transactivation region and a basic DNA-binding domain flanked by a coiled-coil dimerization region (zipper). The C-terminal (CT) domain interacts with the zipper region by forming intra and intermolecular interactions resulting in a hydrophobic pocket (31). These complex interactions are unique among the bZIP members and result in the stabilization of the ZEBRA dimer when bound to DNA.

In the presented work, we have investigated the transduction properties of ZEBRA. We designed different truncated forms of ZEBRA to identify the minimal domain (MD) required for the delivery of different reporter proteins, including EGFP or β-galactosidase, into various cell lines. The 48 amino acids bZIP region of ZEBRA (ZEBRA-MD) was shown to be sufficient to facilitate reporter protein internalization. In addition, we demonstrated that the ZEBRA-MD fused to EGFP required interaction with cell surface heparan sulphate proteoglycans, and crossed the cell membrane in a pathway largely independent from endocytosis. Taken together, our results revealed the powerful transduction properties of ZEBRA-MD, rendering it a promising candidate for the development an efficient protein delivery vector.

EXPERIMENTAL PROCEDURES

Cloning of ZEBRA protein and fragments-The DNA fragments encoding the full-length protein and all truncated forms of ZEBRA were generated by PCR and ligated into the E. coli expression vector pET15b (Novagen) which provided an N-terminal hexahistidine-tag for subsequent purification. Sequences of primers used for generation of truncated ZEBRA fragments, EGFP and LacZ were described elsewhere (32). The reporter genes were C-terminally fused to truncated ZEBRA fragments and cloned into pET15b expression plasmid.

Expression and Purification of recombinant proteins- All recombinant fusion proteins were expressed in E. coli BL21 (DE3) after induction with 0.5 mM IPTG for 15h at 16°C. Cells were lysed by sonication in 20 mM Tris buffer (pH 6.8 or 8) containing 250 mM NaCl and 10% glycerol and subsequently treated with DNase I (Roche) for nucleic acids removal. Purifications of His_6 tagged (His-tag) proteins were performed by nickel affinity chromatography. Proteins were washed using a 0.5-1.5 M NaCl gradient and eluted in 500mM imidazole, 20 mM Tris, 75 mM KCl, 0.5 M

NaCl and 10% glycerol. All purification steps were carried out at 4°C and in presence of protease inhibitors (Pepstatine, E-64, Aprotinin, Pefablock and complete protease inhibitor mix, Roche). Prior to transduction experiments, purified proteins were dialyzed against PBS.

Electrophoretic mobility shift assay (EMSA)- EMSA binding reactions were performed for all purified recombinant proteins. The AP-1 probe was made by annealing two oligonucleotides (5'-AGCACTGACTCATGAAGT-3' and 5'-TACTTCATGAGTCAGTGCT-3'). The cold probe was labeled with Biotin and purified over a Microspin G-25 spin column (Active Motif). Up to 500 µg full-length ZEBRA and truncated proteins were preincubated with 4x Binding buffer B-1, 2x Stabilizing buffer (Generka) and 1 mM DTT for 15 min on ice. The Biotin-labeled probe was mixed with 4x Binding buffer C-1, 2x Stabilizing buffer (Generka), supplemented with 50 ng/µl poly(dI-dC) and added to protein-containing solution. After an incubation of the reaction mix for 15 min at 4°C, the samples were separated on 4-8% nondenaturating polyacrylamid gels in 0.5 x TBE and transferred on Hybond N+ membrane (Amersham). The LightShift Chemiluminescent EMSA Kit (Pierce) was used for detection according to manufacturer's protocol.

Cell culture and transduction experiments- HeLa cells were maintained in Dulbecco's modified Eagle's medium (Gibco), and Saos-2 cells were grown in McCoy's 5A medium (Gibco) supplemented with 10-20% heat-inactivated fetal bovine serum (Gibco), 50 U/ml penicillin, 50 µg/ml streptomycin and 2 mM L-glutamine (Gibco). 7.5 x 10^5 cells/well were seeded on a 12-well plate 24h before transduction experiments. For microscopic analysis, cells (2.5 x 10^5) were plated on 4-well chamber slides at least 24h before treatment. Internalization experiments were performed at 60-80% confluence. Cells were rinsed twice with phosphate buffered saline (PBS) before addition of fresh serum-free culture medium containing indicated amounts of protein. After 4h culture medium was supplemented with 10% heat-inactivated fetal bovine serum (Gibco) for long term incubation.

Drug treatment- Heparin, as well as endocytotic inhibitors such as, wortmannin, nystatin, chlorpromazine hydrochloride and methyl-β-cyclodextrin (MβCD), 2-deoxy-D-glucose and sodium azide was purchased from Sigma. Cells were incubated for 30 min prior to EGFP fusion protein addition in serum-free media containing the indicated concentration of individual drugs (20 µg/ml heparin, 100 nM wortmannin, 50 µg/ml nystatin, 30 µM chlorpromazine hydrochloride and 5-10 mM methyl-β-cyclodextrin (MβCD)). Subsequently, cells were incubated for 3h in the presence of inhibitors and proteins at 37°C or 4°C, and trypsinized (0.5% trypsin-EDTA, Gibco) to remove surface bound protein before analyzing fluorescence by flow cytometry. For depletion of ATP pool, cells were preincubated for 1 h in PBS containing 6 mM 2-deoxy-D-glucose and 10 mM sodium azide.

Immunocytochemistry and fluorescence microscopy- When incubated with EGFP fusion proteins, cells were washed with PBS followed by a mild trypzination (0.5% trypsin-EDTA, Gibco) and several washes with heparin (20 µg/ml). For immunolocalization studies, cells were washed two times for 5 min in heparin (20 µg/ml) in PBS and fixed for 10 min in 4% PFA at room temperature (RT). Cells were permeabilized and blocked with 0.25% TritonX100 and 5% BSA in PBS for 1 h at RT, followed by 1 h incubation at RT with the corresponding primary antibodies in 0.1% TritonX100, 5% BSA in PBS. To detect endogenous endosomal proteins, an Anti-EEA-1 (4 µg/ml, Calbiochem), an Anti-Rab-7 (5 µg/ml, Cell Signaling), an Anti-clathrin or an Anti-caveolin-1 (5 µg/ml, Santa Cruz Biotechnology) antibody, respectively, were applied. After three washes in PBS for 10 min cells were incubated with the corresponding secondary antibody Anti-rabbit Alexa Fluor® 647 (Molecular Probes) in 0.1% TritonX100, 5% BSA in PBS. Cells were washed five times for 10 min with PBS and nuclei were counterstained with Hoechst 33258 (Molecular Probes). Cellular fluorescence on non-fixed cells was visualized using the an inverted fluorescence Nikon Eclipse TE2000-E microscope (Nikon) with a GFP (465- to 495 nm excitation and 515- to 555 nm emission) filter. For localization studies, cells were analyzed by confocal microscopy (TCS-SP2 – Leica Manheim, Germany). Images were acquired sequentially, with 488nm excitation for the MD-EGFP (fluorescence collection

between 500 and 540 nm; displayed in green), 633 nm excitation for Alexa Fluor® 647 - EEA1, Rab7, clathrin, caveolin - 1 (fluorescence collection between 650 and 700nm; displayed in red), and 405 nm excitation for Hoechst (fluorescence collection between 415 and 460nm; displayed in blue).

β-galactosidase staining- After transduction experiments, cells were washed with 20 µg/ml heparin in PBS, and carefully trypsinized for cell surface bound protein removal. Fixation and staining was done according to the β-galactosidase staining kit protocol (Sigma). Briefly, cells were incubated for 10 min at RT with 1x fixation solution containing 2% formaldehyde and 0.2% glutaraldehyde. After three washing steps with PBS at RT, cells were stained with a solution containing magnesium chloride (20 mM), potassium ferricyanide (40 mM), potassium ferrocyanide (40 mM) and 2 mg/mL of X-gal for 3 h at 37°C. Images were taken with a Nikon Eclipse TE2000-E microscope.

Western blot analysis- After transduction experiments, cells were collected and non-internalized proteins were removed by trypzination. Whole cell extracts were prepared by lysing cells in ice cold mammalian cell lysis buffer (Sigma) and separation in cytosolic and nucleic fractions were carried out using cell compartmentation Kit (Pierce), respectively. A total of 50 – 100µg of protein was subjected to SDS-Page separation and transferred to nitrocellulose membranes. Western blotting was carried out as previously described (33). As primary antibodies a monoclonal anti-ZEBRA Z125/Z130 mouse monoclonal antibody (Anti-EB1/Zta Z125 mouse 1:100 in T-TBS), a monoclonal Anti-GFP mouse antibody (Euromedex) 1:500 in T-TBS was used. After an incubation with peroxidase-labeled secondary antibody (Anti-mouse 1:5000 in T-TBS, Amersham), blots were washed again and analyzed with an enhanced chemiluminescence detection system (Amersham).

Flow cytometry analysis- Internalization of EGFP fusion proteins alone or in presence of inhibitors was measured by Flow Cytometry. Cells were treated with 0.5% trypsin and 20 µg/ml heparin during 10 min to remove surface bound proteins before analyzing green fluorescence. Only live cells were assayed using 7-Amino-Actinomycin D (7-AAD) exclusion (34). Flow cytometric analysis was carried out with a fluorescence-activated cell sorting (FACScalibur, Becton Dickinson).

Cytotoxicity Assay- Membrane integrity was measured using the Cytotoxicity Detection Kit from Roche Applied Science. In brief, 1 x 10^4 HeLa or Saos2 cells were seeded in 96-well plates 24 h before treatment with ZEBRA-MD fusion proteins at indicated concentrations in serum-free medium. After 24h, lactate dehydrogenase (LDH) assay was carried out according to manufacture's protocol.

Synthetic liposomes- Synthetic lipid vesicles were prepared as described elsewhere (33). Liposomes were labeled with the 10µM of the lipophilic dye, nile red, and incubated at 37°C in presence of 0.2 µM MD-EGFP and subsequently analyzed by confocal microscopy (TCS-SP2 – Leica Manheim, Germany).

RESULTS

Identification of the minimal domain (MD) required for protein translocation. The full-length ZEBRA protein contains three major regions: a trans-activation domain (TAD, residues 1-140), a highly basic DNA binding domain (DB, residues 175-195) and a dimerization domain (DIM, residues 195-220) (23,26,31). To identify the minimal domain (MD) required for the translocation of ZEBRA into mammalian cells, nine different truncations of the full-length ZEBRA (Z-FL) protein were constructed that covered the entire amino acids sequence of the native protein (Fig. 1A). Proteins extending from residues 1 to 195 covering the TAD (Z1), as well as shorter fragments of the N-terminal part of ZEBRA, were produced (Z2, Z3). The fragments Z4, Z6, and Z9 contained both, DB and DIM, and varied with respect to the regions flanking those functional domains. Furthermore, three fragments bearing either the DB (Z5, Z7) or the DIM (Z8) were constructed (Fig. 1A). The full length and truncated proteins had an N-terminal His-tag to facilitate purification of the soluble protein fractions by nickel affinity chromatography. As shown in Fig. 1B and C, all truncated ZEBRA fragments as well as recombinant EGFP fusions could be successfully overexpressed and purified to near homogeneity. All N-terminal fragments (Z1, Z2, Z3) as well as Z5 showed higher protein yields compared to C-terminal ZEBRA protein fragments (Fig. 1B). Furthermore, fusion of

ZEBRA truncations to EGFP resulted in higher yield of soluble purified protein when compared to β-galactosidase fusions (data not shown).

In order to use ZEBRA as a protein carrier, we first evaluated the transduction properties of the full-length ZEBRA and several different truncations fused to EGFP, including Z2-EGFP, Z3-EGFP, Z4-EGFP, Z5-EGFP, Z6-EGFP, Z8-EGFP and Z9-EGFP. The fusion proteins were added in the culture media of cervical cancer (HeLa) or osteosarcoma (Saos2) cells, incubated for 24h and cell fluorescence was monitored either by flow cytometry or by fluorescence microscopy on live unfixed cells (Fig. 1D and 1E). We found that only full-length Z-FL-EGFP, Z4-EGFP, Z6-EGFP and Z9-EGFP proteins were efficiently transduced into HeLa cells (Fig. 1D). No fluorescence signal was observed in association with the EGFP-fused truncations containing only the N-terminal part (Z3-EGFP) of the wild-type protein, an internal deletion in the zipper domain (Z5-EGFP), or a deletion of the basic domain (Z8-EGFP) (Fig. 1D). Transduction efficiency was further evaluated in HeLa and Saos2 cell lines by flow cytometry after 15 h incubation with 0.2 μM of each protein. The flow cytometric analyses confirmed the efficient uptake of Z4-EGFP, Z6-EGFP and Z9-EGFP into the two cell lines (Fig. 1E). In addition, internalization of Z9-EGFP (MD-EGFP) into mouse myoblasts (C2C12) and Saos2 cells (Fig. 1F) was demonstrated by fluorescence microscopy.

From these results, we concluded that the presence of both the DB and the DIM domains are required and sufficient for internalization. The smallest tested truncated protein containing both domains was Z9 (MD), which facilitated the delivery of EGFP with an almost 100% efficiency (number of fluorescent cells over total cell number) into various mammalian cell lines. Therefore, all translocation experiments described below were performed using the Z9 peptide, which in the following is denoted minimal transduction domain (MD). This MD of ZEBRA is composed of 54 amino acid residues and combines two important domains of the ZEBRA protein; the DNA binding region and the dimerization domain, which together form the bZIP region (Fig. 1G). Additionally to 14 positively charged residues such as lysine and arginine, the MD provides 13 hydrophobic amino acid (leucine, alanine and valine), which are mainly located at the dimerization domain (Fig. 1G).

DNA binding activity. As ZEBRA is a transcription factor which binds DNA through its central basic region (DB, residues 175-195), we investigated whether the DNA binding activity is preserved in different ZEBRA truncations. It was previously shown that ZEBRA recognized the AP-1 consensus heptamer TGA $^{G}/_{C}$ TCA (31). We used this heptamer as a probe to evaluate the DNA binding activity with EMSAs (Fig. 2). The truncations containing both, the DB and DIM domains, (Z4, lane 7,8; Z6, lane 10, 11, 17) bound the AP-1 probe with nearly the same efficiency as the full-length ZEBRA protein (Fig. 2) In contrast, truncations carrying deletions in DB (Z8, lane 13), DIM (Z5,line 9; Z7, line 12), or both domains (Z2, line 5 and 6), failed to bind the AP-1 probe (Fig. 2). In agreement with the work from Petosa and colleagues (31), this data indicated that the presence of the DB and the DIM domain is required and sufficient for DNA binding. However, residual DNA-protein complex formation was also detected for the Z1 truncation which only contained DB but no DIM domain (Fig. 2).

Because the truncated forms Z6 and Z9 (MD) were shown to transduce into cells, we further investigated the DNA binding activity of both peptides when fused N-terminally to EGFP or β-galactosidase reporter proteins. All fusion proteins failed to recognize the AP-1 probe as demonstrated by EMSA (Fig. 2). In contrast, the fusion of EGFP to the full-length ZEBRA or Z4 (data not shown) had no effect on the DNA binding activity (Fig.2). These results suggested that conformational changes occurred after fusion of the reporter proteins with Z6 and MD compromising their ability to bind DNA.

Kinetics of MD-EGFP internalization and cytotoxicity. The translocation of MD(Z9)-EGFP was monitored by the measurement of fluorescence in live cells using flow cytometry analysis. The addition of low concentration of MD(Z9)-EGFP (0.2 μM) to the serum-free culture media of HeLa or Saos2 cells resulted

in a rapid intracellular accumulation of the fusion protein (Fig. 3A). This cellular uptake was detected after removal of cell surface bound protein by extensive trypsin/heparin washes and remained stable for at least 24 h in the cells (Fig. 3A and Sup Fig. 1). The increased fluorescence intensity in Saos2 cells after transduction is most likely due to their larger size compared to smaller HeLa cells, and not caused by better translocation efficiency into the former.

We also investigated the dose-dependent internalization of MD(Z9)-EGFP into these cell lines. Cells were incubated during 4h with different concentration of the fusion protein ranging from 10 to 200 nM. After extensive washing and trypzination, transduction efficiency was analyzed by flow cytometry. Transduced EGFP was already detected in HeLa and Saos2 cells after incubation with low amounts (10 and 20 nM) of MD(Z9)-EGFP (Fig. 3B). About 50% of the cells were transduced in presence of 100 nM MD(Z9)-EGFP (Fig. 3B). Incubation of cells with higher concentrations (200 nM) of MD(Z9)-EGFP resulted in a 100% transduced cell population (Sup Movie 1 and Movie 2). The fluorescence of internalized EGFP increased linearly with the concentration of MD(Z9)-EGFP in the culture medium and reached saturation at 200 nM (data not shown).

The toxicity of both MD(Z9)-EGFP and MD(Z9)-β-galactosidase fusion proteins was tested with a lactate dehydrogenase (LDH) based assay. The cytosolic enzyme LDH can be detected in the cell culture medium after the disruption of cell membranes. Saos2 and HeLa cells were incubated with different concentrations of the fusion protein ranging from 0.1 to 3 µM. 24 h after addition of the MD fusion proteins, no variation in the cell viability was observed as shown by the absence of extracellular LDH activity (Fig. 3C).

Mechanisms of uptake. Several reports have described that cell surface heparan sulfate proteoglycans (HSPGs) play a key role for the cellular internalization of CPPs (14, 35). Mutational analysis of cationic rich sequences demonstrated that the cellular uptake properties of Tat depends mostly on the presence of positively charged residues which facilitate binding to negatively charged HSPGs at the cellular surface (36, 37). To evaluate the role of HSPGs for the uptake of MD-EGFP, HeLa and Saos2 cells were incubated for 30 min with 20 µg/ml heparin prior to addition of the fusion protein. Heparin is a structural homolog of HSPGs and may compete for binding of the latter to MD-EGFP. The uptake of MD-EGFP was significantly inhibited by presence of heparin in the culture medium when compared to the control condition without heparin (Fig. 4A). These data indicated that cellular internalization of MD-EGFP required interactions between negatively charged HSPGs and the basic amino acids in the sequence of MD (Z9) (Fig. 1G).

Recent studies on the uptake mechanisms of Tat or VP22 reported a significant contribution of endocytotic pathways to their cellular internalization (12,15,22,38). Therefore, we first investigated the effect of low temperature and ATP depletion on cellular uptake of MD-EGFP. As shown in Fig. 4B, the intracellular EGFP signal for HeLa and Saos2 cells was strongly reduced after incubation at 4°C. The cellular ATP pool was depleted by a treatment with sodium azide and 2-deoxy-D-glucose. We observed only a 20 - 30% decrease in cell fluorescence in both cell lines (Fig. 4B), indicating that the uptake of MD-EGFP is mostly ATP independent.

To clarify whether MD-EGFP internalization involves endocytosis, we explored the effect of several drugs that specifically inhibit caveolin, clathrin, or lipid raft-dependent endocytosis, respectively. Nystatin is a known inhibitor of caveolin-dependent endocytosis (12). The internalization by a caveolae process is slow and occurs in general upon cell stimulation (39). HeLa and Saos2 cells were treated with 50 µg/ml nystatin prior to addition of 0.2 µM MD-EGFP and internalization was analyzed by flow cytometry. In both cell lines, the intracellular fluorescence signal for MD-EGFP in presence of nystatin was identical to the control conditions (Fig. 4C). Thus, caveolin-dependent endocytosis is not involved in the uptake of MD-EGFP. Macropinocytosis is a rapid and non-specific mechanism of internalization and has been described to be responsible for the cellular uptake of some CPPs (15). Macropinocytosis depends on the activity of phosphatidylinositol-3-kinase (PI3K) and is inhibited by wortmannin (40). We examined the impact of wortmannin on the internalization of MD-EGFP into HeLa and

Saos2 cells. The pretreatment of both cell lines with 100 nM wortmannin did not alter the cellular uptake of MD-EGFP compared to untreated cells (Fig. 4C). Thus, MD-mediated protein translocation does not occur via macropinocytosis. To test whether MD-EGFP uptake involves clathrin-coated pit-mediated endocytosis, MD-EGFP internalization was measured in the presence of chlorpromazine. Saos2 and HeLa cells were incubated with 30 µM chlorpromazine. After 30 min incubation with chlorpromazine, the MD-EGFP fusion protein was added. Interestingly, EGFP fluorescence was significantly reduced in Saos2 cells but not in HeLa cells (Fig. 4C). These results indicate that the internalization process of MD-EGFP may differ depending on the cell type. Finally, we investigated the lipid raft-mediated endocytotic pathway, which has been also reported to be implicated in the uptake of CPPs (15,22). Cells were treated with methyl-β-cyclodextrin (MβCD) to deplete cell surface associated cholesterol resulting in a disruption of lipid rafts. As shown in Fig. 4C, an impaired uptake of MD-EGFP into both cell lines was observed. These data suggest that lipid raft-mediated endocytosis contributes to the uptake of MD-EGFP. However, 60% of MD-EGFP occurred through an alternative route of internalization. This observation is supported by the entry of MD-EGFP into synthetic liposomes (data not shown). The lipophilic dye, nile red (10µM) was added to the synthetic liposomes preparation for fluorescence labeling. Immediately after labeling reaction, liposomes were incubated for 30 min with MD-EGFP and analyzed by confocal microscopy. GFP-fluorescence was detected around and inside the lipid vesicles suggesting a direct translocation across the lipid layer (data not shown).

Intracellular localization of MD-EGFP. In case of an endosomal-dependent pathway of MD uptake, colocalization with early and late endosomes would be expected. We performed immunofluorescence microscopy to study the subcellular co-localization of internalized MD-EGFP with endosomal marker proteins, such as EEA1 (early endosomal marker), Rab7 (endosomal marker, Fig. 5A-D and Sup Fig. 2), caveolin-1 (caveosome marker), and clathrin (marker for clathrin coated pits, Fig. 5E, F) (41). HeLa cells were incubated between 30 min to 15 h with MD-EGFP at 37°C and protein internalization was analyzed by confocal microscopy. The uptake of MD-EGFP was confirmed by direct visualization of the intracellular fluorescence of EGFP or by antibody staining against EGFP.

The majority of the EGFP signals did not co-localize with EEA-1 or Rab-7 signals (Fig. 5A-D). However, a portion of the EGFP signals overlapped with endosomal markers. Variation of the incubation times did change this observation only slightly. At earlier time points (30 min) after the addition of MD-EGFP to the cells we observed minor co-localization of the internalized protein with endosomal markers EEA-1 and at later time points (3 h) with Rab-7. Furthermore, MD-EGFP did not co-localize with caveolin or clathrin signals at any analyzed time points (Fig. 5E, F)

Cellular entry of MD-EGFP was characterized by live cell imaging in HeLa cells. 0.3 µM of the ZEBRA-EGFP fusion protein was added to the cells and directly visualized by fluorescence microscopy for 1 h (Sup Fig. 3). A fast accumulation at the cell membrane level was observed within the first 15 min, followed by a rapid trafficking of EGFP signals inside the cell. Furthermore, internalized proteins were detected inside the cell after immunofluorescence analysis by examining different Z-section of one cell (Sup Fig. 3).

Delivery of β-galactosidase into cells. In order to use MD as a protein carrier, we tested the intracellular functionality of MD-delivered proteins using the 120 kDa enzyme β-galactosidase fused to MD as a model. The fusion protein was added to serum-free culture media of Saos2 and HeLa cells. Cells were fixed and stained according to X-Gal staining kit (Sigma). Fig. 6 shows the successful delivery of functional β-galactosidase into HeLa and Saos2 cells as proven by the blue cellular staining. Analogous to the delivery of EGFP by ZEBRA-MD, we observed a 100% transduced cell population using MD-β-galactosidase. The reporter protein β-galactosidase alone was used as a negative control and no β-galactosidase activity was detected within these control cells (Fig. 6). These results confirmed that β-galactosidase positive staining did not occur through a fixation artifact.

DISCUSSION

With the prospect of developing ZEBRA as a protein delivery tool, it was of interest to identify the minimal transduction domain required for internalization. For this reason, we engineered numerous protein truncations, and characterized their transduction capacities when fused to the reporter protein EGFP. We identified three truncations of ZEBRA, namely Z4, Z6, and Z9 (MD), that had the ability to transfer EGFP into live cells. All truncations with protein translocation ability contained the basic positively charged DB domain, as well as the hydrophobic leucine-rich DIM domain of ZEBRA (26,31), whereas truncated proteins missing either of the two domains failed to translocate EGFP into cells. The 48 amino acid peptide Z9 was the smallest ZEBRA truncation with transduction abilities. It was therefore denoted minimal domain (MD) and further characterized regarding its uptake mechanism, functionality of delivered proteins, as well as cell toxicity.

The uptake of MD-EGFP was temperature-dependent, presumably due to the fluidity loss of the lipid bilayer at low temperatures (18). Since uptake of MD-EGFP into ATP-depleted cells only decreased by 20 %, we conclude that the MD fusion protein is internalized by a largely ATP-independent process. Furthermore, several endocytotic inhibitors, such as nystatin, wortmannin or chlorpromazine, did not interfere with MD-EGFP uptake, indicating no participation of receptor-mediated endocytosis (12,15,22,38,41). This finding was further supported by the lacking colocalization of MD-EGFP with caveolin1 and clathrin. Furthermore, neither the early endosomal marker, EEA-1, nor the late endosomal marker Rab-7, are involved in transport of cargo from early to late endosomes, showed a complete co-localization in microscopic images. Only the incubation with methyl-β-cyclodextrin (MβCD), a drug that inhibits lipid raft mediated endocytosis (22) caused a 40% decreased uptake of MD-EGFP. Thus, the endocytotic pathway may contribute in part to the cellular uptake of MD-EGFP under the applied conditions, but did not account for the majority of the internalized fusion protein. In addition, uptake of MD-EGFP required availability of cell surface HSPGs since its internalization was clearly impaired in the presence of heparin. Similar to other CPPs that are taken up in a HSPG-dependent manner, the cell surface binding of MD appears to be facilitated by the interaction of the highly positively charged DB region and the negatively charged HSPGs (14,42,43). However, as shown by the failure of the DB-containing Z5 truncation to enable protein uptake, the presence of a positively charged domain alone is not sufficient for protein internalization. Only when the DB was present together with the hydrophobic DIM domain, efficient protein uptake was observed. It was earlier established that DB and DIM domains together form a continuous stretch of an α-helix (31), which is similar to other amphipathic CPPs including MAP or Transportan (43,44). For those peptides, an increase in membrane permeability that correlates with the presence of amphiphilic α-helical structures has been observed (45). Accordingly, internalization of MD may require the α-helix formed by DB and DIM domains. Furthermore, the DB domain might mediate surface binding of MD while the DIM domain subsequently facilitates translocation through the lipid bilayer by hydrophobic interactions in a similar way as reported for Penetratin (46). This CPP is internalized via a non-endocytotic, and receptor as well as transporter-independent pathway. Penetratin requires the hydrophobic tryptophan residues and crosses lipid bilayers without pore formation (47,48). In line with these arguments, also the MD-mediated protein translocation did not cause disruption or pore formation in the plasma membrane as shown by the absence of both, 7-AAD uptake and leakage of lactate dehydrogenase (LDH) in transduced cells. Finally, we observed a direct translocation of MD-EGFP into synthetic liposomes (data not shown). Taken together the energy independent uptake of MD-EGFP, the decreased uptake of MD-EGFP into cells at low temperatures, as well as lacking exclusive colocalization with endosomal markers, and incomplete inhibition of MD-EGFP uptake by endocytotic inhibitors suggest that MD-EGFP is, at least in part, translocated directly across the lipid bilayer. This energy-independent internalization property of ZEBRA-MD-EGFP is highly favorable, since endosomal trapping can be circumvent, which seems to be the major bottleneck for most CPP, as for example TAT, which enters cell by macropinocytosis (15) and fails to enter into liposomes(43,49).

Further study to determine the amino acids from MD responsible for the translocation properties will permit to better understand the molecular mechanism of ZEBRA cellular uptake.

In addition, we tested the ability of the truncated ZEBRA proteins to bind DNA. As we expected, constructs encompassing both the basic DB and the DIM domain recognized and bound the AP-1 site *in vitro*. Interestingly, this specific binding was lost when these proteins were fused at the C-terminal with either EGFP or β-galactosidase. As it was shown in the crystal structure of ZEBRA bound to the AP-1 promoter element, DNA binding of the protein requires complex conformation of its C-terminal part, and mutations in the latter were suggested to inactivate transcription factor activity of ZEBRA (31). Thus, the C-terminal fusion of proteins to truncated forms of ZEBRA may have compromised its ability to form protein-DNA complexes. The loss of its DNA-binding activity when fused to proteins is certainly a tremendous advantage for the development of a new potential protein delivery system. However, a possible interaction between Zebras' MD and cellular proteins after its cellular uptake can not be completely ruled out, since it was not examined in the presented study. As the full-length ZEBRA protein can induce growth arrest independently of its ability to bind DNA in host cells through direct interplay with cellular proteins and its basic region (27,28), possible interaction with cellular proteins and control of their activities need to be further analyzed.

In addition to previously reported lymphocyte specific uptake of ZEBRA (25), we observed a rapid internalization of MD-EGFP into a wide range of different cells. MD-delivered proteins remained functional when transduced into cells, as demonstrated by the enzymatic activity of internalized MD-β-galactosidase. In conclusion, MD is a new carrier suitable for the efficient transport of proteins into live mammalian cells. Since its uptake is largely independent from known endocytotic pathways, ZEBRA-MD can carry proteins into cells without being trapped into endosomal compartments. Additionally, it does not show any toxic side effects and transduce a wide range of mammalian cells with 100% efficiency. Taken all together, these favorable biochemical properties of ZEBRA-MD indicate that ZEBRA represents a novel and powerful delivery system for therapeutic proteins.

REFERENCES

1. Murriel, C. L., and Dowdy, S. F. (2006) *Expert Opin Drug Deliv* **3**(6), 739-746
2. Endoh, T., Sisido, M., and Ohtsuki, T. (2008) *Bioconjug Chem* **19**(5), 1017-1024
3. Abes, S., Turner, J. J., Ivanova, G. D., Owen, D., Williams, D., Arzumanov, A., Clair, P., Gait, M. J., and Lebleu, B. (2007) *Nucleic Acids Res* **35**(13), 4495-4502
4. Harada, H., Hiraoka, M., and Kizaka-Kondoh, S. (2002) *Cancer Res* **62**(7), 2013-2018
5. Kilic, U., Kilic, E., Dietz, G. P., and Bahr, M. (2003) *Stroke* **34**(5), 1304-1310
6. Fawell, S., Seery, J., Daikh, Y., Moore, C., Chen, L. L., Pepinsky, B., and Barsoum, J. (1994) *Proc Natl Acad Sci U S A* **91**(2), 664-668
7. Vives, E., Brodin, P., and Lebleu, B. (1997) *J Biol Chem* **272**(25), 16010-16017
8. Derossi, D., Joliot, A. H., Chassaing, G., and Prochiantz, A. (1994) *J Biol Chem* **269**(14), 10444-10450
9. Elliott, G., and O'Hare, P. (1997) *Cell* **88**(2), 223-233
10. Nishi, K., and Saigo, K. (2007) *J Biol Chem* **282**(37), 27503-27517
11. Langel, Ü. (2006) *Handbook of Cell-Penetrating Peptides*, 2 Ed.
12. Richard, J. P., Melikov, K., Brooks, H., Prevot, P., Lebleu, B., and Chernomordik, L. V. (2005) *J Biol Chem* **280**(15), 15300-15306
13. Lundberg, P., and Langel, U. (2003) *J Mol Recognit* **16**(5), 227-233
14. Ziegler, A., and Seelig, J. (2004) *Biophys J* **86**(1 Pt 1), 254-263
15. Kaplan, I. M., Wadia, J. S., and Dowdy, S. F. (2005) *J Control Release* **102**(1), 247-253

16. Ferrari, A., Pellegrini, V., Arcangeli, C., Fittipaldi, A., Giacca, M., and Beltram, F. (2003) *Mol Ther* **8**(2), 284-294
17. Fittipaldi, A., Ferrari, A., Zoppe, M., Arcangeli, C., Pellegrini, V., Beltram, F., and Giacca, M. (2003) *J Biol Chem* **278**(36), 34141-34149
18. Veach, R. A., Liu, D., Yao, S., Chen, Y., Liu, X. Y., Downs, S., and Hawiger, J. (2004) *J Biol Chem* **279**(12), 11425-11431
19. Oliveira, S., Hogset, A., Storm, G., and Schiffelers, R. M. (2008) *Curr Pharm Des* **14**(34), 3686-3697
20. Oliveira, S., van Rooy, I., Kranenburg, O., Storm, G., and Schiffelers, R. M. (2007) *Int J Pharm* **331**(2), 211-214
21. Shiraishi, T., and Nielsen, P. E. (2006) *Nat Protoc* **1**(2), 633-636
22. Wadia, J. S., Stan, R. V., and Dowdy, S. F. (2004) *Nat Med* **10**(3), 310-315
23. Miller, G., El-Guindy, A., Countryman, J., Ye, J., and Gradoville, L. (2007) *Adv Cancer Res* **97**, 81-109
24. Sinclair, A. J. (2003) *J Gen Virol* **84**(Pt 8), 1941-1949
25. Mahot, S., Fender, P., Vives, R. R., Caron, C., Perrissin, M., Gruffat, H., Sergeant, A., and Drouet, E. (2005) *Virus Res* **110**(1-2), 187-193
26. Sinclair, A. J. (2006) *Trends Microbiol* **14**(7), 289-291
27. Rodriguez, A., Armstrong, M., Dwyer, D., and Flemington, E. (1999) *J Virol* **73**(11), 9029-9038
28. Rodriguez, A., Jung, E. J., Yin, Q., Cayrol, C., and Flemington, E. K. (2001) *Virology* **284**(2), 159-169
29. Cayrol, C., and Flemington, E. (1996) *J Biol Chem* **271**(50), 31799-31802
30. Cayrol, C., and Flemington, E. K. (1996) *Embo J* **15**(11), 2748-2759
31. Petosa, C., Morand, P., Baudin, F., Moulin, M., Artero, J. B., and Muller, C. W. (2006) *Mol Cell* **21**(4), 565-572
32. Rothe, R., and Lenormand, J. L. (2008) *Curr Protoc Protein Sci* **Chapter 18**, Unit 18 11
33. Liguori, L., Marques, B., Villegas-Mendez, A., Rothe, R., and Lenormand, J. L. (2008) *J Control Release* **126**(3), 217-227
34. Schmid, I., Krall, W. J., Uittenbogaart, C. H., Braun, J., and Giorgi, J. V. (1992) *Cytometry* **13**(2), 204-208
35. Tyagi, M., Rusnati, M., Presta, M., and Giacca, M. (2001) *J Biol Chem* **276**(5), 3254-3261
36. Ho, A., Schwarze, S. R., Mermelstein, S. J., Waksman, G., and Dowdy, S. F. (2001) *Cancer Res* **61**(2), 474-477
37. Mukai, Y., Sugita, T., Yamato, T., Yamanada, N., Shibata, H., Imai, S., Abe, Y., Nagano, K., Nomura, T., Tsutsumi, Y., Kamada, H., Nakagawa, S., and Tsunoda, S. (2006) *Biol Pharm Bull* **29**(8), 1570-1574
38. Fuchs, S. M., and Raines, R. T. (2004) *Biochemistry* **43**(9), 2438-2444
39. Anderson, R. G. (1998) *Annu Rev Biochem* **67**, 199-225
40. Araki, N., Johnson, M. T., and Swanson, J. A. (1996) *J Cell Biol* **135**(5), 1249-1260
41. Watson, P., Jones, A. T., and Stephens, D. J. (2005) *Adv Drug Deliv Rev* **57**(1), 43-61
42. Fuchs, S. M., and Raines, R. T. (2006) *Cell Mol Life Sci* **63**(16), 1819-1822
43. Zorko, M., and Langel, U. (2005) *Adv Drug Deliv Rev* **57**(4), 529-545
44. Lindgren, M., Gallet, X., Soomets, U., Hallbrink, M., Brakenhielm, E., Pooga, M., Brasseur, R., and Langel, U. (2000) *Bioconjug Chem* **11**(5), 619-626
45. Dietz, G. P., and Bahr, M. (2004) *Mol Cell Neurosci* **27**(2), 85-131
46. Joliot, A., and Prochiantz, A. (2008) *Adv Drug Deliv Rev* **60**(4-5), 608-613

47. Thoren, P. E., Persson, D., Karlsson, M., and Norden, B. (2000) *FEBS Lett* **482**(3), 265-268
48. Terrone, D., Sang, S. L., Roudaia, L., and Silvius, J. R. (2003) *Biochemistry* **42**(47), 13787-13799
49. Kramer, S. D., and Wunderli-Allenspach, H. (2003) *Biochim Biophys Acta* **1609**(2), 161-169

ACKNOWLEDGMENT

This study was funded by a Marie Curie Excellence Grant (n° 014320). The authors thank Kathrin Lang from the Institute of Genetic, TU Dresden, Germany for providing the plasmid with the coding sequence of the β-galactosidase gene. Furthermore, we are grateful to Madiha Derouazi and Thomas Walther for intensive discussion and all helpful comments concerning the manuscript. We also thank Barry Stidder for the proof reading of the manuscript.

FOOTNOTES

The abbreviations used are: ATP, adenosine triphosphate; BSA bovine serum albumin; CPP, cell penetrating peptide; FCS, fetal calf serum; EGFP, enhanced green fluorescence protein; MβCD, methyl-β-cyclodextrin; MD, minimal domain required for transduction; PBS, phosphate-buffered saline; PTD, protein transduction domain,

FIGURE LEGENDS

Fig. 1: Identification of the minimal protein domain (MD) required for protein translocation.

A, Scheme of full-length ZEBRA protein (ZEBRA-FL) and all corresponding protein truncations. The full length ZEBRA (ZEBRA-FL) protein contains activation, DB and DIM domain. Nine truncated forms of ZEBRA (Z1-Z9) were created to characterize the minimal domain (MD) required for transduction.

B, Truncated ZEBRA proteins after expression in *E. coli* BL21 (DE3) and purification by nickel affinity chromatography were separated on a SDS page and detected by Western blotting using an anti-His antibody.

C, Aliquots of ZEBRA-EGFP and MD-β-galactosidase fusion proteins were loaded on a 13% SDS page and visualized by Coomassie Blue staining after electrophoresis.

D, Analysis of intracellular fluorescence after 15 h of incubation with 0.2 µM of each ZEBRA-EGFP fusion protein in living HeLa cells by fluorescence microscopy.

E, Flow cytometric analysis of live HeLa and Saos2 cells after exposure to 0.2 µM ZEBRA-EGFP fusion proteins. Cells were treated with Trypsin prior to flow FACS analysis. The mean cell fluorescence of three independent experiments and the ± S. D. is reported.

F, Uptake of MD-EGFP in C2C12 and Saos2 cells. 0.2 µM MD-EGFP was added to serum-free culture medium. Intracellular fluorescence was visualized by fluorescence microscopy.

G, Amino acid sequence of the MD of the ZEBRA protein. Basic amino acids (7 lysine and 7 arginine residues) are shown in red, whereas in hydrophobic amino acids (one valine, 5 alanine and 7 leucine residues) are presented in blue. The presence of both, the DNA binding region and the dimerization domain, are absolutely required for the translocation property of ZEBRA-MD.

Fig. 2: DNA binding activity

Electrophoretic mobility shift assay (EMSA) of recombinant ZEBRA variants. Truncated ZEBRA proteins and their respective fusion proteins were analyzed for their ability to bind AP-1 DNA probe. Signals were detected by a Chemiluminescent Assay (Pierce).

Fig. 3: Kinetics of MD-EGFP internalization and cytotoxicity

A, Time-dependent intracellular accumulation of MD-EGFP in HeLa and Saos2 cells. Both cell lines were incubated with 0.2 µM of MD-EGFP at 37°C for the times indicated, and subsequently treated with trypsin for 10 min at 37°C. The mean cell fluorescence was analyzed by flow cytometry.

B, Dose-dependent uptake of MD-EGFP in live HeLa and Saos2 cells. Indicated concentrations of MD-EGFP were added to the serum-free cell culture medium. After 4 h cells were washed with PBS, trypsinized for 10 min at 37°C and cell fluorescence was measured by flow cytometry. All transduction experiments were performed in triplicates in two independent analyses, and the ± S.D. are indicated.

C, MD-mediated protein delivery caused no cytotoxicity. HeLa and Saos2 cells were exposed to indicate concentrations of MD-EGFP and MD-β-galactosidase and incubated in growth medium at 37°C for 24 h. Cytotoxicity after the uptake of both fusion proteins was determined by the leakage of LDH into the culture medium. Each column represents the mean viability of two independent experiments performed in triplicates with indicated ± S.D

Fig. 4: Mechanisms of uptake

A, HeLa and Saos2 cells were incubated with 20 µg/ml heparin for 30 min at 37°C and afterwards exposed to 0.2 µM MD-EGFP for 3 h at 37°C. Cells were trypsinized for 10 min at 37°C and washed prior to flow cytometry analysis.
B, The effect of low temperature and depletion cellular ATP on internalization of MD-EGFP. Both cell lines were incubated with 0.2 µM MD-EGFP for 1 h at 4°C. To deplete the cellular ATP pool, HeLa and Saos2 cells were incubated for 1 h with 6 mM 2-deoxy-D-glucose and 10 mM sodium azide and than and exposed to 0.2 µM MD-EGFP for 1h. After trypzination, cells were analyzed by flow cytometry.
C, Effect of endocytotic inhibitors on MD-EGFP transduction. Both cell lines were treated with 30 µM chlorpromazine, 100 nM wortmannin, 50 µg/ml nystatin, or 5-10 mM methyl-β-cyclodextrin (MBCD), respectively, 30 min prior to addition of 0.2 µM MD-EGFP. In general, cellular uptake of pre-treated cells was measured as mean fluorescence and normalized to mean cell fluorescence of untreated control. Each experiment was performed three times in triplicates and the means ± S.D. are indicated.

Fig. 5: Intracellular localization of MD-EGFP in HeLa cells

HeLa cells were exposed to 0.2 µM MD-EGFP for 30 min to 3 h at 37°C. Surface bound proteins were removed by several heparin washes. Cells were then fixed, immuno-stained for endosomal marker proteins EEA-1 (A, C) or Rab-7 (B, D), detected with Alexa Fluor® 647 labeled second antibody, and nuclei were counterstained with Hoechst 33258. Cells were then visualized by confocal microscopy (TCS-SP2 – Leica Manheim, Germany). Images were acquired sequentially, as described in experimental procedures, with MD-EGFP in green, EEA-1 or Rab7 in red and DNA in blue (A, B). C, D, EEA-1 and Rab-7 fluorescence are visualized in red and MD-EGFP in green. An estimation of colocalization was determined with the "CF2D" software from Leica. Diagrams (right) represent the relative intensity of the pixels in the green and red images. Dots gated in the yellow square, corresponding to colocalization, are represented in white in the images.
E, F, HeLa cells were incubated for 3 h with 0.2 µM MD-EGFP at 37°C. Cells were washed with 20 µg/ml heparin in PBS, fixed, and incubated with anti-caveolin-1 (E) or anti-clathrin (F) antibodies and the corresponding secondary anti-rabbit antibody (Alexa Fluor® 647). Fluorescence was analyzed sequentially by confocal microscopy, as previously described. MD-EGFP signals are shown in green, nucleus in blue and clathrin or caveolin-1 marker in red.

Fig. 6: MD-mediated delivery of β-galactosidase into HeLa and Saos2 cells

After 16 h incubation with 0.2 µM of MD-β-galactosidase at 37°C, cells were washed with 20 µg/ml heparin, fixed and stained according to the β-galactosidase Reporter Gene Staining Kit (Sigma). β-galactosidase staining was visualized by contrast phase microscopy.

Figure 1

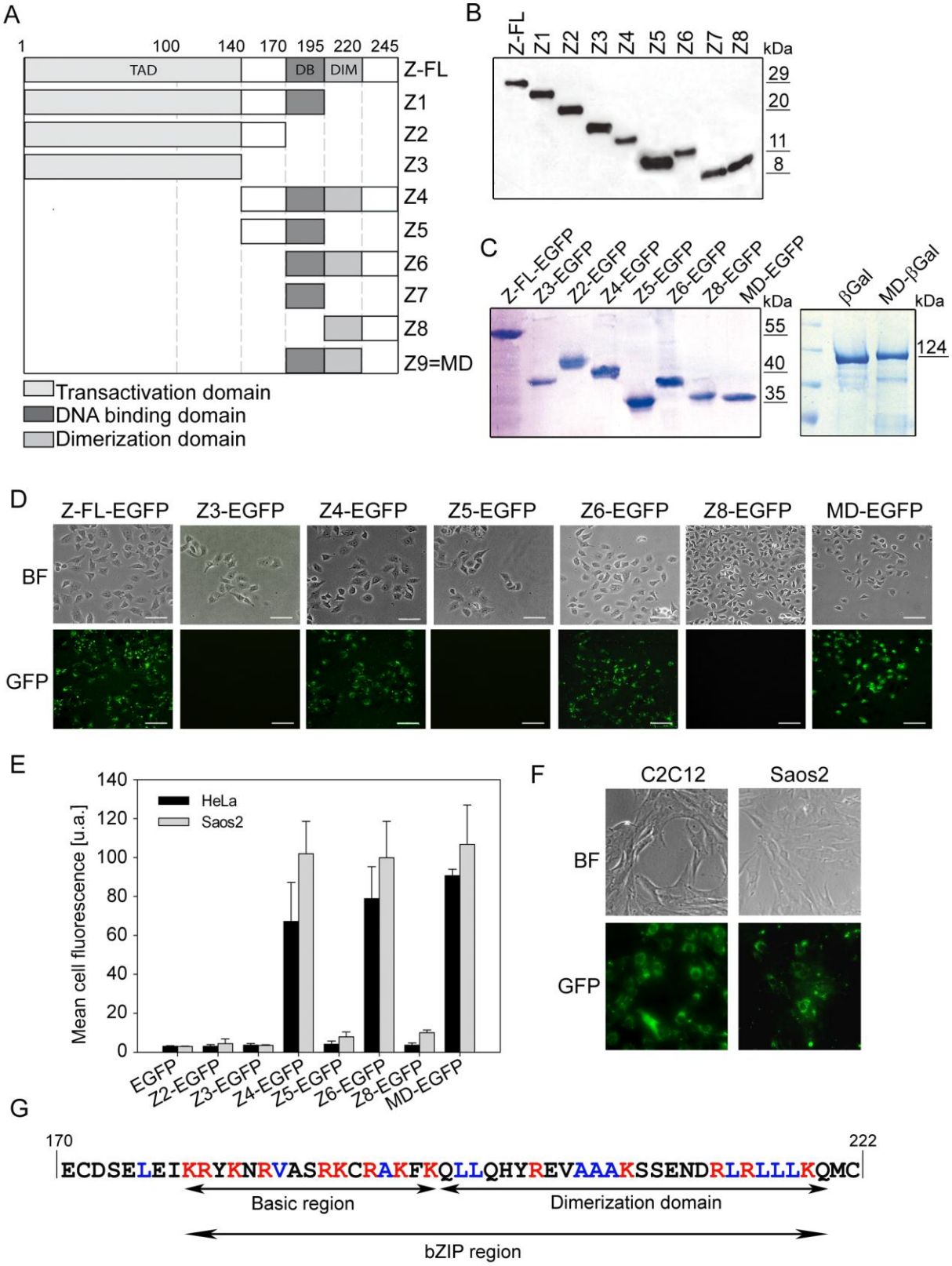
A
1
100
140
170
195
220
245
TAD
DB
DIM
Z-FL
Z1
Z2
Z3
Z4
Z5
Z6
Z7
Z8
Z9=MD
Transactivation domain
DNA binding domain
Dimerization domain
B
Z-FL
Z1
Z2
Z3
Z4
Z5
Z6
Z7
Z8
kDa
29
20
11
8
C
Z-FL-EGFP
Z3-EGFP
Z2-EGFP
Z4-EGFP
Z5-EGFP
Z6-EGFP
Z8-EGFP
MD-EGFP
kDa
55
40
35
βGal
MD-βGal
kDa
124
D
Z-FL-EGFP
Z3-EGFP
Z4-EGFP
Z5-EGFP
Z6-EGFP
Z8-EGFP
MD-EGFP
BF
GFP
E
Mean cell fluorescence [u.a.]
HeLa
Saos2
EGFP
Z2-EGFP
Z3-EGFP
Z4-EGFP
Z5-EGFP
Z6-EGFP
Z8-EGFP
MD-EGFP
F
C2C12
Saos2
BF
GFP
G
170
222
ECDSELEIKRYKNRVASRKCRAKFKQLLQHYREVAAAKSSENDRLRLLLKQMC
Basic region
Dimerization domain
bZIP region

Figure 2

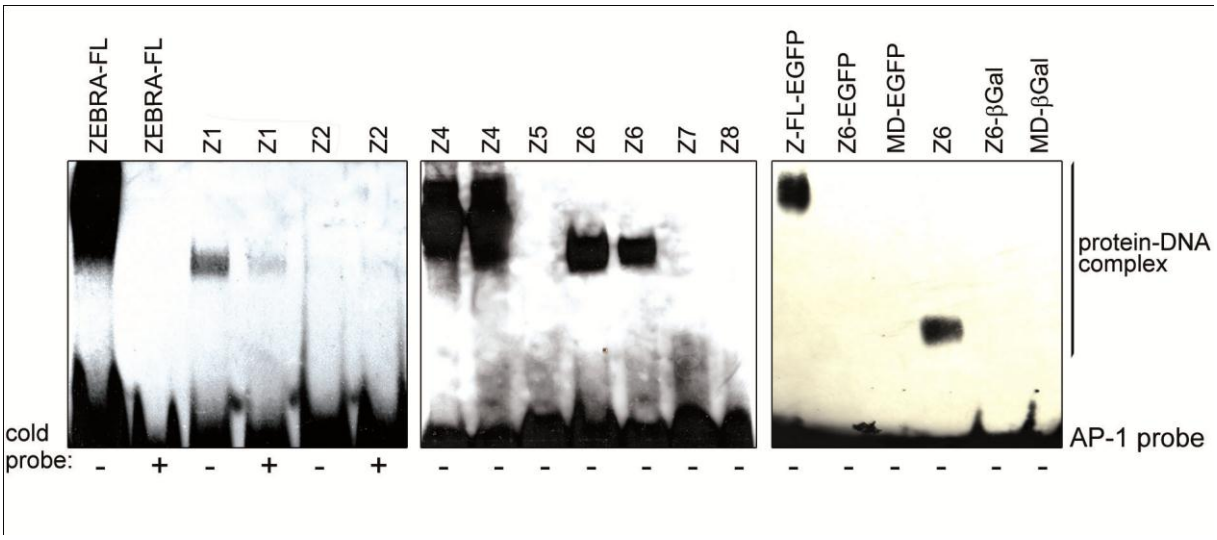
ZEBRA-FL
ZEBRA-FL
Z1
Z1
Z2
Z2
Z4
Z4
Z5
Z6
Z6
Z7
Z8
Z-FL-EGFP
Z6-EGFP
MD-EGFP
Z6
Z6-βGal
MD-βGal
protein-DNA complex
AP-1 probe
cold probe:
- + - + - + - - - - - - - - - - - - -

Figure 3

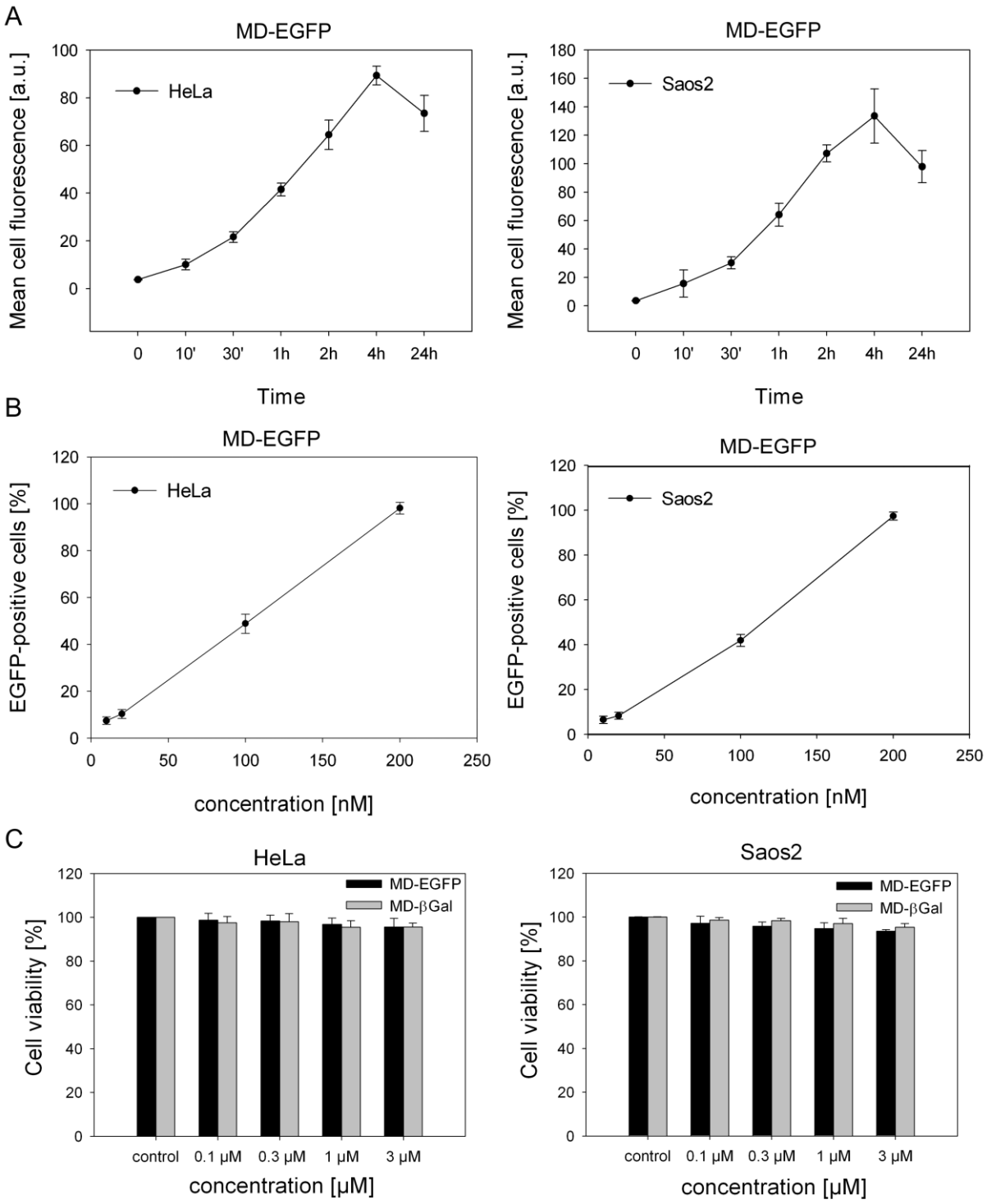
A
MD-EGFP
HeLa
Mean cell fluorescence [a.u.]
Time
0
10'
30'
1h
2h
4h
24h
MD-EGFP
Saos2
Mean cell fluorescence [a.u.]
Time
B
MD-EGFP
HeLa
EGFP-positive cells [%]
concentration [nM]
MD-EGFP
Saos2
EGFP-positive cells [%]
concentration [nM]
C
HeLa
MD-EGFP
MD-βGal
Cell viability [%]
control
0.1 μM
0.3 μM
1 μM
3 μM
concentration [μM]
Saos2
MD-EGFP
MD-βGal
Cell viability [%]
control
0.1 μM
0.3 μM
1 μM
3 μM
concentration [μM]

Figure 4

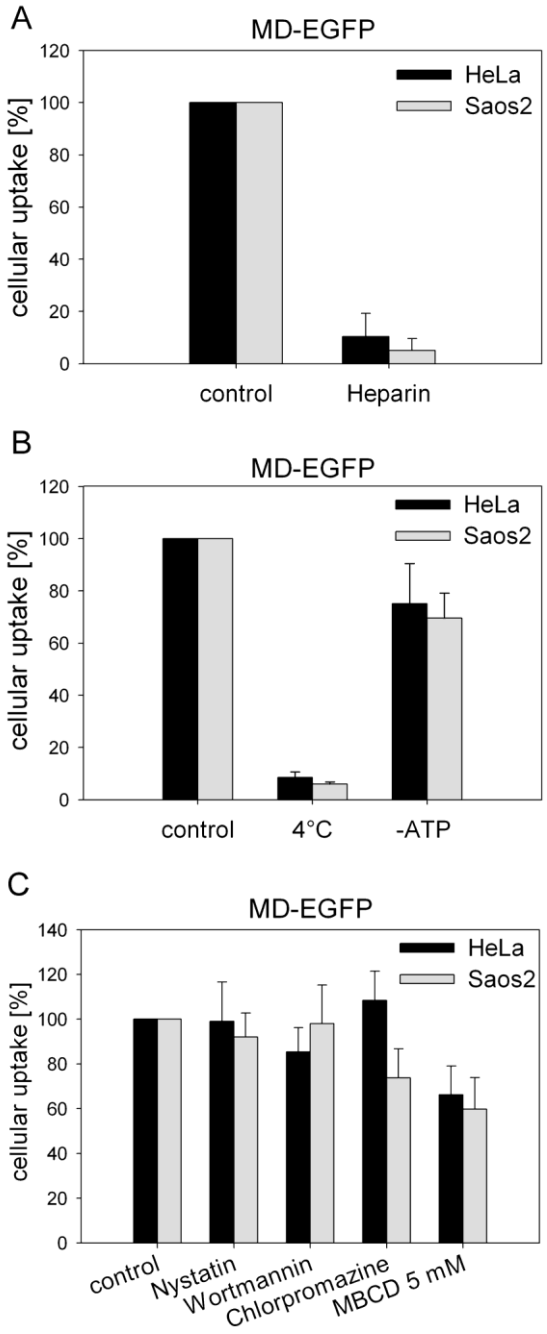
A
MD-EGFP
HeLa
Saos2
cellular uptake [%]
120
100
80
60
40
20
0
control
Heparin
B
MD-EGFP
HeLa
Saos2
cellular uptake [%]
120
100
80
60
40
20
0
control
4°C
-ATP
C
MD-EGFP
HeLa
Saos2
cellular uptake [%]
140
120
100
80
60
40
20
0
control
Nystatin
Wortmannin
Chlorpromazine
MBCD 5 mM

Figure 5

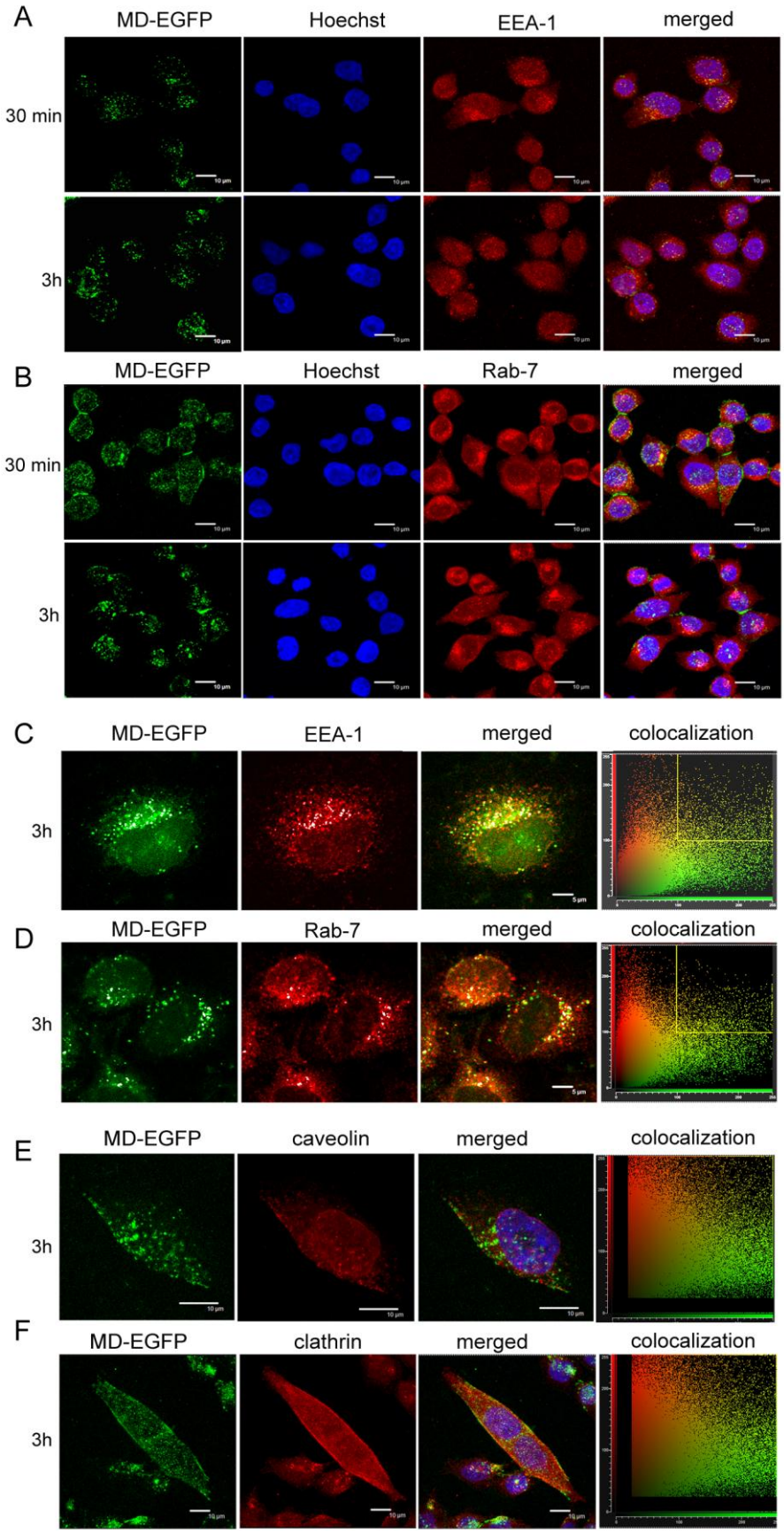
A
MD-EGFP
Hoechst
EEA-1
merged
30 min
3h
B
MD-EGFP
Hoechst
Rab-7
merged
30 min
3h
C
MD-EGFP
EEA-1
merged
colocalization
3h
D
MD-EGFP
Rab-7
merged
colocalization
3h
E
MD-EGFP
caveolin
merged
colocalization
3h
F
MD-EGFP
clathrin
merged
colocalization
3h

Figure 6